University of Alberta

PERFORMANCE ANALYSIS OF DIGITAL COMMUNICATIONS SYSTEMS WITH

FADING AND INTERFERENCE

by

Julian Zhishen Cheng   ©

A thesis submitted to the Faculty of Graduate Studies and Research in partial fulfillment of the

requirements for the degree of **Doctor of Philosophy.**

Department of Electrical and Computer Engineering

Edmonton, Alberta

Spring 2003

National Library
of Canada

Bibliothèque nationale
du Canada

Acquisitions and
Bibliographic Services

Acquisisitons et
services bibliographiques

395 Wellington Street
Ottawa ON K1A 0N4
Canada

395, rue Wellington
Ottawa ON K1A 0N4
Canada

Canada

University of Alberta

Library Release Form

Name of Author: Julian Zhishen Cheng
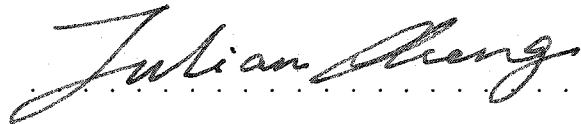
Title of Thesis: Performance Analysis of Digital Communications Systems with Fading and Interference

Degree: Doctor of Philosophy

Year this Degree Granted: 2003

Permission is hereby granted to the University of Alberta Library to reproduce single copies of this thesis and to lend or sell such copies for private, scholarly or scientific research purposes only.

The author reserves all other publication and other rights in association with the copyright in the thesis, and except as hereinbefore provided, neither the thesis nor any substantial portion thereof may be printed or otherwise reproduced in any material form whatever without the author's prior written permission.

Julian Zhishen Cheng

2nd Floor, ECERF,

University of Alberta

Edmonton, Alberta
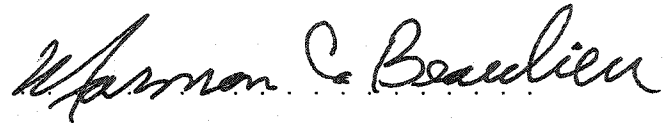
Canada, T6G 2V4

Date: December 23, 2002

University of Alberta

Faculty of Graduate Studies and Research

The undersigned certify that they have read, and recommend to the Faculty of Graduate Studies and Research for acceptance, a thesis entitled **Performance Analysis of Digital Communications Systems with Fading and Interference** submitted by Julian Zhishen Cheng in partial fulfillment of the requirements for the degree of **Doctor of Philosophy**.

Dr. Norman C. Beaulieu (Supervisor)

Dr. Ivan J. Fair

Dr. Chintha Tellambura

Dr. Bruce F. Cockburn

Dr. Laurence B. Milstein   U. of California S.D.

Dr. Douglas P. Wiens

Date December 23, 2002

In Loving Memory of My Father

Abstract

The growing deployment of wireless infrastructures and the decreasing cost of services have resulted in an exponential increase in the usage of wireless communication devices in different fading environments over the past decade. The performance of mature wireless cellular systems remains limited by fading and interference from other user signals. This thesis contributes to the accurate bit error rate (BER) performance analysis of a coherent binary phase shift keying (BPSK) modulation in a general fading and interference environment, as well as contributes to the estimation of the Nakagami-m fading parameter.

A generic BPSK direct-sequence code-division multiple access (DS-CDMA) system using random spreading sequences in flat Rayleigh fading is first considered. A tractable average BER expression is derived using a characteristic function method. The precise BER can be obtained for a system with large processing gain and an arbitrary number of users with modest computational complexity. The result is used to assess the accuracies of several widely used approximations. These results are then extended to a flat Nakagami-m fading channel.

Error analysis for bandwidth-efficient BPSK in a generalized Nakagami/Nakagami fading and cochannel interference (CCI) environment is studied. A tractable analytical BER expression is derived and used to study the effects of fading of an interfering signal on the desired user BER performance. It is found that fading of an interfering signal worsens the BER of the desired signal rather than improving it. The performance of a new novel pulse shape in fading and CCI is also studied. It is shown both analytically and numerically that this novel pulse outperforms the widely used raised-cosine pulse.

The estimation of the Nakagami-m fading parameter is extensively studied. Both moment-based and maximum-likelihood based estimations are considered. Several new estimators are proposed and their properties are thoroughly examined.

Acknowledgment

I am grateful to my thesis advisor Dr. Norman C. Beaulieu for his guidance, advice, encouragement, support, and friendship. I will continue to be influenced by his rigorous scholarship, clarity in thinking, and professional integrity.

I would like to thank Dr. Laurence B. Milstein from University of California, San Diego for his willingness to serve as my external examiner. I am honored to have him on my committee. I would also like to thank Drs. Bruce F. Cockburn, Ivan J. Fair, Chintha Tellambura and Douglas P. Wiens for serving on the committee. One of many good things happened to me since I relocated to Edmonton from Kingston was the opportunity for me to take STAT-512 taught by Dr. Wiens. I am very fortunate that, with his great help, I can apply the concepts and techniques I learned from his class to my research problem. I would also like to thank Dr. Tellambura for his interest in my work as well as his help in several parts of this thesis.

I would also like to thank my girlfriend Yi Song from Queen's University for her continuing encouragement, numerous technical discussions and LaTeX help throughout the writing of this thesis.

This work is in part sponsored by a graduate scholarship from the Natural Sciences and Engineering Research Council (NSERC), the Alberta Informatics Circle of Research Excellence (iCORE), as well as a Graduate Fellowship from Queen's University. Their financial support are greatly appreciated.

Last, I would like to thank my mother for her patience, understanding and support over all these years. I wish my father, whom I lost recently, could see me complete this degree. His enthusiasm

toward life will always inspire me. This thesis is dedicated to him.

Table of Contents

List of Tables

List of Figures

Acronyms

AF	Amount of fading
ARE	Asymptotic relative efficiency
AWGN	Additive white Gaussian noise
BER	Bit error rate
BPSK	Binary phase shift keying
BTRC	Better than raised cosine
CCI	Cochannel interference
CDF	Cumulative distribution function
CDMA	Code division multiple access
CF	Characteristic function
CLT	Central limit theorem
CRLB	Cramér-Rao lower bound
DS-CDMA	Direct sequence - code division multiple access
EM	Expectation-maximization
FDMA	Frequency division multiple access
FF	Fading figure
FH	Frequency hopping
GDE	Greenwood-Durand estimator
IGA	Improved Gaussian approximation
INV	Inverse normalized variance

ISI	Inter-symbol interference
LLF	Log-likelihood function
LOS	Line-of-sight
MA	Multiple access
MAI	Multiple access interference
MGF	Moment generating function
ML	Maximum-likelihood
MVUE	Minimum variance unbiased estimator
PDF	Probability density function
PMF	Probability mass function
PN	Pseudo-noise
PSD	Power spectral density
QPSK	Quaternary phase shift keying
RC	Raised cosine
RV	Random variable
SGA	Standard Gaussian approximation
SIGA	Simplified improved Gaussian approximation
SIR	Signal-to-interference ratio
SNR	Signal-to-noise ratio
SS	Spread spectrum
SSMA	Spread spectrum multiple access
TDMA	Time division multiple access
WLLN	Weak law of large number

List of Symbols

α	Pulse shaping factor
$\delta(\tau)$	Dirac delta function
μ_k	The kth moment
$\hat{\mu}_k$	The kth sample moment
τ_k	Time delay of the kth user
ϕ_k	Phase shift of the kth user
$\phi_X(s)$	Moment generating function of RV X
$\psi(\cdot)$	psi function
$\psi(t)$	Chip waveform
ω_c	Carrier frequency
$\Gamma(\cdot)$	Gamma function
$\Phi_X(\omega)$	Characteristic function of RV X
$\Psi(\cdot;\cdot;\cdot)$	Kummer-U function
Ω	Fading power
$a_k(t)$	Spreading signal of the kth user
$a_j^{(k)}$	The jth chip of the kth user
B	Number of chip boundaries with transitions in User 1's signature waveform
$b_k(t)$	Data signal of the kth user
$b_j^{(k)}$	jth data bit of the kth user
$\text{cov}[X,Y]$	Covariance between RV's X and Y defined as $\mathbb{E}[XY] - \mathbb{E}[X]\mathbb{E}[Y]$

e	Base of natural logarithms
E_b	Energy per bit
$\mathbb{E}[X]$	Mathematical expectation of RV X
$_1F_1(\cdot;\cdot;\cdot)$	Confluent hypergeometric function (Kummer-M function)
$F_X(x)$	Cumulative distribution function of RV X
$f_X(x)$	Probability density function of continuous RV X
G	Processing gain
$G(f)$	Spectrum of $g(t)$
$G_{p,q}^{m,n}(\cdot)$	Meijer's G-function
$g(t)$	Impulse response of the cascade of the transmitter and receiver filters
I	Interference component
$I(\theta)$	Fisher's information
$I_0(\cdot)$	The 0th order modified Bessel function of the first kind
$\mathbf{I}(\theta)$	Fisher's information matrix
$J_v(\cdot)$	vth order Bessel function of the first kind
K	Total number of active users
$\mathscr{K}$	Rician factor
L	Total number of interferers
m	Nakagami m parameter
m_I	Nakagami m parameter for the interferer
m_s	Nakagami m parameter for the desired user
$\mathscr{N}(\mu,\sigma^2)$	Gaussian distribution with mean μ and variance σ^2
$\mathscr{N}(\mu,\Sigma)$	Multivariate Gaussian distribution with mean vector μ and covariance matrix Σ
N	Number of observations
$N_0/2$	Power spectral density of AWGN
$n(t)$	Background AWGN

P_k	Transmitted signal power of the kth user
P_e	Precise average bit error rate
P_e^{SGA}	Average BER using the SGA
P_e^{SIGA}	Average BER using the SIGA
P_e^{SYNC}	Average BER under synchronous operation
$\Pr\{S\}$	Probability of event S
$p_X(i)$	Probability mass function of discrete RV X
$Q(\cdot)$	The standard Q-function defined as $Q(y) = \frac{1}{\sqrt{2\pi}} \int_y^{+\infty} e^{-x^2/2} dx$
R	Nakagami random variable
$R_\psi(\cdot), \hat{R}_\psi(\cdot)$	Partial autocorrelation functions of chip waveform
$S(f)$	Power spectral density
S_k	Fractional chip displacement of the kth interferer relative to the desired user
T	Bit duration
T_c	Chip duration
$\text{var}[X]$	Variance of RV X defined as $\mathbb{E}[X^2] - (\mathbb{E}[X])^2$
Z	Decision statistic

Chapter 1

Introduction

1.1 Introduction

From the beginning, humans have been communicating. It was about three decades ago that computers started to communicate to each other as well, and they have evolved into what we know today as Internet. Recently, smart electrical appliances can also communicate to each other using the Bluetooth technology [67]. With advances in speech recognition technology, humans have started to communicate with these smart appliances and computers. Therefore, communication is everywhere in our daily life. Since the invention of the telephone by Alexander Graham Bell in 1876 [87], wireline communication has dominated most of the consumer communication market. However, in recent years, approximately one hundred years after Marconi patented the first complete wireless telegraph system [87], usage of wireless communication services has experienced an explosive growth. Wireless communications can be based on either satellite technology or cellular technology. However, with the demise of Iridium and other satellite-based companies, the consumer market is clearly in favor of cellular-based wireless communication systems. The number of global cellular subscribers has grown from 10 million in early 1990's to approximately 700 million nowadays. This cellular user population is projected to grow to 2 billion by 2007 [66]. Cellular communication devices are not just convenient communication tools, they are also becoming increasingly important in search and rescue operations, and extremely useful in many emergency situations.

1

When a radio signal is transmitted, the signal strength is subject to attenuation or loss over the transmission path. Signal attenuation is inversely proportional to the distance it travels. The path loss exponent typically takes values of 2-5 depending on the environment. In addition to path loss, the transmitted signal is also subject to shadowing, which is caused by topographical variations such as trees and buildings along the transmission path. In shadowing, the mean received signal strength experiences randomness. The lognormal distribution is typically used to describe this randomness in the received signal power. Path loss is a large scale variation of signal power, possibly over several kilometers in radius. Shadowing is a more local view of the signal power variation, typically over several hundreds of wavelengths. From a smaller scale view, the transmitted radio signal is also subject to multipath fading, signal power variation over a distance of several wavelengths. In addition to fading, the signal can also be corrupted by other user interference. The cause of multipath fading is due to multipath propagation and the cause of other user interference is due to radio frequency reuse and multiple access interference. Since fading and interference are ubiquitous in many wireless systems, we will describe them in more detail in the next section.

1.2   Transmission Environment

In this section, we briefly describe fading and interference, which are two main sources of system performance degradation in any mature cellular system. Section 1.2.1 introduces four basic types of fading channels and reviews some theoretical origins of three useful fading models. In this subsection, we restrict our attention to the first-order statistics for the fading channels. In this thesis, we do not consider the second-order fading statistics; however, they are also of practical importance in certain transmission environment. Section 1.2.2 introduces basic concepts of cellular system. Both cochannel interference and multiple access interference are defined. Three important multiple access schemes are also characterized.

2

1.2.1 Multipath Fading

The wireless channel is a result of random propagation of radio waves; therefore, modeling the wireless channel is typically done in a statistical fashion. Due to ground irregularities, typical wave propagation phenomena such as diffraction, scattering, and reflection lead to diffusion of a transmitted radio wave into a continuum of plane waves with different amplitudes and phases. At the receiver antenna, these incident waves are added up constructively and destructively causing multipath fading, or fading in short. Fading captures the rapid fluctuation of amplitude and phase in a radio signal over a short period of time or distance, typically between a fraction of a wavelength and several wavelengths. Depending on the relative relation between parameters of transmitted signal (i.e., signal bandwidth and symbol period) and parameters of fading channels (i.e., delay spread and Doppler spread), fading channels can be classified into four types: fast frequency-nonselective fading, slow frequency-nonselective fading, fast frequency-selective fading, and slow frequency-selective fading. In the following, we will briefly describe these four basic types of fading.

Delay spread is a parameter which describes the time dispersive nature of the fading channel. The reciprocal of the delay spread is called *coherence bandwidth*. The coherence bandwidth is the range of frequencies over which two frequency components are strongly correlated. If the signal bandwidth is small in comparison with the coherence bandwidth, the channel is said to be frequency-nonselective, or often called *flat* fading. For a frequency-nonselective channel, the frequency components of the transmitted signal undergo the same attenuation and the same phase shift. Therefore, the multipath components are not resolvable in frequency-nonselective fading. On the other hand, if the signal bandwidth is large in comparison with the coherence bandwidth, the channel is said to be frequency-selective. For a frequency-selective channel, the frequency components of the transmitted signal are subject to different gains and different phase shifts. In frequency-selective fading, the received signal are resolvable with resolution commonly defined as the reciprocal of the signal bandwidth. A tapped delay line filter with time-variant tap coefficients is commonly used to model a frequency-selective channel.

3

Doppler spread is a parameter which describes the frequency dispersive nature of a fading channel. The reciprocal of Doppler spread is called *coherence time*. The coherence time is the time duration over which the channel impulse response is essentially time-invariant. If the symbol duration is large in comparison with the coherence time, the channel is said to be *fast* (or called time-selective). On the other hand, if the symbol duration is small in comparison with the coherence time, the channel is said to be slow (or called time-nonselective).

Therefore, delay spread leads to time dispersion and Doppler spread leads to frequency dispersion. These two propagation mechanisms are independent of each other; therefore, as a result, we have four types of fading channels.

In this thesis, we focus on the error analysis of digital systems in slow and flat fading channels. When a signal $s_t(t)$ is transmitted over a flat fading channel, the received signal $s_r(t)$ is given by (neglecting the background noise)

$$s_r(t) = \alpha(t)s_t(t) \tag{1.1}$$

where the complex-valued random process $\alpha(t)$ represents the time-variant characteristics of the fading channel. This fading process is usually assumed to be wide-sense stationary. If the channel is further assumed to be slow, we can replace the random process $\alpha(t)$ by the random variable (RV) α (since $\alpha(t)$ is essentially time-invariant over one symbol duration). A number of statistical models are commonly used to describe the fading amplitude α. The well known models are Rayleigh, Rician, and Nakagami-m. In the following, we will briefly review some theoretical origins of these fading models.

Clarke first developed a model based on statistical characteristics of the received signals using an electromagnetic field representation [18]. Clarke's model assumes a stationary transmitter and a moving mobile. The field incident on the mobile antenna consists of N plane waves, each having equal average amplitude. The z component of the electrical field, denoted by E_z, can be expressed as

$$E_z = \sum_{i=1}^{N} E_i e^{j\phi_i} = Re^{j\theta} = X + jY \tag{1.2}$$

4

where E_i and ϕ_i respectively represent the amplitude and the phase of the ith arriving wave. The distributions of the phases are assumed to be uniform over $[0, 2\pi)$. The random quantities $E_1, E_2, \ldots, E_N; \phi_1, \phi_2, \ldots, \phi_N$ are further assumed to be uncorrelated. When N is sufficiently large, using a Central Limit Theorem (CLT), E_z can be approximated as a complex Gaussian RV, where the real and imaginary components, denoted by X and Y respectively, are Gaussian RV's with means and variances given by

$$\mathbb{E}[X] = \mathbb{E}[Y] = 0; \quad \sigma_x^2 = \sigma_y^2 = \frac{\Omega}{2}, \tag{1.3}$$

and furthermore, $\mathbb{E}[XY] = 0$. The envelope R therefore follows a Rayleigh distribution with probability density function (PDF) given by

$$f_R(r) = \frac{2r}{\Omega} e^{-\frac{r^2}{\Omega}}, \quad r \geq 0 \tag{1.4}$$

where $\mathbb{E}[R^2] = \Omega$. The phase distribution of Rayleigh fading is uniform and the phase is independent of the fading envelope R. The Rayleigh distribution is often observed in an urban transmission environment where there is no line-of-sight (LOS) transmission. If there is a LOS component between the transmitter and the receiver, the envelope R has a Rician distribution. The PDF of Rician is given by

$$f_R(r) = \frac{2r(\mathcal{K}+1)}{\Omega} \exp\left\{-\mathcal{K} - \frac{(\mathcal{K}+1)r^2}{\Omega}\right\} I_0\left(2r\sqrt{\frac{\mathcal{K}(\mathcal{K}+1)}{\Omega}}\right), \quad r \geq 0 \tag{1.5}$$

where $I_0(\cdot)$ is the 0th order modified Bessel function of the first kind [3], and where the parameter $\mathcal{K}$, also known as Rician factor, is defined as

$$\mathcal{K} = \frac{\text{power in line-of-sight component}}{\text{power in scatter component}}. \tag{1.6}$$

When $\mathcal{K} = 0$ (the line-of-sight component vanishes), the Rician distribution degenerates to a Rayleigh distribution. Unlike Rayleigh fading, the envelope and phase of Rician fading are no longer independent. The phase distribution of Rician fading is known and it takes a complicated form. Rician fading is often observed in microcellular and mobile satellite applications.

Another fading model, perhaps more important, is the Nakagami-m fading, which also describes LOS transmission environments. The original work by Nakagami was first documented in Japanese

5

and its English translation didn't appear until 1960 [57]. The Nakagami-m distribution is important because this fading model is deduced directly from fading measurements. Numerous claims have been made, for example in [73], that this fading model fits empirical fading measurements better than the other distributions. The Nakagami-m distribution can be derived under the most general mathematical conditions for the incident waves. To find the distribution of the fading envelope R, we make no assumptions on the joint distribution of $E_1, E_2, \ldots, E_N; \phi_1, \phi_2, \ldots, \phi_N$. Let $\eta = |\sum_{i=1}^{N} E_i e^{j\phi_i}|$ be a positive function of complex RV's $E_1 e^{j\phi_1}, E_2 e^{j\phi_2}, \ldots, E_N e^{j\phi_N}$, the PDF of the fading envelope can be written as

$$f_R(r) = \mathbb{E}_\eta [\delta(r - \eta)] \tag{1.7}$$

where $\delta(\cdot)$ is the Dirac delta function which can be written in terms of Hankel transformation as [80], [57]

$$\delta(r - \eta) = r^{\nu+1} \int_0^{+\infty} \lambda \frac{J_\nu(\lambda r) J_\nu(\lambda \eta)}{\eta^\nu} d\lambda \tag{1.8}$$

where $J_\nu(\cdot)$ is the Bessel function of arbitrary complex order ν with $\mathrm{Re}(\nu) \geq 1/2$. Substitution of (1.8) into (1.7) yields

$$f_R(r) = \frac{r^{\nu+1}}{2^\nu \Gamma(\nu+1)} \int_0^{+\infty} \lambda^{\nu+1} J_\nu(\lambda r) F_\nu(\lambda) d\lambda \tag{1.9}$$

where $\Gamma(\cdot)$ is the Gamma function [3] and

$$F_\nu(\lambda) = 2^\nu \Gamma(\nu+1) \mathbb{E}_\eta \left[\frac{J_\nu(\lambda \eta)}{\lambda^\nu \eta^\nu} \right] \tag{1.10}$$

or

$$F_\nu(\lambda) = \Gamma(\nu+1) \sum_{i=0}^{+\infty} \frac{(-1)^i (\frac{\lambda}{2})^{2i} \mathbb{E}[\eta^{2i}]}{i! \Gamma(\nu+i+1)} \tag{1.11}$$

if the power series expansion is used for the Bessel function. Define

$$m = \frac{(\mathbb{E}[\eta^2])^2}{\mathbb{E}[(\eta^2 - \mathbb{E}[\eta^2])^2]} \tag{1.12}$$

and choose $\nu = m - 1$, we can approximate $F_\nu(\lambda)$ as [1]

$$F_\nu(\lambda) \approx \exp\left(-\frac{\Omega}{4m} \lambda^2 \right). \tag{1.13}$$

---

[1] This approximation becomes exact when both X^2 and Y^2 in $X + jY$ are chi-square distribution with m degrees of freedom and with the PDF $f_Z(z) = \left(\frac{m}{\Omega}\right)^{m/2} \frac{z^{m/2-1}}{\Gamma(m/2)} e^{-\frac{m}{\Omega} z}$.

6
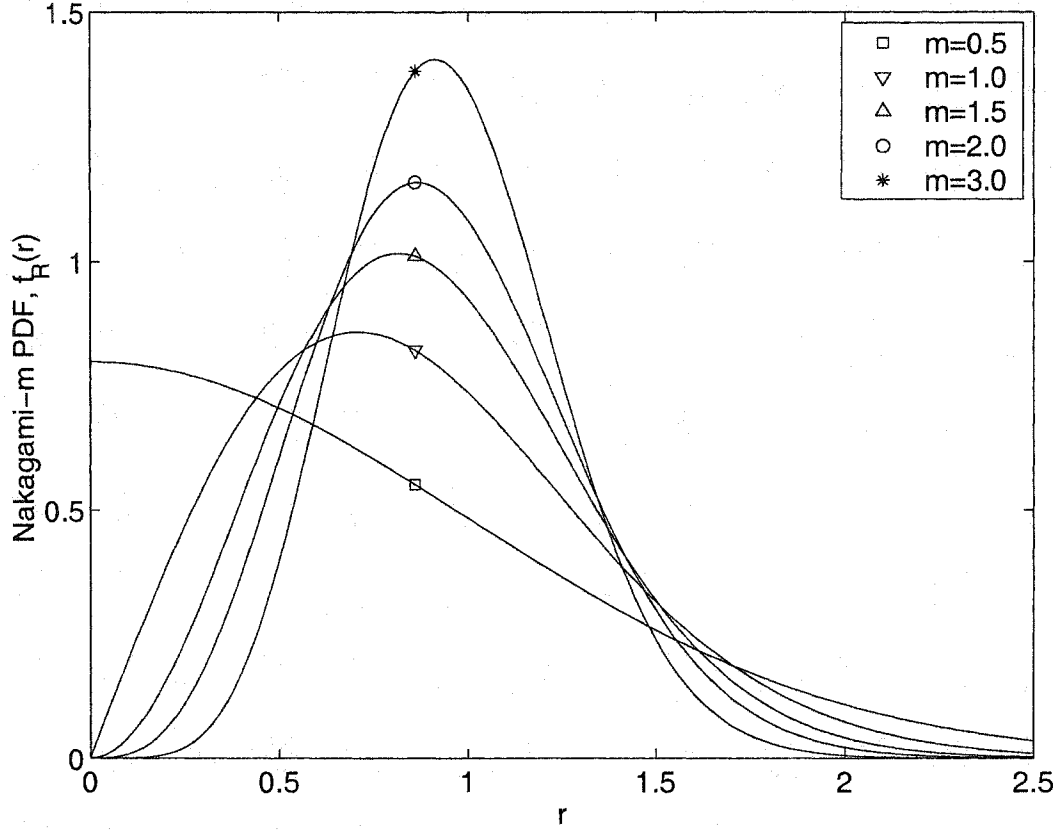
Figure 1.1. Probability density function of Nakagami-m with $\Omega = 1$.

Combining (1.13) and (1.9), we obtain

$$
\begin{aligned}
f_R(r) &\approx \frac{r^m}{2^{m-1}\Gamma(m)} \int_0^{+\infty} \lambda^m J_{m-1}(\lambda r) \exp\left(-\frac{\Omega}{4m}\lambda^2\right) d\lambda \\
&= \frac{2}{\Gamma(m)} \left(\frac{m}{\Omega}\right)^m r^{2m-1} \exp\left(-\frac{m}{\Omega}r^2\right), \quad r \geq 0, \quad m \geq \frac{1}{2}
\end{aligned}
\tag{1.14}
$$

which is the PDF of the Nakagami-m distribution, and m is called the fading parameter. Similar to

the $\mathcal{K}$ factor in Rician distribution, the fading parameter m controls fading severity, and as a result,

the Nakagami model covers a wide range of distributions. These include one-sided Gaussian ($m =$

$1/2$) and Rayleigh ($m = 1$) as special cases. In the limit, when m approaches $+\infty$, the Nakagami-m

distribution approaches an impulsive function corresponding to a static (non-fading) channel. The

PDF of Nakagami-m is plotted in Figure 1.1 for a selected values of m.

The Nakagami-m model is also of theoretical interest since analysis of digital communication

7

systems in Nakagami-m fading often leads to closed-form analytical solutions for important performance measures such as signal outage probability and symbol error rate. Despite its popularity, Nakagami fading is still not well understood at a fundamental level. For example, the phase distribution of the Nakagami-m fading process is not known.

The Nakagami-m is also related to some familiar distributions. For example, if $X = R^2$, where R is Nakagami-distributed according to (1.14), the PDF of X can be found as

$$f_X(x) = \left(\frac{m}{\Omega}\right)^m \frac{x^{m-1}}{\Gamma(m)} \exp\left\{-\frac{m}{\Omega}x\right\} \tag{1.15}$$

which is the PDF of Gamma [70]. After a normalization $G = (m/\Omega)X$, we obtain a familiar form for the PDF of one-parameter Gamma RV as

$$f_G(g) = \frac{g^{m-1}e^{-g}}{\Gamma(m)}, \quad g \geq 0. \tag{1.16}$$

As another example, if we set $m = n/2$ (n is an integer) and $\Omega = n\sigma^2$ in (1.14), after rearrangements, we have

$$f_R(r) = \frac{r^{n-1}}{2^{(n-1)/2}\sigma^n\Gamma(n/2)} \exp\left\{-\frac{r^2}{2\sigma^2}\right\} \tag{1.17}$$

which is the generalized Rayleigh distribution with n degrees of freedom [63].

In order to use a single number to provide a meaningful measure of fading severity for an arbitrary fading distribution, Charash coined the phrase "amount of fading" (AF) [2] in [10]. With his definition, for a fading distribution R, the AF is given by

$$AF = \frac{\text{var}[R^2]}{(\mathbb{E}[R^2])^2}. \tag{1.18}$$

The AF's for aforementioned three fading distributions are tabulated in Table 1.1 according to [68]. The AF is, in general, independent of the average fading power due to the normalization process in (1.18).

---

[2]In his pioneering work, Nakagami used the term fading figure (FF) for AF because m is inversely proportional to the fading range [57]. For this historical reason, we will use the terms AF and FF interchangeably in this thesis.

8

Table 1.1. Amount of fading for Rayleigh, Rician, and Nakagami-m fading distributions.

Fading Type	AF
Rayleigh	1
Rician ($\mathscr{K}$)	$\frac{1+2\mathscr{K}}{(1+\mathscr{K})^2}$
Nakagami-m (m)	$\frac{1}{m}$, $m > \frac{1}{2}$

1.2.2 Interference

Spectrum is a precious resource as well as a commodity. The most challenging problem for wireless communication system design engineers is to achieve the maximum spectral efficiency and to accommodate increasing number of users while maintaining minimum quality of service (QoS). The cellular concept is a breakthrough in solving the spectral congestion problem and user capacity problem. The cellular concepts are introduced in an early paper by MacDonald [51]. The basic idea of cellular communication is first to divide the target coverage area into cells. Each cell is allocated a portion of the total number of channels available to the entire system. Different sets of channels are assigned to adjacent cells and the same set of channels are reused in different cells that are separated sufficiently apart. Fig. 1.2 illustrates the layout of a typical cellular system where the cells labeled with the same letters use the same set of frequencies (channels). These cells are called *cochannel cells*. Therefore, a (desired) mobile user signal is subject to the corruption of the interference generated by other (undesired) users' signals in the cochannel cells operating at the same carrier frequency. This kind of interference is called *cochannel interference*. To accommodate increasing number of users, the cell sizes are often reduced (a microcellular environment) in order to meet this capacity demand. As a result, the radio link performance in a microcellular system is limited dominantly by cochannel interference rather than thermal noise. With advances in low-noise receiver technology, thermal noise plays secondary role in causing the system performance degradations.

9
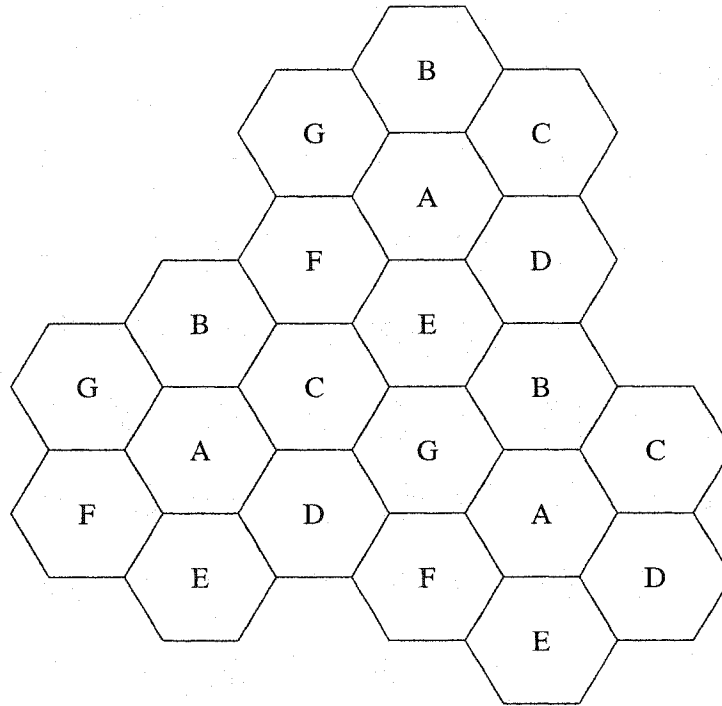
Figure 1.2. A two-tier cell layout with hexagon cell shape to illustrate the concept of frequency reuse.

In cellular systems, multiple access schemes are used to allow many mobile users to share a finite amount of radio spectrum simultaneously. Frequency division multiple access (FDMA), time division multiple access (TDMA) and code division multiple access (CDMA) are the three major competing access techniques. FDMA assigns an individual channel in a frequency slot to each user while TDMA assigns an individual channel in a time slot to each user. Therefore, these two multiple access schemes provide orthogonal transmission in frequency or time. In CDMA, the orthogonality (or quasi-orthogonality) is achieved by spreading the user signals with pseudo-noise (PN) chip sequences, or codes. Since a great number of such sequences can be available, they can be assigned to a large number of potential users and the goal of having a high capacity system can be achieved.

The principle of CDMA is based on the spread spectrum (SS) technology which has been successfully employed in military applications for decades. In a CDMA system, each user's data symbol is modulated (spread) with a much faster changing signature signal over a large bandwidth than

10

what's required for reliable transmission. In addition, all users in the system are occupying the same bandwidth at the same time. By correlating the received signal at the base station with each user's known signature signal, the original data can be recovered for each user. Unlike FDMA or TDMA systems in which the system capacity is a hard number, the capacity of a CDMA system is often described as a soft number. This is because, in addition to the hostile transmission environment, a CDMA system is mainly limited by interference from other users, which is termed multiple access interference (MAI). Hence, it is possible to continue adding additional users at the cost of performance degradation for the existing users. In theory, FDMA, TDMA and CDMA techniques all have the same capacity. However, in a cellular system, we might find that CDMA has some particular advantages over FDMA and TDMA [44]. The principle use of SS for mobile communication systems are described by Pickholtz, Milstein and Schilling [61]. In the same paper, the authors also present the concept of CDMA overlay with existing narrowband systems as well as the concept of narrowband interference rejection in wideband systems. A tutorial article by Flikkema introduces the use of SS for wireless applications from signal processing perspectives [25]. Lee [44] and Gilhousen *et al.* [32] give good introductions to the concept of cellular CDMA and illustrate how this multiple access scheme can be more suitable for the cellular environment than are FDMA and TDMA in terms of higher user capacity. In addition to achieving high system capacity and providing multiple access, CDMA is also well-known for its capabilities to combat multi-path interference and to provide secure communication.

There are two principle forms of CDMA, namely, direct-sequence (DS) and frequency-hopped (FH) CDMA. The DS-CDMA system achieves the bandwidth spreading by using the PN sequences to introduce rapid phase transitions into the carrier containing the data, while FH-CDMA achieves the bandwidth spreading by using the PN sequences to pseudo-randomly hop carrier frequency throughout a large band. A DS-CDMA system is more popular in commercial applications while a FH-CDMA is widely used for military applications. Comprehensive comparisons between the two spreading techniques are outlined in a book by Stüber [70].

This thesis deals with, in part, the system performance for a DS-CDMA cellular system in fading

11

channels using a conventional single-user matched filter receiver and aperiodic random spreading sequences. The matched filter receiver structure is known to be sub-optimal compared to the optimal multi-user receivers described in [78]. However, the optimal multi-user receiver is impractical in a sense that the system complexity increases exponentially with the number of users. Numerous sub-optimal multi-user receivers described in [79] are being proposed for future standards but they require specific knowledge of the signature sequences of the other users, exact timing offsets of all transmitters, and periodicity in spreading sequences. On the other hand, a single-user matched filter receiver doesn't require any of the aforementioned knowledge required by various sub-optimal multi-user receivers. Thus, it is simple and economical.

1.3   Thesis Outline and Contributions

This thesis consists of four major chapters. Each chapter corresponds to one major contribution. At the beginning of each chapter, we review, in detail, some background and literature which are most relevant to the subject of that chapter.

In Chapter 2, we analyze a generic binary phase shift keying (BPSK) DS-CDMA system for Rayleigh-faded users using random spreading sequences under both synchronous and asynchronous operations. The receiver we assume is a single-user correlator receiver. The goal here is to obtain a tractable analytical average bit error rate (BER) expression without making any assumptions on the distribution of the multiple access interference. To do so, we first review a well-known decision statistic for random spreading sequences. Using rigorous probability arguments, we derive a simplified form of the decision statistic. Closed-form expressions are derived for the characteristic function (CF) of the multiple access interference based on both known form and simplified form of the decision statistic. We examine, in detail, the BER dependence on the number of active users in the system for a given signal-to-noise (SNR). A single integral expression is given for the overall average BER and the integrand is shown to be positive and well behaved. Using this expression, we can calculate the average BER to any desired accuracy with modest computational complexity. The

12

BER expression based on the simplified decision statistic is, in particular, capable of analyzing a system with large processing gain. The dependence of the system BER on the number of transitions in the target user signature chip sequence is explicitly derived. Using our newly derived accurate analytical expressions, we also assess the accuracies of several Gaussian approximation methods. It is found that for a Rayleigh-faded environment, even the simplest form of Gaussian approximation can give accurate BER estimates for a system with processing gain of 255 and for a small number of users. Monte Carlo simulations are used to verify our analysis. It is shown that the simulation results are in excellent agreement with the analytical results.

In Chapter 3, we consider the error analysis of a bandwidth efficient BPSK in a TDMA-based microcellular environment. We assume a general Nakagami/Nakagami fading and interference model and derive a precise BER expression for a BPSK modulated signal in fading and cochannel interference environment. Our results are applicable to practical systems since the BER expression takes account arbitrary pulse shaping, symbol timing asynchronism among the active users, as well as cross-signal intersymbol interference caused by each interfering user signal on the desired user signal. We use a characteristic function method, a frequency domain approach, to derive an exact expression for the overall average BER. In doing so, we derive closed-form expressions for the PDF and the CF for the Nakagami fading quadrature components in terms of a pair of Kummer functions. Two Nyquist pulses are considered in this work. One is the popular raised-cosine pulse and the other is a recently proposed novel pulse. We show, for the first time, both analytically and numerically that this new novel pulse shape outperforms the widely used raised-cosine pulse shape in microcellular cochannel interference environment. We demonstrate that at BER $= 10^{-6}$ the novel pulse can achieve about 0.86 dB savings in SNR over the traditional pulse at no extra cost. Our analytical BER results, which are confirmed with Monte Carlo simulations, are also used to show that fading of an interfering signal worsens the BER of the desired signal rather than improving it, a result perhaps contrary to what one's initial thinking. We use convexity property of the Q-function to explain this phenomenon. Finally, we use our precise BER results to assess the accuracy of a Gaussian approximation.

13

In Chapter 4, we extend the results in Chapter 2 to a Nakagami-m flat fading channel. Specifically, we obtain a closed-form expression for the characteristic function of the MAI. An exact single integral BER expression is developed for an asynchronous BPSK DS-CDMA system using random spreading sequences in Nakagami-m fading. The accurate BER results are used to assess the accuracy of the standard Gaussian approximation. It is found that the standard Gaussian approximation is poor for a small number of users in a lightly faded channel.

In Chapter 5, we study estimation of the Nakagami-m fading parameters, in particular, estimation of the m parameter. The Cramér-Rao lower bounds are first derived. Both the maximum-likelihood (ML) method and moment method are considered for this parameter estimation problem. We propose two approximate ML-based estimators based on the asymptotic expansion of the digamma function. We study in detail the properties of a parameter closely associated with these ML estimators. In doing so, we show that the Nakagami-m distribution is a member of two-parameter exponential family, and as a consequence, we obtain the complete sufficient statistics of the fading parameters. Most of previous research in parameter estimation has concentrated primarily on the maximum-likelihood approach and the method of moment approach has received less attention. In this chapter, we propose a family of new moment estimators based on a family of new definitions of m parameter using both integer and non-integer moments. Our new class of moment estimators is general since it contains previous known moment estimators as special cases. A limiting case of this family is particularly of interest, owing to its simplicity in implementation as well as near-ML performance. The derivation of this limiting estimator also leads us to discover a new compact definition of the Nakagami m parameter in terms of a function of the covariance of the instantaneous fading power and its value in dB. We also carry out an asymptotic study of our new moment estimators. Using the multivariate delta method drawn from large-sample theory, we obtain closed-form expressions for the asymptotic variances for this class of estimators. Based on these analytical results, we conclude that the limiting case of this class of moment estimators is almost fully efficient asymptotically. Finally, we use Monte Carlo simulation to study the finite-sample performances of our proposed estimators and compare them to that of Greenwood-Durand estimator (GDE).

14

Chapter 6 concludes this thesis by outlining major findings of this thesis. Future work is also suggested.

15

Chapter 2

Accurate DS-CDMA BER Calculation in Flat Rayleigh Fading

2.1 Introduction

It is well-known that spread spectrum multiple access (SSMA) has the ability to combat multi-path interference, increase system capacity, and improve quality of service. Much work has been reported on the calculation of the user average BER for direct sequence - code division multiple access (DS-CDMA) systems. Two approaches for DS-CDMA, operating on additive white Gaussian noise channels, have been widely reported.

The first approach presumes that exact BER evaluation is intractable or numerically cumbersome, so accurate BER approximations are sought [64], [7], [26], [56], [38], [53], [54], [76], [49], [11], [55]. Perhaps the most widely cited and most widely used approximation is the so-called standard Gaussian approximation (SGA) first proposed by Pursley [64]. In the SGA, a central limit theorem is employed to approximate the sum of the multiple access interference (MAI) signals as an additive white Gaussian process additional to the background Gaussian noise process. The receiver design, thus, consists of a conventional single-user matched filter (correlation receiver) to detect the desired user signal. The variance of the MAI averaged over all possible operating conditions is used to compute the signal-to-noise ratio (SNR) at the filter (correlator) output. The SGA is widely

16

used because it is easy to apply; however, it was shown by Morrow and Lehnert that performance analyses based on using the SGA often overestimate the system performance, especially when the number of users in the system is small [56]. These limitations have motivated research to improve the accuracy of the SGA. In [49], Long *et al.* improved the accuracy of the SGA using the standard Hermite polynomial error correction method. In [47], Lehnert and Pursley studied extensively the statistics of the MAI signals with random signature sequences. Based on the work of [47], Morrow and Lehnert [56] later introduced a method termed improved Gaussian approximation (IGA). The IGA is more accurate than the SGA, especially for a small number of active users [56]. However, the IGA computation requires numerical integration and multiple numerical convolutions. This method was simplified in [38] by Holtzman such that neither knowledge of the conditional variance distribution, nor numerical integration, nor convolution is necessary to achieve acceptable BER estimation. Thus, it is termed simplified improved Gaussian approximation (SIGA) [38]. More recently, Morrow [55] further simplified the expression attained in [38] without significant penalty in the BER accuracy.

The second approach is to perform the evaluation of the SS multiple access system BER without knowledge of, or assumptions about the MAI distribution. Many of these techniques are based on extensions of previous studies of inter-symbol interference (ISI) systems. These methods include the moment space technique [83], characteristic function method [30], method of moments [40], [82], and an approximate Fourier series method [71], [72]. Generally, these techniques can achieve more accurate BER estimate than CLT based approximations at the expense of much higher computational complexity.

Fewer results exist for BER's of DS-CDMA systems operating in Rayleigh fading channels and employing *random* sequences. System performance analysis employing random sequences often leads to tractable results. Besides this attractive mathematical feature, there are other important reasons for random sequences to be used for SSMA system performance evaluation. First, random sequences can be used to describe some complex characteristics of some practical sequences which

17

have very long periods. Over a few data symbols, these long codes behave pseudo-randomly. Second, when the communication engineer is given little or no knowledge of the sequences to be used, random sequence can be considered a good substitute. Finally, computational complexity of the exact SSMA performance analysis can be prohibitive for a large number of users using deterministic sequences, while random sequences do not suffer this shortcoming. In this work, we provide a new accurate, yet tractable BER calculation solution for a binary DS-CDMA system operating in slowly fading Rayleigh channels with random sequences. Our treatment of the subject furthers the work reported in [56], [47], [30], [29].

Previous related work includes the following. Borth and Pursley [7] studied the SNR at the output of a correlator receiver for Rician fading channels. The performance of a DS-CDMA system in a frequency non-selective Rayleigh fading channel was evaluated by Gardner and Orr [26] for deterministic sequences using the SGA. In [30], Geraniotis and Pursley used the characteristic function method to evaluate SSMA system performance in an additive white Gaussian noise channel. Later, Geraniotis [28] extended this technique to frequency non-selective and selective Rician fading channels for deterministic sequences. In [27], the characteristic function method was used in studying the performance of DS-SS systems on specular multipath fading channels with multipath ISI; however, MAI was not considered in this work. More recently, Liu *et al.* proposed a low-complexity characteristic function method to evaluate binary and quaternary DS-SSMA over flat Rican channels using deterministic signature sequences [48]. In [71] and [72], Sunay and McLane used an approximate Fourier series method to study BER performance under both frequency non-selective and selective Rayleigh fading. Additionally, the system degradations due to imperfect chip and phase synchronization were assessed.

The contributions of this work are as follows. We analyze a generic DS-CDMA system with Rayleigh-distributed users under both synchronous and asynchronous operations for random sequences. We examine in detail the BER dependence on the number of active users in the system for a given SNR. For asynchronous operation, we provide an explicit closed-form expression for the characteristic function of the MAI. A single integral expression is given for the overall BER and the

18

integrand is shown to be positive and well-behaved. With this expression, we can calculate the BER to any desired accuracy and with minimal computational complexity. The IGA and SIGA methods are extended to a fading channel system. Numerical results obtained from our accurate method are used to assess the accuracies of the SGA and SIGA for Rayleigh fading channels. Accurate comparisons of the performances of asynchronous and synchronous systems operating in Rayleigh fading are made using our new solution.

The remainder of this chapter is organized as follows. In Section 2.2, we introduce the system and channel models. Review of the important properties of the receiver decision statistic for random sequences is provided in Section 2.3 for completeness. In this section, we also derive a simplified form of the decision statistic. This form of decision statistic is suitable for calculating the average BER for a system with a large processing gain. The SGA, IGA, and SIGA for a Rayleigh fading channel are examined in Section 2.4. System performance evaluations for synchronous and asynchronous operations are presented in Sections 2.5 and 2.6, respectively. Numerical results and discussions are provided in Section 2.7. In Section 2.8, we summarize our chapter results.

2.2 System and Channel Models

The spread spectrum multiple access system model for our study is shown in Fig. 2.1. We consider a general asynchronous binary direct sequence system which supports K active users. More specifically, we study the system performance under the reverse link (mobiles to basestation) assumption. The kth transmitted signal is described by

$$s_k(t) = \sqrt{2P_k}b_k(t)a_k(t)\cos(\omega_c t + \theta_k) \tag{2.1}$$

where P_k represents the transmitted signal power, $b_k(t)$ is the data signal, $a_k(t)$ is the spreading signal, ω_c is the carrier frequency and θ_k is the carrier phase. The kth user's data signal, $b_k(t)$, is a random process which is a rectangular waveform, taking values from $\{-1, +1\}$ with service rate

$R_s = 1/T$ and it is expressed as

$$b_k(t) = \sum_{j=-\infty}^{+\infty} b_j^{(k)} P_T(t - jT) \tag{2.2}$$

where $P_T(t) = 1$ for $0 \leq t < T$, and $P_T(t) = 0$, otherwise. The jth data bit of the kth user is denoted as $b_j^{(k)}$. Data sources are assumed uniform, i.e., $\Pr\{b_j^{(k)} = +1\} = \Pr\{b_j^{(k)} = -1\} = 1/2$. The spreading signal, $a_k(t)$, can be expressed as

$$a_k(t) = \sum_{l=-\infty}^{+\infty} a_l^{(k)} \psi(t - lT_c) \tag{2.3}$$

where $\psi(t)$ is an arbitrary chip waveform which is time-limited to $[0, T_c)$ and T_c is the chip duration. It is convenient, and entails no loss of generality, to normalize the energy of the chip waveform $\psi(t)$ to

$$\int_0^{T_c} \psi^2(t) dt = T_c . \tag{2.4}$$

The lth chip of the kth user is denoted by $a_l^{(k)}$ which assumes values from $\{-1, +1\}$. All signature sequences, $\{a_l^{(k)}\}$, are assumed to be random in the following sense. Every chip polarity is determined by flipping an unbiased coin . There are G chips per data symbol and the period of the sequence is G [1] We further normalize the chip duration so that $T_c = 1$ and, thus, $T = G$. Note that if the chip waveform is rectangular, i.e., $a_k(t) = \sum_{j=-\infty}^{+\infty} a_j^{(k)} P_{T_c}(t - jT_c)$, the transmitted signal, $s_k(t)$, becomes the well-known phased-coded SS model [64]. In this thesis, we will only concentrate on rectangular chip waveform. SSMA performance analysis for other chip waveforms has recently been considered in [58] and [85].

Each signal, $s_k(t)$, is transmitted over a frequency non-selective fading channel where the user signal and the interfering signals all experience mutually independent Rayleigh fading. The fading is also assumed to be slow such that coherent detection is feasible. This channel model is widely used in system design and performance studies for DS-CDMA systems [53], [76], [11], [79]. It is also a special case of the indoor wireless channel model studied in [40]. In frequency non-selective fading,

---

[1] It can be shown in Appendix A that the periodic condition of the random sequence can be removed without affecting the decision statistic presented in the sequel. Therefore, our assumption, made for analytical simplicity, is realistic for long codes (sequence of period much longer than the duration of data symbol) often employed in practical systems.

20
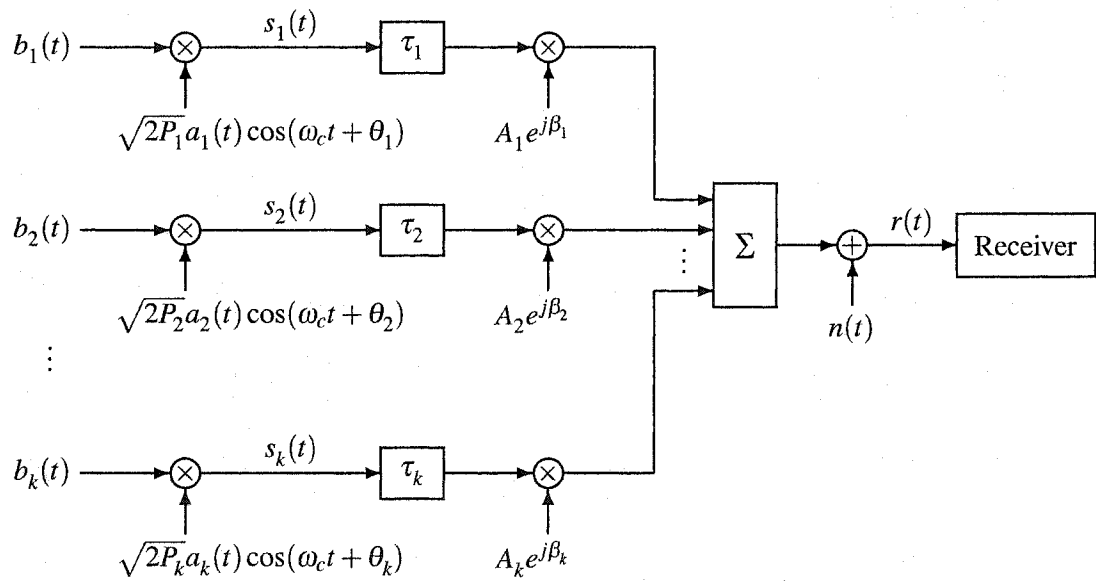
Figure 2.1. A DS-CDMA/SSMA system model.

21

the spread bandwidth of the signal is smaller than the coherence bandwidth of the channel. This assumption, which is typically incorrect for a large spread signal, is made for two reasons; one is analytical simplicity, and the other is that the flat fading model can lead to a worst case performance prediction since in practice a RAKE receiver is commonly used to exploit the multipath fading.

The channel impulse response for the kth transmitted signal is given by

$$h_k(t) = A_k e^{j\beta_k} \delta(t - \tau_k) \tag{2.5}$$

where the fading random variables $\{A_k\}_{k=1}^K$ are independent, Rayleigh-distributed and account for the fading channel attenuation of all signals. Each RV, A_k, represents the envelope of a complex Gaussian process with unit variance in each quadrature component. The first-order probability density function of A_k is given by

$$f_{A_k}(a) = a e^{-\frac{a^2}{2}} I_{[0,+\infty)}(a) \tag{2.6}$$

such that $\mathbb{E}[A_k^2] = 2$. Here, $I_A(x)$ is the indicator function whose value is 1 when $x \in A$ and 0 otherwise. In (2.5), $\{\beta_k\}_{k=1}^K$ are the phases introduced by the fading channel and are assumed uniform over $[0, 2\pi)$ and independent. The random variables $\{\tau_k\}_{k=1}^K$ represent time delays and account for the lack of time coordinations (asynchronism) among the K transmitters as well as the channel transmission delays. These time delays are random variables assumed uniform over $[0, T)$ and independent. The transmitted signal is further assumed to experience an additive background noise process $n(t)$, which is characterized as a zero-mean, stationary white Gaussian process with two-sided power spectral density $N_0/2$ (Watt/Hz). Note that setting $A_k = 1, k = 1, \ldots, K$ in (2.5) results in an AWGN transmission model with randomly phased signals.

The received signal $r(t)$ at the input of the matched filter receiver is given by

$$
\begin{aligned}
r(t) &= \sum_{k=1}^K s_k(t) * h_k(t) + n(t) \\
&= \sum_{k=1}^K \sqrt{2P_k} A_k b_k(t - \tau_k) a_k(t - \tau_k) \cos(\omega_c t + \phi_k) + n(t)
\end{aligned}
\tag{2.7}
$$

where $*$ denotes convolution and $\phi_k = \beta_k + \theta_k - w_c \tau_k$ is assumed a uniform random variable over $[0, 2\pi)$. The average received power of the kth signal is $\mathbb{E}[A_k^2] P_k$. For simplicity, we assume all

22

transmitted signals have the same transmitted power [2] and set this value to 2, i.e., $P_1 = P_2 = \cdots = P_k = 2$. Under our assumption, on average the received signal power at the basestation for each active user is the same and this power control scheme is sometimes referred as the average power control [65].

Since all the aforementioned random variables are generated from different physical sources, we assume the random variables $\left\{ \{A_k\}_{k=1}^K; \{\phi_k\}_{k=1}^K; \{(b_j^{(k)})\}_{k=1}^K; \{(a_j^{(k)})\}_{k=1}^K \right\}$ are mutually independent.

A synchronous system model is obtained when $\tau_k \ (\mathrm{mod}\ T) = 0, k = 1, \ldots, K$ in (2.7). All other assumptions remain the same as for the asynchronous system model.

2.3 Receiver Decision Statistic

Consider using a conventional single-user matched filter receiver to coherently demodulate the desired user signal in an asynchronous system. The average bit error rate is the same for all users by symmetry. We assume, without loss of generality, that the target user signal has index $k = 1$ and $\tau_1 = \phi_1 = 0$. After despreading, the output of the demodulator is

$$
\begin{aligned}
Z_1' &= \int_0^T r(t) a_1(t) \cos(\omega_c t) dt \\
&= \int_0^T \left(\sum_{k=1}^K 2 A_k b_k(t - \tau_k) a_k(t - \tau_k) \cos(\omega_c t + \phi_k) + n(t) \right) a_1(t) \cos(\omega_c t) dt \\
&= \int_0^T A_1 b_1(t) [\cos(0) + \cos(2\omega_c t)] dt \\
&\quad + \sum_{k=2}^K A_k \int_0^T b_k(t - \tau_k) a_k(t - \tau_k) a_1(t) [\cos(\phi_k) + \cos(2\omega_c t + \phi_k)] dt \\
&\quad + \int_0^T n(t) a_1(t) \cos(\omega_c t) dt.
\end{aligned}
\tag{2.8}
$$

For practical transmission systems, the condition $f_c = \frac{\omega_c}{2\pi} \gg 1/T$ is usually satisfied; therefore, the double frequency terms can be eliminated by the lowpass filtering (LPF). The decision statistic at

---

[2] If unequal transmitted powers are assumed, the resulting MAI terms will not be i.i.d.; however, one can invoke the Liapounoff version of the central limit theorem in the standard Gaussian approximation [53].

23

the output of the LPF is given by

$$Z_1 = s_1 + I + n_1. \tag{2.9}$$

In (2.9), the first term s_1 is the desired signal component and it is given by

$$s_1 = \int_0^T A_1 b_1(t)dt = A_1 b_0^{(1)} T = A_1 b_0^{(1)} G \tag{2.10}$$

where $b_0^{(1)}$ denotes the 0th data symbol for User 1 and it is a symmetric Bernoulli RV. Also in the

first term, G is now usefully reinterpreted as the *processing gain*. The last term n_1 is the component

due to background noise and it is a Gaussian random variable with mean

$$
\begin{aligned}
\mathbb{E}[n_1] &= \mathbb{E}\left[\int_0^T n(t)a_1(t)\cos(\omega_c t)dt\right] \\
&= \int_0^T \mathbb{E}[n(t)]\mathbb{E}[a_1(t)]\cos(\omega_c t)dt \\
&= 0
\end{aligned}
\tag{2.11}
$$

and with variance

$$
\begin{aligned}
\mathrm{var}[n_1] &= \mathbb{E}[n_1^2] \\
&= \int_0^T \int_0^T \mathbb{E}[n(s)n(t)]\mathbb{E}[a_1(s)a_1(t)]\cos(\omega_c s)\cos(\omega_c t)dtds \\
&= \int_0^T \int_0^T \frac{N_0}{2}\delta(s-t)\mathbb{E}[a_1(s)a_1(t)]\cos(\omega_c s)\cos(\omega_c t)dtdts \\
&= \frac{N_0}{2}\int_0^T \mathbb{E}[a_1^2(t)]\cos^2(\omega_c t)dt \\
&= \frac{N_0 T}{4} \\
&= \frac{N_0 G}{4}.
\end{aligned}
\tag{2.12}
$$

The second component, I, is the multiple access interference from the other $K-1$ active users and

it is given by

$$
\begin{aligned}
I &= \sum_{k=2}^K A_k \int_0^T b_k(t-\tau_k)a_k(t-\tau_k)a_1(t)\cos(\phi_k)dt \\
&= \sum_{k=2}^K A_k \left[b_{-1}^{(k)}\int_0^{\tau_k} a_k(t-\tau_k)a_1(t)dt + b_0^{(k)}\int_{\tau_k}^T a_k(t-\tau_k)a_1(t)dt\right]\cos(\phi_k).
\end{aligned}
\tag{2.13}
$$

If we define the continuous-time partial cross-correlation functions between $a_k(t)$ and $a_i(t)$ as [64]

$$R_{k,i}(\tau) = \int_0^\tau a_k(t-\tau)a_i(t)dt \tag{2.14}$$

24

and

$$\hat{R}_{k,i}(\tau) = \int_{\tau}^{T} a_k(t-\tau)a_i(t)dt, \qquad (2.15)$$

we can write the MAI term as

$$I = \sum_{k=2}^{K} A_k W_k \cos(\phi_k) \qquad (2.16)$$

where

$$W_k = b_{-1}^{(k)} R_{k,1}(\tau_k) + b_0^{(k)} \hat{R}_{k,1}(\tau_k). \qquad (2.17)$$

In their work on random sequences for the AWGN channel, Lehnert and Pursley [47] simplified W_k, conditioning on User 1's signature sequence, as

$$W_k = P_k R_\psi(S_k) + Q_k \hat{R}_\psi(S_k) + X_k(\hat{R}_\psi(S_k) + R_\psi(S_k)) + Y_k(\hat{R}_\psi(S_k) - R_\psi(S_k)) \qquad (2.18)$$

where S_k is a uniform RV over $[0, 1)$, which accounts for the fractional chip displacement of the kth interferer's chip relative to User 1, $R_\psi(S_k)$ and $\hat{R}_\psi(S_k)$ are the partial autocorrelation functions of the chip waveform defined as

$$R_\psi(s) = \int_0^s \psi(t)\psi(t+T_c-s)dt, \quad 0 \le s \le T_c \qquad (2.19)$$

and

$$\hat{R}_\psi(s) = \int_s^{T_c} \psi(t)\psi(t-s)dt, \quad 0 \le s \le T_c \qquad (2.20)$$

and zero otherwise. The detailed derivation of (2.18) is presented in Appendix A where the RV's X_k, Y_k, P_k, and Q_k are precisely defined.

For a rectangular chip waveform $\psi(t) = P_1(t)$, $R_\psi(\tau) = \tau$ and $\hat{R}_\psi(\tau) = 1 - \tau$. Thus, (2.18) becomes

$$W_k = P_k S_k + Q_k(1 - S_k) + X_k + Y_k(1 - 2S_k). \qquad (2.21)$$

In (2.21), according to Appendix A, P_k and Q_k are symmetric Bernoulli RV's and X_k is a discrete RV which represents the sum of A independent symmetric Bernoulli RV's where A equals the number of chip boundaries *without* transitions in User 1's signature waveform. Similarly, Y_k represents the sum of B independent symmetric Bernoulli RV's where B equals the number of chip boundaries

25

with transitions in User 1's signature waveform. Clearly, $A + B = G - 1$ and the marginal PMF's of X_k and Y_k are given by

$$p_{X_k}(i) = \binom{A}{\frac{i+A}{2}} 2^{-A}, \quad i \in \mathscr{A} = \{-A, -A+2, \ldots, A-2, A\} \tag{2.22}$$

and

$$p_{Y_k}(j) = \binom{B}{\frac{j+B}{2}} 2^{-B}, \quad j \in \mathscr{B} = \{-B, -B+2, \ldots, B-2, B\}. \tag{2.23}$$

Equation (2.18) has two-fold significance. First, it expresses the partial cross-correlation functions (see (2.17)) between the spreading waveforms in terms of the partial autocorrelation functions of the chip waveforms. This permits further simplification to forms such as (2.21) which will be used in the sequel. Secondly, for a target user, the simplifications also classify the total possible 2^G signature sequences into G classes. As discussed later, the system average BER performance depends on the number of chip boundaries with (or without) transitions in the target user's signature sequence. Appropriate use of this fact (classification of the signature sequences) aids in determining tractable BER expressions.

Our analysis will make use of a number of important results which are repeated here for completeness. The proofs and further discussions of these results are given in the Appendix A.

Fact 1: The $(K - 1)$ MAI terms conditioned on B are independent.

Fact 2: The RV's P_k, Q_k, X_k and Y_k conditioned on B are independent.

Fact 3: The RV's P_k, Q_k, X_k and Y_k conditioned on B are zero-mean.

Based on above facts, it is further shown in Appendix A that

Fact 4: The MAI terms are uncorrelated (unconditionally).

The decision statistic in (2.18) is used in calculating the packet error rate of a DS/SSMA system by exploiting the inherent bit-to-bit error dependence [56], and it is also useful for observing the BER dependence on the amount of spreading in User 1's signature sequence (B). However, this

dependence on B can be removed. In Appendix A, we have shown the decision statistic in (2.18) can be further simplified to

$$W_k = \Gamma_k \hat{R}_\psi(S_k) + \Delta_k R_\psi(S_k) \tag{2.24}$$

where the RV Γ_k is a sum of G i.i.d. symmetric Bernoulli RV's and the PMF of Γ_k is given by

$$p_{\Gamma_k}(i) = \binom{G}{\frac{i+G}{2}} 2^{-G}, \quad i \in \mathscr{I} = \{-G, -G+2, \ldots, G-2, G\}; \tag{2.25}$$

and where Δ_k is a sum of G i.i.d. symmetric Bernoulli RV's and the PMF of Δ_k is given by

$$p_{\Delta_k}(j) = \binom{G}{\frac{j+G}{2}} 2^{-G}, \quad j \in \mathscr{I} = \{-G, -G+2, \ldots, G-2, G\}. \tag{2.26}$$

Furthermore, RV's Γ_k and Δ_k are statistically independent.

2.4 Central Limit Theorem Approximations

2.4.1 Standard Gaussian Approximation

In the SGA, as used in AWGN, a CLT is invoked to approximate the MAI process as Gaussian, as the additional background Gaussian noise process. The SGA is widely used because of its simplicity; however, the SGA is also known to seriously overestimate system performance (or underestimate the BER values) for small values of K in AWGN channels [56].

In the SGA, the variance of the MAI averaged over all operating conditions is used to compute the equivalent noise power. To find this variance, let us first examine the conditional variance of the MAI. Let $\mathscr{S} = \{S_2, S_3, \ldots, S_K\}$ and $\phi = \{\phi_2, \phi_3, \ldots, \phi_K\}$, the variance of the MAI conditioned on $\{A_k\}_{k=2}^K$, $\mathscr{S}$, ϕ, and B is

$$
\begin{aligned}
\zeta &= \operatorname{var}\left[I | \{A_k\}_{k=2}^K, \mathscr{S}, \phi, B\right] \\
&= \mathbb{E}\left[\left(\sum_{k=2}^K A_k W_k \cos(\phi_k)\right)^2 \Bigg| \{A_k\}_{k=2}^K, \mathscr{S}, \phi, B\right] \\
&= \sum_{k=2}^K A_k^2 \mathbb{E}[W_k^2 | S_k, B] \mathbb{E}[\cos^2(\phi_k) | \phi_k].
\end{aligned}
\tag{2.27}
$$

27

Since

$$\mathbb{E}[\cos^2(\phi_k)|\phi_k] = \cos^2(\phi_k) = \frac{1}{2}\left[1 + \cos(2\phi_k)\right], \tag{2.28}$$

averaging over ϕ_k and using the fact $\mathbb{E}[\cos(2\phi_k)] = 0$, we get

$$\mathbb{E}[\cos^2(\phi_k)] = \frac{1}{2}. \tag{2.29}$$

Using (2.21), we have

$$\mathbb{E}[W_k^2|S_k,B] = \mathbb{E}[P_k^2 S_k^2|S_k] + \mathbb{E}[Q_k^2(1-S_k)^2|S_k] + \mathbb{E}[X_k^2|B] + \mathbb{E}[Y_k^2(1-2S_k)^2|S_k,B] \tag{2.30}$$

where in obtaining the above result we have invoked Fact 2 stated in Section 2.3. Since the variances of the zero-mean symmetric Bernoulli RV's P_k and Q_k are unity, we have

$$\mathbb{E}[P_k^2 S_k^2|S_k] = S_k^2 \mathbb{E}[P_k^2] = S_k^2 \tag{2.31}$$

and

$$E[Q_k^2(1-S_k)^2|S_k] = (1-S_k)^2 \mathbb{E}[Q_k^2] = (1-S_k)^2. \tag{2.32}$$

Recall from Section 2.3 that the RV X_k is a summation of A i.i.d. symmetric Bernoulli RV's (b_j) where $A = G - 1 - B$, thus, we have

$$\begin{aligned}
\mathbb{E}[X_k^2|B] &= \sum_{j=1}^{A} \mathrm{var}[b_j] \\
&= \sum_{j=1}^{G-1-B} \mathrm{var}[b_j] \\
&= G - 1 - B.
\end{aligned} \tag{2.33}$$

Similarly, since the RV Y_k is a summation of B i.i.d. Bernoulli RV's (b_j), we have

$$\begin{aligned}
\mathbb{E}[Y_k^2(1-2S_k)^2|S_k,B] &= (1-2S_k)^2 \sum_{j=1}^{B} \mathrm{var}[b_j] \\
&= B(1-2S_k)^2.
\end{aligned} \tag{2.34}$$

Substitution of (2.31), (2.32), (2.33) and (2.34) into (2.30) yields

$$E[W_k^2|S_k,B] = S_k^2 + (1-S_k)^2 + (G-1-B) + B(1-2S_k)^2$$

28

$$= (4B+2)S_k^2 - (4B+2)S_k + G$$

$$= (4B+2)(S_k^2 - S_k) + G. \tag{2.35}$$

Averaging (2.35) with respect to the PDF of S_k and using the fact that $\mathbb{E}[S_k^2 - S_k] = -1/6$, we have

$$\mathbb{E}[W_k^2|B] = G - \frac{2B+1}{3}. \tag{2.36}$$

Averaging (2.36) with respect to the PDF of B and using the fact that $\mathbb{E}[B] = \frac{G-1}{2}$, we obtain

$$\mathbb{E}[W_k^2] = \frac{2G}{3}. \tag{2.37}$$

From (2.27), (2.29) and (2.37), we obtain the variance of the MAI, conditioned on $\{A_k\}_{k=2}^K$, as

$$\sigma_{\mathrm{MAI}|\{A_k\}_{k=2}^K}^2 = \frac{G}{3} \sum_{k=2}^K A_k^2. \tag{2.38}$$

Averaging (2.38) across the interferers' Rayleigh fading amplitudes, we obtain the equivalent noise power as

$$\sigma_{\mathrm{MAI}}^2 = \frac{G}{3} \sum_{k=2}^K \mathbb{E}[A_k^2] = \frac{2G}{3}(K-1). \tag{2.39}$$

The average BER given A_1 for each user is then approximated by

$$P_{e|A_1}^{\mathrm{SGA}} \approx Q\left(\frac{A_1 G}{\sqrt{\frac{N_o G}{4} + \frac{2G}{3}(K-1)}} \right) \tag{2.40}$$

where $Q(y) = \frac{1}{\sqrt{2\pi}} \int_y^{+\infty} e^{-x^2/2} dx$. Averaging A_1 in (2.40) with respect to the Rayleigh distribution (2.6) and using the integral identity [79, p. 101, eqn. (3.61)]

$$\int_0^{+\infty} xe^{-x^2/2} Q\left(\frac{x}{\sigma}\right) dx = \frac{1}{2}\left(1 - \frac{1}{\sqrt{\sigma^2+1}}\right), \tag{2.41}$$

we approximate the average BER in Rayleigh fading using the SGA as

$$P_e^{\mathrm{SGA}} \approx \frac{1}{2}\left[1 - \frac{1}{\sqrt{\frac{N_o}{4G} + \frac{2(K-1)}{3G} + 1}} \right]. \tag{2.42}$$

29

2.4.2 Improved Gaussian Approximation

The improved Gaussian approximation is also a technique based on a CLT. Unlike the SGA, which assumes an average variance value for the MAI (or the first moment of the conditional variance ζ), the improved Gaussian approximation exploits the knowledge of the distribution of the conditional variance ζ (or all moments of ζ). The central idea of the improved Gaussian approximation is based on the observation that the MAI is approximated Gaussian when conditioned on the delays and the phases of all the interfering signals, and on B. To show this we rewrite the MAI as

$$I = \sum_{k=2}^{K} A_k W_k \cos(\phi_k) = \sum_{k=2}^{K} G_k W_k \qquad (2.43)$$

where $G_k = A_k \cos(\phi_k)$ is zero-mean Gaussian with unit variance, i.e., $G_k \sim \mathcal{N}(0,1)$. This is true since A_k is Rayleigh-distributed, ϕ_k is uniform over $[0, 2\pi)$ and A_k, ϕ_k are independent [60, p. 146]. However I is not Gaussian, as shown in Section 2.6. In the IGA, the MAI is considered Gaussian conditioned on $\mathcal{S}$, $\mathcal{G}$ and B where $\mathcal{G} = \{G_2, G_3, \ldots, G_K\}$. We can rewrite the conditional variance of the MAI as

$$\zeta \;=\; \sum_{k=2}^{K} G_k^2 [(4B+2)(S_k^2 - S_k) + G] \qquad (2.44)$$

$$\;=\; \sum_{k=2}^{K} Z_k \qquad (2.45)$$

where Z_k are identically distributed and conditionally independent on B, and each Z_k is given by

$$Z_k = U_k V_k \qquad (2.46)$$

where

$$U_k = G_k^2 \qquad (2.47)$$

$$V_k = (4B+2)(S_k^2 - S_k) + G. \qquad (2.48)$$

Note that in (2.44), ζ is a function of the random variables $\mathcal{G}$, $\mathcal{S}$, and B. Therefore, ζ itself is a RV and has its own distribution. If we denote the PDF of ζ by $f_\zeta(\zeta)$, we can approximate the BER in an interference-limited environment, given A_1, by

$$P_{e|A_1}^{IGA} \;\approx\; \int_{0}^{+\infty} Q\left(\frac{A_1 G}{\sqrt{\zeta}}\right) f_\zeta(\zeta) d\zeta$$

30

$$= \mathbb{E}\left[Q\left(\frac{A_1 G}{\sqrt{\zeta}} \right) \right]. \tag{2.49}$$

The evaluation of the PDF for ζ requires knowledge of the PDF of Z_k conditioned on B, and numerically evaluating a $(K - 2)$-fold convolution and taking the expectation with respect to B. That is,

$$f_\zeta(\zeta) = \mathbb{E}\left[f_{Z|B}(z) * \ldots * f_{Z|B}(z) \right]. \tag{2.50}$$

Finally, two additional numerical integrations are required to obtain the overall average BER. It was shown in [56] that, consequently, the BER for an AWGN channel obtained from the IGA is significantly more accurate than the BER obtained from the SGA especially for small values of K. As shown, the IGA method can be cumbersome to use; therefore, it should be avoided if possible. Fortunately, as we see in Section 2.7, the IGA for our problem is not necessary.

At this point we comment that the SGA utilizes the first moment of the conditional variance, ζ; while the IGA utilizes the distribution of the conditional variance, $f_\zeta(\zeta)$, therefore all moments of ζ. Holtzman [38] further simplified the calculation of (2.49) by using only the first and the second moments of ζ, provided certain prior analyses are done. The inaccuracies of Holtzman's simplification have been shown to be minor [38].

The central idea of Holtzman's approximation can be illustrated as follows. Let $f(\Theta)$ be a real function of a RV Θ with mean μ and variance σ^2, and we assume that all the nth order derivatives of $f(\Theta)$ exist. We expand the real function $f(\Theta)$ using the Talyor series around the mean μ and get

$$f(\Theta) = f(\mu) + f'(\mu)(\Theta - \mu) + \frac{f''(\mu)}{2}(\Theta - \mu)^2 + \cdots. \tag{2.51}$$

Averaging $f(\Theta)$ over Θ and using a second-order approximation, we can approximate the expected value of $f(\Theta)$ as

$$\mathbb{E}[f(\Theta)] \approx f(\mu) + \frac{f''(\mu)}{2}\sigma^2. \tag{2.52}$$

If we use a three-point difference formula for the continuous-time second order derivative, we can further approximate the above expression as

$$\mathbb{E}[f(\Theta)] \approx f(\mu) + \frac{f(\mu + h) - 2f(\mu) + f(\mu - h)}{2h^2}\sigma^2 \tag{2.53}$$

31

where the parameter h controls the accuracy of the finite difference approximation. Holtzman suggested $\sqrt{3}\sigma$ as a good choice of h. With this value of h, we have

$$\mathbb{E}[f(\Theta)] \approx \frac{2}{3}f(\mu) + \frac{1}{6}f(\mu + \sqrt{3}\sigma) + \frac{1}{6}f(\mu - \sqrt{3}\sigma). \tag{2.54}$$

For our problem, from (2.49), if we let $\Theta = \zeta$ and $f(x) = Q(\frac{A_1 G}{\sqrt{x}})$ [3], the conditional BER for an interference-limited environment, given A_1, can be approximated by

$$P_{e|A_1}^{SIGA} \approx \frac{2}{3}Q\left(\frac{A_1 G}{\sqrt{\mu_\zeta}}\right) + \frac{1}{6}Q\left(\frac{A_1 G}{\sqrt{\mu_\zeta + \sqrt{3}\sigma_\zeta}}\right) + \frac{1}{6}Q\left(\frac{A_1 G}{\sqrt{\mu_\zeta - \sqrt{3}\sigma_\zeta}}\right) \tag{2.55}$$

where μ_ζ and σ_ζ are respectively the mean and the standard deviation of the conditional variance ζ. Averaging the conditional BER with respect to the PDF of A_1, we obtain the approximate average BER as

$$\begin{aligned}
P_e^{SIGA} \approx & \frac{1}{3}\left[1 - \frac{G}{\sqrt{\mu_\zeta + G^2}}\right] + \frac{1}{12}\left[1 - \frac{G}{\sqrt{\mu_\zeta + \sqrt{3}\sigma_\zeta + G^2}}\right] \\
& + \frac{1}{12}\left[1 - \frac{G}{\sqrt{\mu_\zeta - \sqrt{3}\sigma_\zeta + G^2}}\right]
\end{aligned} \tag{2.56}$$

where the above error rate estimation is valid provided $\mu_\zeta + G^2 > \sqrt{3}\sigma_\zeta$. Therefore, to use Holzman's approximation for error rate estimation, we are only required to have knowledge of μ_ζ and σ_ζ^2. The mean of ζ is

$$\begin{aligned}
\mu_\zeta &= \mathbb{E}[\zeta] \\
&= \sum_{k=2}^{K} \mathbb{E}[Z_k] \\
&= \sum_{k=2}^{K} \mathbb{E}[G_k^2]\mathbb{E}[(4B+2)(S_k^2 - S_k) + G)] \\
&= \sum_{k=2}^{K} \mathbb{E}[G_k^2](\mathbb{E}[4B+2]\mathbb{E}[S_k^2 - S_k] + G) \\
&= \frac{2G}{3}(K-1)
\end{aligned} \tag{2.57}$$

as we expect. The variance of ζ is

$$\sigma_\zeta^2 = \mathrm{var}[\zeta]$$

---

[3] All the nth order derivatives of $f(x)$ exist since the derivatives of $Q(x)$ take the form of Hermite polynomials.

32

$$
\begin{aligned}
&= \mathbb{E}\left[\left(\sum_{k=2}^{K} Z_k - \sum_{k=2}^{K} \overline{Z}_k\right)^2\right] \\
&= \mathbb{E}\left[\left((Z_2 - \overline{Z}_2) + (Z_3 - \overline{Z}_3) + \ldots + (Z_K - \overline{Z}_K)\right)^2\right] \\
&= \mathbb{E}\left[\sum_{k=2}^{K}(Z_k - \overline{Z}_k)^2 + \sum_{\substack{i=2 \\ i \neq j}}^{K}\sum_{j=2}^{K}(Z_i - \overline{Z}_i)(Z_j - \overline{Z}_j)\right] \\
&= (K-1)\mathrm{var}[Z_k] + (K-1)(K-2)\mathrm{cov}_{i \neq j}[Z_i, Z_j] \\
&= (K-1)\left(\mathbb{E}[Z_k^2] - (\mathbb{E}[Z_k])^2 + (K-2)\mathrm{cov}_{i \neq j}[Z_i, Z_j]\right).
\end{aligned} \tag{2.58}
$$

Therefore, in order to compute σ_ζ^2, we need to compute $\mathbb{E}[Z_k]$, $\mathbb{E}[Z_k^2]$, and $\mathrm{cov}_{i \neq j}[Z_i, Z_j]$ separately. Clearly, we have

$$
\mathbb{E}[Z_k] = \frac{2G}{3}. \tag{2.59}
$$

Using the definitions of U_k and V_k, we have

$$
\begin{aligned}
\mathbb{E}[Z_k^2] &= \mathbb{E}[U_k^2 V_k^2] \\
&= \mathbb{E}[G_k^4]\mathbb{E}[V_k^2] \\
&= 3\mathbb{E}[((4B+2)(S_k^2 - S_k) + G)^2] \\
&= 12\mathbb{E}\left[(4B^2 + 4B + 1)(S_k^2 - S_k)^2 + G(2B+1)(S_k^2 - S_k) + \frac{G^2}{4}\right].
\end{aligned} \tag{2.60}
$$

Using the distribution of B and S_k, it is straightforward to show that

$$
\mathbb{E}[4B^2 + 4B + 1] = G^2 + G - 1 \tag{2.61}
$$

$$
\mathbb{E}[(S_k^2 - S_k)^2] = \frac{1}{30} \tag{2.62}
$$

$$
\mathbb{E}[2B + 1] = G \tag{2.63}
$$

$$
\mathbb{E}[S_k^2 - S_k] = -\frac{1}{6}. \tag{2.64}
$$

Substituting the above expressions into (2.60), we obtain

$$
\mathbb{E}[Z_k^2] = \frac{7G^2 + 2G - 2}{5}. \tag{2.65}
$$

Finally, to compute the covariance between Z_i and Z_j for $i \neq j$, we have

$$
\mathrm{cov}(Z_i, Z_j) = \mathbb{E}[Z_i Z_j] - \mathbb{E}[Z_i]\mathbb{E}[Z_j]
$$

33

$$= \mathbb{E}\left[G_i^2((4B+2)(S_i^2-S_i)+G)]G_j^2((4B+2)(S_j^2-S_j)+G)\right] - \frac{4G^2}{9}$$

$$= \frac{G-1}{9}. \tag{2.66}$$

Substitution of (2.59), (2.65), and (2.66) into (2.58) yields

$$\sigma_\zeta^2 = (K-1)\left[\frac{43G^2+18G-18}{45} + \frac{(K-2)(G-1)}{9}\right]. \tag{2.67}$$

Alternatively, (2.56), (2.57) and (2.67) can be derived by taking account of the distribution of the received power, P_r. The instantaneous power for the kth user is $P_r = P_k A_k^2$ or $2\chi^2$, where χ^2 is a chi-square RV with two degrees of freedom and unit variance. In [65], Holtzman's method is extended by including the first and the second moments for the received signal power, Using $\mathbb{E}[P_r] = 4$ and $\mathbb{E}[P_r^2] = 32$, we well as [65, eqns. (C.96)-(C.98)], we again obtain (2.56), (2.57) and (2.67).

To include the background noise in the approximation, we can modify the conditional BER as

$$P_{e|A_1}^{\text{SIGA}} \approx \frac{2}{3}Q\left(\frac{A_1}{\sqrt{\frac{\mu_\zeta}{G^2}+\frac{N_0}{2E_b}}}\right) + \frac{1}{6}Q\left(\frac{A_1}{\sqrt{\frac{\mu_\zeta+\sqrt{3}\sigma_\zeta}{G^2}+\frac{N_0}{2E_b}}}\right) + \frac{1}{6}Q\left(\frac{A_1}{\sqrt{\frac{\mu_\zeta-\sqrt{3}\sigma_\zeta}{G^2}+\frac{N_0}{2E_b}}}\right) \tag{2.68}$$

where E_b is the energy per bit and it is given by $E_b = PT$. Averaging (2.68) over the PDF of A_1, we get

$$P_e^{\text{SIGA}} \approx \frac{1}{3}\left[1 - \frac{1}{\sqrt{\mu_\zeta/G^2+N_0/2E_b+1}}\right] + \frac{1}{12}\left[1 - \frac{1}{\sqrt{(\mu_\zeta+\sqrt{3}\sigma_\zeta)/G^2+N_0/2E_b+1}}\right]$$

$$+ \frac{1}{12}\left[1 - \frac{1}{\sqrt{(\mu_\zeta-\sqrt{3}\sigma_\zeta)/G^2+N_0/2E_b+1}}\right] \tag{2.69}$$

where the above expression is valid provided $(\mu_\zeta - \sqrt{3}\sigma)/G^2 + N_0/2E_b + 1 > 0$. In Section 2.6, we will assess the accuracies of both SGA and SIGA using the exact method which does not reply on any form of CLT.

2.5 Synchronous BER Analysis

In this section, we consider the BER calculation for a synchronous system, i.e. $\tau_1 = \tau_2 = \ldots = \tau_k = 0$ in (2.7). The BER for a synchronous system operating in flat Rayleigh fading is known; however,

34

the present derivation both serves completeness and clarifies the derivation and understanding of the asynchronous results to follow. The results will also be used later to compare the performances of asynchronous and synchronous systems. We first assume all signature sequences are deterministic and $\phi_1 = 0$. The output of the matched filter, after LPF, for User 1 is given by [79]

$$
\begin{aligned}
y_1 &= \int_0^T r(t)a_1(t)\cos(w_c t)dt \\
&= S_1 + I_1 + n_1
\end{aligned}
\tag{2.70}
$$

where n_1 is a zero-mean Gaussian RV with variance $\sigma_{n_1}^2 = \frac{N_0 G}{4}$, S_1 is the signal component, $S_1 = \pm A_1 G$, and the interference term I_1 is given by

$$
\begin{aligned}
I_1 &= \sum_{k=2}^K A_k b_0^{(k)} \cos(\phi_k) \int_0^T a_k(t)a_1(t)dt \\
&= \sum_{k=2}^K G\rho_{k1} b_0^{(k)} A_k \cos(\phi_k) \tag{2.71a} \\
&= \sum_{k=2}^K G\rho_{k1} b_0^{(k)} G_k' \tag{2.71b} \\
&= \sum_{k=2}^K G\rho_{k1} G_k. \tag{2.71c}
\end{aligned}
$$

In (2.71a), we have defined the full-period cross-correlation coefficient ρ_{k1} between the kth and User 1's signature sequences as

$$
\rho_{k1} \stackrel{\text{def}}{=} \frac{1}{GT_c} \int_0^{GT_c} a_k(t)a_1(t)dt. \tag{2.72}
$$

We set $G_k' = A_k \cos(\phi_k)$ and $G_k = b_0^{(k)} G_k'$. Note that, as before, G_k' is a zero-mean, unit variance Gaussian RV. Since $b_0^{(k)}$ takes values from $\{-1, +1\}$ with equal probability independently of the values of G_k', G_k is also a zero-mean, unit variance Gaussian RV. Now, note that the independence of $\{A_2, A_3, \ldots, A_K; \phi_2, \phi_3, \ldots, \phi_K; b_0^{(2)}, b_0^{(3)}, \ldots, b_0^{(K)}\}$ implies the independence of $\{G_2, G_3, \ldots, G_K\}$. Since a sum of independent Gaussian RV's has a Gaussian distribution, it follows that I_1 is a Gaussian RV with zero-mean and variance $\sigma_{I_1}^2 = \sum_{k=2}^K G^2 \rho_{k1}^2$. By symmetry and using the independence of I_1 and n_1, one has

$$
P_{e|A_1}^{\text{SYNC}} = Q\left(\frac{A_1 G}{\sqrt{\frac{N_0 G}{4} + \sum_{k=2}^K G^2 \rho_{k1}^2}} \right). \tag{2.73}
$$

35

Averaging over the PDF of A_1, we obtain the BER for a Rayleigh-faded user as

$$P_e^{\text{SYNC}} = \frac{1}{2}\left[1 - \frac{1}{\sqrt{1 + \frac{N_o}{4G} + \Sigma_{k=2}^{K}\rho_{k1}^2}}\right].$$

(2.74)

The BER expression (2.74) is the same as the expression derived in [79, eqn. (3.135)] as expected. Physically from (2.74), one sees that the interferers act like additional independent Gaussian background noise. This is because the MAI on the flat Rayleigh fading channel (inclusion of the modulation on the carriers) has a Gaussian first-order distribution assuming synchronous transmission. Importantly, this implies that the optimum receiver (that does not perform user-interference cancellation) is a whitening filter followed by a correlator detector. In the next section, it is shown that this is not the case for asynchronous transmission.

For uniform random signature sequences, $E[\rho_{k1}^2] = 1/G$ [79], and

$$P_e^{\text{SYNC}} = \frac{1}{2}\left[1 - \frac{1}{\sqrt{1 + \frac{N_o}{4G} + \frac{K-1}{G}}}\right].$$

(2.75)

2.6 Asynchronous BER Analysis

In this section, we will use the characteristic function method to compute the average BER under asynchronous transmission conditions in flat Rayleigh fading. For completeness, the exact BER expressions are derived using the known decision statistic as well as the simplified decision statistic developed in Appendix A. It will be shown in the next section that, with this CF method, the average BER can be obtained to any desired accuracy.

2.6.1 BER Analysis using the Known Decision Statistic

In this subsection, we derive the exact average BER expression using the decision statistic proposed by Lehnert and Pursley [47]. To do so, we first examine the statistics of each interferer, I_k. From (2.43), we have $I_k = G_k W_k$, where G_k is a zero-mean, unit variance Gaussian RV and W_k is defined in (2.21). Thus, given W_k, I_k is a Gaussian RV with zero mean and conditional variance $\sigma_{I_k|W_k}^2 = W_k^2$. This implies through (2.21) that I_k given $P_k, Q_k, X_k, Y_k, S_k, B$ is Gaussian and the conditional PDF

36

for I_k follows as

$$f_{I_k|P_k,Q_k,X_k,Y_k,S_k,B}(i_k) = \frac{1}{\sqrt{2\pi}|P_kS_k + Q_k(1-S_k) + X_k + Y_k(1-2S_k)|}$$

$$\times \exp\left\{-\frac{i_k^2}{2[P_kS_k + Q_k(1-S_k) + X_k + Y_k(1-2S_k)]^2}\right\} \quad (2.76)$$

where a modulus operation is required in (2.76) since W_k may take negative values. Averaging over P_k, Q_k, X_k, Y_k (which is equivalent to averaging over all interferers' spreading sequences and data sequences, see [47, eqn. (12)]) yields

$$f_{I_k|S_k,B}(i_k) = \frac{1}{4\sqrt{2\pi}}2^{-(G-1)}\sum_{i\in\mathscr{A}}\sum_{j\in\mathscr{B}}\binom{A}{\frac{i+A}{2}}\binom{B}{\frac{j+B}{2}}$$

$$\times \left\{\sum_{l=1,2,3,4}\frac{1}{\sigma_l(i,j,S_k)}\exp\left\{-\frac{i_k^2}{2\sigma_l^2(i,j,S_k)}\right\}\right\} \quad (2.77a)$$

where

$$\sigma_1^2(i,j,S_k) = [1+i+j(1-2S_k)]^2, \quad (2.77b)$$

$$\sigma_2^2(i,j,S_k) = [2S_k-1+i+j(1-2S_k)]^2, \quad (2.77c)$$

$$\sigma_3^2(i,j,S_k) = [1-2S_k+i+j(1-2S_k)]^2, \quad (2.77d)$$

$$\sigma_4^2(i,j,S_k) = [-1+i+j(1-2S_k)]^2. \quad (2.77e)$$

Note that to obtain (2.77a), Fact 2 has been used, i.e., X_k and Y_k given B are independent. It is clear from (2.77a) that the PDF of I_k given S_k and B is not Gaussian, though the functional form is a weighted summation of "Gaussian-like" terms. We postpone averaging S_k here since they appear in the denominators of the exponential function arguments giving an intractable integral. The characteristic function of I_k, given S_k and B, is

$$\Phi_{I_k|S_k,B}(\omega) = \frac{2^{-(G-1)}}{4}\sum_{i\in\mathscr{A}}\sum_{j\in\mathscr{B}}\binom{A}{\frac{i+A}{2}}\binom{B}{\frac{j+B}{2}}\left\{\sum_{l=1,2,3,4}\exp\left\{-\frac{1}{2}\sigma_l^2(i,j,S_k)\omega^2\right\}\right\}. \quad (2.78)$$

The S_k's now appear in the numerators of the exponential function arguments and averaging can be carried out to give

$$\Phi_{I_k|B}(\omega) = \int_0^1 \Phi_{I_k|S_k,B}(\omega)dS_k$$

37

$$= \frac{2^{-(G-1)}}{4} \sum_{i \in \mathscr{A}} \sum_{j \in \mathscr{B}} \binom{A}{\frac{i+A}{2}} \binom{B}{\frac{j+B}{2}}$$

$$\times \left\{ \int_0^1 \exp\left[-\frac{1}{2}\sigma_1^2(i,j,S_k)\omega^2 \right] dS_k \right.$$

$$+ \int_0^1 \exp\left[-\frac{1}{2}\sigma_2^2(i,j,S_k)\omega^2 \right] dS_k$$

$$+ \int_0^1 \exp\left[-\frac{1}{2}\sigma_3^2(i,j,S_k)\omega^2 \right] dS_k$$

$$\left. + \int_0^1 \exp\left[-\frac{1}{2}\sigma_4^2(i,j,S_k)\omega^2 \right] dS_k \right\} \tag{2.79}$$

where in (2.79), the first integral becomes

$$\int_0^1 \exp\left[-\frac{1}{2}\sigma_1^2(i,j,S_k)\omega^2 \right] dS_k$$

$$= \int_0^1 \exp\left\{ -\frac{1}{2}\left[1+i+j(1-2S_k) \right]^2 \omega^2 \right\} dS_k$$

$$= \frac{1}{2} \int_{-1}^1 \exp\left\{ -\frac{1}{2}(1+i+ju)^2\omega^2 \right\} du$$

$$= \frac{1}{2} \int_{-1}^1 \exp\left\{ -\frac{\left(u + \frac{1+i}{j} \right)^2}{2\left(\frac{1}{j^2\omega^2} \right)} \right\} du$$

$$= \frac{\sqrt{\frac{\pi}{2}}}{|j\omega|} \left\{ Q\left(\frac{|j\omega|[(i+1)-j]}{j} \right) - Q\left(\frac{|j\omega|[(i+1)+j]}{j} \right) \right\}$$

$$= \frac{\sqrt{\frac{\pi}{2}}}{j|\omega|} \left\{ Q(|\omega|\cdot[(i+1)]-j]) - Q(|\omega|\cdot[(i+1)+j]) \right\} \tag{2.80}$$

where the last equality follows from the fact $Q(-x) = 1 - Q(x)$ and where in the special case when

$j = 0$, the above integral specializes to $\exp(-\frac{1}{2}i^2\omega^2)$. If we define

$$J(i,j) = \begin{cases} \exp(-\frac{1}{2}i^2\omega^2) & j = 0, \\ \frac{\sqrt{\frac{\pi}{2}}}{j|\omega|}\left\{ Q\left(|\omega|\cdot(i-j) \right) - Q\left(|\omega|\cdot(i+j) \right) \right\} & j, \omega \neq 0, \end{cases} \tag{2.81}$$

we can simply express the integral of (2.80) as

$$\int_0^1 \exp\left[-\frac{1}{2}\sigma_1^2(i,j,S_k)\omega^2 \right] dS_k = J(i+1,j). \tag{2.82}$$

Similarly we can show

$$\int_0^1 \exp\left[-\frac{1}{2}\sigma_2^2(i,j,S_k)\omega^2 \right] dS_k = J(i,j-1), \tag{2.83}$$

38

and

$$\int_0^1 \exp\left[-\frac{1}{2}\sigma_3^2(i,j,S_k)\omega^2\right] dS_k = J(i,j+1), \tag{2.84}$$

and

$$\int_0^1 \exp\left[-\frac{1}{2}\sigma_4^2(i,j,S_k)\omega^2\right] dS_k = J(i-1,j). \tag{2.85}$$

Observe from (2.79) that $\Phi_{I_k|B}(w)$ is real. This implies $f_{I_k|B}(i_k)$ is symmetric about $i_k = 0$, as expected. The function $J(i,j)$ defined in (2.81) has an interesting geometric interpretation. To see this, for $j \neq 0$, we write

$$\begin{aligned}
J(i,j) &= \frac{\sqrt{\frac{\pi}{2}}}{j|\omega|}\left\{Q(i|\omega| - j|\omega|) - Q(i|\omega| + j|\omega|)\right\} \\
&= -\sqrt{2\pi}\left\{\frac{Q(i|\omega| + j|\omega|) - Q(i|\omega| - j|\omega|)}{2j|\omega|}\right\} \\
&= -\sqrt{2\pi}Q'(i|\omega|) - \sqrt{2\pi}\frac{j^2|\omega|^2}{6}Q^{(3)}(\xi) \tag{2.86}
\end{aligned}$$

where ξ lies between $i|\omega| - j|\omega|$ and $i|\omega| + j|\omega|$, $Q'(x) = -\frac{1}{\sqrt{2\pi}}e^{-\frac{x^2}{2}}$ is the first-order derivative of the Q-function and $Q^{(3)}(x) = \frac{1}{\sqrt{2\pi}}e^{-x^2/2}[1-x^2]$ is the third-order derivative of the Q-function. From (2.86), it's clear that, for $j \neq 0$, the function $J(i,j)$ is just the three-point approximation (scaled by a constant factor) of the derivative of the standard Q-function evaluated at $i|\omega|$. For $j = 0$, the second term in (2.86) vanishes for all values of i and ω, and this approximation becomes an exact scaling of the derivative of the Q-function evaluated at $i|\omega|$.

Using the fact that the I_k's given B are independent, we have the characteristic function for the total interference term I, given B, as

$$\Phi_{I|B}(\omega) = \prod_{k=2}^{K} \Phi_{I_k|B}(\omega). \tag{2.87}$$

Let $\xi|B = I|B + n_1$, where n_1, representing the background noise, is a zero-mean Gaussian RV with variance $\sigma_{n_1}^2 = N_0 G/4$, $I|B$ is the total other-user interference given B, and $\xi|B$ is the total disturbance given B. Since the other-user interference and background noise are independent, we have

$$\Phi_{\xi|B}(\omega) = \Phi_{I|B}(\omega)\Phi_{n_1}(\omega)$$

39

$$= \Phi_{n_1}(\omega) - [1 - \Phi_{I|B}(\omega)]\Phi_{n_1}(\omega) \qquad (2.88)$$

where $\Phi_{n_1}(\omega)$ is the CF of the background noise and it is given by $\exp(-\omega^2\sigma_{n_1}^2/2)$.

We use the Fourier inversion formula for the real integral [59, p. 40, eqn. (3-22)] to find the distribution function of $\xi|B$, $F_{\xi|B}(\cdot)$, which is to be used to calculate the BER, as

$$F_{\xi|B}(\xi) = \frac{1}{2} + \frac{1}{\pi}\int_0^{+\infty}\frac{\Phi_{I|B}(\omega)}{\omega}\sin(\xi\omega)d\omega. \qquad (2.89)$$

The conditional BER for our target user can be expressed, by symmetry, as

$$\begin{aligned}
P_{e|A_1,B} &= \Pr\{\xi < -A_1 G\} \\
&= 1 - F_\xi(A_1 G) \\
&= \frac{1}{2} - \frac{1}{\pi}\int_0^{+\infty}\frac{\sin(A_1 G\omega)}{\omega}\Phi_{\xi|B}(\omega)d\omega \\
&= Q\left(\frac{A_1 G}{\sigma_{n_1}}\right) + \frac{1}{\pi}\int_0^{+\infty}\frac{\sin(A_1 G\omega)}{\omega}[1 - \Phi_{I|B}(\omega)]\Phi_{n_1}(\omega)d\omega.
\end{aligned} \qquad (2.90)$$

Averaging over the PDF of A_1, and using the integral identity [33, eqn. 3.952-1]

$$\int_0^{+\infty}\sin(kx)xe^{-\frac{x^2}{2}}dx = \sqrt{\frac{\pi}{2}}ke^{-\frac{k^2}{2}}, \qquad (2.91)$$

we have

$$P_{e|B} = \frac{1}{2}\left[1 - \frac{G}{\sqrt{\sigma_{n_1}^2 + G^2}}\right] + \frac{G}{\sqrt{2\pi}}\int_0^{+\infty}[1 - \Phi_{I|B}(\omega)]\Phi_{n_1}(\omega)\exp\left\{-\frac{1}{2}\omega^2 G^2\right\}d\omega. \qquad (2.92)$$

When the effect of the background noise is negligible, $\sigma_{n_1}^2 \approx 0$ and $\Phi_{n_1}(w) \approx 1$, so (2.92) becomes

$$\begin{aligned}
P_{e|B} &\approx \frac{G}{\sqrt{2\pi}}\int_0^{+\infty}[1 - \Phi_{I|B}(\omega)]\Phi_{n_1}(\omega)\exp\left\{-\frac{1}{2}\omega^2 G^2\right\}d\omega \\
&= \frac{1}{2} - \frac{G}{\sqrt{2\pi}}\int_0^{+\infty}\Phi_{I|B}(\omega)\exp\left\{-\frac{1}{2}\omega^2 G^2\right\}d\omega.
\end{aligned} \qquad (2.93)$$

Eqns. (2.92), (2.87), and (2.79) (or (2.93), (2.87) and (2.79) for the noiseless case) give the average BER experienced by a target user with a signature sequence that has a given value of B. The average BER for all users, or for one target user averaged over all signature sequences randomly assigned by a base station for each service request, is

$$P_e = 2^{-(G-1)}\sum_{B=0}^{G-1}\binom{G-1}{B}P_{e|B}. \qquad (2.94)$$

40

An interesting result seen in (2.94) is that the average BER over all signature sequences can be obtained by averaging over G classes [4] of sequences rather than over 2^G possible random sequences. Consequently, the order of the computational complexity in the number of user sequences is reduced from exponential to linear. This conclusion was stated previously in [47].

2.6.2 BER Analysis using the Simplified Decision Statistic

In this subsection, a computationally efficient and accurate average BER expression is derived using the simplified decision statistic presented in Section 2.3. Recall that W_k can be alternatively expressed as $W_k = \Delta_k S_k + \Gamma_k(1 - S_k)$ where Δ_k, Γ_k each consists of a sum of G i.i.d. Bernoulli RV's. Since $I_k = W_k G_k$ where G_k is a zero-mean unit variance Gaussian RV, conditioning on W_k, and thus, on Δ_k, Γ_k and S_k, we can write the PDF of the kth interferer as

$$f_{I_k|\Gamma_k,\Delta_k,S_k}(i_k) \frac{1}{\sqrt{2\pi}|\Delta_k S_k + \Gamma_k(1 - S_k)|} \exp\left\{-\frac{i_k^2}{2[\Delta_k S_k + \Gamma_k(1 - S_k)]^2}\right\}. \tag{2.95}$$

Since Γ_k and Δ_k are independent (see Appendix A), the joint PDF of Γ_k and Δ_k equals the product of the marginals. Averaging over the joint PDF of Δ_k and Γ_k, the conditional PDF of I_k becomes

$$f_{I_k|S_k}(i_k) = 2^{-2G} \sum_{i \in \mathscr{I}} \sum_{j \in \mathscr{I}} \binom{G}{\frac{i+G}{2}} \binom{G}{\frac{j+G}{2}} \frac{1}{\sqrt{2\pi}|iS_k + j(1 - S_k)|}$$
$$\times \exp\left\{-\frac{i_k^2}{2[iS_k + j(1 - S_k)]^2}\right\} \tag{2.96}$$

and its characteristic function (conditioned on S_k) follows as

$$\Phi_{I_k|S_k}(\omega) = 2^{-2G} \sum_{i \in \mathscr{I}} \sum_{j \in \mathscr{I}} \binom{G}{\frac{i+G}{2}} \binom{G}{\frac{j+G}{2}} \exp\left\{-\frac{1}{2}\omega^2[iS_k + j(1 - S_k)]^2\right\}. \tag{2.97}$$

To obtain the unconditional CF for the kth interferer, we average the conditional CF with respect to the PDF of S_k and obtain

$$\Phi_{I_k}(\omega) = 2^{-2G} \sum_{i \in \mathscr{I}} \sum_{j \in \mathscr{I}} \binom{G}{\frac{i+G}{2}} \binom{G}{\frac{j+G}{2}} \tilde{J}(i, j) \tag{2.98}$$

where, for convenience, we have defined a function $\tilde{J}(i, j)$ as

$$\tilde{J}(i, j) = \begin{cases} \exp(-\frac{1}{2}i^2\omega^2) & i = j, \\ \frac{\sqrt{2\pi}}{(i-j)|\omega|}\{Q(j|\omega|) - Q(i|\omega|)\} & i \neq j. \end{cases} \tag{2.99}$$

---

[4]In each class, all signature sequences have the same total number of transitions at the chip boundaries.

41

In Appendix A, we point out that, in general, RV's W_k and W_{k+1} are dependent with correlator receiver. Here, for simplicity, we assume W_k and W_{k+1} are independent. Since $I_k = W_k G_k$, the independence between W_k and W_{k+1} as well as the independence between G_k and G_{k+1} imply that the MAI terms I_k and I_{k+1} are also statistically independent. Therefore, the CF of the total MAI becomes

$$\Phi_I(\omega) = \prod_{k=2}^{K} \Phi_{I_k}(\omega). \tag{2.100}$$

As before, the average BER in terms of the CF of the MAI and background noise can be shown as

$$P_e = \frac{1}{2}\left[1 - \frac{G}{\sqrt{\sigma_{n_1}^2 + G^2}}\right] + \frac{G}{\sqrt{2\pi}} \int_0^{+\infty} [1 - \Phi_I(\omega)]\Phi_{n_1}(\omega)\exp\left\{-\frac{1}{2}\omega^2 G^2\right\}d\omega. \tag{2.101}$$

Comparing (2.101) and (2.92), we comment that (2.92) represents the conditional BER only, while (2.101) represents the desired average BER and no additional statistical averaging is required. Clearly, the BER derived using the simplified decision statistic is computationally more efficient than the BER derived using the known decision statistic proposed by Lehnert and Pursley. In the following section, we will compare the computational complexities of these two BER expressions in detail.

2.7 Numerical Results and Discussions

In previous analyses of SS multiple access system performance based on the characteristic function method, the characteristic function of each interferer is given as iterated integrals [30], [72] with 2-3 levels of numerical integration. At best, it can be expressed as a single integral for a BPSK system with rectangular chip waveform for the AWGN channel, but the integrand is not well-behaved [30, eqn. (14)]. In (2.79), we present an explicit closed-form expression for the characteristic function involving only the exponential function and the Q-function. It can be shown that the expression requires computation and summation of at most $(G-1)^2$ terms. Since the error function is widely available in many scientific software tools such as Matlab and Maple, this expression can be readily programmed for direct evaluation. A typical plot of $\Phi_{I_k|B}(\omega)$ is illustrated in Fig. 2.2 for $G = 31$

and $B = 30$. Observe that $\Phi_{I_k|B}(\omega)$ has Gaussian-like shape which decays exponentially in ω^2 for increasing frequency ω (the Q-function can be well approximated as exponential in $-\omega^2$ for large values of arguments). Note that (2.79) implies that the PDF of the MAI has support over $(-\infty, +\infty)$; this is in contrast to the the AWGN channel case where the support of the MAI PDF is finite over $[-k,k]$, where k is a constant. Consequently, the BER bounding technique described in [47] is not applicable to Rayleigh fading channels.

The conditional BER expressions in (2.92) and (2.93) are important new results. Known error rate expressions are given in a form similar to (2.89) but with an integrand which contains a singularity point, and moreover, is oscillatory with a varying period (dependent on ω). This is a very undesirable feature for numerical integration. A series expansion method was suggested in [30] to enhance the accuracy; however, large numbers of terms are required to obtain a good approximation and the speed of convergence depends on certain parameters. The integrand functions in (2.92) and (2.93) are extremely well-behaved in the sense that they are smooth, strictly non-negative, have no oscillations and decay exponentially with increasing ω. This is clearly seen from typical integrand functions plotted in Fig. 2.3 for the case of a system with background noise and in Fig. 2.4 for the case without background noise. Hence, simple numerical integration techniques can be employed to obtain the BER to any desired accuracy. In this chapter, all numerical results were obtained using the composite Simpson's rule. Compared to the approximate Fourier series method [72], our new integral solution also provides greater dynamic range for the average error rate. This is because the series given in [72] is an alternating series.

Fig. 2.5 shows numerical results for the conditional BER with three values of B, $B = 0$, $B = G - 1$, and $B = \mathbb{E}[B] = (G - 1)/2$. A short sequence period of $G = 7$ and no background noise are assumed. For $B = 0$, User 1's signature sequence has no transitions at any chip boundary. This corresponds to a narrow-band signal subject to wide-band interferences; hence it yields the worst BER performance. On the other hand, for $B = G - 1$, User 1's signature sequence has transitions at every chip boundary, and consequently, highest spreading gain; this results in the best BER performance. However, the unfavorable autocorrelation properties of such sequences may introduce

43
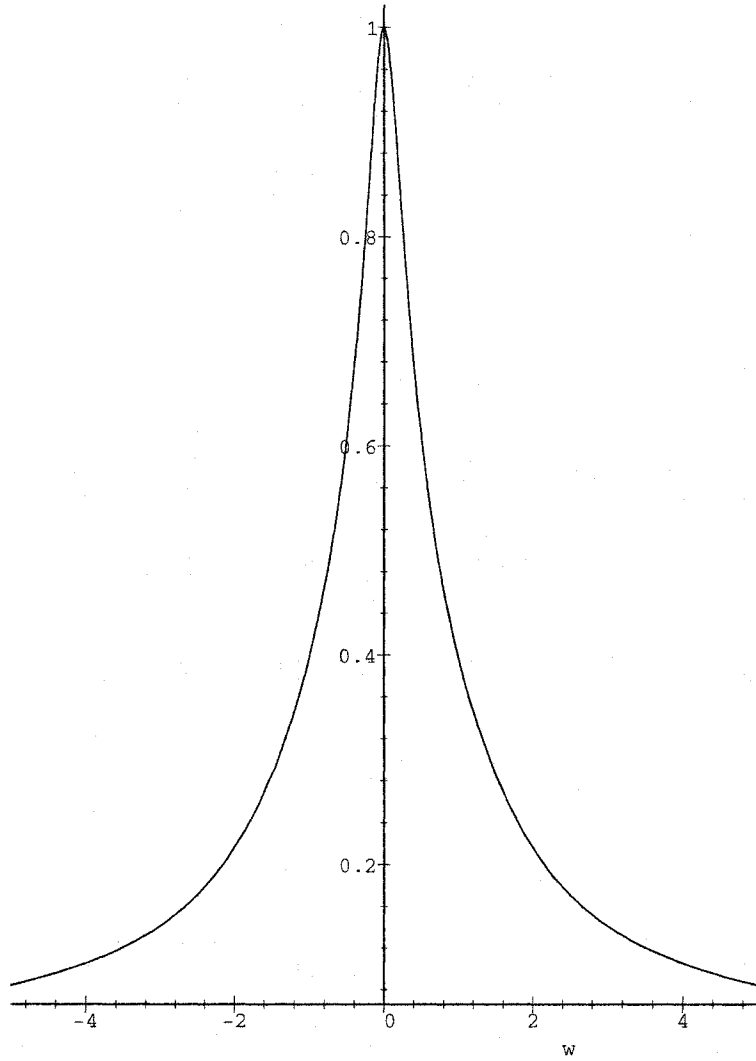
Figure 2.2. Conditional characteristic function for each interferer $\Phi_{I_k|B}(\omega)$ with $G = 31$ and $B = 30$.

44
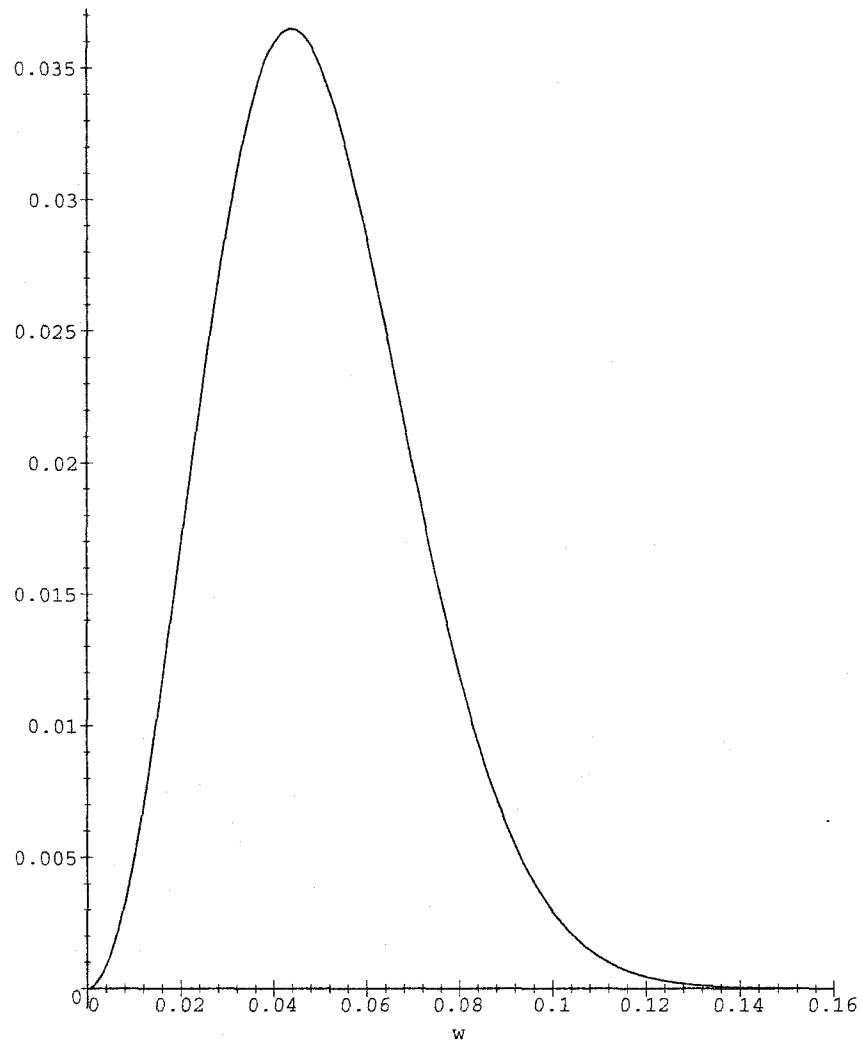
Figure 2.3. Integrand of (2.92) with $K = 5$, $G = 31$ and $B = 15$ for received SNR = 20 dB.

45
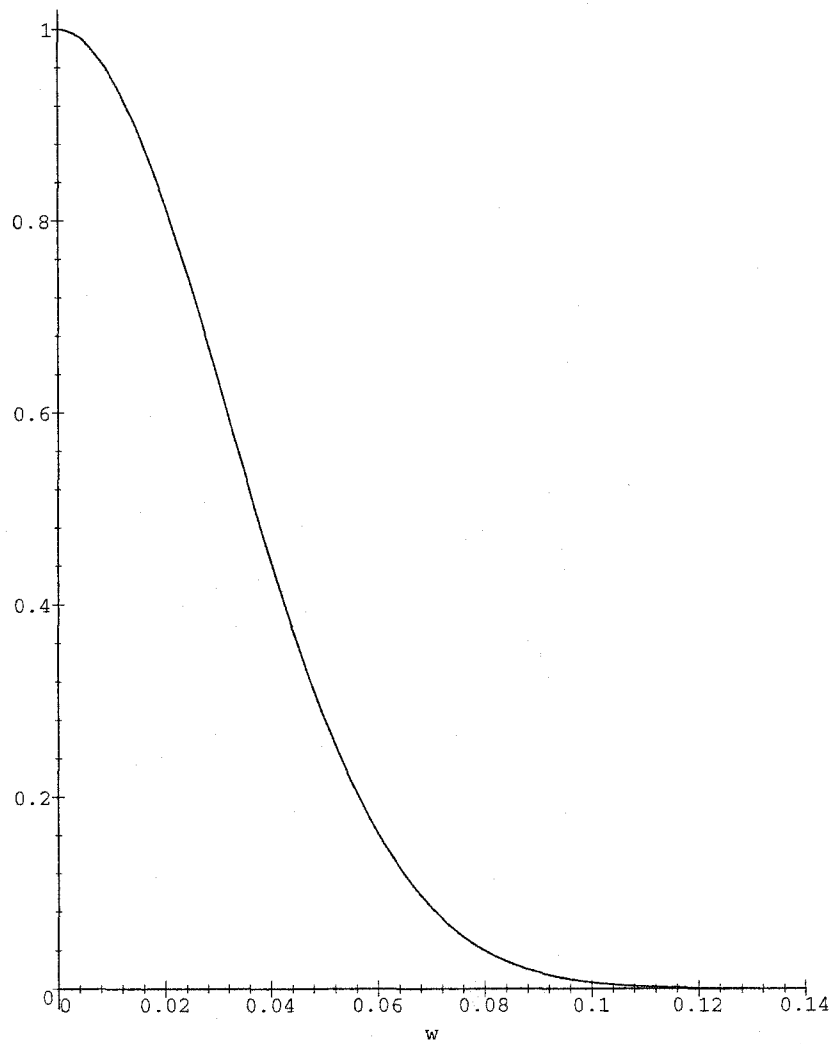
Figure 2.4. Integrand of (2.93) with $K = 5$, $G = 31$ and $B = 30$.

46
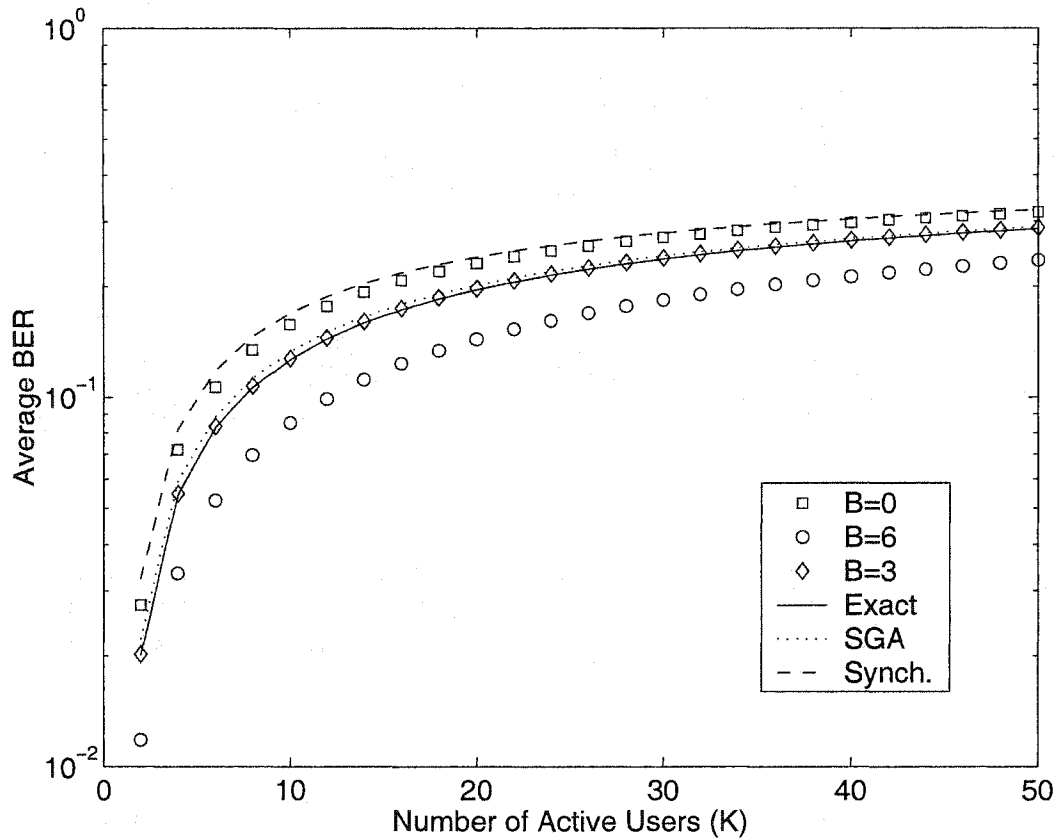
Figure 2.5. System BER performance without background noise for $G = 7$.

difficulties for chip synchronization [55]. These two extreme case performances provide upper and lower bounds for the BER experienced by any user in the system for a single particular transmission using a particular signature sequence. User sequences having the mean value of B, i.e. $(G-1)/2$, have transitions at half of the chip boundaries of User 1. As expected, the BER lies between the BER's of the $B = 0$ and $B = G - 1$ cases.

Fig. 2.5 shows the accurate BER computed using the characteristic function method described in the previous section, as well as the BER obtained by the SGA. Several interesting observations can be made. As shown, the accurate BER, averaging over all possible values of B's, is well approximated by the average BER obtained by assuming the mean value of B. We also observe from Fig.

47

2.5 that the SGA provides excellent approximation to the accurate BER computed via the characteristic function method and this is true even for the case of a single interferer. We observe, from our numerical results, that the BER estimates based on the SGA consistently *overestimate* the accurate BER. This is in contrast to the situation for AWGN channels where the SGA underestimates the BER [56], [38]. Fig. 2.6 examines a system with larger processing gain, $G = 31$. Similar observations and conclusions can be drawn. Comparing Fig. 2.5 with Fig. 2.6, we see that the SGA is a better approximation for $G = 31$ than $G = 7$. This is expected in consideration of a CLT. These tests on the validity of the SGA suggest there is no substantial benefit to using the SIGA rather than the SGA for our fading channel system. Indeed, our numerical results for $G = 31$ show that, in most cases, the improvements in the BER accuracy achieved using the SIGA are in the third significant digits.

Our definition of synchronous operation in Section 2.2 implies perfect chip alignment but no phase alignment. The BER's under synchronous operation are plotted in Figs. 2.5 and 2.6. We observe that the BER under synchronous operation is no better than the worst case BER (upper bound for $B = 0$) under asynchronous operation. The poor error rate performance under synchronous operation for our fading channel system agrees with previous findings for the AWGN channel [56].

Fig. 2.7 shows the accurate BER results and the SGA for a system operating with different background noise levels for $G = 31$. We observe that for all values of SNR the SGA provides excellent approximation to the accurate BER computed via the characteristic function method, even for a system with a single interfering signal.

All the BER's presented so far have been obtained using the first approach outlined in Section 2.6.1 for moderate levels of processing gain. This approach, which is based on the known decision statistic, however becomes cumbersome or even prohibitive to use for a system with a large, say $G = 127$, processing gain. Fortunately, in the second approach, the BER expression of (2.101), which is based on the simplified decision statistic, becomes useful for a system with large processing gain. In order to compare the computational complexities of these two approaches, we define the complexity here as the number of calls to $J(i, j)$ or $\tilde{J}(i, j)$, which are respectively defined in (2.81)

48
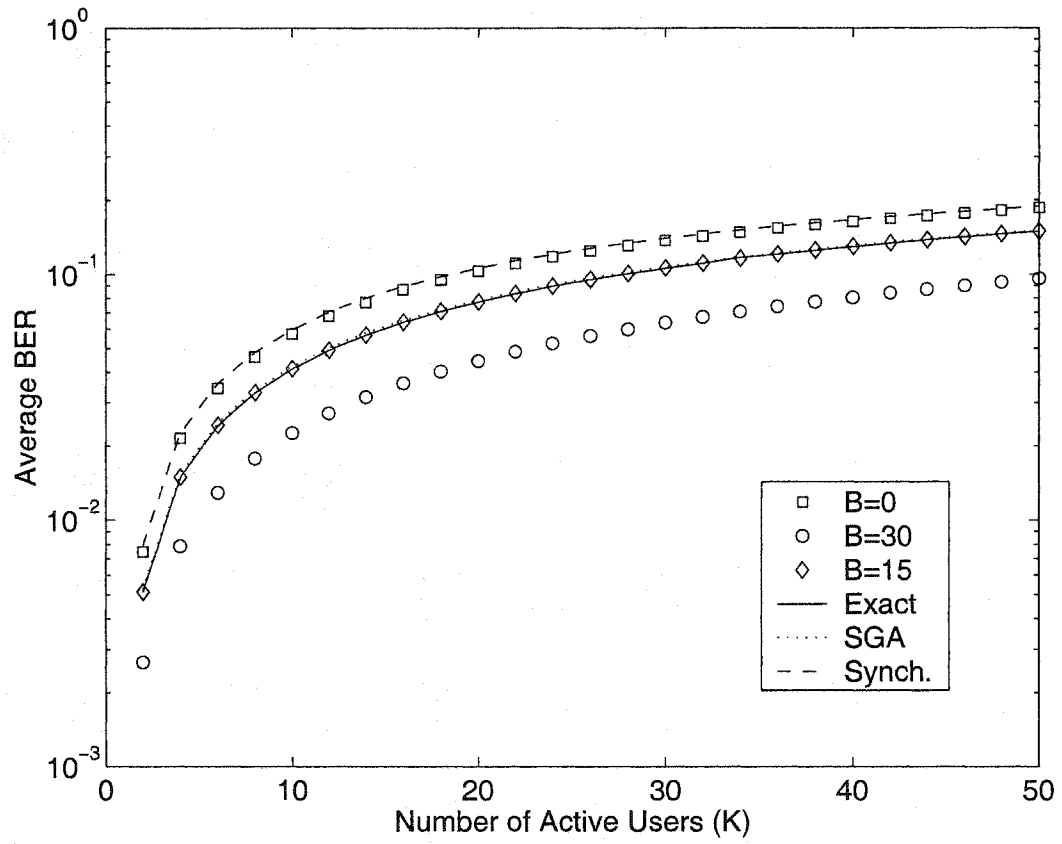
Figure 2.6. System BER performance without background noise for $G = 31$.

49
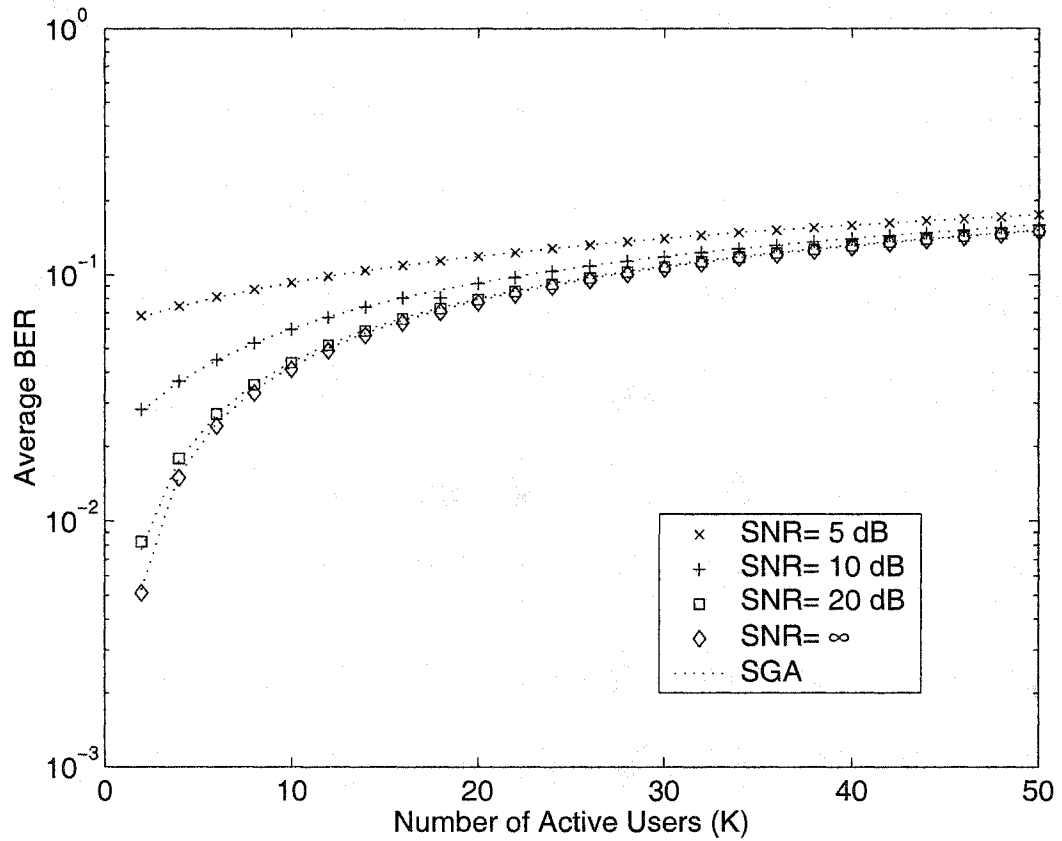
Figure 2.7. System BER performance with background noise for $G = 31$.

50

and (2.99). This measure of complexity is reasonable since these two functions have almost identical computational complexity (each calls the Q-function twice). To compute the total number of calls to $J(i,j)$ in the first approach, we first recognize the cardinality of the set $\{-B, -B+2, \ldots, B-2, B\}$ is $B+1$. Using the first approach, from (2.77a), we observe that for a particular value of B, the index j has $B+1$ different choices and the index i has $(G-1-B)+1 = G-B$ different choices. Since B takes integer values from 0 to $G-1$, to evaluate the CF at each ω, the total number of calls to $J(i,j)$ is

$$
\begin{aligned}
& 4\sum_{B=0}^{G-1}(G-B)(B+1) \\
= \; & 4\left[\sum_{B}^{G-1}G + (G-1)\sum_{B=0}^{G-1}B - \sum_{B=0}^{G-1}B^2\right] \\
= \; & \frac{2}{3}G(G+1)(G+2).
\end{aligned}
$$

On the other hand, with the second approach, from (2.97), only a total number of $(G+1)^2$ calls to $\tilde{J}(i,j)$ are required. For large processing gain, it is clear that the computational complexity of the second approach is an order smaller than that of the first approach. For example, with processing gain of $G=127$, only $16,384$ calls to $\tilde{J}(i,j)$ are required for each ω; while $1,398,016$ calls to $J(i,j)$ are required for the first approach.

Assuming an interference-limited environment, Table 2.1 tabulates the BER's obtained using the simplified approach outlined in Section 2.6.2 for a system with processing gain of $G=127$. In this table, we have also included the simulated BER's based on the raw decision statistic in (2.17). As shown, the BER's obtained using the simplified approach are in excellent agreement with the Monte Carlo results. In some cases, the accuracies are obtained even in the third significant digits. These results indicate that the loss in accuracies due to the independence assumption for the MAI terms is negligible. In Table 2.1, we have also included the BER's estimated with the SGA and the SIGA methods. It is obvious that both approximations are in good agreement with the exact results for a wide range of number of active users. Similar observations can be made from Table 2.2 in which the processing gain has been increased to $G=255$. Therefore, even though the MAI

51

of our DS-CDMA system is not exactly Gaussian, as shown in Section 2.6.1, the SGA gives quick and accurate estimation of the system performance in terms of the BER versus the number of active users.

2.8 Summary

Accurate, analytical solutions for the BER of a DS-CDMA system using random spreading sequences operating over Rayleigh fading channels have been derived. New closed-form expressions are provided for the characteristic function of the interfering signals. In contrast to previous analytical solutions, our new solutions are of moderate complexity, requiring a single numerical integration of an exponentially decaying positive integral for any number of system users. The solutions are suitable for small, moderate, and large values of processing gain. Any arbitrary degree of accuracy in the results can be achieved by using standard techniques of numerical integration. The new solutions have been applied to assess the validities of Gaussian BER approximations for Rayleigh fading and to compare the BER performances of asynchronous systems to synchronous systems in Rayleigh fading. Though only Rayleigh fading is considered in this chapter, the same analytical technique can be applied for a more general fading channel model. In Chapter 4, we will extend this work to a Nakagami-m fading model.

Table 2.1. Comparisons of average BER's for a DS-CDMA SSMA using random spreading sequences with processing gain $G = 127$ in an interference-limited environment.

Users (K)	SGA	SIGA	Simplified	Simulation
2	1.3072E-03	1.2961E-03	1.2987E-03	1.3058E-03
4	3.8911E-03	3.8588E-03	3.8619E-03	3.8215E-03
6	6.4352E-03	6.3828E-03	6.3863E-03	6.3732E-03
8	8.9406E-03	8.8689E-03	8.8729E-03	8.8134E-03
10	1.1408E-02	1.1318E-02	1.1323E-02	1.1334E-02
12	1.3839E-02	1.3731E-02	1.3737E-02	1.3765E-02
14	1.6234E-02	1.6109E-02	1.6115E-02	1.6106E-02
16	1.8593E-02	1.8453E-02	1.8460E-02	1.8479E-02
18	2.0919E-02	2.0764E-02	2.0771E-02	2.0771E-02
20	2.3211E-02	2.3042E-02	2.3049E-02	2.3014E-02
22	2.5471E-02	2.5287E-02	2.5296E-02	2.5317E-02
24	2.7699E-02	2.7502E-02	2.7512E-02	2.7465E-02
26	2.9896E-02	2.9686E-02	2.9697E-02	2.9727E-02
28	3.2062E-02	3.1840E-02	3.1852E-02	3.1742E-02
30	3.4199E-02	3.3966E-02	3.3978E-02	3.3856E-02
32	3.6307E-02	3.6063E-02	3.6076E-02	3.5945E-02
34	3.8386E-02	3.8131E-02	3.8146E-02	3.8181E-02
36	4.0437E-02	4.0173E-02	4.0188E-02	4.0215E-02
38	4.2462E-02	4.2188E-02	4.2204E-02	4.2203E-02
40	4.4460E-02	4.4177E-02	4.4194E-02	4.4110E-02

Table 2.2. Comparisons of average BER's for a DS-CDMA SSMA using random spreading sequences with processing gain $G = 255$ in an interference-limited environment.

Users (K)	SGA	SIGA	Simplified	Simulation
2	6.5231E-04	6.4957E-04	6.4961E-04	6.5949E-04
4	1.9494E-03	1.9411E-03	1.9413E-03	1.9560E-03
6	3.2363E-03	3.2228E-03	3.2231E-03	3.2293E-03
8	4.5133E-03	4.4948E-03	4.4951E-03	4.4553E-03
10	5.7805E-03	5.7570E-03	5.7574E-03	5.7574E-03
12	7.0381E-03	7.0097E-03	7.0102E-03	7.0004E-03
14	8.2861E-03	8.2529E-03	8.2536E-03	8.2065E-03
16	9.5246E-03	9.4868E-03	9.4876E-03	9.4879E-03
18	1.0753E-02	1.0711E-02	1.0712E-02	1.0763E-02
20	1.1974E-02	1.1927E-02	1.1928E-02	1.1841E-02
22	1.3184E-02	1.3133E-02	1.3134E-02	1.3198E-02
24	1.4387E-02	1.4331E-02	1.4332E-02	1.3968E-02
26	1.5580E-02	1.5520E-02	1.5522E-02	1.5394E-02
28	1.6764E-02	1.6701E-02	1.6703E-02	1.6692E-02
30	1.7940E-02	1.7873E-02	1.7874E-02	1.7842E-02
32	1.9107E-02	1.9036E-02	1.9038E-02	1.9004E-02
34	2.0266E-02	2.0191E-02	2.0193E-02	2.0266E-02
36	2.1416E-02	2.1338E-02	2.1340E-02	2.1124E-02
38	2.2558E-02	2.2476E-02	2.2478E-02	2.2218E-02
40	2.3693E-02	2.3607E-02	2.3609E-02	2.3333E-02

Chapter 3

Error Rate Analysis of Bandwidth-Efficient BPSK in

Nakagami Fading and Cochannel Interference

3.1 Introduction

The performances of mature wireless cellular systems are limited by fading and cochannel interference (CCI). Multipath propagation causes rapid signal fading and frequency reuse leads to cochannel interference. While the Rayleigh fading model has been widely used to represent fading environments, propagation conditions in some wireless systems may not be well described by this model, e.g., microcellular systems, where the fading is not as severe as Rayleigh fading. The Nakagami-m distribution can be used to model fading of various degrees of severity [57]. This is particularly useful for microcellular environments where the fading of the desired signal and the fadings of the interfering signals may be statistically different. In [84], a Nakagami/Nakagami model, denoted here as m_s/m_I, was proposed where the Nakagami fading parameter for the desired user (m_s) is not the same as the fading parameter for the undesired users (m_I). This fading and interference model is general enough to cover a wide range of fading and interference conditions. For example, Rayleigh fading is a special case of Nakagami-m fading, and Rician fading can be approximated reasonably well by Nakagami-m fading [57]. Furthermore, the Nakagami-m distribution is sometimes a good approximation to the log-normal distribution, which is considered a good model for

55

shadowing. Therefore, in this chapter, we will assume a m_S/m_I model to investigate the bit error rate (BER) performance of coherent binary phase shift keying (BPSK) modulation in a fading CCI environment.

The BER performance of digital modulations in fading and CCI was studied in [52], [43], [5], [4], [1], [17], [50]. In [52], using Stein's approach [69], Maciejko analyzed the BER performance of a coherent PSK system with a single interferer in Rayleigh fading. In [43], Krishnamurthi and Gupta derived closed-form BER expressions for PSK modulations with one Rayleigh-faded interferer. Chong and Leung recently studied the exact BER of a noncoherent frequency shift keying (NCFSK) system in fading and cochannel interference [17]. Beaulieu and Abu-Dayya analyzed the BER performance for bandlimited QPSK using an approximate Fourier series method [5]. This work was extended in [4] to some limited diversity cases. All these works consider only Rayleigh-faded interferers. Ma *et al.* recently studied the BER of binary coherent PSK and differential PSK for diversity systems assuming multiple Rician-faded interferers [50]. The model assumed in [50] is, however, a simplified one. It allows only synchronized interferers. There are important shortcomings inherent in this assumption. First, in many practical systems, the interferers are not synchronized. Second, this assumption circumvents dealing with the cross-signal intersymbol interference (ISI) that exists in practical systems that use bandwidth efficient pulse shaping. In a recent letter [1], Aalo and Zhang derived a BER expression for coherent BPSK in CCI and Nakagami-m fading. The analysis in [1, eqn. (9)] assumes a BER expression that is valid only for the case of a BPSK signal corrupted by additive white Gaussian noise (AWGN). This assumption is not rigorously correct for the transmission environment assumed. It can be justified as an approximation by assuming that the total interference is Gaussian. However, as shown in this paper, the Gaussian approximation (GA) can yield poor BER estimates under certain operating conditions.

In this work, building on the system model used in [5], we use a characteristic function (CF) method to derive a precise BER expression for a BPSK modulated signal in CCI and AWGN. Our BER expression is general. It takes account of arbitrary pulse shaping, symbol timing asynchronism between the desired user and the undesired users, as well as the cross-signal intersymbol interference

caused by each interfering signal. Thus, our results are applicable to practical BPSK systems. They are used in application examples to draw two interesting conclusions. First, the results are used to show that a novel pulse shape published in [6] outperforms the widely used raised-cosine pulse shape in microcellular CCI environments. Second, the results are used to show that fading of an interfering signal worsens (increases) the BER of the desired signal rather than improving (decreasing) it, perhaps contrary to what one might expect. Further, we use our results to assess the accuracy of a Gaussian approximation. We point out that only BPSK modulation is considered here. While our approach permits deriving new and useful precise results for BPSK, it can not be extended to quaternary phase shift keying (QPSK) in a straightforward manner.

This chapter is organized as follows. In Section 3.2, we describe our system model. In Section 3.3, we derive closed form expressions for the PDF and CF of the Nakagami fading quadrature component. These analytical expressions will be useful in the ensuing development. In 3.4, precise BER expressions using the CF method are derived for both asynchronous and synchronous interfering signals. An approximate BER expression is developed in Section 3.5 using the Gaussian assumption. Numerical results and discussion are presented in Section 3.6. In particular, the BER performance of a novel pulse shape is compared to that of the raised-cosine pulse shape. In addition, the effect of fading of an interference signal on the BER of the desired signal is examined and an unexpected conclusion is drawn. In Section 3.7, we summarize major findings of this chapter.

3.2 System Model

The transmitted signal of the desired user is

$$S_d(t) = \sqrt{2P_s T} s_d(t) \cos(\omega_c t) \tag{3.1}$$

where $\omega_c = 2\pi f_c$ and f_c is the carrier frequency in Hertz; $s_d(t)$ is the desired user baseband signal and it is given by

$$s_d(t) = \sum_{k=-\infty}^{+\infty} a[k] g_T(t - kT) \tag{3.2}$$

57

where $1/T$ is the symbol transmission rate and $g_T(t)$ is the impulse response of the transmitter pulse shaping filter and its Fourier transform is denoted by $G_T(f)$. We assume that the transmitter pulse shape has its energy normalized to unity, i.e., $\int_{-\infty}^{+\infty} g_T^2(t)dt = 1$. In BPSK modulation, $a[k]$ takes values from $\{+1, -1\}$ with equal probabilities. The transmitted power for the desired user signal is P_s. To show this, from (3.2), the power spectral density (PSD) of the data stream process, $s_d(t)$, is [36, p. 239]

$$S_d(f) = \frac{1}{T}|G_T(f)|^2 \sum_{n=-\infty}^{+\infty} \mathbb{E}[a[k]a[k-n]]\exp(-j2\pi nfT)] \qquad (3.3)$$

$$= \frac{1}{T}|G_T(f)|^2 \qquad (3.4)$$

where $\mathbb{E}[\cdot]$ denotes the expectation. For BPSK modulation with uncorrelated data bits, we have $\mathbb{E}[a[k]a[k-n]] = 1$, when $n = 0$, and zero otherwise. Therefore, the power spectral density of the transmitted signal becomes

$$S(f) = \frac{(\sqrt{2P_sT})^2}{4}\left[S_d(f-f_c)+S_d(f+f_c)\right] \qquad (3.5)$$

and the power of the transmitted signal for the desired user is

$$\int_{-\infty}^{+\infty} S(f)df = \frac{P_sT}{2}\left[\int_{-\infty}^{+\infty} S_d(f-f_c)df + \int_{-\infty}^{+\infty} S_d(f+f_c)df\right] \qquad (3.6)$$

$$= \frac{P_sT}{2}\left[\int_{-\infty}^{+\infty} \frac{1}{T}|G_T(f-f_c)|^2df + \int_{-\infty}^{+\infty} \frac{1}{T}|G_T(f+f_c)|^2df\right] \qquad (3.7)$$

$$= \frac{P_s}{2}\left[\int_{-\infty}^{+\infty} g_T^2(t)dt + \int_{-\infty}^{+\infty} g_T^2(t)dt\right] \qquad (3.8)$$

$$= \frac{P_s}{2}[1+1] \qquad (3.9)$$

$$= P_s \qquad (3.10)$$

where in obtaining (3.8), we have invoked Parseval's theorem.

When $S_d(t)$ is transmitted, it is subject to fading, as well as interference caused by other user signals occupying the same channel. A reasonable assumption is that all interfering signals have the same modulation format as the desired user signal. Thus, the transmitted signal for the ith interfering signal is

$$S_i(t) = \sqrt{2P_iT}s_i(t)\cos(\omega_c t) \qquad (3.11)$$

58

where P_i is the transmitted power for the ith interfering user signal and $s_i(t)$ is the ith interferer baseband signal and it is given by

$$s_i(t) = \sum_{k=-\infty}^{+\infty} b_i[k] g_T(t - kT) \qquad (3.12)$$

where $b_i[k]$ is the ith interferer's information bit taking values from $\{+1, -1\}$ with equal probabilities.

We assume that both the desired user signal and the L interfering signals are transmitted over a frequency-nonselective slowly fading channel. The received signal becomes

$$R(t) = \sqrt{2P_s T R_s} s_d(t) \cos(\omega_c t + \theta_s) + \sum_{i=1}^{L} \sqrt{2P_i T R_i} s_i(t - \tau_i) \cos(\omega_c(t - \tau_i) + \theta_i) + n(t) \qquad (3.13)$$

where τ_i, representing the symbol asynchronism, is the possible random misalignment of the ith interfering user symbol with respect to the desired user symbol, and it is assumed to be uniform over $[0, T)$. In (3.13), $n(t)$ is a zero-mean white Gaussian background noise process with two-sided PSD $N_0/2$ (Watt/Hz); the phases θ_s and θ_i, for the desired user and the ith interferer, respectively, representing the random phases introduced by the fading channels, are assumed to be mutually independent and uniformly distributed over $[0, 2\pi)$. The respective random variables (RV's)[1] R_s and R_i represent the fading channel gains. We assume that the desired user's fading amplitude follows the Nakagami-m distribution with parameters (m_s, Ω_s) and its PDF is given by [63]

$$f_{R_s}(r_s) = \frac{2}{\Gamma(m_s)} \left(\frac{m_s}{\Omega_s}\right)^{m_s} r_s^{2m_s - 1} e^{-\frac{m_s r_s^2}{\Omega_s}} \qquad (3.14)$$

where $\mathbb{E}[R_s^2] = \Omega_s$. Similarly, we assume that all L interfering users' fading amplitudes follow the Nakagami-m distribution with parameter (m_I, Ω_I) and with PDF given by

$$f_{R_i}(r_i) = \frac{2}{\Gamma(m_I)} \left(\frac{m_I}{\Omega_I}\right)^{m_I} r_i^{2m_I - 1} e^{-\frac{m_I r_i^2}{\Omega_I}} \qquad (3.15)$$

where $\mathbb{E}[R_i^2] = \Omega_I$ for $i = 1, 2, \ldots, L$. Note that these parameters are not necessarily identical to those of the desired user. We further assume that both the desired user and all the interfering users experience independent fadings. The fading parameters m_s in (3.14) and m_I in (3.15) control the

---

[1]Under the slow fading assumption, the fading process is constant over a symbol duration.

59

severity of the fading conditions. For the worst transmission cases, when m_s or m_I equals 0.5, the fading distribution corresponds to a one-sided Gaussian distribution with a large tail probability. For the best transmission case, in the limit, when m_s or m_I approaches infinity, the fading distribution corresponds to an impulsive function, a nonfading channel.

Since the fading is assumed slow, a coherent receiver can be implemented. In the coherent receiver design, the desired user's signal phase is assumed to be estimated and compensated perfectly. Therefore, the demodulated signal becomes

$$
\begin{aligned}
Z(t) &= R(t)\cos(\omega_c t + \theta_s) \\
&= \sqrt{2P_s T}\, R_s s_d(t)\cos(\omega_c t + \theta_s)\cos(\omega_c t + \theta_s) \\
&\quad + \sum_{i=1}^{L} \sqrt{2P_i T}\, R_i s_i(t - \tau_i)\cos(\omega_c t - \omega_c \tau_i + \theta_i)\cos(\omega_c t + \theta_s) \\
&\quad + n(t)\cos(\omega_c t + \theta_s) \\
&= \sqrt{\frac{P_s T}{2}}\, R_s s_d(t)[\cos(0) + \cos(2\omega_c t + 2\theta_s)] \\
&\quad + \sum_{i=1}^{L} \sqrt{\frac{P_i T}{2}}\, R_i s_i(t - \tau_i)[\cos(\theta_i - \theta_s - \omega_c \tau_i) + \cos(2\omega_c t + \theta_i + \theta_s - \omega_s \tau_i)] \\
&\quad + n(t)\cos(\omega_c t + \theta_s).
\end{aligned}
\tag{3.16}
$$

The demodulated signal is then passed through a low-pass filter with spectrum matched to the spectrum of the transmitter pulse shape. The frequency response of this filter is zero outside the interval $[-(1+\alpha)/2T, (1+\alpha)/2T]$ where $0 \le \alpha \le 1$. Since $f_c \gg 1/T$ for $\alpha \le 1$, the double frequency components in (3.16) can be eliminated by the low-pass filter and the output becomes

$$
Z_{\mathrm{LP}}(t) = \sqrt{\frac{P_s T}{2}}\, R_s V_s(t) + \sum_{i=1}^{L} \sqrt{\frac{P_i T}{2}}\, R_i V_i(t)\cos(\phi_i) + n_0(t)
\tag{3.17}
$$

where

$$
V_s(t) = \sum_{k=-\infty}^{+\infty} a[k]g(t - kT)
\tag{3.18}
$$

and

$$
V_i(t) = \sum_{k=-\infty}^{+\infty} b[k]g(t - kT - \tau_i)
\tag{3.19}
$$

60

where $\phi_i = \theta_i - \theta_s - \omega_c \tau_i$ is assumed to be uniformly distributed over $[0, 2\pi)$ and $n_0(t)$ is the filtered Gaussian noise process. Here $g(t)$ is the overall impulse response of the cascade of the transmitter and receiver filters. In this work, we assume that this overall impulse response is a Nyquist pulse [63]. Two Nyquist pulses are considered in this paper. The first is the popular raised-cosine (RC) pulse which is widely used in modem design. The RC pulse is given by [63]

$$g(t) = \frac{\sin(\pi t/T)}{\pi t/T} \cdot \frac{\cos(\pi \alpha t/T)}{1 - 4\alpha^2 t^2/T^2} \tag{3.20}$$

and its spectrum is

$$G_{\mathrm{RC}}(f) = \begin{cases} T & 0 \leq |f| \leq \frac{1-\alpha}{2T} \\ \frac{T}{2}\left\{ 1 + \cos\left[\frac{\pi T}{\alpha}\left(|f| - \frac{1-\alpha}{T} \right) \right] \right\} & \frac{1-\alpha}{2T} \leq |f| \leq \frac{1+\alpha}{2T} \\ 0 & |f| > \frac{1+\alpha}{2T} \end{cases} \tag{3.21}$$

where α is the pulse shaping factor (also called the excess bandwidth) whose value is restricted to be between zero and one. The second pulse considered in this study is the pulse recently proposed by Beaulieu *et al.* [6]. It is given by

$$g(t) = \frac{\sin(\pi t/T)}{\pi t/T} \cdot \frac{4\beta \pi t \sin(\pi \alpha t/T) + 2\beta^2 \cos(\pi \alpha t/T) - \beta^2}{4\pi^2 t^2 + \beta^2} \tag{3.22}$$

where $\beta = \frac{2T\ln 2}{\alpha}$. The spectrum of this pulse is [2]

$$G_{\mathrm{BTRC}}(f) = \begin{cases} T & 0 \leq |f| \leq \frac{1-\alpha}{2T} \\ T\exp\left\{ \frac{2T\ln 2}{\alpha}\left[\frac{1-\alpha}{2T} - |f| \right] \right\} & \frac{1-\alpha}{2T} \leq |f| \leq \frac{1}{2T} \\ T - T\exp\left\{ \frac{2T\ln 2}{\alpha}\left[|f| - \frac{1+\alpha}{2T} \right] \right\} & \frac{1}{2T} \leq |f| \leq \frac{1+\alpha}{2T} \\ 0 & |f| \geq \frac{1+\alpha}{2T} \end{cases} \tag{3.23}$$

where α is again the excess bandwidth. This new pulse, termed better than raised-cosine (BTRC) in this work, has a better eye diagram, and a smaller symbol error probability in the presence of ISI and symbol timing error in a baseband system [6]. In this chapter, we will show that the BTRC pulse also outperforms the RC pulse in fading and CCI environments for the system model considered.

[2]Eqns. (3.20), (3.23), (3.22), respectively, correct typographical errors in [6, eqns. (2), (3), and (4)].

61
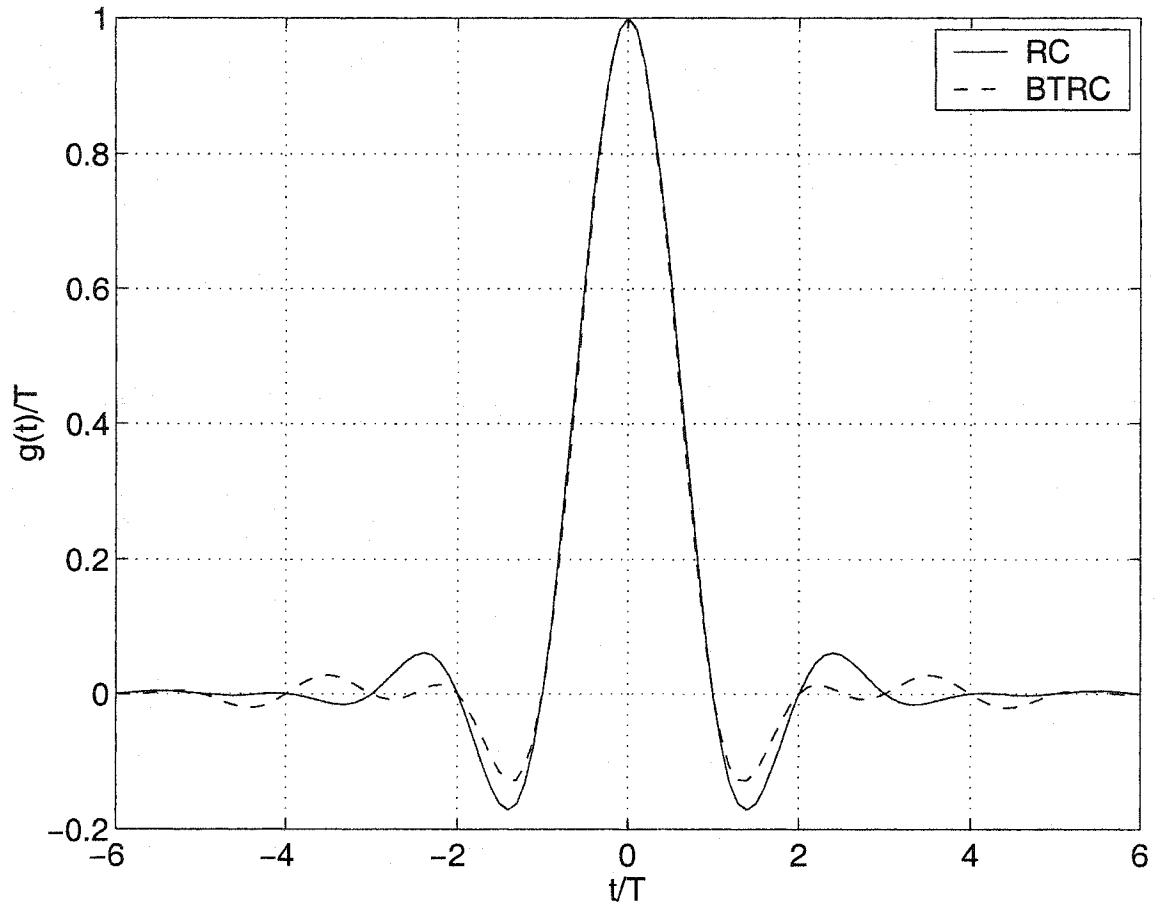
Figure 3.1. Normalized RC pulse and BTRC pulse with excess bandwidth ($\alpha = 0.35$).

The normalized RC pulse and BTRC pulse are plotted in Fig. 3.1 for a representative α value. The corresponding spectra are plotted in Fig. 3.2. We note that the RC and BTRC pulse have the same amount of excess bandwidth. Therefore, these performance improvements are obtained at no additional cost. Unless otherwise specified, $\alpha = 0.5$ is used in the numerical results. In the development that follows, it will be clear that the value of α offers a trade-off between spectral efficiency and detection performance.

Without loss of generality, we assume that the bit $a[0]$ is to be detected. Sampling $Z_{\mathrm{LP}}(t)$ at $t = 0$, the decision statistic becomes

$$Z_{\mathrm{LP}}[0] = \sqrt{\frac{P_s T}{2}} R_s a[0] + \sum_{i=1}^{L} \sqrt{\frac{P_i T}{2}} R_i \cos(\phi_i) \rho_i + n_0 \qquad (3.24)$$

62
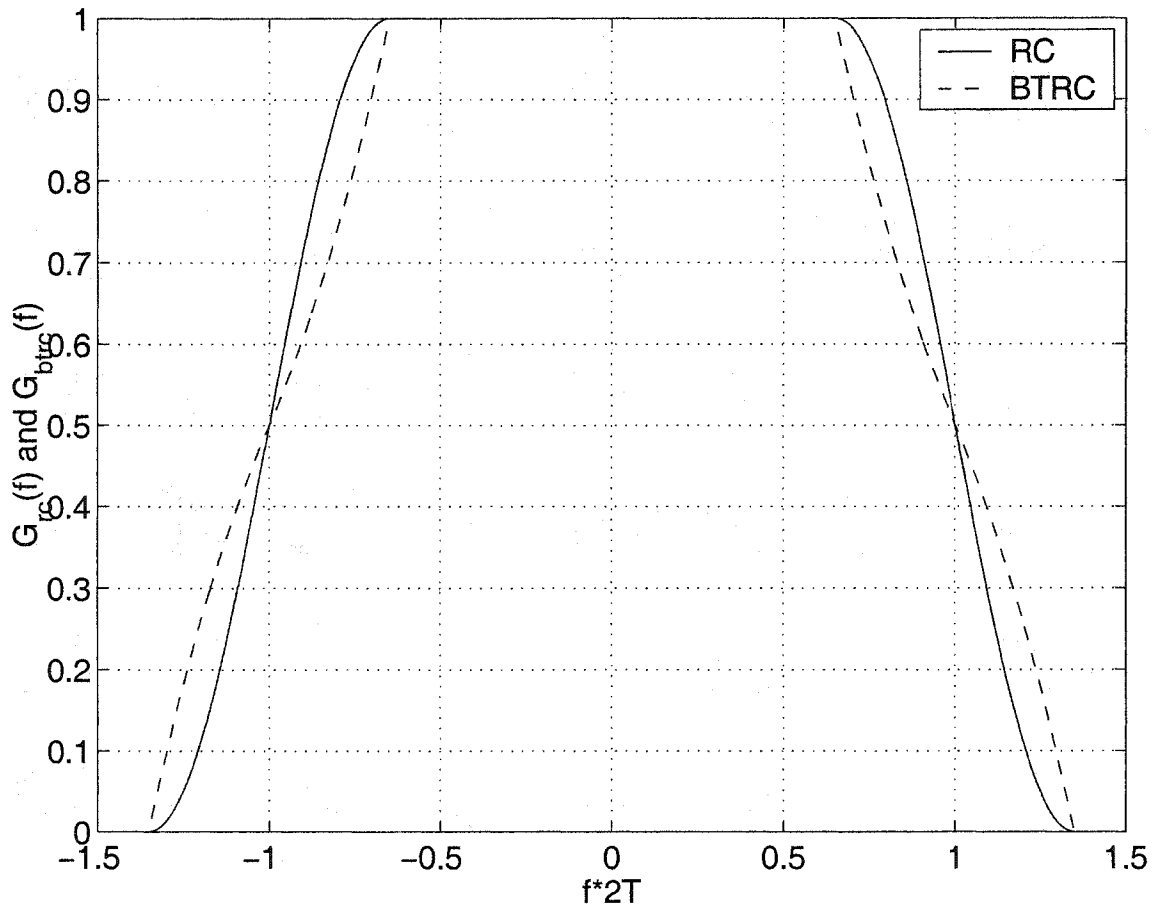
Figure 3.2. Normalized spectra for RC pulse and BTRC pulse with excess bandwidth ($\alpha = 0.35$).

where

$$\rho_i = \sum_{k=-\infty}^{+\infty} b_i[k]g(-kT - \tau_i).$$ (3.25)

In (3.24), the first term represents the desired signal component; the second term represents the undesired CCI components and each of these components contains cross-signal ISI terms from each interferer; the third term represents the undesired noise component, where $n_0 = n_0(0)$ is a zero-mean Gaussian RV. Without loss of generality, we assume that the output noise power is unity, i.e., $\text{var}[n_0] = 1$. Therefore, with our conventions, the (average) signal-to-noise power ratio and the (average) signal-to-interference power ratio for our system model can be expressed, respectively, as

$$SNR\ (dB) = 10\log_{10}\left(\frac{P_s T \Omega_s}{2}\right)$$ (3.26)

and

$$SIR\ (dB) = 10\log_{10}\left(\frac{\Omega_s}{\Omega_I} \cdot \frac{P_s}{\sum_{i=1}^{L} P_i}\right).$$ (3.27)

3.3 PDF and CF of Nakagami Quadrature Components

In this section, we take a digression and derive closed-form expressions for the PDF and the CF of in-phase and quadrature components for Nakagami-m fading process (assuming uniform random phase). These expressions are useful in the development of the precise BER calculation using the characteristic function method.

We denote the fading amplitude by R which is Nakagami-m distributed with parameters (m, Ω). We let Θ be its corresponding random phase which is distributed uniformly over $[0, 2\pi)$. We wish to derive the PDF and the CF of the in-phase and quadrature components i.e., $X = R\cos\Theta$ and $Y = R\sin\Theta$ [3], assuming that the fading amplitude and phase are independent. Since each component has the same distribution, we will only consider the in-phase component $X = R\cos\Theta$ here. We will first consider the case of integer m values, and then consider more general case of arbitrary m

---

[3] In general, the in-phase and the quadrature components are independent. We are slightly abusing the terminology here since it can be shown that the in-phase component ($X = R\cos\Theta$) and the quadrature component ($Y = R\sin\Theta$) are dependent except for the case when $m = 1$.

values. The results for the integer case are included because the its derivation does not depend on any complicated integral identity, and more importantly, these closed-form expressions can reveal some interesting structure, which may not be easily obtained otherwise.

3.3.1 Case of integer m values

The conditional distribution of X given R can be shown to be [60, p. 98]

$$f_{X|R}(x|r) = \frac{2}{2\pi\sqrt{r^2 - x^2}}, \quad |x| < r. \tag{3.28}$$

Averaging (3.28) over the PDF of R, we have

$$
\begin{aligned}
f_X(x) &= \int_{|x|}^{+\infty} \frac{2}{\Gamma(m)} \left(\frac{m}{\Omega}\right)^m r^{2m-1} e^{-\frac{mr^2}{\Omega}} \frac{2}{2\pi\sqrt{r^2 - x^2}} dr \\
&= \frac{1}{2\pi} \frac{2}{\Gamma(m)} \left(\frac{m}{\Omega}\right)^m \int_0^{+\infty} \frac{(u + x^2)^{m-1}}{\sqrt{u}} e^{-\frac{m}{\Omega}(u + x^2)} du \\
&= \frac{1}{2\pi} \frac{2}{\Gamma(m)} \left(\frac{m}{\Omega}\right)^m e^{-\frac{m}{\Omega}x^2} \int_0^{+\infty} \sum_{k=0}^{m-1} \binom{m-1}{k} u^{k-\frac{1}{2}} x^{2(m-1-k)} e^{-\frac{m}{\Omega}u} du \\
&= \frac{1}{2\pi} \frac{2}{\Gamma(m)} \left(\frac{m}{\Omega}\right)^m e^{-\frac{m}{\Omega}x^2} \sum_{k=0}^{m-1} \binom{m-1}{k} x^{2(m-1-k)} \int_0^{+\infty} u^{k-\frac{1}{2}} e^{-\frac{m}{\Omega}u} du.
\end{aligned}
\tag{3.29}
$$

In the derivation of (3.29), we have used the substitution $u = r^2 - x^2$ and the binomial expansion. Applying the integral identity [33, (3.381)]

$$\int_0^{+\infty} u^n e^{-au} du = \frac{\Gamma(n+1)}{a^{n+1}}$$

in (3.29), we get

$$f_X(x) = \frac{1}{2\pi} \frac{2}{\Gamma(m)} \left(\frac{m}{\Omega}\right)^m e^{-\frac{m}{\Omega}x^2} \sum_{k=0}^{m-1} \binom{m-1}{k} \frac{\Gamma(k + \frac{1}{2})}{(\frac{m}{\Omega})^{k+\frac{1}{2}}} x^{2(m-1-k)}. \tag{3.30}$$

Letting $l = m - 1 - k$ and using the fact that $\binom{m-1}{l} = \binom{m-1}{m-1-l}$, we have the PDF of the Nakagami quadrature component as

$$f_X(x) = \underbrace{\frac{1}{\sqrt{2\pi}\sqrt{\frac{\Omega}{2m}}} e^{-\frac{m}{\Omega}x^2}}_{\text{Gaussian PDF}} \sum_{l=0}^{m-1} A_l x^{2l} \tag{3.31a}$$

where

$$A_l = \frac{\binom{m-1}{l}}{\sqrt{\pi}} \frac{\Gamma(m - l - \frac{1}{2})}{\Gamma(m)} \left(\frac{m}{\Omega}\right)^l. \tag{3.31b}$$

65

We observe that the PDF of X takes the form of a product of a Gaussian PDF with a polynomial function of even powers, where the highest even power is $2(m-1)$.

By definition, the CF of X, $\Phi_X(\omega)$, is

$$
\begin{aligned}
\Phi_X(\omega) &= \int_{-\infty}^{+\infty} f_X(x) e^{j\omega x} dx \\
&= \int_{-\infty}^{+\infty} \frac{1}{\sqrt{2\pi}\sqrt{\frac{\Omega}{2m}}} e^{-\frac{m}{\Omega}x^2} \sum_{l=0}^{m-1} A_l x^{2l} e^{j\omega x} dx
\end{aligned}
\tag{3.32}
$$

where $j^2 = -1$. Completing the square gives,

$$
\exp\left\{-\frac{m}{\Omega}x^2 + j\omega x\right\} = \exp\left\{-\frac{m}{\Omega}\left(x - j\frac{\omega\Omega}{2m}\right)^2\right\} \exp\left\{-\frac{\Omega}{4m}\omega^2\right\}
$$

and the CF of X becomes

$$
\Phi_X(\omega) = \underbrace{\exp\left\{-\frac{\Omega}{4m}\omega^2\right\}}_{Gaussian\ CF} \sum_{l=0}^{m-1} A_l M_{2l}
\tag{3.33}
$$

where

$$
M_{2l} = \int_{-\infty}^{+\infty} x^{2l} \frac{1}{\sqrt{2\pi}\sqrt{\frac{\Omega}{2m}}} \exp\left\{-\frac{(x - j\frac{\omega\Omega}{2m})^2}{2(\frac{\Omega}{2m})}\right\} dx.
\tag{3.34}
$$

Let $s = x - j\frac{\omega\Omega}{2m}$ be a complex RV, and we have

$$
M_{2l} = \int_{-\infty-j\frac{\omega\Omega}{2m}}^{+\infty-j\frac{\omega\Omega}{2m}} \left(s + j\frac{\omega\Omega}{2m}\right)^{2l} \frac{1}{\sqrt{2\pi}\sqrt{\frac{\Omega}{2m}}} \exp\left\{-\frac{s^2}{2(\frac{\Omega}{2m})}\right\} ds
\tag{3.35}
$$

where the integration is along a line parallel to the real axis. Consider the contour of integration shown in Fig. 3.3. Since the integrand function is analytical (has no poles) inside the contour of integration, the integration around the contour is zero by Cauchy integral theorem. It is straightforward to show that the integrations along each of two vertical contours become zero as a goes to infinity. Therefore,

$$
\begin{aligned}
M_{2l} &= \int_{-\infty}^{+\infty} \sum_{k=0}^{2l} \binom{2l}{k}\left(j\frac{\omega\Omega}{2m}\right)^k s^{2l-k} \frac{1}{\sqrt{2\pi}\sqrt{\frac{\Omega}{2m}}} \exp\left\{-\frac{s^2}{2(\frac{\Omega}{2m})}\right\} ds \tag{3.36} \\
&= \sum_{k=0}^{2l} \binom{2l}{k}\left(j\frac{\omega\Omega}{2m}\right)^k \int_{-\infty}^{+\infty} s^{2l-k} \frac{1}{\sqrt{2\pi}\sqrt{\frac{\Omega}{2m}}} \exp\left\{-\frac{s^2}{2(\frac{\Omega}{2m})}\right\} ds \tag{3.37} \\
&= \sum_{k=0\ k\ even}^{2l} \binom{2l}{k}\left(j\frac{\omega\Omega}{2m}\right)^k \int_{-\infty}^{+\infty} s^{2l-k} \frac{1}{\sqrt{2\pi}\sqrt{\frac{\Omega}{2m}}} \exp\left\{-\frac{s^2}{2(\frac{\Omega}{2m})}\right\} ds \tag{3.38}
\end{aligned}
$$

66
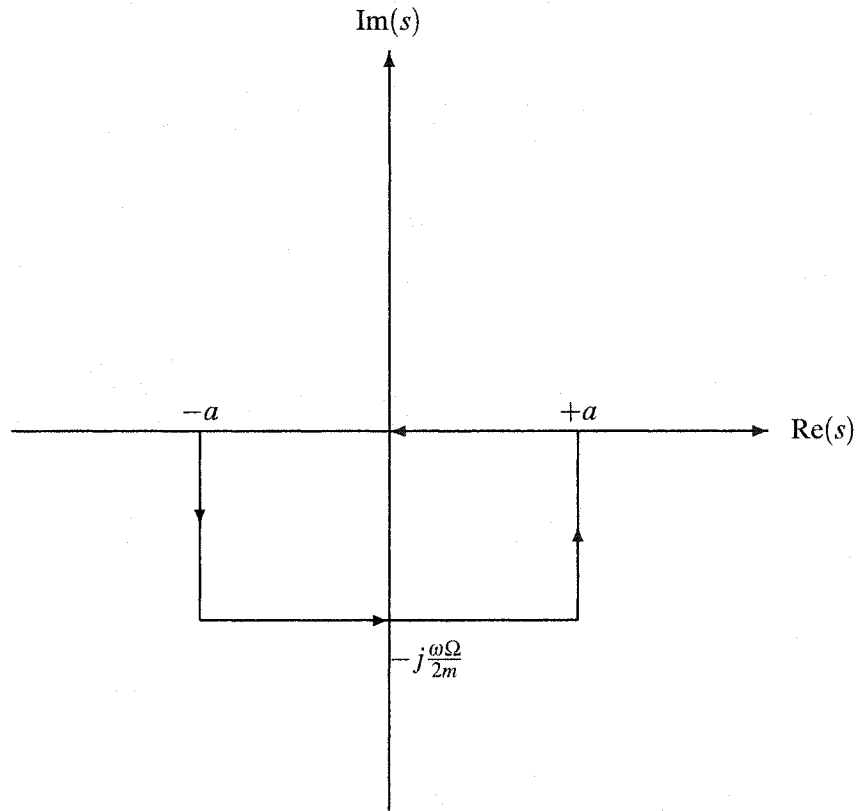
Figure 3.3. The contour of integration for evaluating (3.35) when $\Omega > 0$.

$$= \sum_{\substack{k=0 \\ k \text{ even}}}^{2l} \binom{2l}{k} \left(j\frac{\omega\Omega}{2m}\right)^k (2l-k-1)!! \left(\sqrt{\frac{\Omega}{2m}}\right)^{2l-k} \tag{3.39}$$

where $(n-1)!! = (n-1)(n-3)\cdots(5)(3)(1)$. In deriving (3.36), we have used the central moment

expression for the zero-mean Gaussian RV. Here M_{2l} can be interpreted as the even moments of a

Gaussian RV with mean $j\frac{\omega\Omega}{2m}$ and variance $\frac{\Omega}{2m}$.

Combining (3.32) and (3.36), we observe that, similar to the PDF of X, the CF of X takes the

form of a product of a Gaussian CF with a polynomial function of even powers, where the highest

even power is $2(m-1)$. In addition, as expected, the CF of X is real since the PDF of X is even

symmetric about zero.

67

3.3.2 Case of arbitrary m values

For the case of arbitrary m values, it is advantageous to derive the CF first. To show this, we use the definition of CF as $\Phi_X(\omega) = \mathbb{E}[e^{j\omega X}]$ and invoke the fundamental theorem of expectation [81] as well as the independence assumption for R and Θ, and get

$$
\begin{aligned}
\Phi_X(\omega) &= \int_0^{+\infty} f_R(r)dr \left[\int_0^{2\pi} \frac{1}{2\pi} e^{jr\omega\cos\theta} d\theta \right] \tag{3.40} \\
&= \int_0^{+\infty} f_R(r)dr \left[\frac{1}{2\pi} \int_0^{\pi} e^{jr\omega\cos\theta} d\theta + \frac{1}{2\pi} \int_\pi^{2\pi} e^{jr\omega\cos\theta} d\theta \right] \tag{3.41} \\
&= \int_0^{\infty} f_R(r)dr \left[\frac{1}{2\pi} \int_0^{\pi} (e^{jr\omega\cos\theta} + e^{-jr\omega\cos\theta}) d\theta \right] \tag{3.42} \\
&= \int_0^{\infty} f_R(r)dr \left[\frac{1}{\pi} \int_0^{\pi} \cos(r\omega\cos\theta) d\theta \right] \tag{3.43} \\
&= \int_0^{\infty} J_0(r\omega) f_R(r)dr \tag{3.44} \\
&= {}_1F_1\left(m; 1; -\frac{\Omega}{4m}\omega^2 \right) \tag{3.45}
\end{aligned}
$$

where $J_0(\cdot)$ is the 0th order Bessel function of the first kind and it is defined as $J_0(z) = \frac{1}{\pi} \int_0^\pi \cos(z\sin\theta)d\theta = \frac{1}{\pi} \int_0^\pi \cos(z\cos\theta)d\theta$ [3] and the last equality follows from a complicated integral identity [33, 6.631]

$$
\int_0^{+\infty} x^\mu e^{-\alpha x^2} J_\nu(\beta x)dx = \frac{\beta^\nu \Gamma(\frac{1}{2}\nu + \frac{1}{2}\mu + \frac{1}{2})}{2^{\nu+1}\alpha^{\frac{1}{2}(\mu+\nu+1)}\Gamma(\nu+1)} \\
\times {}_1F_1\left(\frac{\nu+\mu+1}{2}; \nu+1; -\frac{\beta^2}{4\alpha} \right) \tag{3.46}
$$

where $J_\nu(\cdot)$ is the νth order Bessel function of the first kind and ${}_1F_1(\cdot;\cdot;\cdot)$ is the confluent hypergeometric function, which is also called Kummer-M function [3]. Using Kummer's transformation [3]

$$
{}_1F_1(a;b;z) = e^z {}_1F_1(b-a;b;-z), \tag{3.47}
$$

the CF of X can be alternatively expressed in a form as

$$
\Phi_X(\omega) = \exp\left(-\frac{\Omega}{4m}\omega^2 \right) {}_1F_1\left(1-m; 1; \frac{\Omega}{4m}\omega^2 \right) \tag{3.48}
$$

where we observe that the exponential factor denotes the CF of a zero-mean Gaussian RV.

To obtain the PDF for X, we take inverse Fourier transform of $\Phi_X(\omega)$ and get

$$
f_X(x) = \frac{1}{2\pi} \int_{-\infty}^{+\infty} e^{-j\omega x} \Phi_X(\omega)d\omega \tag{3.49}
$$

68

$$= \frac{1}{\pi} \int_0^{+\infty} \cos(\omega x)_1 F_1\left(m; 1; -\frac{\Omega}{4m}\omega^2\right) d\omega \tag{3.50}$$

$$= \frac{1}{\sqrt{\pi}\Gamma(m)} \left(\frac{m}{\Omega}\right)^m |x|^{2m-1} e^{-\frac{mx^2}{\Omega}} \Psi\left(\frac{1}{2}; m+\frac{1}{2}; \frac{mx^2}{\Omega}\right) \tag{3.51}$$

where in obtaining the last equality, we have used the following integral identity[4] [33, 7.642]

$$\int_0^{+\infty} \cos(2xy)_1 F_1(a; c; -x^2) dx = \frac{\sqrt{\pi}}{2} \frac{\Gamma(c)}{\Gamma(a)} |y|^{2a-1} e^{-y^2} \Psi\left(c - \frac{1}{2}; a + \frac{1}{2}; y^2\right) \tag{3.52}$$

where $\Psi(\cdot; \cdot; \cdot)$ is known as the Kummer-U function [3].

In summary, for the case of arbitrary m values, we have expressed the PDF and the CF of Nakagami-m in-phase components in terms of Kummer-U and Kummer-M functions, respectively. In the special cases when m takes integer values, it has been shown that these closed-form expressions can be presented in terms of elementary functions.

Fig. 3.4 plots the Nakagami in-phase component PDF for $m = 0.75, 1, 6, 11, 16$ when $\Omega = 2$. Observe that, for the special case when $m = 1$, the PDF of X becomes zero-mean Gaussian, as expected. In the limit, when m approaches $+\infty$, the channel becomes nonfading and the Nakagami in-phase component distribution approaches to that of (3.28). The asymptotic PDF evaluated at $x = 0$ is $\lim_{m\to+\infty} f_X(0) = \frac{1}{\pi\sqrt{\Omega}}$, where $\sqrt{\Omega}$ is the root mean-square value of the Nakagami RV. Fig. 3.5 plots the Nakagami in-phase component CF for $m = 0.75, 1, 6, 11, 16$ when $\Omega = 2$. Observe that, when $m = 1$, the CF of X becomes Gaussian and positive everywhere, as expected. For values of m greater than 1, the CF of X assumes both positive and negative values; however, its envelope decays rapidly with ω for decreasing m values.

Using these newly derived analytical expressions, we can calculate the precise BER for the BPSK-modulated signal in the general fading and CCI environment in the following section.

---

[4]A typographical error in (3.52) has recently been corrected by the author and this has been acknowledged by A. Jeffrey and D. Zwillinger, Editors for Gradshteyn and Ryzhik's *Table of Integrals, Series, and Products*, 6th edition.
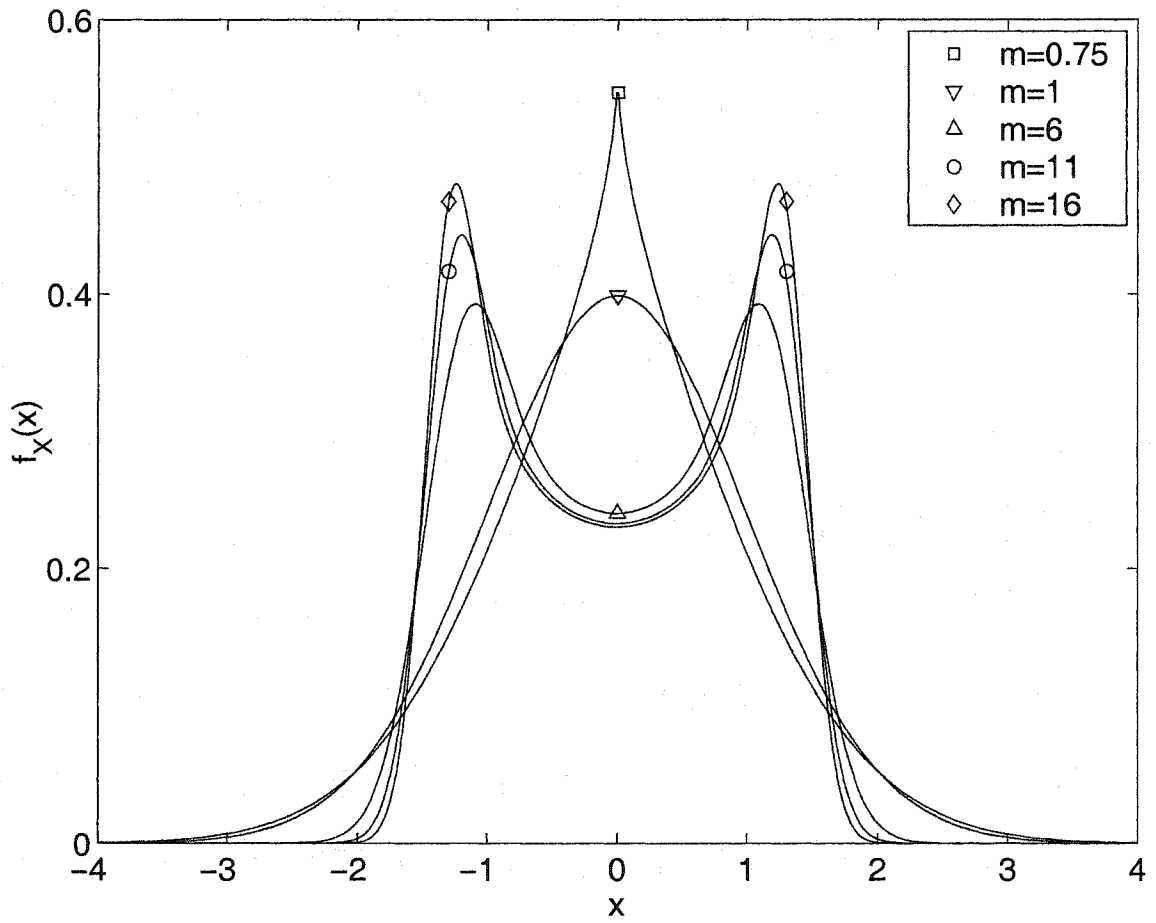
Figure 3.4. Probability density function (PDF) of $X = R\cos\Theta$ for $\Omega = 2$ and $m = 0.75, 1, 6, 11, 16$.

70
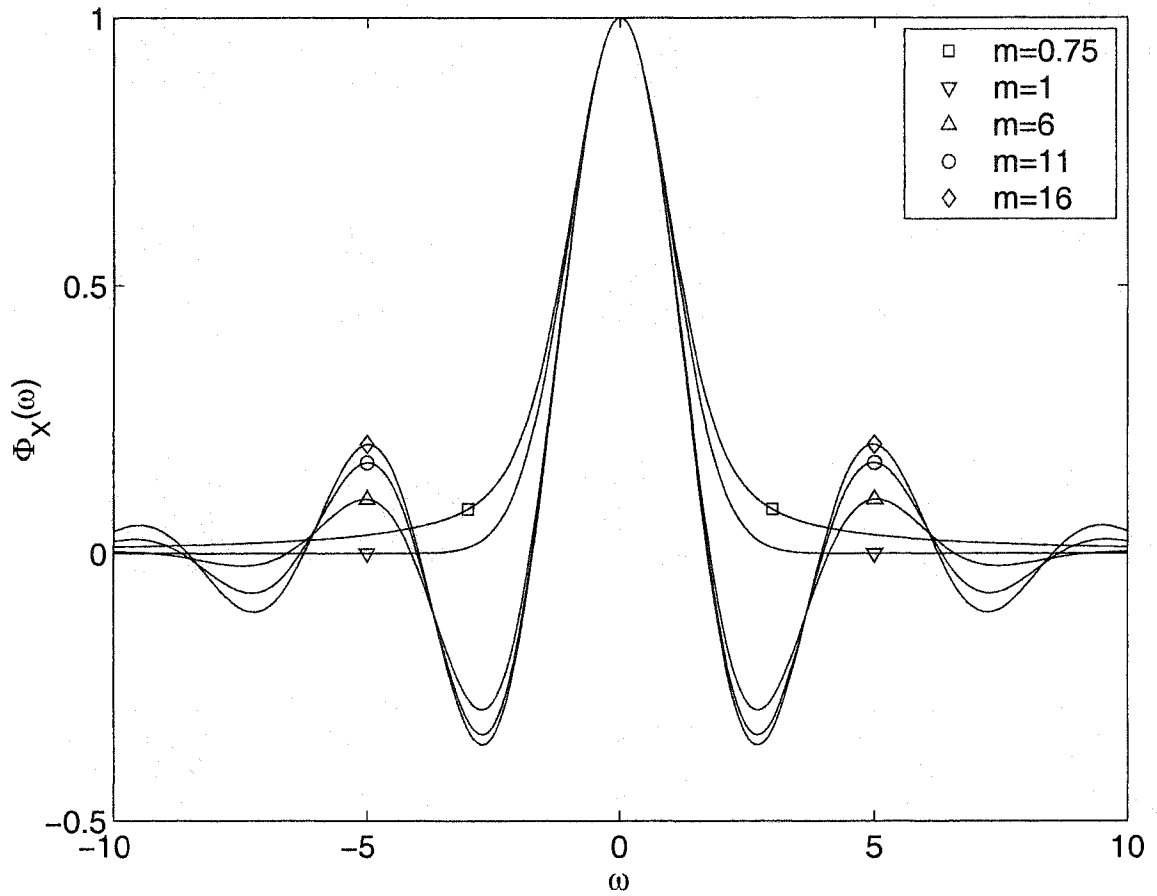
Figure 3.5. Characteristic function (CF) of $X = R\cos\Theta$ for $\Omega = 2$ and $m = 0.75, 1, 6, 11, 16$.

71

3.4   BER Calculation Using the CF Method

In this section, we study the exact BER analysis for our fading and CCI problem. Section 3.4.1 derives the exact BER expression for the BPSK-modulated signal corrupted by multiple Nakagami-faded asynchronous interferers and AWGN. In Section 3.4.2, closed-form expression of the characteristic function for the CCI is derived and the result is required in the exact BER calculation. Finally, in Section 3.4.3, we treat the special case when all interfering signals are synchronous with the desired user signal.

3.4.1   Exact Bit Error Rate Expression

We denote the total interference component by I and write

$$I = \sum_{i=1}^{L} \sqrt{\frac{P_i T}{2}} R_i \cos(\phi_i) \rho_i \tag{3.53}$$

where ρ_i has been previously defined in (3.25). Letting $\Lambda = I + n_0$ and using the independence assumption of the CCI and the background noise, we can express the CF of the CCI plus noise term, Λ, as the product of the CF of the total interference and the CF of the background noise as

$$\Phi_\Lambda(\omega) = \Phi_I(\omega) \Phi_{n_0}(\omega)$$

$$= \Phi_{n_0}(\omega) - [1 - \Phi_I(\omega)] \Phi_{n_0}(\omega). \tag{3.54}$$

The cumulative distribution function (CDF) of Λ can be expressed in terms of its CF as [59, p. 40, eqn. (3-23)]

$$F_\Lambda(\lambda) = \frac{1}{2} + \frac{1}{\pi} \int_0^{+\infty} \frac{\sin(\lambda\omega)}{\omega} \Phi_\Lambda(\omega) d\omega. \tag{3.55}$$

The average BER, conditioned on R_s, for the desired user is

$$
\begin{aligned}
P_{e|R_s} &= \Pr\left[\sqrt{\frac{P_s T}{2}} R_s a[0] + I + n_0 < 0 \,\middle|\, a[0] = +1 \right] \\
&= \Pr\left[I + n_0 < -\sqrt{\frac{P_s T}{2}} R_s \right] \\
&= 1 - F_\Lambda\left(\sqrt{\frac{P_s T}{2}} R_s \right)
\end{aligned}
$$

72

$$= \frac{1}{2} - \frac{1}{\pi} \int_0^{+\infty} \frac{\sin(\sqrt{\frac{P_sT}{2}}R_s\omega)}{\omega} \Phi_\Lambda(\omega)d\omega$$

$$= Q\left(\sqrt{\frac{P_sT}{2}}R_s\right) + \frac{1}{\pi} \int_0^{+\infty} \frac{\sin(\sqrt{\frac{P_sT}{2}}R_s\omega)}{\omega}[1 - \Phi_I(\omega)]\Phi_{n_0}(\omega)d\omega \qquad (3.56)$$

where $Q(x) = \frac{1}{\sqrt{2\pi}}\int_x^{+\infty} e^{-y^2/2}dy$. Averaging over the PDF of R_s, and using the integral identities [79, eqn. (3.63)]

$$\int_0^{+\infty} x^{2n-1}e^{-x^2/2}Q\left(\frac{x}{\sigma}\right)dx = \frac{(n-1)!}{2}[1 - (\sigma^2 + 1)^{-1/2}]^n$$
$$\times \sum_{k=0}^{n-1} 2^{-k}\binom{n-1+k}{k}[1 + (\sigma^2 + 1)^{-1/2}]^k \qquad (3.57)$$

and [33, eqn. (3.952)]

$$\int_0^{+\infty} x^{\mu-1}e^{-\beta x^2}\sin\gamma x\, dx = \frac{\gamma e^{-\frac{\gamma^2}{4\beta}}}{2\beta^{\frac{\mu+1}{2}}}\Gamma\left(\frac{1+\mu}{2}\right) {}_1F_1\left(1 - \frac{\mu}{2}; \frac{3}{2}; \frac{\gamma^2}{4\beta}\right), \qquad (3.58)$$

respectively for the first and second term in (3.56), we get

$$P_e = P_e^{(1)} + P_e^{(2)}. \qquad (3.59a)$$

The first error term, $P_e^{(1)}$, represents the BER contribution due to the background noise only, and it is given by (assuming m_s takes only integer values)

$$P_e^{(1)} = \frac{1}{2^{m_s}}\left[1 - (\sigma_n^2 + 1)^{-1/2}\right]^{m_s}$$
$$\times \sum_{k=0}^{m_s-1} 2^{-k}\binom{m_s - 1 + k}{k}\left[1 + (\sigma_n^2 + 1)^{-1/2}\right]^k \qquad (3.59b)$$

where $\sigma_n^2 = \frac{4m_s}{P_sT\Omega_s}$. The second error term, $P_e^{(2)}$, represents the BER contribution due to both the background noise and the cochannel interference, and it is given by

$$P_e^{(2)} = \frac{1}{\pi}\frac{\Gamma(m_s + \frac{1}{2})}{\Gamma(m_s)}\sqrt{\frac{\Omega_s P_s T}{2m_s}}\int_0^{+\infty}[1 - \Phi_I(\omega)]\,\Phi_{n_0}(\omega)$$
$$\times {}_1F_1\left(m_s + \frac{1}{2}; \frac{3}{2}; \frac{\Omega_s P_s T}{8m_s}\omega^2\right)d\omega. \qquad (3.59c)$$

The integral in (3.59c) does not seem to have a closed-form expression; however, it is readily evaluated using numerical integration.

73

3.4.2 CF of CCI and Background Noise

Since n_0 is a zero mean, unit variance Gaussian RV, the CF of n_0 is $\Phi_{n_0}(\omega) = e^{-\omega^2/2}$. To find the CF for the total interference, we write

$$I \approx \sum_{i=1}^{L} \sqrt{\frac{P_i T}{2}} R_i \cos(\phi_i) \left(\sum_{k=-P}^{P} b_i[k] g_{k,i} \right) \tag{3.60}$$

where $g_{k,i} = g(-kT - \tau_i)$ and we have assumed that the cross-term ISI contribution from the ith interferer is limited to $2P+1$ terms. Letting $X_i = R_i \cos(\phi_i)$ and $Y_i = \sum_{k=-P}^{P} b_i[k] g_{k,i}$, we rewrite the total interference component as

$$I = \sum_{i=1}^{L} I_i = \sum_{i=1}^{L} \sqrt{\frac{P_i T}{2}} X_i Y_i. \tag{3.61}$$

Conditioning on τ_i, the CF of Y_i is

$$\Phi_{Y_i|\tau_i}(\omega) = \mathbb{E}\left[e^{j\omega Y_i} \right] \tag{3.62}$$

$$= \mathbb{E}\left[e^{j\omega \sum_{k=-P}^{P} b_i[k] g_{k,i}} \right] \tag{3.63}$$

$$= \mathbb{E}\left[\prod_{k=-P}^{P} e^{j\omega b_i[k] g_{k,i}} \right] \tag{3.64}$$

$$= \prod_{k=-P}^{P} \mathbb{E}\left[e^{j\omega b_i[k] g_{k,i}} \right] \tag{3.65}$$

$$= \prod_{k=-P}^{P} \left(\frac{1}{2} e^{j\omega g_{k,i}} + \frac{1}{2} e^{-j\omega g_{k,i}} \right) \tag{3.66}$$

$$= \prod_{k=-P}^{P} \cos(g_{k,i} \omega) \tag{3.67}$$

where (3.65) follows from the fact that the ith interfering user's data bits are independent, and hence, uncorrelated. Conditioning on X_i and τ_i, and using the scaling property of the Fourier transform, from (3.61) and (3.67), we have the CF of I_i as

$$\Phi_{I_i|X_i,\tau_i}(\omega) = \prod_{k=-P}^{P} \cos\left(\sqrt{\frac{P_i T}{2}} g_{k,i} X_i \omega \right). \tag{3.68}$$

Averaging out X_i and τ_i, we obtain the CF of the ith interferer as

$$\Phi_{I_i}(\omega) = \mathbb{E}_{X_i}\left[\mathbb{E}_{\tau_i}\left[\Phi_{I_i|X_i,\tau_i}(\omega) \right] \right] \tag{3.69}$$

74

$$= \mathbb{E}_{X_i} \left[\mathbb{E}_{\tau_i} \left[\prod_{k=-P}^{P} \cos \left(\sqrt{\frac{P_i T}{2}} g_{k,i} X_i \omega \right) \right] \right] \qquad (3.70)$$

or

$$\Phi_{I_i}(\omega) = \frac{2}{T} \int_0^T \left[\int_0^{+\infty} f_X(x) dx \prod_{k=-P}^{P} \cos \left(\sqrt{\frac{P_i T}{2}} g(-kT - \tau) x \omega \right) \right] d\tau \qquad (3.71)$$

where $X = R \cos \Theta$ and $f_X(x)$ is the PDF of an auxiliary function, $X = R \cos \Theta$ (R is a Nakagami-m distributed RV and Θ is an independent uniformly distributed RV), which has been derived in Section 3.3 (See (3.49)).

Finally, using the assumption that all interfering components are independent, we obtain the CF of the total interference as

$$\Phi_I(\omega) = \prod_{i=1}^{L} \Phi_{I_i}(\omega). \qquad (3.72)$$

Evaluation of (3.72) requires, in turn, evaluation of (3.71). The inner, improper integral in (3.71) has an integral with envelope $f_X(x)$, the PDF of X, which has been plotted in Fig. 3.4 for a number of m parameter values. Our empirical trials have indicated that the infinite range of integration of X can be approximated with a finite range over $[0, 5\sqrt{\Omega_I/2}]$ for all permissible values of the fading parameter. This approximation improves with increasing values of m. Therefore, without loss of much numerical accuracy, we can approximate (3.71) well using definite, proper integrals as

$$\Phi_{I_i}(\omega) = \frac{2}{T} \int_0^T \left[\int_0^{5\sqrt{\Omega_I/2}} f_X(x) dx \prod_{k=-P}^{P} \cos \left(\sqrt{\frac{P_i T}{2}} g(-kT - \tau) x \omega \right) \right] d\tau \qquad (3.73)$$

3.4.3 BER Under Synchronous Operation

In the special case when all the interfering signals have the same symbol timing as the desired user, there is no cross-term ISI and the total interference component can be simplified to

$$I = \sum_{i=1}^{L} \sqrt{\frac{P_i T}{2}} R_i \cos(\phi_i) b_i[0] \qquad (3.74)$$

$$= \sum_{i=1}^{L} \sqrt{\frac{P_i T}{2}} X_i b_i[0] \qquad (3.75)$$

$$\equiv \sum_{i=1}^{L} \sqrt{\frac{P_i T}{2}} X_i \qquad (3.76)$$

75

where $X \equiv Y$ denotes that the RV's X and Y have the same statistics. The last equality in (3.76) follows a Lemma which states that the product of a symmetric Bernoulli RV [5] and a zero mean symmetric RV gives back the symmetric RV with the same statistics. A formal statement of this Lemma and its proof are as follows.

Lemma: *Suppose $Z = XY$, where X and Y are two independent RV's. The RV X has a zero-mean symmetric PDF; i.e., $f_X(x) = f_X(-x)$ and Y is a Bernoulli RV taking values from $\{+1, -1\}$ with equal probabilities. Then, $f_Z(z) = f_X(z)$.*

Proof: The PDF of Y is

$$f_Y(y) = \frac{1}{2}\delta(y-1) + \frac{1}{2}\delta(y+1) \tag{3.77}$$

where $\delta(\cdot)$ is the δ-function. The conditional PDF of Z given Y is [81]

$$f_{Z|Y}(z) = \frac{1}{|y|}f_X\left(\frac{z}{y}\right). \tag{3.78}$$

Averaging over the PDF of Y, one gets

$$
\begin{aligned}
f_Z(z) &= \mathbb{E}[f_{Z|Y}(z)] \\
&= \frac{1}{2}\int_{-\infty}^{+\infty}\delta(y-1)f_{Z|Y}(z)dy + \frac{1}{2}\int_{-\infty}^{+\infty}\delta(y+1)f_{Z|Y}(z)dy \\
&= \frac{1}{2}f_X(z) + \frac{1}{2}f_X(-z) \\
&= f_X(z)
\end{aligned}
\tag{3.79}
$$

■

Now using the assumption that the L interfering signals are independent, the CF of the total interference (under the synchronous assumption) can be obtained as

$$
\begin{aligned}
\Phi_I(\omega)\Big|_{\text{sync}} &= \prod_{i=1}^{L}\Phi_X\left(\sqrt{\frac{P_iT}{2}}\,\omega\right) \\
&= \prod_{i=1}^{L}{}_1F_1\left(m_I; 1; -\frac{\Omega_I P_i T}{8m_I}\omega^2\right).
\end{aligned}
\tag{3.80}
$$

where the last equality follows from a result which has been derived in Section 3.3 (see (3.40)).

---

[5] A symmetric Bernoulli RV is defined here as a RV taking values from $\{+1, -1\}$ with equal probabilities.

76

In general, the exact BER of BPSK modulation in CCI environment depends on the power distribution of the interfering signals. This is true for both asynchronous and synchronous interfering signals since the characteristic functions in (3.72) and (3.80) both depend on the power distribution of the interfering signals. However, when $m_I = 1$ (Rayleigh fading), using a Kummer transformation [3, eqn. (13.1.27)] and the fact [3, eqn. (13.1.2)]

$$_1F_1\left(0; 1; \frac{\Omega_I P_i T}{8m_I}\omega^2\right) = 1,$$

the CF of I assuming synchronous interferer becomes

$$\Phi_I(\omega)\bigg|_{\text{sync},m_I=1} = \prod_{i=1}^{L} \exp\left(-\frac{\Omega_I P_i T}{8m_I}\omega^2\right) {}_1F_1\left(1 - m_I; 1; \frac{\Omega_I P_i T}{8m_I}\omega^2\right)$$

$$= \exp\left(-\frac{\Omega_I T \sum_{i=1}^{L} P_i}{8}\omega^2\right) \tag{3.81}$$

which corresponds to a zero-mean Gaussian PDF with variance $(\Omega_I T/4)\sum_{i=1}^{L} P_i$. Therefore, we conclude that the first-order distribution of the sum of synchronous, Rayleigh-faded, BPSK-modulated cochannel signals is exactly zero-mean Gaussian. The variance of this Gaussian sample depends only on the total interference signal power. The exact BER in this situation can be evaluated using the Gaussian approximation recalled in the next section.

3.5 BER Calculation Using Gaussian Approximation

The exact distribution for the total cochannel interference is, in general, difficult to obtain. It has been reported only for restricted special cases [16]. Therefore, a central limit theorem (CLT) is usually invoked to approximate the distribution of the total cochannel interference, I, as Gaussian. Recall that the first and the second moments of I completely describe the Gaussian distribution. It can be shown that the first moment of I is zero and the second moment of I, or here, its variance, is given by

$$\text{var}[I] = \mathbb{E}[I^2] = \frac{\Omega_I T \sum_{i=1}^{L} P_i \mathbb{E}[\rho_i^2]}{4}. \tag{3.82}$$

In (3.82), $\mathbb{E}[\rho_i^2]$ can be further simplified to a compact form and this quantity is the same for all interfering users. We recall that the term ρ_i, defined in (3.25), represents the cross-signal ISI

77

from the ith user corrupting the desired user signal. Averaging over the information data bits and the random delay, we obtain $\mathbb{E}[\rho_i^2]$ as

$$\mathbb{E}[\rho_i^2] = \sum_{k=-\infty}^{+\infty} \mathbb{E}[b_i^2[k]]\mathbb{E}[g^2(-kT-\tau_i)] \tag{3.83}$$

$$= \sum_{k=-\infty}^{+\infty} \mathbb{E}[g^2(-kT-\tau_i)] \tag{3.84}$$

$$= \frac{1}{T} \sum_{k=-\infty}^{+\infty} \int_0^T g^2(-kT-\tau)d\tau \tag{3.85}$$

$$= \frac{1}{T} \sum_{k=-\infty}^{+\infty} \int_{-kT}^{-(k+1)T} g^2(t)dt \tag{3.86}$$

$$= \frac{1}{T} \int_{-\infty}^{+\infty} g^2(t)dt \tag{3.87}$$

$$= \frac{1}{T} \int_{-\infty}^{+\infty} |G(f)|^2 df \tag{3.88}$$

where (3.83) follows from the assumption that the delay of the ith user and the information bits of the ith user are independent; eqn. (3.86) follows from a substitution $t = -kT - \tau$; and (3.88) follows from Parseval's theorem. Using the RC pulse spectrum defined in (3.21), we have

$$\frac{1}{T} \int_{-\infty}^{+\infty} |G_{\text{RC}}(f)|^2 df = \frac{1}{T}\left\{2T^2\left(\frac{1-\alpha}{2T}\right) + \frac{T^2}{2}\int_{\frac{1-\alpha}{2T}}^{\frac{1+\alpha}{2T}}\left\{1+\cos\left[\frac{\pi T}{\alpha}\left(f-\frac{1-\alpha}{2T}\right)\right]\right\}^2 df\right\}$$

$$= (1-\alpha) + \frac{\alpha}{2}\int_0^1 (1+\cos\pi u)^2 du$$

$$= 1 - \frac{\alpha}{4}. \tag{3.89}$$

Similarly, using the BTRC pulse spectrum defined in (3.23), we have

$$\frac{1}{T} \int_{-\infty}^{+\infty} |G_{\text{BTRC}}(f)|^2 df = \frac{1}{T}\left\{2T^2\left(\frac{1-\alpha}{2T}\right) + 2T^2\int_{\frac{1-\alpha}{2T}}^{\frac{1}{2T}}\exp\left\{\frac{4T\ln 2}{\alpha}\left[\frac{1-\alpha}{2T}-f\right]\right\}df\right.$$

$$\left. + 2T^2\int_{\frac{1}{2T}}^{\frac{1+\alpha}{2T}}\left\{1-\exp\left\{\frac{2T\ln 2}{\alpha}\left[f-\frac{1+\alpha}{2T}\right]\right\}\right\}^2 df\right\}$$

$$= (1+\alpha) + \left(\frac{3}{8}\right)\left(\frac{\alpha}{\ln 2}\right) + \left[\alpha - \frac{\alpha}{\ln 2} + \left(\frac{3}{8}\right)\left(\frac{\alpha}{\ln 2}\right)\right]$$

$$= 1 - \frac{\alpha}{4}\left(\frac{1}{\ln 2}\right). \tag{3.90}$$

78

To summarize, we have derived

$$\mathbb{E}[\rho_i^2] = \begin{cases} 1 - \frac{\alpha}{4} & \text{RC} \\ 1 - \frac{\alpha}{4}\left(\frac{1}{\ln 2}\right) & \text{BTRC.} \end{cases} \tag{3.91}$$

The total equivalent noise power is

$$\sigma_t^2 = 1 + \text{var}[I]. \tag{3.92}$$

Hence, the average BER, conditioned on R_s, is given by

$$P_{e|R_s} = Q\left(\frac{\sqrt{\frac{P_s T}{2}}R_s}{\sigma_t}\right). \tag{3.93}$$

Note that BER estimates obtained from the GA depend only on the total interfering signal power (see (3.82)). Also observe that larger values of α give smaller values for $\mathbb{E}[\rho_i^2]$, and thus, smaller values for $\text{var}[I]$ and σ_t^2. Then, from (3.93), it is clear that the BER will also be correspondingly reduced. Therefore, the Gaussian approximation (3.93) shows directly and explicitly that the value of excess bandwidth α provides a trade-off between spectral efficiency and detection performance, as is well known [5], [20].

We now use the Gaussian approximation to compare the performance of the two Nyquist pulses for an unfaded desired user signal. Clearly, with the same amount of excess bandwidth, the BTRC pulse gives smaller equivalent noise power, thus, lower BER values. To maintain the same BER performance, or identical equivalent noise powers, one must require

$$1 - \frac{\alpha_{\text{RC}}}{4} = 1 - \frac{\alpha_{\text{BTRC}}}{4\ln 2}$$

or $\alpha_{\text{BTRC}} = 0.693\alpha_{\text{RC}}$. In other words, under the assumption that the Gaussian approximation is valid, for a given BER performance, the BTRC pulse has about 30% savings in excess bandwidth. For practical interest, a more meaningful question is to ask: given the target BER (P_e), the SIR value, and the amount of excess bandwidth (α), how much savings in the signal-to-noise ratio we can achieve if we employ the BTRC pulse in lieu of the RC pulse in our system?

79

To answer the aforementioned question, without loss of generality, we first assume $P_s = \sum_{i=1}^{L} P_i$.

From (3.93), we obtain

$$[Q^{-1}(P_e)]^2 = \frac{\frac{P_s T R_s^2}{2}}{\sigma_t^2} = \frac{\frac{P_s T \Omega_s}{2}}{\sigma_t^2} \tag{3.94}$$

where the last equality follows from the fact $\Omega_s = R_s^2$ when the desired user signal is unfaded. For a RC pulse, from (3.82), (3.91), and (3.92), we have

$$[Q^{-1}(P_e)]^2 = \frac{\left(\frac{P_s T \Omega_s}{2}\right)}{1 + \frac{P_s T \Omega_I}{4}\left(1 - \frac{\alpha}{4}\right)}$$

$$= \frac{\left(\frac{P_s T \Omega_s}{2}\right)}{1 + \frac{1 - \frac{\alpha}{4}}{2SIR}\left(\frac{P_s T \Omega_s}{2}\right)} \tag{3.95}$$

where the last equality follows from the fact that $\Omega_I = \frac{\Omega_s}{SIR}$. Denote the signal-to-noise ratio $\frac{P_s T \Omega_s}{2}$ by SNR_{RC} and solve (3.95) for SNR_{RC}, we have the required signal-to-noise ratio for the RC pulse as

$$SNR_{RC} = \frac{[Q^{-1}(P_e)]^2}{1 - \frac{(1 - \frac{\alpha}{4})}{2SIR}[Q^{-1}(P_e)]^2}. \tag{3.96}$$

Similarly we can show that the required signal-to-noise ratio for the BTRC pulse as

$$SNR_{BTRC} = \frac{[Q^{-1}(P_e)]^2}{1 - \frac{(1 - \frac{\alpha}{4\ln 2})}{2SIR}[Q^{-1}(P_e)]^2}. \tag{3.97}$$

Therefore, the amount of SNR savings in dB, denoted by ΔSNR, becomes

$$\Delta SNR\,(dB) = SNR_{RC}\,(dB) - SNR_{BTRC}\,(dB)$$

$$= 10\log_{10}\frac{2(SIR) - (1 - \frac{\alpha}{4\ln 2})[Q^{-1}(P_e)]^2}{2(SIR) - (1 - \frac{\alpha}{4})[Q^{-1}(P_e)]^2}. \tag{3.98}$$

As an example, with $SIR = 10\,dB$ and $\alpha = 1.00$, eqn. (3.98) predicts that the RC pulse will require additional $1.19\,dB$ in SNR in order to achieve the same BER performance as the BTRC pulse when the target BER performance is at $P_e = 10^{-6}$.

The approximate analytical expression derived in (3.98) is easy to compute; however, as it will be shown in Section 3.6, the Gaussian approximation can be poor in many situations. Our analysis using the Gaussian approximation only predicts that, in terms of relative BER performance, the BTRC pulse will outperform the RC pulse. We will use our precise analytical expressions to accurately compare the performances of these two pulses in Section 3.6.

80

Finally, averaging (3.93) over the PDF of R_s yields the average BER (for the Gaussian approximation) as

$$P_e^{GA} = \mathbb{E}_{R_s}\left[Q\left(\frac{R_s}{\sigma_t}\right)\right]$$

$$= \int_0^{+\infty} \frac{2}{\Gamma(m_s)}\left(\frac{m_s}{\Omega_s}\right)^{m_s} r_s^{2m_s-1} e^{-\frac{m_s r_s^2}{\Omega_s}} Q\left(\frac{\sqrt{\frac{P_s T}{2}}r_s}{\sigma_t}\right) dr_s. \tag{3.99}$$

The integral (3.99) does not simplify to a closed-form expression for arbitrary values of m_s. However, for integer values of m_s, using the integral identity [79, eq. (3.63)], we can show that

$$P_e^{GA} = \frac{1}{2^{m_s}}\left[1 - (\sigma_g^2 + 1)^{-1/2}\right]^{m_s}$$

$$\times \sum_{k=0}^{m_s-1} 2^{-k}\binom{m_s-1+k}{k}\left[1 + (\sigma_g^2 + 1)^{-1/2}\right]^k \tag{3.100}$$

where $\sigma_g^2 = \frac{4m_s}{P_s T \Omega_s}\sigma_t^2$. Some results obtained using the GA are presented in the next Section.

3.6 Numerical Results and Discussion

In this section, we use our precise analytical results to study the average BER performance of BPSK in Nakagami fading and CCI. First, the new analytical average BER expression derived in Section 3.4 is validated by computer simulation. Next, we study the impact of the interfering users' fading on the desired user error rate. We then use the new results to compare the average BER performance of a CCI BPSK system using the classical raised-cosine pulse to that of a system using the novel shape pulse in various fading and interference environments. Finally, we assess the accuracy of the Gaussian approximation developed in Section 3.5.

We assume that the total interference power is distributed uniformly among all the active interfering signals, i.e, $\sum_{i=1}^L P_i = LP_I$, where P_I is the transmitter power of each interfering signal. Further, as in [5], we fix the total transmitter power of the interfering signals to equal the transmitter power of the desired signal, i.e., $\sum_{i=1}^L P_i = P_s$. Our results do not require these assumptions which are made for illustrative purposes only.

Based on our empirical trials, we have found that taking account of seven adjacent pulses ($P = 3$)

81

is sufficient to capture the effect of cross-signal ISI on the average BER without loss of numerical accuracy.

Fig. 3.6 shows the average BER versus the SNR for a moderately faded desired user signal ($m_s = 5$) and a single asynchronous Rayleigh-faded ($m_I = 1$) interferer both using the RC pulse at $SIR = 10\ dB$ and $SIR = 15\ dB$. The solid lines show the average BER's obtained using the precise analysis and the crosses denotes the average BER's obtained using Monte Carlo simulation. The theoretical results and the simulation results are in excellent agreement. Therefore, in the remaining examples we will only show numerical results obtained using the precise analytical expression. Observe in Fig. 3.6 that an error rate floor occurs for large SNR values. This phenomenon is expected and is due to the cross-signal ISI.

Fig. 3.7 shows the average BER versus the SNR for a strong (lightly faded) desired user signal ($m_s = 8$) corrupted by one or six Rayleigh-faded ($m_I = 1$) interferers all using the RC pulse at $SIR = 10\ dB$ and $SIR = 15\ dB$ under both synchronous and asynchronous operations. Comparing Fig. 3.7 with Fig. 3.6, for the case of one asynchronous Rayleigh-faded interferer, we note that the average BER performance improves (BER decreases) when the desired signal is less severely faded, as expected. Fig. 3.7 also shows that the average BER corresponding to the situation when the total interference power is uniformly distributed among six interferers ($L = 6$) is smaller than the BER corresponding to the situation when the same total interference power is concentrated in one interferer ($L = 1$). This observation is consistent with the findings in [5] for the case of a non-faded desired user signal (which corresponds to $m_s = +\infty$). Fig. 3.7 also shows the average BER performance when all interfering signals are symbol timing synchronized with the desired signal. For the special case of Rayleigh-faded interfering signals ($m_I = 1$), as discussed in Section 3.4, the resulting average BER depends only on the total interference power. Finally, Fig. 3.7 indicates that the BER under asynchronous operation with a single interferer ($L = 1$) is always greater than the BER under synchronous operation. However, with six interferers ($L = 6$), the BER under synchronous operation can be either smaller or greater than the BER under asynchronous operation depending on the value of SIR.

82

In Fig. 3.8, we examine a case where the desired signal is strong (lightly faded) with $m_s = 8$, but the interfering signals are subjected to less fading, as represented by increasing the value of m_I. Comparing Fig. 3.8 ($m_I = 5$) with Fig. 3.7 ($m_I = 1$), we observe that as the interfering signals become less faded, the BER of the desired signal decreases. Or conversely, subjecting the interfering signals to more severe fading results in increasing of BER of the desired signal. This might seem counter-intuitive. Insight into this behavior is furthered by considering the case of an unfaded desired signal and faded interferers. Recall that the interference power is constant. In Fig. 3.9, BER curves are plotted for an unfaded desired user signal corrupted by interfering signals faded with various amounts of severity. It is clear that for an unfaded user, the BER increases when the interfering signals are more severely faded (corresponding to decreasing m_I from $m_I = 5$ to $m_I = 1$). This behavior is a consequence of the upward concavity of the Q-function, and can be explained by referring to the results published by Jenq [39]. Though he considered ISI rather than CCI, a similar argument applies here to the CCI case. Consider first the error rate of BPSK in AWGN. It is well known that $P_e = Q(\frac{s}{\sigma})$, where s is the signal strength and σ is the noise standard deviation. In the presence of an interferer taking values $-d$ and $+d$ with equal probabilities, the resulting BER is $P_e' = [Q(\frac{s+d}{\sigma}) + Q(\frac{s-d}{\sigma})]/2$. Since the Q-function is concave up, it is clear that $P_e' > P_e$ by Jensen's inequality [3]. The fading "smears" the interference to assume different values of d. While the symmetry around s is not present (that is, one cannot pair $-d$ with $+d$ for all values of d), the fading skews the values of d toward larger values since the fading distribution is one sided on $[0, +\infty)$. The result is an increased BER. A small m_I value corresponds to a situation when d takes large values with high probability, and thus, it gives greater error rate. On the other hand, a large m_I value corresponds to a situation when d takes large values with low probability, and thus, it gives smaller error rate. Note in Fig. 3.9 that this argument holds for all values of SNR and, therefore, it does not depend on the assumption that the desired signal is unfaded. Thus, as demonstrated in Figs. 3.8 and 3.9, the BER performance of the desired faded signal improves (BER decreases) when the interfering signals are less faded.

In Section 3.5, the Gaussian approximation was used to predict that the BTRC pulse gives

83

better BER performance than the RC pulse. Many numerical examples confirm this prediction. For example, Fig. 3.10 compares the BER performances for the two Nyquist pulses with shaping factor $\alpha = 1.00$ at $SIR = 5, 10$ and 15 dB. As shown, the BTRC pulse yields smaller BER values than those of the RC pulse over a wide range of SNR values. In particular, with $SIR = 15$ dB, the BER of the BTRC pulse is about half the BER of the RC pulse at $SNR = 30$ dB, and the BTRC pulse has about 0.86 dB savings in SNR over the RC pulse at BER $= 10^{-6}$. Additional numerical examples can be found in Table 3.6 to demonstrate the advantage of the new novel pulse.

Figs. 3.6–3.8 also show the accuracy of the Gaussian approximation. From Fig. 3.6, it is seen that the GA is in good agreement with the exact analysis for low SNR values. However, the GA fails to accurately predict the error rate floor for high SNR values. Similar observations can be drawn from Fig. 3.7. Fig. 3.8 indicates that the GA agrees with the exact analyses reasonably well for six interferers under both asynchronous and synchronous operations. However, the GA *overestimates* the exact BER when a single interferer is lightly faded. This observation is in contrast to the observation in Fig. 3.7 where the GA *underestimates* the BER when the single interferer is severely faded. Thus, the GA is not a reliable predictor and needs not be used given the tractable, precise method derived here.

3.7 Summary

In this chapter, we studied the error rate of a bandwidth efficient BPSK signal in fading and cochannel interference. The model we adopted is the general m_s/m_I model which covers a wide range of fading and cochannel interference conditions. We obtained a precise BER expression using the characteristic function method. Using this precise method, we found that less faded interfering signals improve the BER performance of the desired user signal. We also studied the performance of a novel pulse in fading and CCI environments. This new pulse outperforms the classical RC pulse for all cases considered. The performance gains over the RC pulse, although moderate in most cases, are attained at no additional cost. Therefore, this new pulse will be useful for future wireless
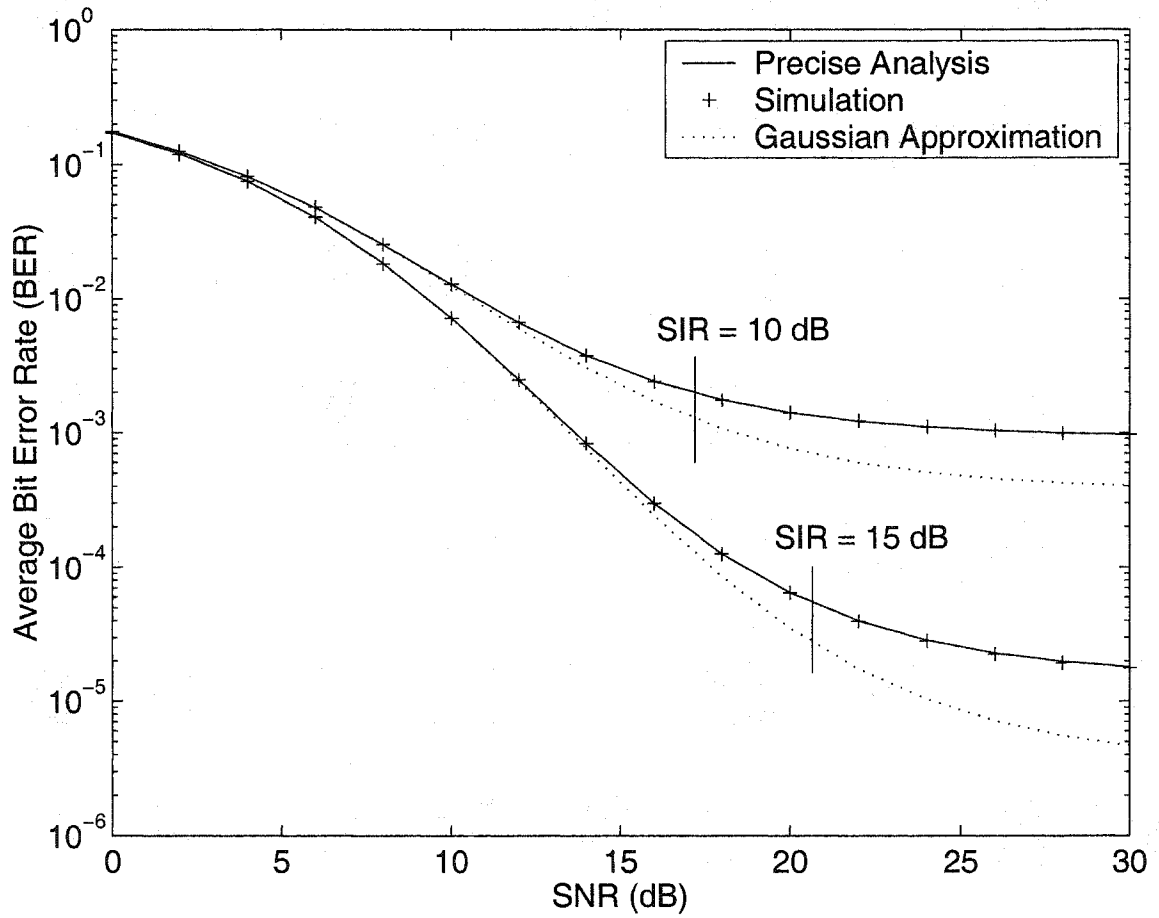
Figure 3.6. Average BER versus *SNR* for $m_s = 5$ and $m_I = 1$ with a single asynchronous interferer and RC pulse ($\alpha = 0.5$) at *SIR* $= 10$ *dB* and *SIR* $= 15$ *dB*.

85
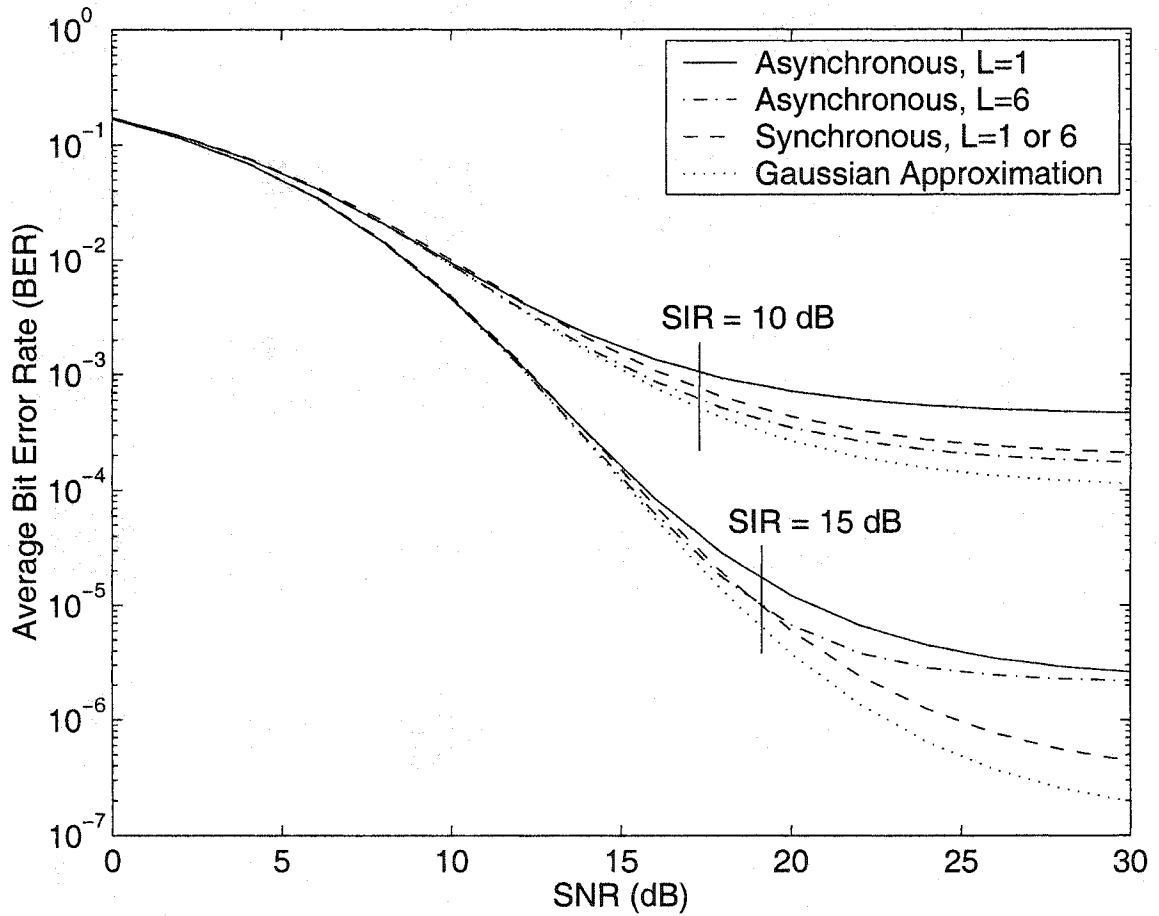
Figure 3.7. Average BER versus *SNR* for $m_s = 8$ and $m_I = 1$ with $L = 1, 6$ and RC pulse ($\alpha = 0.5$) at *SIR* = 10 *dB* and *SIR* = 15 *dB*.

86
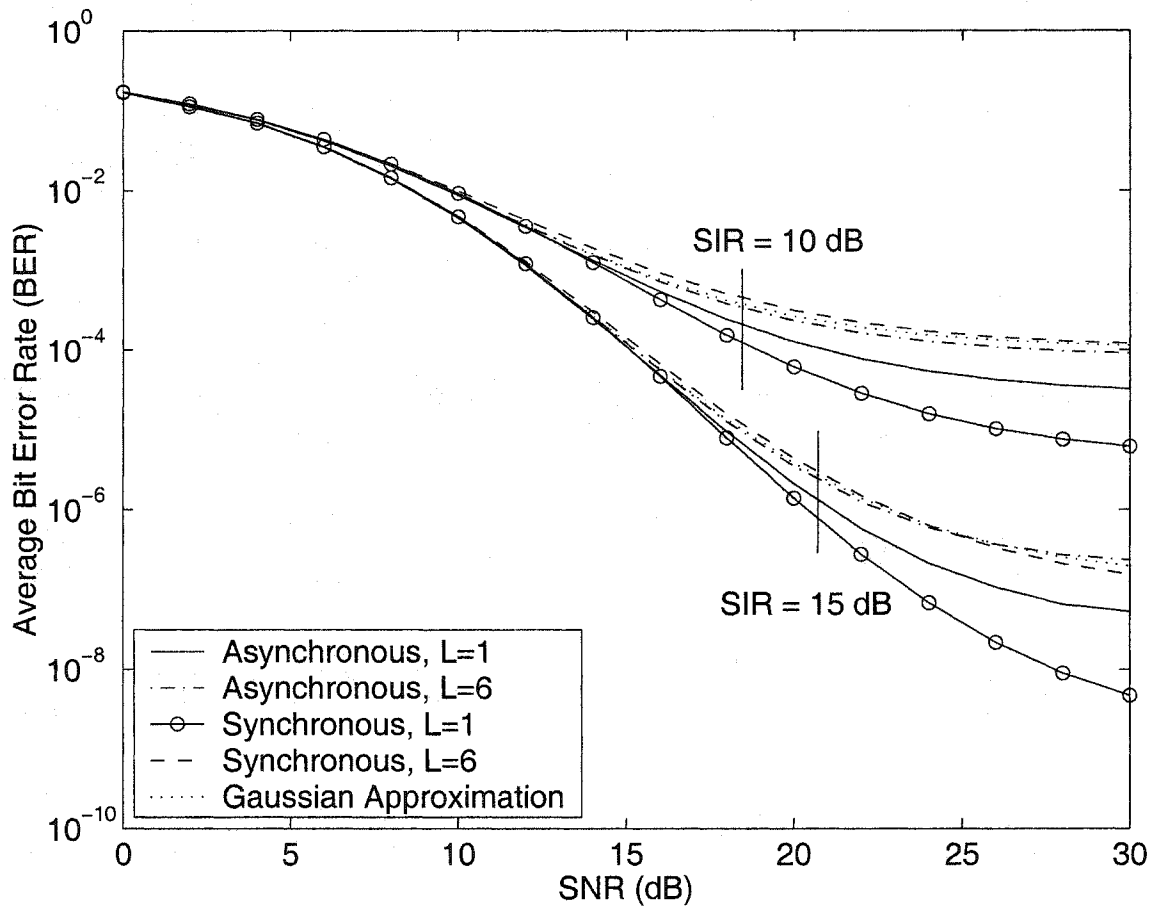
Figure 3.8. Average BER versus SNR for $m_s = 8$ and $m_I = 5$ with $L = 1, 6$ and RC pulse ($\alpha = 0.5$) at $SIR = 10$ dB and $SIR = 15$ dB.

87
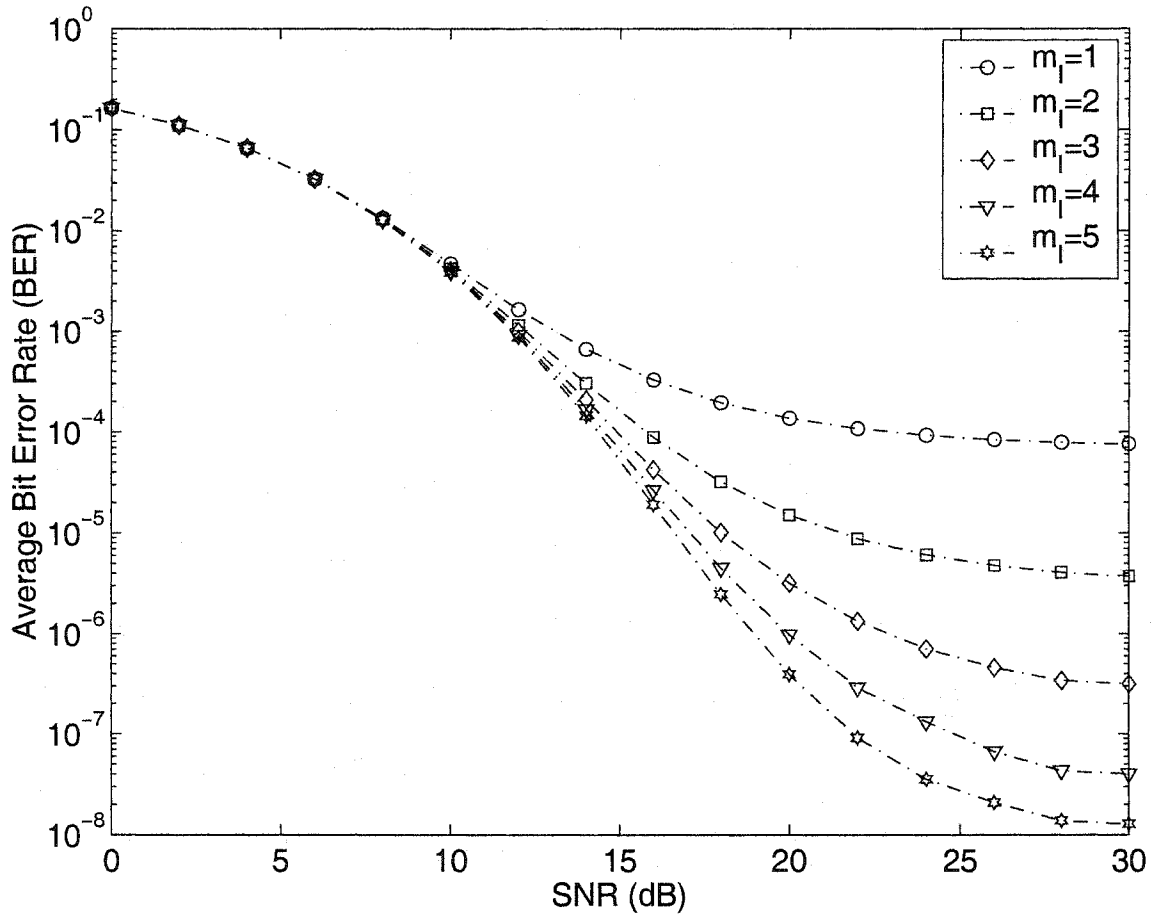
Figure 3.9. Average BER versus *SNR* for unfaded desired user signal and $m_I = 1,2,3,4,5$ with

$L = 6$ and RC pulse ($\alpha = 0.5$) at *SIR* $= 10$ *dB*.

88
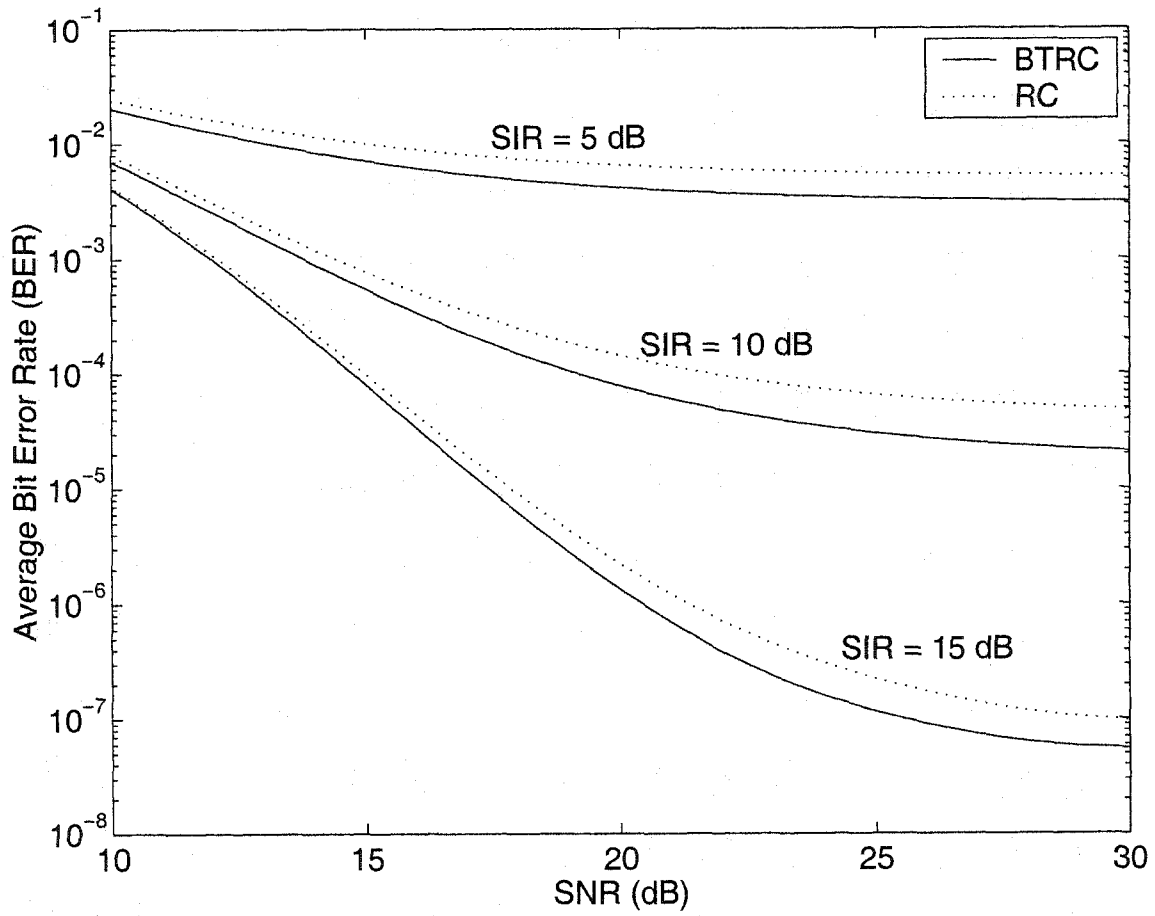
Figure 3.10. Average BER versus *SNR* for $m_s = 8$ and $m_I = 2$ with $L = 6$, RC pulse ($\alpha = 1.00$) and BTRC pulse ($\alpha = 1.00$) at *SIR* = 5, 10, and 15 *dB*.

89

Table 3.1. The average BER of BPSK in generalized Nakagami fading for the RC pulse and the BTRC pulse with $SIR = 15\ dB$, $m_s = 10$, $m_I = 2$ and $L = 6$.

	α	SNR=5 dB	10 dB	15 dB	20 dB	25 dB	30 dB
RC	0.25	5.07E-02	4.69E-03	1.38E-04	5.37E-06	8.80E-07	4.35E-07
	0.50	5.05E-02	4.57E-03	1.23E-04	3.96E-06	5.41E-07	2.47E-07
	0.75	5.02E-02	4.44E-03	1.10E-04	2.94E-06	3.38E-07	1.47E-07
	1.00	5.00E-02	4.32E-03	9.83E-04	2.19E-06	2.19E-07	9.42E-08
BTRC	0.25	5.06E-02	4.64E-03	1.31E-04	4.68E-06	7.05E-07	3.35E-07
	0.50	5.03E-02	4.46E-03	1.11E-04	3.30E-06	3.56E-07	1.55E-07
	0.75	4.99E-02	4.29E-03	9.47E-05	2.00E-06	1.93E-07	8.31E-08
	1.00	4.95E-02	4.11E-03	8.03E-05	1.33E-06	1.13E-07	5.37E-08

systems. Using our precise BER expression, we assessed definitely the accuracy of the GA with various system parameters. It was found that the GA can be poor under many operating conditions.

90

Chapter 4

Error Rate of Asynchronous DS-CDMA in Nakagami

Fading

In this chapter, using the CF of an auxiliary function derived in Chapter 3, we extend the results on accurate DS-CDMA BER calculation in flat Rayleigh fading to flat Nakagami-m fading. This chapter is organized as follows. Section 4.1 briefly reviews the system model and an important decision statistic presented in Chapter 2. Section 4.2 derives the BER estimate using the standard Gaussian approximation. Section 4.3 derives an accurate BER expression without making assumptions on the distribution of the MAI. Section 4.4 presents numerical results and discussions. Finally, Section 4.5 summarizes the chapter results.

4.1 System Model and Receiver Decision Statistic

Recall the DS-CDMA/SSMA system model described in Fig. 2.1 for K asynchronous users. The received signal, $r(t)$, at the input of the desired user matched filter receiver is given by

$$r(t) = \sum_{k=1}^{K} \sqrt{2P_k} R_k b_k (t - \tau_k) a_k (t - \tau_k) \cos(\omega_c t - \phi_k) + n(t) \tag{4.1}$$

P_k represents the transmitted signal power, ω_c is the carrier frequency, $\{\tau_k\}_{k=1}^{K}$ represent the delays which account for user asynchronism, $\phi_k = \beta_k + \theta_k - \omega_c \tau_k$ is assumed a uniform RV over $[0, 2\pi)$ where β_k is the phase introduced by the fading channel on the kth user signal and θ_k is the phase

91

of the kth user's transmitted signal. The kth user data signal, $b_k(t)$, is a random process which is a rectangular waveform, taking values from $\{-1, +1\}$ with symbol rate $R_s = 1/T$ and its expression is given in (2.2). The spreading signal, $a_k(t)$, can be expressed as

$$a_k(t) = \sum_{l=-\infty}^{+\infty} a_l^{(k)} \psi(t - lT_c) \tag{4.2}$$

where $\psi(t)$ is a rectangular chip waveform which is time-limited to $[0, T_c)$ and normalized according to $\int_0^{T_c} \psi^2(t)dt = T_c$. The lth chip of the kth user is denoted as $a_l^{(k)}$ and takes values from $\{-1, +1\}$ with the polarities of all chips assumed random. There are G chips for one data symbol and we normalize the chip duration so that $T_c = 1$ and, thus, $T = G$. The channel fading is represented by the RV's $\{R_k\}_{k=1}^K$ which are Nakagami-m distributed and have the PDF given by

$$f_R(r) = \frac{2}{\Gamma(m)} \left(\frac{m}{\Omega} \right)^m r^{2m-1} e^{-\frac{mr^2}{\Omega}}, \ r \geq 0 \tag{4.3}$$

where $\Omega = \mathbb{E}[R^2]$. Here, for simplicity, we have assumed all active users experience the same amount of fading and m takes integer values.

The received signal is usually corrupted by an additive background zero-mean white Gaussian noise process, $n(t)$. For large signal to background noise ratio, the effect of background noise is negligible in a mainly interference-limited system [53]. Thus, in the following analysis, we do not consider background noise for simplicity. Without loss of generality, we further assume that $\{\tau_k\}_{k=1}^K$ are uniformly distributed over $[0, T)$; that $P_1 = P_2 = \ldots = P_k = 2$, i.e., the users have equal transmitted signal powers; that average power control is used for the received signal, i.e. $\mathbb{E}[R_k^2] = \Omega$ for $k = 1, \cdots K$; and that all aforementioned RV's, $\left\{ \{R_k\}_{k=1}^K; \{\tau_k\}_{k=1}^K; \{\phi_k\}_{k=1}^K; \{(b_j^{(k)})\}_{k=1}^K; \{(a_l^{(k)})\}_{k=1}^K \right\}$, are mutually independent.

We assume, without loss of generality, that the target user has index $k = 1$ and $\tau_1 = \phi_1 = 0$. The channel is assumed to be slowly fading so that coherent detection can be perfectly implemented. Using a suboptimal single-user matched filter receiver, the decision statistic at the output of the correlator, after low-pass filtering, is given by

$$Z_1 = R_1 b_0^{(1)} G + \sum_{k=2}^K R_k W_k \cos(\phi_k). \tag{4.4}$$

92

Here, $b_0^{(1)}$ denotes the 0th data symbol for User 1, and it is shown in Appendix A that

$$W_k = \Delta_k S_k + \Gamma_k (1 - S_k). \tag{4.5}$$

In (4.5), the RV S_k is uniform over $[0, 1)$ and accounts for the fractional chip displacement of the kth interferer's chip relative to User 1; the RV's Δ_k and Γ_k are shown in Appendix A to be sums of G i.i.d. Bernoulli RV's. The PMF's for Δ_k and Γ_k are, respectively, given by

$$p_{\Gamma_k}(i) = \binom{G}{\frac{i+G}{2}} 2^{-G}, \quad i \in \mathscr{I} = \{-G, -G+2, \dots, G-2, G\}, \tag{4.6}$$

and

$$p_{\Delta_k}(j) = \binom{G}{\frac{j+G}{2}} 2^{-G}, \quad j \in \mathscr{I} = \{-G, -G+2, \dots, G-2, G\}. \tag{4.7}$$

Furthermore, the RV's Γ_k and Δ_k are statistically independent.

4.2 Standard Gaussian Approximation

In the SGA, a CLT is invoked to approximate the sum of the MAI as an additive zero-mean Gaussian noise process. From (4.4), we denote the sum of the MAI signals, at the output of the matched filter receiver, as $I = \sum_{k=2}^{K} R_k W_k \cos(\phi_k)$. The variance of I, denoted by σ_I^2, is obtained by averaging over all operating conditions as

$$\begin{aligned} \sigma_I^2 &= \frac{G}{3} \sum_{k=2}^{K} \mathbb{E}[R_k^2] \\ &= \frac{G}{3}(K-1)\Omega. \end{aligned}$$

The average BER, given R_1, for each user is then approximated by

$$P_{e|R_1}^{SGA} \approx Q\left(\frac{R_1 G}{\sigma_I}\right). \tag{4.8}$$

Averaging over R_1 in (4.8) with respect to the Nakagami-m distribution defined in (4.3) and using the integral identity [79, eq. (3.63)], we approximate the average BER in Nakagami-m fading (for integer values of m) using the SGA as

$$P_e^{SGA} \approx \frac{1}{2^m}\left[1 - (\alpha^2 + 1)^{-\frac{1}{2}}\right]^m \sum_{k=0}^{m-1} 2^{-k} \binom{m-1+k}{k}\left[1 + (\alpha^2 + 1)^{-\frac{1}{2}}\right]^k \tag{4.9}$$

where $\alpha^2 = \frac{2m}{3G}(K-1)$. Note that the average BER, for a mainly interference-limited environment, does not depend on Ω. This is because both the desired signal power and the interfering signal power scale linearly as Ω.

4.3 Accurate BER Calculation

The total other-user interference at the output of the matched filter receiver is $I = \sum_{k=2}^{K} I_k$ where $I_k = R_k W_k \cos(\phi_k)$, and W_k is defined in (4.5). Similar to the development described in Section 2.6, the conditional BER, given R_1, for our target user can be expressed as

$$
\begin{aligned}
P_{e|R_1} &= \Pr\{I < -R_1 G\} \\
&= 1 - F_I(R_1 G) \\
&= \frac{1}{2} - \frac{1}{\pi} \int_0^{+\infty} \frac{\sin(R_1 G\omega)}{\omega} \Phi_I(\omega) d\omega
\end{aligned}
\tag{4.10}
$$

where in the derivation of (4.10), we have used the Fourier inversion formula [59, p. 40] for the real integral.

The overall BER, obtained by averaging over the PDF of R_1 and using the integral property [33, (3.952)], becomes

$$
P_e = \frac{1}{2} - \frac{G}{\pi} \frac{\Gamma(m+\frac{1}{2})}{\Gamma(m)} \sqrt{2} \int_0^{+\infty} \Phi_I'(u) \exp\left\{-\frac{1}{2}G^2 u^2\right\} {}_1F_1\left(1-m;\frac{3}{2};\frac{G^2 u^2}{2}\right) du
\tag{4.11}
$$

where $\Phi_I'(u)$ is the CF of the total interfering signals with its frequency scaled by $\sqrt{\frac{\Omega}{2m}}$. Note that, for the special case when $m=1$ (Rayleigh), using the fact that ${}_1F_1(0;\frac{3}{2};\frac{G^2\omega^2}{2}) = 1$, $\Gamma(\frac{3}{2}) = \frac{\sqrt{\pi}}{2}$, and $\Gamma(1) = 1$, we have

$$
P_{e|m=1} = \frac{1}{2} - \frac{G}{\sqrt{2\pi}} \int_0^{+\infty} \Phi_I'(u) \exp\left\{-\frac{1}{2}G^2 u^2\right\} du,
\tag{4.12}
$$

which is consistent with the results (2.93) and (2.101) obtained in Chapter 2.

Following Section 2.6.2, we again assume that $\{W_k\}_{k=2}^{K}$ are independent, and thus $\{I_k\}_{k=2}^{K}$ are also independent. Therefore, The CF of the total interfering signal becomes

$$
\Phi_I(\omega) = \prod_{k=2}^{K} \Phi_{I_k}(\omega).
\tag{4.13}
$$

94

To find $\Phi_{I_k}(\omega)$, we write $I_k = W_k \chi_k$ where $\chi_k = R_k \cos(\phi_k)$. Then, given W_k, the PDF of I_k is

$$f_{I_k|W_k}(i_k) = \frac{1}{|W_k|} f_{\chi_k}\left(\frac{i_k}{W_k}\right). \tag{4.14}$$

Using the scaling property of the Fourier transform, we obtain

$$\Phi_{I_k|W_k}(\omega) = \Phi_{\chi_k}(\omega W_k) \tag{4.15}$$

where $\Phi_{\chi_k}(\cdot)$ is the CF of χ_k, which has been derived in Chapter 3 in (3.33) as

$$\Phi_\chi(\omega) = \underbrace{\exp\left\{-\frac{\Omega}{4m}\omega^2\right\}}_{Gaussian\ CF} \sum_{l=0}^{m-1} A_l M_{2l} \tag{4.16}$$

where

$$A_l = \frac{\binom{m-1}{l}}{\sqrt{\pi}} \frac{\Gamma(m-l-\frac{1}{2})}{\Gamma(m)} \left(\frac{m}{\Omega}\right)^l, \tag{4.17}$$

and

$$M_{2l} = \sum_{\substack{k=0 \\ k\ even}}^{2l} \binom{2l}{k} \left(j\frac{\omega\Omega}{2m}\right)^k (2l-k-1)!! \left(\sqrt{\frac{\Omega}{2m}}\right)^{2l-k}. \tag{4.18}$$

Thus, averaging (4.15) with respect to the PMF's of Δ_k and Γ_k and letting $\Phi'_{I_k|S_k}(\omega) = \Phi_{I_k|S_k}(\sqrt{\frac{\Omega}{2m}}\omega)$, we get

$$
\begin{aligned}
\Phi'_{I_k|S_k}(\omega) &= \sum_{i'\in\mathscr{S}} \sum_{j'\in\mathscr{S}} \binom{G}{\frac{i'+G}{2}} 2^{-G} \binom{G}{\frac{j'+G}{2}} 2^{-G} \Phi_{\chi_k}(\omega[i'S_k + j'(1-S_k)]) \\
&= 2^{-2G} \sum_{i'\in\mathscr{S}} \sum_{j'\in\mathscr{S}} \binom{G}{\frac{i'+G}{2}} \binom{G}{\frac{j'+G}{2}} \exp\left\{-\frac{1}{2}\omega^2[i'S_k + j'(1-S_k)]^2\right\} \\
&\quad \times \sum_{l=0}^{m-1} \underbrace{\frac{\binom{m-1}{l}}{2^l\sqrt{\pi}} \frac{\Gamma(m-l-\frac{1}{2})}{\Gamma(m)}}_{a_l(m)} M'_{2l}
\end{aligned} \tag{4.19}
$$

where

$$M'_{2l} = \sum_{\substack{q=0,\ q\ even}}^{2l} \binom{2l}{q} (2l-q-1)!!(j\omega)^q[i'S_k + j'(1-S_k)]^q. \tag{4.20}$$

Averaging (4.19) over the PDF of S_k, yields

$$\Phi'_{I_k}(\omega) = \int_0^1 \Phi'_{I_k|S_k}(\omega)\,dS_k. \tag{4.21}$$

95

Carrying out above integration, we obtain $\Phi_{I_k}'(\omega)$ as

$$\Phi_{I_k}'(\omega) = 2^{-2G} \sum_{i' \in \mathscr{S}} \sum_{j' \in \mathscr{S}} \binom{G}{\frac{i'+G}{2}} \binom{G}{\frac{j'+G}{2}} \widehat{J}(i',j',\omega) \tag{4.22a}$$

where for $i' = j' = i$,

$$\widehat{J}(i,j,\omega) = \exp\left\{ -\frac{1}{2}\omega^2 i^2 \right\} \sum_{l=0}^{m-1} a_l(m) \left\{ \sum_{q=0,\,q\ \text{even}}^{2l} \binom{2l}{q} (2l-q-1)!!(j\omega)^q i^q \right\} \tag{4.22b}$$

and for $i' \neq j'$,

$$\widehat{J}(i',j',\omega) = \sum_{l=0}^{m-1} a_l(m) \left\{ \sum_{q=0,\,q\ \text{even}}^{2l} \binom{2l}{q} (2l-q-1)!!(j\omega)^q B(j';i';\omega;q) \right\} \tag{4.22c}$$

where we have defined the function $B(a;b;k;q)$ as

$$B(a;b;k;q) = \frac{1}{b-a} \int_a^b u^q e^{-\frac{1}{2}k^2 u^2} du, \quad a \neq b. \tag{4.23}$$

Note that $B(a;b;k;q)$ is always positive for all permissible values of a, b, k, and q. The function $B(a;b;k;q)$ can be evaluated exactly as follows. For given a, b and k, we denote I_q (where q is a positive even number) as

$$I_q \overset{\triangle}{=} B(a;b;k;q) = \frac{1}{b-a} \int_a^b u^q e^{-\frac{1}{2}k^2 u^2} du. \tag{4.24}$$

Integrating by parts, we obtain a recursive expression for I_q as

$$I_q = \frac{1}{k^2(a-b)} \left[b^{q-1} e^{-\frac{1}{2}k^2 b^2} - a^{q-1} e^{-\frac{1}{2}k^2 a^2} \right] + \frac{q-1}{k^2} I_{q-2}, \quad q \geq 2 \tag{4.25}$$

where $I_{q-2} \overset{\triangle}{=} \frac{1}{b-a} \int_a^b u^{q-2} e^{-\frac{1}{2}k^2 u^2} du$. For $q = 0$, we have

$$\begin{aligned}
I_0 &= \frac{1}{b-a} \int_a^b e^{-\frac{1}{2}k^2 u^2} \\
&= \frac{\sqrt{2\pi}}{(b-a)|k|} \left\{ Q(a|k|) - Q(b|k|) \right\}.
\end{aligned} \tag{4.26}$$

Using (4.25) and (4.26), we can recursively evaluate I_q or $B(a;b;k;q)$ in (4.24) for all permissible values of q without resorting to numerical integration.

Finally, for the special case when $m = 1$ (Rayleigh), we can obtain a more compact expression for $\widehat{J}(i',j',\omega)$. That is, for $i' = j' = i$,

$$\widehat{J}(i',j',\omega) = \exp\left\{ -\frac{1}{2}\omega^2 i^2 \right\}, \tag{4.27a}$$

96

and for $i' \neq j'$,

$$\widehat{J}(i',j',\omega) = \frac{\sqrt{2\pi}}{(i'-j')|\omega|}\left\{ Q(j'|\omega|) - Q(i'|\omega|) \right\}. \tag{4.27b}$$

We note that, as expected, $\widehat{J}(i',j',\omega)$ in (4.27) is identical to $\widetilde{J}(i,j)$ in (2.99) obtained in Chapter 2.

4.4 Numerical Results and Discussions

The exact average BER expression derived in (4.11) is an important new result. It is expressed in terms of a single integral. In this integral, the CF of the MAI has been derived in closed-form expression (it involves only exponential function and the standard Q-function). For the special case when $m = 1$ (Rayleigh), it has been shown in Chapter 2 that the integrand function is strictly non-negative, decaying exponentially. For parameter values $m > 1$, the integrand function takes both positive and negative values; however, its envelope decays exponentially. A typical integrand function is plotted in Fig. 4.1 for $m = 2$, $K = 6$, and $G = 31$. In general, the rate of envelope decay for the integrand function decreases with large values of parameter m, but increases with processing gain.

The average BER is plotted as a function of the number of active users in Fig. 4.2 for different integer values of parameter m and for two different processing gains, namely, $G = 7$ and $G = 31$. We observe that for a given processing gain and a fixed number of users, the system performance increases with increasing parameter m value. This is expected since a larger parameter m value corresponds to a lightly faded channel, thus, smaller BER results. We also observe that, for a given processing gain, the amount of performance improvement diminishes nonlinearly with linearly-spaced increasing parameter m values. Notably, the largest BER improvement is obtained between $m = 1$ and $m = 2$ and for small numbers of users in the system. All analyses in this work are performed for integer-valued m; however, interpolation techniques can be used to estimate the BER for real-valued parameter m.

Fig. 4.3 compares the BER estimated using the SGA to the corresponding BER calculated using the accurate solution for $G = 31$. As shown, the accuracy of the SGA is excellent under a strong

97
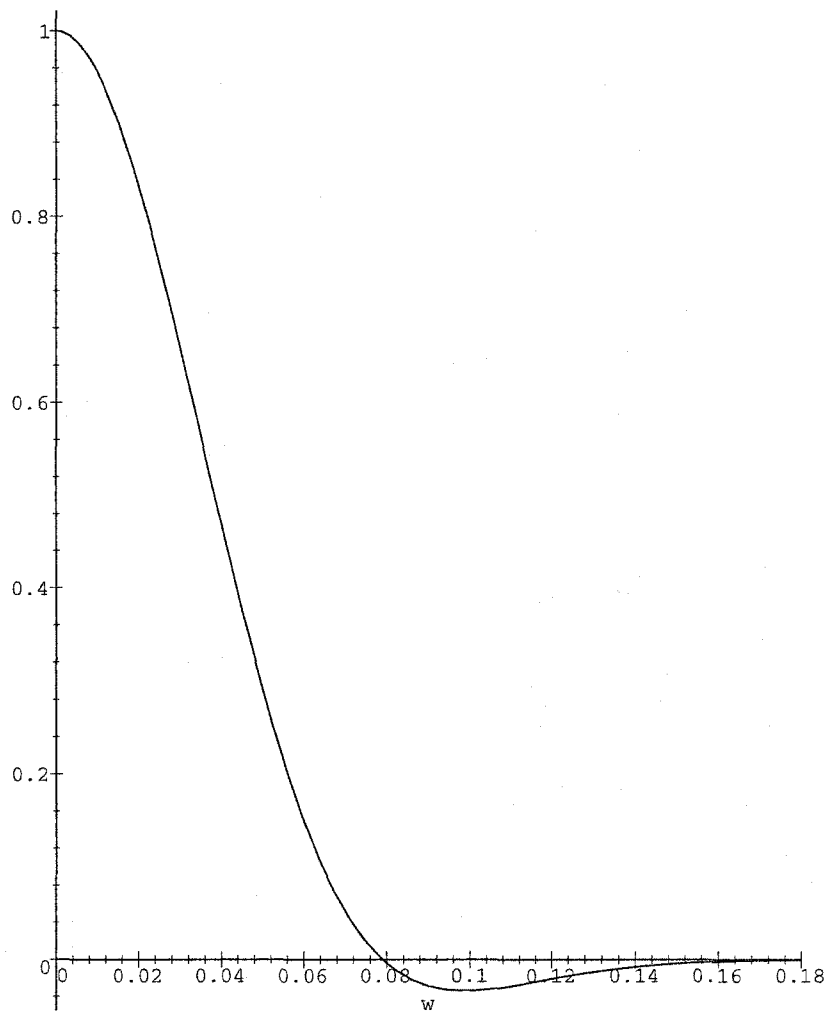
Figure 4.1. Integrand of (4.11) with $m = 2$, $K = 6$, and $G = 31$.

98
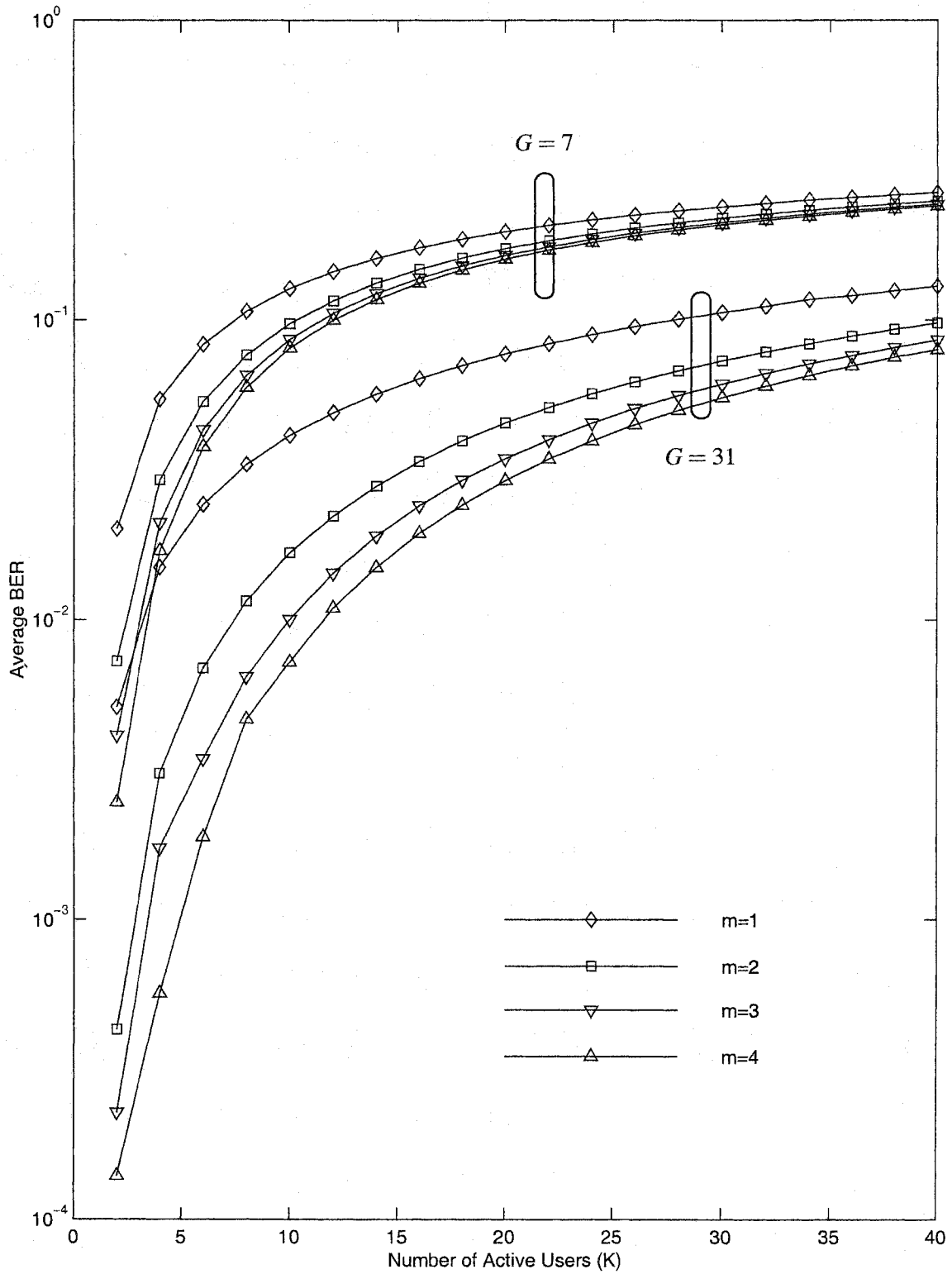
Figure 4.2. System BER performance in an interference-limited environment for $G = 7$ and $G = 31$.

99

fading environment when $m = 1$ (Rayleigh). This is even true for a system with a single interferer. However, it is clear that the SGA can significantly underestimate the BER for $m > 1$ in a system with small numbers of users, especially for large m parameter values. Since large values of parameter m imply light fading environments (or the static non-fading case when $m \to +\infty$), our observation is consistent with the findings in [56].

4.5 Summary

In this chapter, we have derived an accurate, analytical solution using the characteristic function method for the BER of a DS-CDMA system operating in flat Nakagami-m fading. Using any standard numerical integration technique, we can perform rapid and accurate BER calculation for a system in a generalized fading environment. The validity of the standard Gaussian approximation for Nakagami fading channels has also been assessed. It has been found that the SGA can underestimate the BER for a system with a small number of users and moderate processing gain in a lightly faded environment.
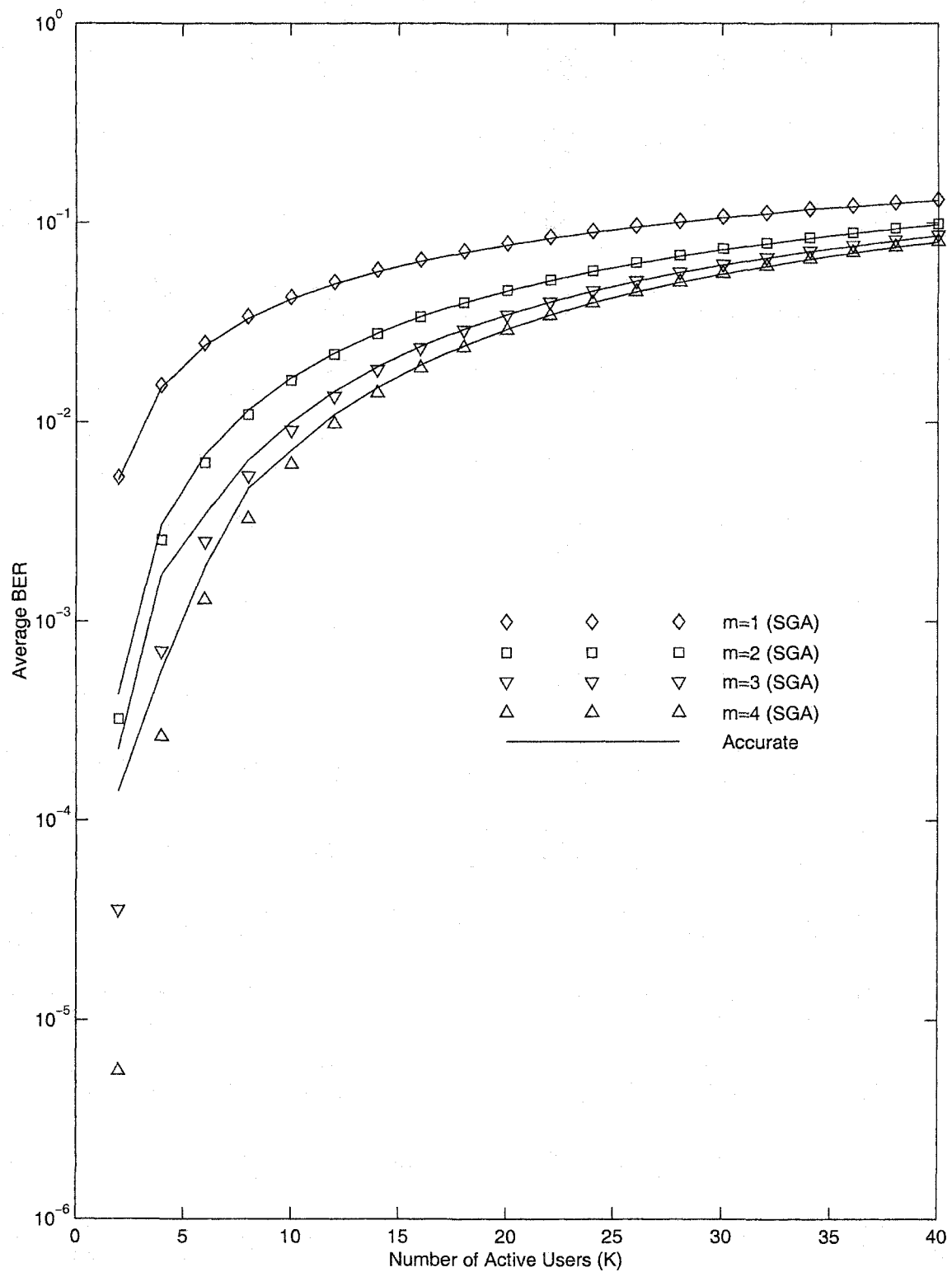
Figure 4.3. Comparison of BER estimated from the SGA with the accurate solution for $G = 31$.

101

Chapter 5

Estimation of the Nakagami Fading Parameters

5.1 Introduction

As we have shown in previous chapters, the Nakagami-m fading model is useful in describing a generalized fading and cochannel interference transmission environment. This is because the Nakagami-m distribution is flexible in modeling a variety of fading conditions. This fading model is also of practical importance because the distribution was originally deduced from experimental data [57]. Extensive empirical measurements confirmed the usefulness of the Nakagami-m distribution for modeling the radio links over a wide range of frequency bands (See [22] and the references therein).

We summarize, for convenience, the most salient features of the Nakagami-m distribution here. The probability density function of the Nakagami-m distribution is given by

$$f_R(r) = \frac{2}{\Gamma(m)} \left(\frac{m}{\Omega}\right)^m r^{2m-1} e^{-mr^2/\Omega}, \quad r \geq 0 \tag{5.1}$$

where Ω is the second moment, i.e., $\Omega = \mathbb{E}[R^2]$, and the m parameter, sometimes known as inverse of the fading figure, is defined as

$$m = \frac{\Omega^2}{\mathbb{E}[(R^2 - \Omega)^2]}, \quad m \geq 1/2. \tag{5.2}$$

As we develop, we will reveal that another compact definition of this m parameter is also possible. The Nakagami-m distribution covers a wide range of fading conditions; when $m = 1/2$, it is a

102

one-sided Gaussian distribution and when $m = 1$, it is a Rayleigh distribution. In the limit as m approaches infinity, the channel becomes static and its corresponding PDF becomes an impulsive function located at $\sqrt{\Omega}$, its root-mean-square value. The kth moment expression for the Nakagami-m distribution is given by

$$\mu_k = \mathbb{E}[R^k] = \frac{\Gamma(m+k/2)}{\Gamma(m)} \left(\frac{\Omega}{m}\right)^{k/2}. \tag{5.3}$$

The motivations of this work are as follows. In order to use the Nakagami-m distribution to model a given set of empirical fading data, one must determine or estimate the value of m from these measured data. The knowledge of the m parameter is also required by the receiver for optimal reception of signals in Nakagami fading [10]. The later application calls for a good m estimator with a form which is suitable for fast and efficient on-line implementation. The knowledge of the m parameter can also be fed back to the transmitter side so that the transmitter can be designed by taking account of the channel information.

Throughout this work we assume a high signal-to-noise power ratio environment. Therefore, the background noise can be neglected in our analysis. The estimation problem can be formally stated as follows. Given $R_1, R_2, \ldots, R_N$ i.i.d. random samples according to the Nakagami-m distribution given in (5.1), we seek good estimators $\hat{m}$ and $\hat{\Omega}$ (which are functions of $R_1, R_2, \ldots, R_N$) for m and Ω.

Two popular approaches to this problems are maximum-likelihood based estimation and moment-based estimation. In this chapter, we will study our Nakagami-m fading parameter problem using these two approaches.

The rest of this chapter is organized as follows. Section 5.2 reviews some fundamental statistical concepts which are required in the remainder of the chapter. In this section we also review the literature related to our fading parameter estimation. The Cramér-Rao lower bound is derived in Section 5.3. Section 5.4 considers the maximum-likelihood estimation, while Section 5.5 considers the moment-based estimation. In Section 5.6, we perform a detailed numerical study of our proposed estimators. Finally, we summarize our results in Section 5.7.

103

5.2 Background Review

This section consists of two parts. In the first part, we review some fundamental concepts and theorems drawn from statistical inference theory. These include the definitions of minimum variance unbiased estimator, Cramér-Rao lower bound, sufficiency, completeness, and exponential family. Major theorems covered are Rao-Blackwell, Lehmann-Scheffé, Central Limit Theory, as well as the delta method. Both scalar and multivariate delta method will be used extensively in this chapter. In the second part, we review some relevant literature related to our work.

5.2.1 Review of Statistical Concepts

In this subsection, we summarize some statistical concepts and theorems which are useful in the subsequent development. The theory of mathematical statistics is rich; it is not our intention to summarize all the results in a few pages. Instead, we will only introduce those important concepts which are required in our work. Most theorems, with exception of the delta method, are stated without proofs. The proofs can be found in several popular statistics references [9], [21], [46], or in engineering references [62], [41]. We consider a PDF, $f_X(x; \theta)$, which is of a known form containing a fixed [1] but unknown parameter $\theta \in \Omega$, where Ω is called the *parameter space*. Let $X_1, X_2, \ldots, X_N$ denote a sequence of i.i.d. random samples drawn according to $f_X(x; \theta)$. We are interested in finding a statistic U, which is a function of these observed random samples, i.e., $\hat{\theta} = U(X_1, X_2, \ldots, X_N)$, as a good estimator for θ. The problem of this nature is called point estimation in statistics literature or is called signal estimation in the engineering literature.

Typically, we are only interested in *unbiased estimators*. An estimator $\hat{\theta}$ is called an unbiased estimator if $\mathbb{E}[\hat{\theta}] = \theta$, and $b(\hat{\theta}) = \mathbb{E}[\hat{\theta}] - \theta$ is commonly defined as the bias in the estimator $\hat{\theta}$. Among the class of unbiased estimators, in addition, we seek an unbiased estimator which has minimum variance. The resulting estimator is called a *minimum variance unbiased estimator* (MVUE). In practice, MVUE can not always be found even it exists. In the following, we will introduce

---

[1]If the parameter θ is not fixed and has a known *a priori* distribution, Bayesian parameter estimation is more appropriate.

104

several techniques which may be used to find the MVUE.

For any given unbiased estimator, we can assess the performance of this estimator by comparing its variance to a variance lower bound. If, by coincidence, the variance of the estimator attains this lower bound, we declare a MVUE is found. There exist several such variance lower bounds [41]; however, the Cramér-Rao lower bound (CRLB) is by far the most popular variance lower bound because it is easy to determine.

Let $\mathbf{x} = [x_1, x_2, \ldots, x_N]^T$ and denote the log-likelihood function (LLF) with a scalar unknown parameter θ by $\ln f_X(\mathbf{x}; \theta)$. The CRLB can be stated as follows [41].

Theorem 5.2.1 (Cramér-Rao Lower Bound) *Assume that the LLF satisfies a regularity condition, i.e., $\mathbb{E}[\partial \ln f_X(\mathbf{x}; \theta)/\partial \theta] = 0$ for all θ, where the expectation is taken with respect to $f_X(\mathbf{x}; \theta)$. Then, the variance of any unbiased estimator $\hat{\theta}$ satisfies*

$$var[\hat{\theta}] \geq \frac{1}{-\mathbb{E}\left[\frac{\partial^2 \ln f_X(\mathbf{x}; \theta)}{\partial \theta^2}\right]}. \tag{5.4}$$

Furthermore, an unbiased estimator may be found to attain the bound if and only if

$$\frac{\partial \ln f_X(\mathbf{x}; \theta)}{\partial \theta} = I(\theta)(g(\mathbf{x}) - \theta) \tag{5.5}$$

for some functions g and I. The MVUE is $\hat{\theta} = g(\mathbf{x})$ and the minimum variance is $1/I(\theta)$.

If an unbiased estimator attains the CRLB, we call this estimator an *efficient estimator*. In (5.5), the non-negative quantity $I(\theta)$ is called the Fisher information. Intuitively, the more information we have, the lower the variance bound becomes, as we expect. If we now have a vector of s unknown parameters, $\theta = [\theta_1, \theta_2, \ldots, \theta_s]^T$, we can modify the above variance lower bound [2] to

$$\text{var}[\hat{\theta}_i] \geq [\mathbf{I}^{-1}(\theta)]_{ii} \tag{5.6}$$

where $\mathbf{I}[\theta]$ is a $s \times s$ Fisher information matrix and it is defined by

$$[\mathbf{I}(\theta)]_{ij} = -\mathbb{E}\left[\frac{\partial^2 \ln f_X(\mathbf{x}; \theta)}{\partial \theta_i \partial \theta_j}\right] \tag{5.7}$$

---

[2]The regularity condition here requires the equation $1 = \int f_{\mathbf{x}}(\mathbf{x}; \theta)d\mathbf{x}$ can be differentiated twice w.r.t. θ under the integral sign.

105

where $i, j = 1, 2, \ldots, s$. The proof of the CRLB uses the Cauchy-Schwarz inequality and it can be found, for example, in Kay [41].

We note that the CRLB sometimes can result an efficient estimator, and thus, a MVUE. If, however, no unbiased estimator can be found to attain the CRLB, it is still of interest to find the MVUE, provided it exists. To do so, we require the concept of sufficient statistic.

Definition 5.2.1 (Sufficient Statistic) [9] *A statistic $T = U(X_1, X_2, \ldots, X_N)$ is said to be a sufficient statistic for θ if the conditional distribution of X given $T = t$, i.e., $f_X(x|T = t)$, is independent of θ.*

Definition 5.2.1 has limited practical use in finding the sufficient statistic. A useful method is to use the factorization theorem, which is due to Neyman [37].

Theorem 5.2.2 (Factorization Theorem) *Let $X_1, X_2, \ldots, X_N$ be random samples from $f_X(x; \theta)$ and $f_X(\mathbf{x}; \theta)$ be the joint PDF, $Y = U(X_1, X_2, \ldots, X_N)$ is a sufficient statistic for θ if and only if*

$$f_X(\mathbf{x}; \theta) = \prod_{i=1}^{N} f_X(x_i; \theta) = g(y; \theta) h(\mathbf{x}) \tag{5.8}$$

where g is a function of y and θ only, and h is a function of x only.

In general, the sufficient statistic is not unique. A sufficient statistic Y^* is said to be *minimal sufficient statistic* for θ if Y^* is a function of any other sufficient statistic T, i.e., $Y^* = H(T)$. The usefulness of the sufficient statistic can be seen from the Rao-Blackwell theorem.

Theorem 5.2.3 (Rao-Blackwell) [9] *Let $X_1, X_2, \ldots, X_N$ be a random sample from $f_X(x; \theta)$; $T = U_1(X_1, X_2, \ldots, X_N)$ be a sufficient statistic for θ; and $Y = U_2(X_1, X_2, \ldots, X_N)$ be any unbiased estimator of θ. Then, $\phi(T) = \mathbb{E}[Y|T]$ is an unbiased estimator of θ and $var[\phi(T)] \leq var[Y]$.*

The uniqueness of an unbiased estimator can be established through the concept of completeness.

Definition 5.2.2 (Completeness) [9] *Let $Y = U(X_1, X_2, \ldots, X_N)$ be a statistic based on $X_1, X_2, \ldots, X_N$ from $f_X(x; \theta)$. The statistic Y is said to be complete statistic if $\mathbb{E}_\theta[g(Y)] = 0$ for all θ implies $g(y) = 0$ almost everywhere y.*

We comment that a complete sufficient statistic implies a minimal sufficient statistic. However,

106

the converse may not be true [46]. The following short but important theorem due to Lehmann and Scheffé can be used to determine the uniqueness of unbiased estimators.

Theorem 5.2.4 (Lehmann-Scheffé) *Unbiased estimators based on complete sufficient statistics are unique.*

It is clear that Theorems 5.2.3 and 5.2.4 can be combined to find the MVUE. The resulting theorem is sometimes referred as the Rao-Blackwell-Lehmann-Scheffé theorem [41].

The complete sufficient statistic can be obtained easily for certain family of distributions. Probably, the most important family of distributions is the exponential family. Many important distributions, such as Gaussian, Rayleigh, Gamma, etc., belong to this family.

Definition 5.2.3 (Exponential Family) [62] *A family of distributions* $\{F_X(x;\theta)\}$ *where* $\theta = [\theta_1, \theta_2, \ldots, \theta_s]^T$ *is said to form a s-parameter exponential family if the distributions have densities of the form*

$$f_X(x;\theta) = C(\theta)\exp\left\{\sum_{i=1}^{s}\eta_i(\theta)T_i(x)\right\}h(x) \qquad (5.9)$$

where $C, \eta_1, \eta_2, \ldots, \eta_s, T_1, T_2, \ldots, T_s$ *and h are real-valued functions.*

If a distribution is a member of exponential family, the following theorem can be used to determine the complete sufficient statistic [62].

Theorem 5.2.4 (Complete Sufficient Statistic for Exponential Family) *If N i.i.d. random samples* $X_1, X_2, \ldots, X_N$ *are drawn according to a probability density function which is a member of an s-parameter,* $\theta = [\theta_1, \theta_2, \ldots, \theta_s]^T$, *exponential family with the form*

$$f_X(x;\theta) = C(\theta)\exp\left\{\sum_{i=1}^{s}\eta_i(\theta)T_i(x)\right\}h(x), \qquad (5.10)$$

then $\left(\sum_{i=1}^{N}T_j(X_i), j = 1, 2, \ldots, s\right)$ *is a joint complete sufficient statistic for* θ *provided that the natural parameter space* $\Xi = \{(\eta_1(\theta), \ldots, \eta_s(\theta))\} \subseteq \mathbb{R}^s$ *contains an s-dimensional rectangle. In other words, the natural parameter space* Ξ *has full rank.*

We now define several types of convergence for a sequence of random variables and review several important theorems built on these concepts. The simplest type of convergence is convergence in probability and it is defined as follows [9].

107

Definition 5.2.4 (Convergence in Probability) *We say that a sequence of RV's, $\{X_n\}$, converge to a constant c in probability, denoted by $X_n \xrightarrow{Pr} c$, if for any $\varepsilon > 0$,*

$$Pr\{|X_n - c| \geq \varepsilon\} \longrightarrow 0, \quad as \quad n \rightarrow +\infty.$$

The concept of convergence in probability can be used to define consistency of an estimator. If an estimator $\hat{\theta}$ converges to its true value θ in probability, then we say that $\hat{\theta}$ is a *consistent estimator* of θ. An important result associated with the consistent estimator in probability theory is the Weak Law of Large Number (WLLN). It states that if $\overline{X}_n = \frac{1}{n} \sum_{i=1}^{n} X_i$ is the average of i.i.d. RV's $X_1, X_2, \ldots, X_n$ with mean $\mathbb{E}[X_i] = \mu$, then $\overline{X}_n \xrightarrow{Pr} \mu$, i.e., the sample mean $\overline{X}_n$ is a consistent estimator of μ. The following result is useful to establish the consistency for a function of an estimator [21].

Theorem 5.2.5 *If $X_n \xrightarrow{Pr} c$ and the function $g(x)$ is continuous at c, then $g(X_n) \xrightarrow{Pr} g(c)$.*

Another important type of convergence for a sequence of RV's is the convergence in law, or sometimes called convergence in distribution.

Definition 5.2.5 (Convergence in Law) [9] *A sequence of RV's $\{X_n\}$ is said to converge to X in law, denoted by $X_n \xrightarrow{L} X$, if*

$$Pr\{X_n \leq x\} \longrightarrow Pr\{X \leq x\} = F_X(x) \tag{5.11}$$

as $n \rightarrow +\infty$ at every continuity point x of the distribution function for X, $F_X(x)$.

Probably the most important theorem in mathematical statistics is the central limit theorem (CLT), which builds on the concept of convergence in law. The CLT has many important engineering applications. As we have shown in previous chapters, the CLT is useful in obtain quick, and sometimes accurate, BER estimations. One version of the CLT, often called the classical CLT [45], can be stated as follows.

Theorem 5.2.6 (Classical Central Limit Theorem) *If $Z_1, Z_2, \ldots$ are a sequence of i.i.d. RV's such that $\mathbb{E}[Z_i] = \mu$ and $var[Z_i] = \sigma^2$ $(0 < \sigma^2 < \infty)$. Let $X_n = \frac{1}{n} \sum_{i=1}^{n} Z_i$, then*

$$\sqrt{n}(X_n - \mu) \xrightarrow{L} Z \sim \mathcal{N}(0, \sigma^2).$$

108

The proof of the CLT is quite involved and it uses the concept of matching of moment generating functions. The proof can be found, for example, in Cassella and Berger [9]. Now, combining the concept of convergence in probability and the concept of convergence in law, we have the following useful properties. Formal proofs of these properties can be found, for example, in Cramér [21].

Properties of Convergence

(1) If $Y_n \xrightarrow{L} Y$, and a and b are constants with $b \neq 0$, then $bY_n + a \xrightarrow{L} bY + a$;

(2) (Slusky's Theorem) If $Y_n \xrightarrow{L} Y$, and $A_n \xrightarrow{Pr} a$ and $B_n \xrightarrow{Pr} b$, then $A_n + B_nY_n \xrightarrow{L} a + bY$;

(3) If c is a constant, then $Y_n \xrightarrow{Pr} c \Leftrightarrow Y_n \xrightarrow{Pr} c$;

(4) If $Y_n \xrightarrow{L} Y$ and $R_n \xrightarrow{Pr} 0$, then $Y_n + R_n \xrightarrow{L} Y$.

We now demonstrate the usefulness of these properties in the proof of following important theorem.

Theorem 5.2.7 (Delta Method) [45] *Let $\{X_n\}$ be a sequence of RV's such that $X_n \xrightarrow{Pr} \mu$ and $\sqrt{n}(X_n - \mu) \xrightarrow{L} X \sim \mathcal{N}(0, \sigma^2)$. Let g be a function which is differentiable. We further assume that $g'(\mu)$ exists and is not zero. Then*

$$\sqrt{n}(g(X_n) - g(\mu)) \xrightarrow{L} \mathcal{N}(0, \sigma^2(g'(\mu))^2). \tag{5.12}$$

Proof: The Taylor expansion of $g(X_n)$ around $X_n = \mu$ gives

$$g(X_n) - g(\mu) = g'(\mu)(X_n - \mu) + \frac{g''(\xi_n)}{2!}(X_n - \mu)^2 \tag{5.13}$$

where ξ_n is between μ and X_n. Then

$$\sqrt{n}(g(X_n) - g(\mu)) = g'(\mu)(\sqrt{n}(X_n - \mu)) + \frac{g''(\xi_n)}{2\sqrt{n}}(\sqrt{n}(X_n - \mu))^2. \tag{5.14}$$

Now since $\sqrt{n}(X_n - \mu) \xrightarrow{L} X \sim \mathcal{N}(0, \sigma^2)$, we have

$$g'(\mu)(\sqrt{n}(X_n - \mu)) \xrightarrow{L} g'(\mu)X \sim \mathcal{N}(0, \sigma^2(g'(\mu))^2) \tag{5.15}$$

by Property 1. Also, since $(\sqrt{n}(X_n - \mu))^2 \xrightarrow{L} X^2$ and $g''(\xi_n)/2\sqrt{n} \xrightarrow{Pr} 0$, by Slusky's theorem, we have the remainder

$$\frac{g''(\xi_n)}{2\sqrt{n}}(\sqrt{n}(X_n - \mu))^2 \xrightarrow{L} 0, \tag{5.16}$$

109

or, the remainder converges to zero in probability by Property 3, Therefore, by Property 4, we have

$$\sqrt{n}(g(X_n) - g(\mu)) \xrightarrow{L} \mathcal{N}(0, \sigma^2(g'(\mu))^2)$$

as desired. ∎

In essence, as Lehmann explains [45], the delta method involves approximating the difference $g(X_n) - g(\mu)$ by a linear function $g'(\mu)(X_n - \mu)$. Since X_n is Gaussian, one would expect that $g'(\mu)(X_n - \mu)$ is also Gaussian since a linear transformation of a Gaussian gives a Gaussian. The delta method method can be extended to multivariate case and it is stated as follows.

Theorem 5.2.8 (Multivariate Delta Method) [45] *Suppose* $\mathbf{X} = [X_1, X_2, \ldots, X_p]^T$ *is a* $p \times 1$ *random vector. Let* $\mathbf{X}_n$ *be a sequences of random vectors such that* $\mathbf{X}_n \xrightarrow{Pr} \mu$ *where* $\mu = [\mu_1, \mu_2, \ldots, \mu_p]^T$, *and*

$$\sqrt{n}(\mathbf{X}_n - \mu) \xrightarrow{L} \mathbf{X} \sim \mathcal{N}(\mathbf{0}, \Sigma) \tag{5.17}$$

where Σ *is the* $p \times p$ *covariance matrix of* $\mathbf{X}$. *Let* g *be a function such that* $g : \mathcal{R}^p \to \mathcal{R}$, *then*

$$\sqrt{n}(g(\mathbf{X}_n) - g(\mu)) \xrightarrow{L} \mathcal{N}\left(\mathbf{0}, (\nabla_g(\mu))^T \Sigma \nabla_g(\mu)\right) \tag{5.18}$$

where $\nabla_g(\mu)$ *is the gradient* $\nabla_g(\mathbf{x}) = \left[\frac{\partial g}{\partial x_1}, \frac{\partial g}{\partial x_2}, \ldots, \frac{\partial g}{\partial x_p}\right]^T$ *evaluated at* $\mathbf{x} = \mu$.

The primary tool used in solving the point estimation problem is the maximum-likelihood estimation (MLE) method. If we denote the likelihood function by $L(\theta)$ and it is given by

$$L(\theta) = \prod_{i=1}^{N} f(x_i; \theta) \tag{5.19}$$

where $\theta = [\theta_1, \theta_2, \ldots, \theta_s]^T$ are the parameters to be estimated, then the MLE involves taking partial derivative of $L(\theta)$ with respect to θ_i, setting

$$\frac{\partial}{\partial \theta_i} L(\theta) = 0, \quad i = 1, 2, 3, \ldots s,$$

and solving for $\theta_1, \theta_2, \ldots, \theta_s$. In general, MLE does not yield closed-form expression for the estimators. Numerical techniques such as Newton-Raphson method or expectation-maximization (EM) algorithms are called to determine the MLE numerically.

110

MLE is favored because it satisfies several optimal criteria. If $\theta^* = [\theta_1^*, \theta_2^*, \ldots, \theta_s^*]$ is the true parameter and $\theta = [\theta_1, \theta_2, \ldots, \theta_s]$ is any other parameter, then it can be shown that $\Pr(L(\theta^*) > L(\theta)) \longrightarrow 1$ as $N \longrightarrow +\infty$.

The maximum-likelihood estimation is widely used also because the resulting estimation is asymptotically unbiased and asymptotically efficient (attaining the CRLB) for large sample size. This can be seen from the following theorem.

Theorem 5.2.9 (Asymptotic Property of MLE) [41]   *If the joint PDF $f_X(x; \theta)$ of the data* $x = [x_1, x_2, \ldots, x_N]^T$ *satisfies some regularity conditions, then the MLE of the unknown parameter* $\theta = [\theta_1, \theta_2, \ldots, \theta_s]^T$ *is asymptotically distributed according to*

$$\hat{\theta} \xrightarrow{L} \mathscr{N}(\theta, \mathbf{I}^{-1}(\theta)) \tag{5.20}$$

where $\mathbf{I}(\theta)$ is the Fisher's information matrix evaluated at the true value of the unknown parameter.

From the asymptotic distribution, it is seen that the MLE is asymptotically unbiased and asymptotically attains the CRLB.

Contrary to MLE, method of moment estimation often results in closed-form expressions for the estimators. In general, moment-based estimators are consistent. However, no optimality is guaranteed. To obtain the moment estimators, we equate the kth distribution moments, $\mathbb{E}[X^k]$, to the corresponding sample moments, $(1/N)\sum_{i=1}^n X^k$, beginning with $k = 1$ and continuing until there are enough number of equations to solve for $\theta_1, \theta_2, \ldots, \theta_s$. Often, we are interested in those moment estimators which use low order sample moments since outliers can cause higher order sample moments to deviate from the true distribution moments when the sample size is not large enough.

5.2.2   Literature Review on Nakagami Parameter Estimation

In this subsection, we review the literature related to the Nakagami fading parameter estimation. The ML estimation of the Nakagami fading parameter was first considered by Cheng and Beaulieu in [13] (See Section 5.4) where two approximate ML-based estimators were proposed. The same result has recently been claimed by Ko and Alouini in a submitted manuscript [42]. In a recent

111

note [86], Zhang pointed out that estimation of the m parameter can be put in the framework of Gamma density parameter estimation. This is because the square of a Nakagami RV follows the Gamma distribution. The mapping from Nakagami to Gamma is one-to-one; therefore, by the data processing theorem [19], we can estimate the Nakagami m parameter based on Gamma samples without losing any information from the mapping process. Estimation of the Gamma parameters has been extensively studied in the statistics community. A comprehensive survey of this subject has been compiled in a monograph by Bowman and Shenton [8]. A popular ML-based Gamma shape parameter estimator is the Greenwood-Durand estimator (GDE) [34]. It can be shown that the log-likelihood function of Nakagami-m and Gamma samples will both lead to a non-linear equation as

$$g(\hat{m}) = \ln(\hat{m}) - \psi(\hat{m}) = \Delta; \qquad m = g^{-1}(\Delta) \tag{5.21}$$

where $\psi(\cdot)$ is the psi function, also called the digamma function, defined in [3], and $\Delta = \ln\left[\frac{1}{N}\sum_{i=1}^{N} r_i^2\right] - \frac{1}{N}\sum_{i=1}^{N}\ln r_i^2$, a function of N observed Nakagami-m samples. Based on tabulated data for $\ln(m) - \psi(m)$, Greenwood and Durand devised a Hasting-type [35] rational approximation to the ML estimator as

$$\hat{m}_{GDE} = f_{GDE}(\Delta) = \begin{cases} f_1(\Delta) & \Delta < 0.5772 \\ f_2(\Delta) & 0.5772 \leq \Delta \leq 17 \end{cases} \tag{5.22}$$

where

$$f_1(\Delta) = \frac{0.5000876 + 0.1648852\Delta - 0.0544274\Delta^2}{\Delta} \tag{5.23}$$

and

$$f_2(\Delta) = \frac{8.898919 + 9.059950\Delta - 0.9775373\Delta^2}{(17.79728 + 11.968477\Delta + \Delta^2)\Delta}. \tag{5.24}$$

According to [34], the maximum errors of above approximations are 0.0088% and 0.0054%, respectively, for $f_1(\Delta)$ and $f_2(\Delta)$.

Moment-based estimation of the Nakagami-m parameter was first considered by Abdi and Kaveh in [2] where a moment estimator was proposed based on the second and the fourth Nakagami sample moments. A better moment estimator which uses the first and the third sample moments was proposed by Cheng and Beaulieu [12]. Using both integer and non-integer sample moments, Cheng

112

and Beaulieu [15] (See Section 5.5) proposed a family of new moment estimators for m and conducted a simulation study. It was shown that this family of moment estimators also includes known integer moment estimators as special cases. More recently, Tepedelenlioglu [74] proposed moment estimators of the form

$$f_{l,k}(\hat{m}) = \frac{\hat{\mu}_l^k}{\hat{\mu}_k^l}; \quad \hat{m} = f_{l,k}^{-1}\left(\frac{\hat{\mu}_l^k}{\hat{\mu}_k^l}\right) \tag{5.25}$$

where $\hat{\mu}_k$ is the kth Nakagami sample moment. It has been shown that $f_{1,2}^{-1}(\hat{\mu}_1^2/\hat{\mu}_2)$ outperforms all published integer-based moment estimators. However the inverse function $f_{l,k}^{-1}(\cdot)$ in general does not have closed-form expression and it needs to be numerically computed and stored.

Moment-based estimators can often be used as a good initial value for some estimators which are iterative in nature. For example, Bowman and Sheton [8] suggested solving the ML equation of (5.21) recursively using

$$\hat{m}^{(i)} = \frac{\hat{m}^{(i-1)} g(\hat{m}^{(i-1)})}{\Delta} \tag{5.26}$$

where a good moment estimator can be used as the initial value $\hat{m}^{(0)}$.

5.3 Cramér-Rao Lower Bound

In this section, we derive the CRLB for the variances of unbiased estimators of the Nakagami-m fading parameters. Letting $\mathbf{r} = [r_1, r_2, \ldots, r_N]^T$ and $\theta = [m, \Omega]^T$, the Fisher's information matrix for the Nakagami-m distribution is given by

$$I(\theta) = \begin{bmatrix} -\mathbb{E}\left[\frac{\partial^2 \ln f_R(\mathbf{r};\theta)}{\partial m^2}\right] & -\mathbb{E}\left[\frac{\partial^2 \ln f_R(\mathbf{r};\theta)}{\partial m \partial \Omega}\right] \\ -\mathbb{E}\left[\frac{\partial^2 \ln f_R(\mathbf{r};\theta)}{\partial \Omega \partial m}\right] & -\mathbb{E}\left[\frac{\partial^2 \ln f_R(\mathbf{r};\theta)}{\partial \Omega^2}\right] \end{bmatrix} \tag{5.27}$$

where $\ln f_R(\mathbf{r}; \theta)$ is the log-likelihood function of N i.i.d. Nakagami-m distributed observations and it is given by

$$\begin{aligned} \ln f_R(\mathbf{r};\theta) &= \ln\left[\prod_{i=1}^{N} f_R(r_i;\theta)\right] \\ &= \ln\left[\prod_{i=1}^{N} \frac{2}{\Gamma(m)}\left(\frac{m}{\Omega}\right)^m r_i^{2m-1} e^{-\frac{mr_i^2}{\Omega}}\right] \end{aligned}$$

113

$$= N \ln \left[\frac{2}{\Gamma(m)} \left(\frac{m}{\Omega} \right)^m \right] + (2m-1) \sum_{i=1}^{N} \ln r_i - \frac{m}{\Omega} \sum_{i=1}^{N} r_i^2. \tag{5.28}$$

Using (5.28), we can easily find the first-order and the second-order partial derivatives as

$$\frac{\partial \ln f_R(\mathbf{r}; \theta)}{\partial m} = N \left[-\psi(m) + \ln m - \ln \Omega + 1 \right] + 2 \sum_{i=1}^{N} \ln r_i - \frac{1}{\Omega} \sum_{i=1}^{N} r_i^2 \tag{5.29}$$

$$\frac{\partial \ln f_R(\mathbf{r}; \theta)}{\partial \Omega} = -\frac{mN}{\Omega} + \frac{m}{\Omega^2} \sum_{i=1}^{N} r_i^2 \tag{5.30}$$

$$\frac{\partial^2 \ln f_R(\mathbf{r}; \theta)}{\partial m^2} = N \left[-\psi'(m) + \frac{1}{m} \right] \tag{5.31}$$

$$\frac{\partial^2 \ln f_R(\mathbf{r}; \theta)}{\partial m \partial \Omega} = -\frac{N}{\Omega} + \frac{1}{\Omega^2} \sum_{i=1}^{N} r_i^2 \tag{5.32}$$

$$\frac{\partial^2 \ln f_R(\mathbf{r}; \theta)}{\partial \Omega^2} = \frac{mN}{\Omega^2} - \frac{2m}{\Omega^2} \sum_{i=1}^{N} r_i^2 \tag{5.33}$$

where $\psi(\cdot)$ is the digamma function, defined as $\psi(m) = \frac{d}{dm} \ln \Gamma(m) = \Gamma'(m)/\Gamma(m)$ [3, p. 258, eqn. 6.3.1], and $\psi'(\cdot)$ is the first-order derivative of the digamma function, also known as the trigamma function [3, p. 260].

Upon taking the negative expectations, we obtain the Fisher's information matrix as

$$I(\theta) = \begin{bmatrix} \frac{mN}{\Omega^2} & 0 \\ 0 & N \left[\psi'(m) - \frac{1}{m} \right] \end{bmatrix}, \tag{5.34}$$

and the inverse becomes

$$I^{-1}(\theta) = \begin{bmatrix} \frac{\Omega^2}{mN} & 0 \\ 0 & \frac{1}{N \left[\psi'(m) - \frac{1}{m} \right]} \end{bmatrix}. \tag{5.35}$$

Therefore, according to Theorem 4.2.1, the CRLB for any unbiased estimator $\hat{m}$ is

$$\text{var}[\hat{m}] \geq \frac{1}{N \left[\psi'(m) - \frac{1}{m} \right]}, \tag{5.36}$$

and the CRLB for any unbiased estimator $\hat{\Omega}$ is

$$\text{var}[\hat{\Omega}] \geq \frac{\Omega^2}{mN}. \tag{5.37}$$

Furthermore, since we can rewrite (5.30) as

$$\frac{\partial \ln f_R(\mathbf{r}; \theta)}{\partial \Omega} = \underbrace{\frac{mN}{\Omega^2}}_{I(\Omega)} \left[\frac{1}{N} \sum_{i=1}^{N} r_i^2 - \Omega \right], \tag{5.38}$$

114

according to Theorem 4.2.1, the unbiased estimator $\hat{\Omega} = \frac{1}{N}\sum_{i=1}^{N} r_i^2$ in fact has the minimum variance. However, it is not too difficult to convince ourself that it is impossible to find a function $g(\mathbf{r})$ such that the following equality

$$\frac{\partial \ln f_R(\mathbf{r};\theta)}{\partial m} = \underbrace{N\left[\psi'(m) - \frac{1}{m}\right]}_{I(m)}[g(\mathbf{r}) - m] \tag{5.39}$$

can be satisfied. Therefore, again according to Theorem 4.2.1, we conclude that there exists no unbiased m estimator which can attain the CRLB for arbitrary sample size N. The minimum variance unbiased estimator for m may however still exist, even it can not be easily found.

5.4 Maximum-likelihood Based Estimation

In this section, we consider ML estimation of the Nakagami-m fading parameter. In general, minimum variance unbiased estimators may not always be found; however, the ML estimator can be considered, asymptotically for large sample size, as an approximation to the MVUE [41]. We propose two approximate ML-based estimators and study the properties of a parameter which is closely associated with these ML estimators

Let $R_1, R_2, \ldots, R_N$ be random variables which are i.i.d. according to (5.1). The log-likelihood function (LLF) of the independent multivariate Nakagami distribution based on the experimental observations $R_1 = r_1, R_2 = r_2, \ldots, R_N = r_N$ has been derived in (5.28). Taking the first-order derivative of the LLF with respect to m, and setting it equal to zero, we obtain

$$-\psi(m) + \ln m = \frac{\frac{1}{N}\sum_{i=1}^{N} r_i^2}{\Omega} - 1 + \ln\Omega - \frac{1}{N}\sum_{i=1}^{N} \ln r_i^2. \tag{5.40}$$

To show that the zero of (5.40) corresponds to the maximum of the LLF, we are required to show that the second-order derivative of the LLF with respect to m is non-positive, i.e., $\partial^2 \text{LLF}/\partial m^2 \leq 0$. Since

$$\frac{\partial^2}{\partial m^2}\text{LLF} = N\left[\frac{1}{m} - \psi'(m)\right], \tag{5.41}$$

115

using an integral representation of the digamma function [33, eqn. 8.361.8]

$$\psi(z) = \ln z + \int_0^{+\infty} e^{-tz} \left[\frac{1}{t} - \frac{1}{1 - e^{-t}} \right] dt,$$

we have

$$
\begin{aligned}
\frac{1}{m} - \psi'(m) &= \frac{1}{m} - \frac{1}{m} - \frac{\partial}{\partial m} \int_0^{+\infty} e^{-tm} \left[\frac{1}{t} - \frac{1}{1 - e^{-t}} \right] dt \\
&= -\int_0^{+\infty} \left(\frac{\partial}{\partial m} e^{-tm} \right) \left[\frac{1}{t} - \frac{1}{1 - e^{-t}} \right] dt \\
&= -\int_0^{+\infty} e^{-tm} \left[1 - \frac{t}{1 - e^{-t}} \right] dt \\
&= -\int_0^{+\infty} e^{-tm} \left[\frac{e^{-t} - (1 - t)}{1 - e^{-t}} \right] dt \\
&\leq 0
\end{aligned}
$$

where the inequality follows from the fact that $e^{-tm} \geq 0$ and $1 - t \leq e^{-t} \leq 1$. Therefore, applying above inequality to (5.41), we have $\partial^2 \text{LLF} / \partial m^2 \leq 0$, or the solution (zero for m) for (5.40) is a maximizer of the LLF.

The statistic for m in (5.40) requires knowledge of Ω which is typically not known. Substitution of the unbiased maximum likelihood estimators of Ω, $\hat{\Omega} = \frac{1}{N} \sum_{i=1}^N r_i^2$, into (5.40) yields

$$-\psi(m) + \ln m \approx \Delta \tag{5.42}$$

where the approximation in (5.42) becomes exact as N approaches infinity, and where

$$\Delta = \ln \left[\frac{1}{N} \sum_{i=1}^N r_i^2 \right] - \frac{1}{N} \sum_{i=1}^N \ln r_i^2. \tag{5.43}$$

The parameter Δ is determined by the observed samples only and it is independent of m. In the sequel, we give a physical interpretation of Δ and discuss some of its properties.

The ML estimation of the m parameter requires solving the nonlinear equation (5.42), which does not lead to a closed-form expression for the estimator. The asymptotic expansion [3] of $\psi(z)$ is given as [3, p. 259, eqn. 6.3.18]

$$\psi(z) \sim \ln z - \frac{1}{2z} - \frac{1}{12z^2} + \frac{1}{120z^4} - \frac{1}{252z^6} + \cdots. \tag{5.44}$$

---

[3] Asymptotic expansions are in general divergent series which are of practical importance in computing functions for large value of arguments.

116

Using the first-order approximation $\psi(z) \approx \ln z - 1/2z$ in (5.42), we obtain

$$\hat{m}_{ML(1)} = \frac{1}{2\Delta} \cdot \tag{5.45}$$

Using the second-order approximation $\psi(z) \approx \ln z - 1/2z - 1/12z^2$ in (5.42), and solving $12\Delta m^2 - 6m - 1 = 0$ for m, we obtain [4]

$$\hat{m}_{ML(2)} = \frac{6 + \sqrt{36 + 48\Delta}}{24\Delta} \cdot \tag{5.46}$$

Here, in obtaining $\hat{m}_2$, we have discarded the negative solution since the m parameter only assumes positive values.

Now, we rewrite (5.43) as

$$\Delta = \ln\left[\left(\frac{1}{N}\sum_{i=1}^{N} r_i^2\right)\right] - \ln\left[\left(r_1^2 r_2^2 \ldots r_N^2\right)^{\frac{1}{N}}\right]$$

$$= \ln\left[\frac{\frac{1}{N}\sum_{i=1}^{N} r_i^2}{\left(r_1^2 r_2^2 \ldots r_N^2\right)^{\frac{1}{N}}}\right] . \tag{5.47}$$

It is clear that the parameter Δ is just the logarithm of the ratio of the arithmetic mean and the geometric mean for the instantaneous fading power.

Both approximate ML estimators contain the parameter Δ, which in turn depends only on the observed samples. We now study several interesting properties of Δ as follows.

Property 1: The Δ defined in (5.47) is always positive. In the limit, when m approaches $+\infty$, Δ goes to zero.

To show that Δ is positive, we apply the well-known Arithmetic-Geometric inequality [3, p. 10, eqn. 3.2.1]

$$\frac{1}{N}\sum_{i=1}^{N} x_i^2 \geq \left(x_1^2 x_2^2 \ldots x_N^2\right)^{\frac{1}{N}},$$

to (5.47) and immediately have $\Delta \geq 0$. Observe from (5.45) and (5.46) that $\Delta \geq 0$ implies that $\hat{m}_1 \geq 0$ and $\hat{m}_2 \geq 0$, respectively, as expected. In the limit as m approaches infinity, Δ becomes zero.

---

[4] As noted by Zhang [86], same approximate ML estimators were proposed by Thom [75] in the framework of Gamma parameter estimation. Recently, these results have also been reported by Ko and Alouini [42].

117

To see this, we note that

$$\lim_{m \to +\infty} \Delta = \lim_{m \to +\infty} \ln \left[\frac{\frac{1}{N} \sum_{i=1}^{N} r_i^2}{\left(r_1^2 r_2^2 \ldots r_N^2 \right)^{\frac{1}{N}}} \right]$$

$$= \ln \left[\frac{\frac{1}{N} N \Omega}{\left(\Omega^N \right)^{\frac{1}{N}}} \right]$$

$$= \ln \left[\frac{\Omega}{\Omega} \right] = 0. \tag{5.48}$$

In deriving (5.48), we have used the fact that when m approaches infinity, the Nakagami-m PDF becomes an impulsive function (i.e., zero variance) located at $\sqrt{\Omega}$, that is, $\{r_1, r_2, \ldots, r_N\}$ approaches $\{\sqrt{\Omega}, \sqrt{\Omega}, \ldots, \sqrt{\Omega}\}$ as $m \to +\infty$. Conversely, when $\Delta = 0$, eqns. (5.45) and (5.46) in turn suggest that m is infinity, which is correct.

Property 2: The parameter Δ defined in (5.47) is a function of the complete sufficient statistic for (m, Ω).

We first show that the Nakagami-m distribution, with m and Ω as unknown parameters, is a member of two-parameter exponential family. To show this, we rewrite the Nakagami-m PDF as

$$f_R(r; m, \Omega) = \frac{2}{\Gamma(m)} \left(\frac{m}{\Omega} \right)^m r^{2m-1} e^{-\frac{mr^2}{\Omega}}$$

$$= \frac{2}{\Gamma(m)} \left(\frac{m}{\Omega} \right)^m \exp\left\{ \ln r^{2m} \right\} \frac{1}{r} \exp\left\{ \frac{mr^2}{\Omega} \right\}$$

$$= \frac{2}{\Gamma(m)} \left(\frac{m}{\Omega} \right)^m \exp\left\{ -\frac{m}{\Omega} r^2 + m \ln r^2 \right\} \frac{1}{r}. \tag{5.49}$$

If we let $C(m, \Omega) = \frac{2}{\Gamma(m)} \left(\frac{m}{\Omega} \right)^m$, $\eta_1(m, \Omega) = -m/\Omega$, $\eta_2(m, \Omega) = m$, $T_1(r) = r^2$, $T_2(r) = \ln r^2$ and $h(r) = 1/r$, then from Definition 5.2.3, we conclude that the Nakagami-m distribution is a member of two-parameter, (m, Ω), exponential family.

From (5.49), the natural parameter space for the Nakagami-m distribution becomes $\Xi = \{ (-\frac{m}{\Omega}, m) :$ $m > 1/2, \Omega > 0 \} \subseteq \mathbb{R}^2$. Let $u = -m/\Omega$ and $v = m$, we plot the natural parameter space in Fig. 5.1 as the shaded area. Clearly, as shown, one can construct a two-dimensional rectangle inside this natural parameter space. It has been shown that the Nakagami-m distribution also belongs to the two-parameter exponential family; therefore, by Theorem 5.2.4, we conclude that $(\sum_{i=1}^{N} R_i^2, \sum_{i=1}^{N} \ln R_i^2)$ is a (joint) complete sufficient statistic for (m, Ω). We observe that the parameter Δ defined in (5.43)

118
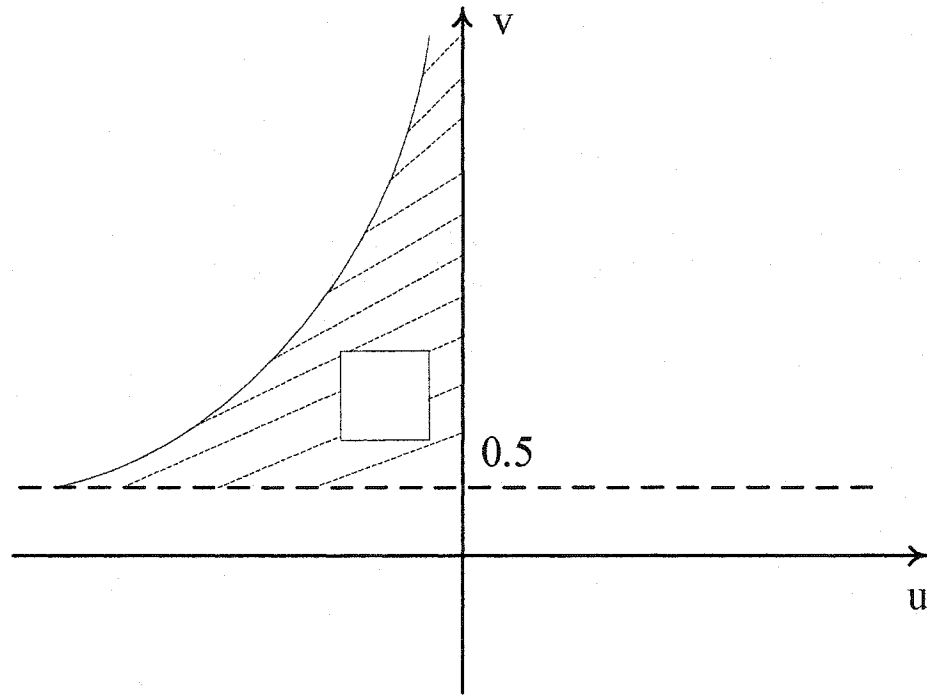
Figure 5.1. The natural parameter space $\Xi = \{(u,v) = (-\frac{m}{\Omega}, m) : m > 1/2, \Omega > 0\} \subseteq \mathbb{R}^2$ of the Nakagami-m distribution.

in our ML estimators is also a function of the joint complete sufficient statistic. In general, it can be shown, by the Neyman factorization Theorem, that the ML estimator is always a function of a sufficient statistic [37].

One can often use the complete sufficient statistic to find the MVUE. As an example of a two-parameter distribution, let $\mathbf{x} = [X_1, X_2, \ldots, X_N]^T$ be N i.i.d. observed samples, if $\check{\theta} = [\check{\theta}_1, \check{\theta}_2]^T$ is an unbiased estimator of $\theta = [\theta_1, \theta_2]^T$ and $(T_1(\mathbf{x}), T_2(\mathbf{x}))$ be a complete and sufficient statistic for (θ_1, θ_2). Then $\hat{\theta} = \mathbb{E}[\check{\theta} \,|\, T_1(\mathbf{x}), T_2(\mathbf{x})]$, if it exists, will yield the MVUE for θ. The procedure just described is called the Rao-Blackwell-Lehmann-Scheffé Theorem [41]. For our problem, to this end, we have found that $(\sum_{i=1}^N R_i^2, \sum_{i=1}^N \ln R_i^2)$ is a complete sufficient statistic for (m, Ω). Unfortunately, no unbiased estimator for m is known, and further, it is not known if any unbiased estimator for m exists. Therefore, the aforementioned technique to find the MVUE using the complete sufficient

119

statistic is not applicable. However, we can still make a good use of the complete and sufficient statistic here. To see this, given Ω, it is obvious that the Nakagami-m distribution is a one-parameter (m) exponential family and

$$T = \sum_{i=1}^{N} \ln R_i^2 - \frac{\sum_{i=1}^{N} R_i^2}{\Omega} \tag{5.50}$$

is a complete sufficient statistic for m. We now attempt to derive an estimator for m based on T. To do this, we take the expectation of T as

$$
\begin{aligned}
\mathbb{E}[T] &= \sum_{i=1}^{N} \mathbb{E}[\ln R_i^2] - \frac{1}{\Omega} \sum_{i=1}^{N} \mathbb{E}[R_i^2] \\
&= N\mathbb{E}[\ln R_i^2] - N \\
&= N \int_0^{+\infty} \frac{2}{\Gamma(m)} \left(\frac{m}{\Omega}\right)^m r^{2m-1} e^{-\frac{m}{\Omega}r^2} \ln r^2 \, dr - N \\
&= N \frac{(\frac{m}{\Omega})^m}{\Gamma(m)} \int_0^{+\infty} u^{m-1} e^{-\frac{m}{\Omega}u} \ln u \, du - N.
\end{aligned}
\tag{5.51}
$$

Using an integral identity [33, eqn. 4.352.1]

$$\int_0^{+\infty} x^{\nu-1} e^{-ux} \ln x \, dx = \frac{1}{u^\nu} \Gamma(\nu)[\psi(\nu) - \ln u]$$

in (5.51), we obtain

$$\mathbb{E}[T] = N[\psi(m) - \ln(m) + \ln\Omega] - N. \tag{5.52}$$

Now setting $\mathbb{E}[T] = T$, combining (5.52) and (5.50), and using $\Omega \approx \frac{1}{N}\sum_{i=1}^{N} r_i^2$, after re-arrangements, we obtain

$$-\psi(m) + \ln m \approx \Delta$$

which is the identical nonlinear equation derived from the maximum-likelihood principle. Therefore, by applying the moment-type estimation of the Nakagami m parameter sufficient statistic, we can also obtain the MLE solution. This observation, though we have only demonstrated that moment-type estimation can lead to MLE for the Nakagami-m, can be extended to all exponential-type distributions. This result, which is not widely known in the engineering community, was first investigated in detail by Davidson and Solomon [23].

120

Property 4: Finally, as a side result, we show that the moment generating function (MGF) of the parameter Δ, denoted by $\phi_\Delta(s)$, can be expressed in a compact form as

$$\phi_\Delta(s) = \frac{\Gamma(mN)[\Gamma(m-s/N)]^N}{N^s[\Gamma(m)]^N\Gamma(mN-s)} \tag{5.53}$$

where s is complex. To arrive the above result we start from the definition of moment generating function for Δ as

$$
\begin{aligned}
\phi_\Delta(s) &= \mathbb{E}[e^{s\Delta}] \\
&= \mathbb{E}\left[\frac{(\sum_{i=1}^N r_i^2)^s}{N^s(\prod_{i=1}^N r_i^2)^{\frac{s}{N}}}\right] \\
&= \underbrace{\int_0^{+\infty}\cdots\int_0^{+\infty}}_{N}\left[\frac{2}{\Gamma(m)}\left(\frac{m}{\Omega}\right)^m r_1^{2m-1}e^{-\frac{m}{\Omega}r_1^2}\right] \\
&\quad \times \left[\frac{2}{\Gamma(m)}\left(\frac{m}{\Omega}\right)^m r_2^{2m-1}e^{-\frac{m}{\Omega}r_2^2}\right]\cdots\left[\frac{2}{\Gamma(m)}\left(\frac{m}{\Omega}\right)^m r_N^{2m-1}e^{-\frac{m}{\Omega}r_N^2}\right] \\
&\quad \times \left[\frac{(\sum_{i=1}^N r_i^2)^s}{N^s(\prod_{i=1}^N r_i^2)^{\frac{s}{N}}}\right]dr_1 dr_2\cdots dr_N \\
&= \frac{\left[\frac{2}{\Gamma(m)}\left(\frac{m}{\Omega}\right)^m\right]^N}{N^s}\int_0^{+\infty}\cdots\int_0^{+\infty}\prod_{i=1}^N r_i^{2m-\frac{2s}{N}-1} \\
&\quad \times \left(\sum_{i=1}^N r_i^2\right)^s \exp\left\{-\frac{m}{\Omega}\sum_{i=1}^N r_i^2\right\}dr_1 dr_2\cdots dr_N. \tag{5.54}
\end{aligned}
$$

If we let $c = 2m - \frac{2s}{N}$, after a change of variable ($r_i^2 = x_i$), we can re-write (5.54) as

$$
\begin{aligned}
\phi_\Delta(s) &= \frac{\left[\frac{1}{\Gamma(m)}\left(\frac{m}{\Omega}\right)^m\right]^N}{N^s}\int_0^{+\infty}\cdots\int_0^{+\infty}x_1^{d-1}x_2^{d-1}\cdots x_N^{d-1} \\
&\quad \times \left(\sum_{i=1}^N x_i\right)^s \exp\left\{-\frac{m}{\Omega}\sum_{i=1}^N x_i\right\}dx_1 dx_2\cdots dx_N \tag{5.55}
\end{aligned}
$$

where $d = m - s/N$. We can now reduce the multiple N integrals in (5.55) into a single integral by invoking a useful integral identity from Gibson [31, p. 483], which is given by

$$
\begin{aligned}
&\int_0^{+\infty}\cdots\int_0^{+\infty}x_1^{\alpha_1-1}x_2^{\alpha_2-1}\cdots x_n^{\alpha_n-1}f(x_1+x_2+\cdots+x_n)\,dx_1 dx_2\cdots dx_n \\
&= \frac{\Gamma(\alpha_1)\Gamma(\alpha_2)\cdots\Gamma(\alpha_n)}{\Gamma(\alpha_1+\alpha_2+\cdots+\alpha_n)}\int_0^{+\infty}u^{\alpha_1+\alpha_2+\cdots+\alpha_n-1}f(u)\,du. \tag{5.56}
\end{aligned}
$$

121

Letting $\alpha_1 = \alpha_2 = \cdots \alpha_N = d$ and $f(x) = x^s \exp\{-\frac{m}{\Omega}x\}$, applying (5.56) to (5.55), we obtain

$$\phi_\Delta(s) = \frac{\left[\frac{1}{\Gamma(m)}\left(\frac{m}{\Omega}\right)^m\right]^N}{N^s} \cdot \frac{\Gamma(d)\Gamma(d)\cdots\Gamma(d)}{\Gamma(Nd)} \int_0^{+\infty} u^{Nd-1} u^s \exp\left\{-\frac{m}{\Omega}u\right\} du$$

$$= \frac{\left[\frac{1}{\Gamma(m)}\left(\frac{m}{\Omega}\right)^m\right]^N}{N^s} \cdot \frac{[\Gamma(m-s/N)]^N}{\Gamma(Nm-s)} \int_0^{+\infty} u^{Nm-1} \exp\left\{-\frac{m}{\Omega}u\right\} du. \tag{5.57}$$

Using the definition of the Gamma function

$$\Gamma(n) = \int_0^{+\infty} t^{n-1} e^{-t} dt \tag{5.58}$$

and changing the variable in (5.57), after some simplifications, we arrive at the expression of the MGF for Δ in (5.53) as desired.

The PDF of Δ can be obtained from its MGF expression by using the inverse Laplace transform and it is given by

$$f_\Delta(\delta) = \frac{1}{2\pi j} \int_{c-j\infty}^{c+j\infty} \phi_\Delta(-s) e^{s\delta} ds \tag{5.59}$$

where $j^2 = -1$ and c is a suitably chosen positive constant. Substitution of (5.53) into (5.59) yields

$$f_\Delta(\delta) = \frac{\theta_1}{2\pi j} \int_{c-j\infty}^{c+j\infty} \frac{N^s[\Gamma(m+\frac{s}{N})]^N}{\Gamma(mN+s)} e^{s\delta} ds \tag{5.60}$$

where

$$\theta_1 = \frac{\Gamma(mN)}{[\Gamma(m)]^N}. \tag{5.61}$$

If we now let $y = s/N$, the PDF of Δ becomes

$$f_\Delta(\delta) = \frac{N\theta_1}{2\pi j} \int_{c'-j\infty}^{c'+j\infty} \frac{N^{Ny}[\Gamma(m+y)]^N}{\Gamma(N(m+y))} e^{Ny\delta} dy \tag{5.62}$$

where c' is another positive constant. With the aid of Gauss's Formula for the product of the Gamma function

$$\Gamma(nx) = (2\pi)^{\frac{1-n}{2}} n^{nx-\frac{1}{2}} \prod_{k=0}^{n-1} \Gamma\left(x+\frac{k}{n}\right), \tag{5.63}$$

the denominator of the integrand in (5.62) can be written as

$$\Gamma(N(m+y)) = (2\pi)^{\frac{1-N}{2}} N^{N(m+y)-\frac{1}{2}} \prod_{k=0}^{N-1} \Gamma\left(m+y+\frac{k}{N}\right). \tag{5.64}$$

122

Substituting (5.64) into (5.62), after some simplifications, the PDF of Δ can be written as

$$f_\Delta(\delta) = \frac{N\theta_2}{2\pi j} \int_{c'-j\infty}^{c'+j\infty} \frac{\prod_{k=1}^{N} \Gamma(1-(1-m)+y)}{\prod_{k=1}^{N} \Gamma\left(1-(1-m)-\frac{1}{N}+\frac{k}{N}+y\right)} \left(e^{N\delta}\right)^y dy \qquad (5.65)$$

where

$$\theta_2 = \frac{\theta_1}{(2\pi)^{\frac{1-N}{2}} N^{Nm-\frac{1}{2}}}. \qquad (5.66)$$

Now comparing (5.65) with the definition of the Meijer's G-function [33, eqn. 9.301]

$$G_{p,q}^{m,n}\left(x \left| \begin{array}{ccc} a_1 & \cdots & a_p \\ b_1 & \cdots & b_q \end{array} \right.\right) = \frac{1}{2\pi j} \int \frac{\prod_{j=1}^{m}\Gamma(b_j-s)\prod_{j=1}^{n}\Gamma(1-a_j+s)}{\prod_{j=m+1}^{q}\Gamma(1-b_j+s)\prod_{j=n+1}^{p}\Gamma(a_j-s)} x^s ds, \qquad (5.67)$$

we can simply write the PDF of Δ as

$$f_\Delta(\delta) = (N\theta_2) G_{N,N}^{0,N}\left(e^{N\delta} \left| \begin{array}{ccccc} 1-m & 1-m & 1-m & \cdots & 1-m \\ 1-m & 1-m-\frac{1}{N} & 1-m-\frac{2}{N} & \cdots & 1-m-\frac{N-1}{N} \end{array} \right.\right). \qquad (5.68)$$

Because two approximate ML-based estimators in (5.45) and (5.46) are both functions of the parameter Δ only, the PDF of Δ can be used to assess the performances of these two estimators analytically. The Meijer's G-function is widely available in popular software packages such as Maple and Mathematica. However, the computational complexity of the Meijer's G-function with large numbers of arguments is huge, and thus, it is not feasible to use $f_\Delta(\delta)$ for practical numbers of observation sample size. Therefore, we will use Monte Carlo simulation to determine the performances of our proposed ML estimators. Before we present these numerical results in Section 5.6, we will first study the same estimation problem using the method of moments.

5.5   Moment-Based Estimation

In this section, we study moment-based estimation of the Nakagami m fading parameter. As shown in the previous section, ML-based estimation of the Nakagami fading parameter leads to finding solution of a non-linear equation. This undesirable feature has, in part, motivated some researchers to find an estimator of the fading parameter using method of moment. In general, as we have stated in Section 5.2.1, moment-based estimators are consistent; however, no optimality is guaranteed.

123

Fortunately, for our problem, as it will be be shown, highly efficient moment-based estimators can be found.

Given $r_1, r_2, \ldots, r_N$ as N independent realizations of the Nakagami-m RV, Abdi and Kaveh [2] reported a moment-based estimator for the m fading parameter, denoted by $\hat{m}_s$, as

$$\hat{m}_s = \frac{\hat{\mu}_2^2}{\hat{\mu}_4 - \hat{\mu}_2^2} \qquad (5.69)$$

where $\hat{\mu}_k = (1/N) \sum_{i=1}^{N} r_i^k$ is the kth sample moment. This estimator, which uses the second and the fourth sample moments, is also called the inverse normalized variance (INV) estimator [2], since it can be derived directly from the Nakagami m parameter definition by substituting sample moments for distribution moments. Alternatively, the estimator in (5.69) can be derived by taking the ratio of the second and the fourth Nakagami-m distribution moments and solving for m. If we take the ratio of the first and the third moment, and use the property of the Gamma function $\Gamma(m+1) = m\Gamma(m)$ [3], we obtain

$$\begin{aligned} \frac{\mu_3}{\mu_1} &= \frac{\Gamma(m+\frac{3}{2})}{\Gamma(m+\frac{1}{2})} \left(\frac{\Omega}{m} \right) \\ &= \left(m + \frac{1}{2} \right) \left(\frac{\Omega}{m} \right). \end{aligned} \qquad (5.70)$$

Solve for m, we have

$$m = \frac{\mu_1 \mu_2}{2(\mu_3 - \mu_1 \mu_2)}. \qquad (5.71)$$

This suggests a new moment estimator, denoted by $\hat{m}_t$, as

$$\hat{m}_t = \frac{\hat{\mu}_1 \hat{\mu}_2}{2(\hat{\mu}_3 - \hat{\mu}_1 \hat{\mu}_2)}. \qquad (5.72)$$

Since the highest order of sample moment that $\hat{m}_t$ uses is three and that $\hat{m}_s$ uses is four, one would expect that the variance of $\hat{m}_t$ is smaller than that of $\hat{m}_s$, and thus, $\hat{m}_t$ is a better estimator than $\hat{m}_s$ (higher order sample moments can deviate significantly from the true moments if the sample size is not large enough because of outliers). Our numerical results presented in Section 5.6 confirms this intuition.

Better moment-based estimators than $\hat{m}_t$ can be found if we admit the use of non-integer moments. The computation and use of non-integer moments, for any applications, seems rare in the

124

engineering literature. Thus, our generalization of the design of the estimator to employ non-integer moments is novel. To show how these new estimators can be derived, we first take the pth root of our observed samples, $R_i, i = 1, 2, \ldots, N$, as

$$X_i = (R_i)^{1/p} \quad i = 1, 2, \ldots, N; \quad p > 0. \tag{5.73}$$

Denoting the RV at the output of our nonlinear transformation of the observation samples by X, the kth moment of X becomes

$$
\begin{aligned}
\mathbb{E}[X^k] &= \int_0^{+\infty} r^{\frac{k}{p}} \frac{2}{\Gamma(m)} \left(\frac{m}{\Omega}\right)^m r^{2m-1} e^{-\frac{m}{\Omega}r^2} dr \\
&= \frac{2}{\Gamma(m)} \left(\frac{m}{\Omega}\right)^m \int_0^{+\infty} r^{(2m+\frac{k}{p})-1} e^{-\frac{m}{\Omega}r^2} dr \\
&= \frac{\Gamma(m+k/2p)}{\Gamma(m)} \left(\frac{\Omega}{m}\right)^{2p} \tag{5.74}
\end{aligned}
$$

where in obtaining the last equality, we have used the following integral identity [33, eqn. 3.478]

$$\int_0^{+\infty} x^{\nu-1} e^{-\mu x^p} dx = \frac{1}{p} \mu^{-\frac{\nu}{p}} \Gamma\left(\frac{\nu}{p}\right).$$

Note that, from (5.74), when $p = 1$ we obtain, as expected, the kth moment expression for a Nakagami-m RV in (5.3). For a given p value, one can take the ratio of any two moments of X, solve for m, and obtain an expression for m. In general, such procedure involves solving a transcendental equation and does not lead to closed-form expressions for the estimator. If we, however, take the ratio of the $(2p+1)$th moment and the first moment of X, we get

$$
\begin{aligned}
\frac{\mathbb{E}[X^{2p+1}]}{\mathbb{E}[X]} &= \frac{\Gamma(m+\frac{1}{2p}+1)}{\Gamma(m+\frac{1}{2p})} \left(\frac{\Omega}{m}\right) \\
&= \left(1 + \frac{1}{2mp}\right) \Omega. \tag{5.75}
\end{aligned}
$$

Solving (5.75) for m, we obtain in closed-form

$$m = \frac{\mathbb{E}[X]\Omega}{2p(E[X^{2p+1}] - E[X]\Omega)}. \tag{5.76}$$

Using (5.73) in (5.76), we obtain a family of new definitions for m parameter as

$$m_{\frac{1}{p}} = \frac{\mu_{\frac{1}{p}} \mu_2}{2p(\mu_{2+\frac{1}{p}} - \mu_{\frac{1}{p}} \mu_2)}, \quad p > 0. \tag{5.77}$$

125

Eqn. (5.77) suggests a family of new moment-based estimators for the fading parameter m, denoted by $\hat{m}_{\frac{1}{p}}$, as

$$\hat{m}_{\frac{1}{p}} = \frac{\hat{\mu}_{\frac{1}{p}}\hat{\mu}_2}{2p(\hat{\mu}_{2+\frac{1}{p}} - \hat{\mu}_{\frac{1}{p}}\hat{\mu}_2)}. \tag{5.78}$$

The estimator derived in (5.78) is an interesting result since it uses both integer and non-integer sample moments. This estimator can be derived alternatively by taking the ratio of the $(2 + (1/p))$th and the $(1/p)$th moments of a Nakagami-m RV and solving for m. Varying the parameter p yields a family of estimators. Generally, the performances of these estimators improve with increasing p values. Known integer-moment based estimators are obtained as special cases for appropriate values of p. In particular, when $p = 1/2$, we obtain $\hat{m}_2 = \hat{m}_s$, which is the INV estimator first proposed by Abdi and Kaveh [2]. When $p = 1$, we obtain our new integer-moment estimator $\hat{m}_1 = \hat{m}_t$. Letting $p = 2$, we obtain a fractional moment estimator as

$$\hat{m}_{\frac{1}{2}} = \frac{\hat{\mu}_{\frac{1}{2}}\hat{\mu}_2}{4(\hat{\mu}_{\frac{5}{2}} - \hat{\mu}_{\frac{1}{2}}\hat{\mu}_2)}. \tag{5.79}$$

Since the highest order of sample moments in (5.79) is 2.5 (which is less than 3), we would expect that the variance of $\hat{m}_{\frac{1}{2}}$ is smaller than that of $\hat{m}_s$ and $\hat{m}_t$. Our numerical results presented in Section 5.6 will verify this expectation.

To this end, we have presented a family of new definitions for the Nakagami-m fading parameter in (5.77). This family is controlled by a positive real number p. We now investigate the limiting case when p approaches $+\infty$. Put $k = 1/p$, we can rewrite (5.77) as

$$m_k = \frac{k\mu_k\mu_2}{2(\mu_{2+k} - \mu_k\mu_2)} = \frac{\mu_2}{\rho_k} \tag{5.80}$$

where

$$\rho_k = \frac{2(\mu_{k+2} - \mu_k\mu_2)}{k\mu_k}. \tag{5.81}$$

Note that when the real number k approaches zero, ρ_k approaches the form of $0/0$! Therefore, by invoking l'Hôpital's rule, we can obtain the limit value of ρ_k when $k \to 0$ as

$$\lim_{k \to 0} \rho_k = \lim_{k \to 0} \frac{2(\mu_{k+2} - \mu_k\mu_2)}{k\mu_k}$$

126

$$= \lim_{k \to 0} \frac{2(\mathbb{E}[R^{k+2}] - \mathbb{E}[R^k]\mathbb{E}[R^2])}{k\mathbb{E}[R^k]}$$

$$= \lim_{k \to 0} \frac{2\left(\mathbb{E}[\frac{d}{dk}R^{k+2}] - \mathbb{E}[\frac{d}{dk}R^k]\mathbb{E}[R^2]\right)}{\frac{d}{dk}(k\mathbb{E}[R^k])}$$

$$= \lim_{k \to 0} \frac{2(\mathbb{E}[R^{k+2}\ln R] - \mathbb{E}[R^k \ln R]\mathbb{E}[R^2])}{\mathbb{E}[R^k] + k\mathbb{E}[R^k \ln R]}$$

$$= 2(\mathbb{E}[R^2 \ln R] - \mathbb{E}[\ln R]\mathbb{E}[R^2])$$

$$= \mathbb{E}[R^2 \ln R^2] - \mathbb{E}[R^2]\mathbb{E}[\ln R^2]$$

$$= \text{cov}[R^2, \ln R^2]. \tag{5.82}$$

Combining (5.80) and (5.82), we obtain, in essence, a new compact definition for the Nakagami-m fading parameter as

$$m = \frac{\mathbb{E}[R^2]}{\text{cov}[R^2, \ln R^2]}. \tag{5.83}$$

This result is intuitively correct. As a sanity check, when m approaches infinity (no fading), both R^2 and $\ln R^2$ approach their respective means, and thus, $\lim_{m \to +\infty} \text{cov}[R^2, \ln R^2] = 0$, which in turn suggests that m is infinity according to (5.83).

Recall from Chapter 1 that the fading figure for the Nakagami-m fading is given by FF $= 1/m$. According to (5.83), we can obtain an alternative expression for the Nakagami fading figure as

$$\text{FF} = \frac{\text{cov}[R^2, \ln R^2]}{\mathbb{E}[R^2]} \tag{5.84}$$

$$= \frac{\text{cov}[R^2, 10\log_{10} R^2]}{c\mathbb{E}[R^2]} \tag{5.85}$$

where $c = 10\log_{10} e$. In words, eqn. (5.85) says that the fading figure for the Nakagami-m fading model can be interpreted as the covariance of the instantaneous fading power and its value in dB [5] normalized by its average fading power and some constant. The covariance term $\text{cov}[R^2, \ln R^2]$ has its own interesting physical interpretation. To see this, since FF $= \text{var}[R^2]/(\mathbb{E}[R^2])^2$, from (5.84), we have

$$\text{cov}[R^2, \ln R^2] = \frac{\text{var}[R^2]}{\mathbb{E}[R^2]}$$

---

[5]We comment that, coincidentally, the original Nakagami distribution was deduced from the distribution of the intensity in dB [57].

127

$$= \frac{\text{Variance of the instantaneous fading power}}{\text{Mean of the instantaneous fading power}} . \tag{5.86}$$

The new compact definition of the m fading parameter in (5.83) suggests that we can have a new estimator for m based on sample moments and sample covariance. Let $r_1, r_2, \ldots, r_N$ be N independent realizations of the Nakagami-m RV, the new estimator becomes

$$\hat{m}_0 = \frac{a}{\frac{1}{N-1} \sum_{i=1}^{N} (r_i^2 - a)(\ln r_i^2 - b)} \tag{5.87}$$

where

$$a = \frac{1}{N} \sum_{i=1}^{N} r_i^2, \quad b = \frac{1}{N} \sum_{i=1}^{N} \ln r_i^2 \tag{5.88}$$

where the factor $\frac{1}{N-1}$ in the denominator of $\hat{m}_0$ is required to obtain an unbiased estimator of the covariance for a finite sample size. This new m parameter estimator is compact and computationally simpler than those estimators presented in (5.78). It is of interest to observe that $\hat{m}_0$ is also a function of the complete and sufficient statistic derived in Section 5.4 for m and Ω. Intuitively we would expect that $\hat{m}_0$ to be a good estimator. In the sequel, we will study the asymptotic properties of our new moment-based estimators.

It is difficult to obtain the analytical performances of the estimators in (5.78) and (5.87) with finite sample size. We can, however, obtain their asymptotic large-sample performances analytically. To do so, we first rewrite the estimators in (5.78) and (5.87) to the forms, which are suitable for our following analysis, as

$$\hat{m}_k = \begin{cases} \frac{k}{2\left(\frac{\hat{\mu}_{k+2}}{\hat{\mu}_k \hat{\mu}_2} - 1\right)} & k > 0 \\ \left(\frac{\frac{1}{N} \sum_{i=1}^{N} r_i^2 \ln r_i^2}{\hat{\mu}_2} - \frac{1}{N} \sum_{i=1}^{N} \ln r_i^2\right)^{-1} & k = 0 \end{cases} \tag{5.89}$$

where, for mathematical convenience, we have replaced $\frac{1}{N-1}$ by $\frac{1}{N}$ in $\hat{m}_0$ since these two factors are equivalent when N approaches infinity. We now summarize our main result on the large-sample properties of our new moment-based estimators in the following theorem.

Theorem 4.5.1 *The estimators in (5.89), indexed by $k \geq 0$, are consistent, i.e.*

$$\hat{m}_k \xrightarrow{Pr} m \quad as \quad N \longrightarrow +\infty \tag{5.90}$$

128

and asymptotically normal-distributed

$$\sqrt{N}(\hat{m}_k - m) \xrightarrow{L} \mathcal{N}(0, \sigma_k^2) \quad as \quad N \longrightarrow +\infty \tag{5.91}$$

where for $k > 0$, the asymptotic variance is

$$\sigma_k^2 = m^2 \left[\frac{v_{2k}}{v_k^2} + \frac{v_{2k+2} - \frac{v_{k+2}^2}{v_2}}{(k/2)^2 v_k^2} \right] \tag{5.92}$$

where $v_k = \Gamma(m + k/2)/\Gamma(m)$; and where for $k = 0$, the asymptotic variance is

$$\sigma_0^2 = m^2[1 + m\psi'(m+1)]. \tag{5.93}$$

Proof: Recall from Section 1.2.1, if R is a Nakagami-m distributed RV, then $G = (m/\Omega)R^2$ has one-parameter Gamma density function with shape parameter m, which is restricted to be $m > 1/2$, i.e.,

$$f_G(g) = \frac{g^{m-1}e^{-g}}{\Gamma(m)}, \quad g > 0. \tag{5.94}$$

The mean and variance of G are $\mathbb{E}[G] = m$ and $\text{var}[G] = m$, respectively. The kth moment of G is given by

$$\mathbb{E}[G^k] = \frac{\Gamma(m+k)}{\Gamma(m)} \tag{5.95}$$

and therefore,

$$v_k = \frac{\Gamma(m+k/2)}{\Gamma(m)} = \mathbb{E}[G^{k/2}]. \tag{5.96}$$

We first observe that the estimators in (5.89) share a property of scale invariance such that if $\hat{m}_k = T_k(r_1^2, r_2^2, \ldots, r_N^2)$, then

$$T_k(cr_1^2, cr_2^2, \ldots, cr_N^2) = T_k(r_1^2, r_2^2, \ldots, r_N^2) \tag{5.97}$$

for any constant $c > 0$. To see this, when $k > 0$,

$$T_k(cr_1^2, cr_2^2, \ldots, cr_N^2) = \frac{k}{2 \left\{ \frac{\frac{1}{N}\sum_{i=1}^N (cr_i^2)^{\frac{k+2}{2}}}{\left[\frac{1}{N}\sum_{i=1}^N (cr_i^2)^{\frac{k}{2}} \right]\left[\frac{1}{N}\sum_{i=1}^N (cr_i^2) \right]} - 1 \right\}}$$

129

$$= \frac{k}{2\left[\dfrac{c^{\frac{k+2}{2}}\hat{\mu}_{k+2}}{c^{\frac{k}{2}+1}\hat{\mu}_k\hat{\mu}_2} - 1\right]}$$

$$= \frac{k}{2\left[\dfrac{\hat{\mu}_{k+2}}{\hat{\mu}_k\hat{\mu}_2} - 1\right]}$$

$$= T_k(r_1^2, r_2^2, \dots, r_N^2).$$

Similarly, one can show that $\hat{m}_0$ is also scale invariant. As a consequence, if we choose $c = m/\Omega$, this invariant property allows us to write

$$
\begin{aligned}
\hat{m}_k &= T_k(r_1^2, r_2^2, \dots, r_N^2) \\
&= T_k((m/\Omega)r_1^2, (m/\Omega)r_2^2, \dots, (m/\Omega)r_N^2) \\
&= T_k(g_1, g_2, \dots, g_N)
\end{aligned}
\tag{5.98}
$$

where $g_1, g_2, \dots, g_N$ are samples from the one-parameter Gamma density given in (5.94). Furthermore, we have the identity $v_k = \mu_k$. We emphasize that the above substitution is carried out for mathematical convenience only, as in general $c = m/\Omega$ is unknown, m and Ω are the parameters we try to estimate.

For $\hat{m}_k$ $(k > 0)$, to establish consistency, we note that

$$
\begin{aligned}
\hat{\mu}_k &= \frac{1}{N}\sum_{i=1}^{N}(r_i^2)^{k/2} \\
&= \frac{1}{N}\left[(r_1^2)^{k/2} + (r_2^2)^{k/2} + \dots + (r_N^2)^{k/2}\right] \\
&= \frac{1}{N}\left[g_1^{k/2} + g_2^{k/2} + \dots + g_N^{k/2}\right].
\end{aligned}
$$

$$\tag{5.99}$$

Therefore, by the Weak Law of Large Number, we have

$$\hat{\mu}_k \xrightarrow{Pr} \mathbb{E}[G^{k/2}] = v_k = \mu_k. \tag{5.100}$$

Since $\hat{m}_k$ is a continuous function of $\hat{\mu}_k$, we have

$$\hat{m}_k \xrightarrow{Pr} \frac{k}{2\left(\dfrac{v_{k+2}}{v_k v_2} - 1\right)} = m. \tag{5.101}$$

130

To find the asymptotic variance σ_k^2, we note that, by the multivariate Central Limit Theorem,

$$\sqrt{N}\begin{bmatrix} \hat{\mu}_2 - v_2 \\ \hat{\mu}_k - v_k \\ \hat{\mu}_{k+2} - v_{k+2} \end{bmatrix} \xrightarrow{L} \mathcal{N}(0, \Sigma_k) \tag{5.102}$$

where $\mathcal{N}(0, \Sigma_k)$ is a trivariate normal distribution with mean vector $0 = [0,\ 0,\ 0]^T$ and covariance matrix Σ_k given by

$$\Sigma_k = \begin{bmatrix} \mathrm{var}[G] & \mathrm{cov}[G, G^{k/2}] & \mathrm{cov}[G, G^{(k+2)/2}] \\ \mathrm{cov}[G, G^{k/2}] & \mathrm{var}[G^{k/2}] & \mathrm{cov}[G^{k/2}, G^{(k+2)/2}] \\ \mathrm{cov}[G, G^{(k+2)/2}] & \mathrm{cov}[G^{k/2}, G^{(k+2)/2}] & \mathrm{var}[G^{(k+2)/2}] \end{bmatrix}. \tag{5.103}$$

Using (5.95) and (5.96), we can show

$$\mathrm{var}[G] = \mathbb{E}[G^2] - (\mathbb{E}[G])^2 = v_4 - v_2^2$$

$$\mathrm{var}[G^{k/2}] = \mathbb{E}[G^k] - (\mathbb{E}[G^{k/2}])^2 = v_{2k} - v_k^2$$

$$\mathrm{var}[G^{(k+2)/2}] = \mathbb{E}[G^{k+2}] - (\mathbb{E}[G^{k+2}/2]^2) = v_{2k+4} - v_{k+2}^2$$

$$\mathrm{cov}[G, G^{k/2}] = \mathbb{E}[GG^{k/2}] - \mathbb{E}[G]\mathbb{E}[G^{k/2}] = v_{k+2} - v_2 v_k$$

$$\mathrm{cov}[G, G^{(k+2)/2}] = \mathbb{E}[GG^{(k+2)/2}] - \mathbb{E}[G]\mathbb{E}[G^{(k+2)/2}] = v_{k+4} - v_2 v_{k+2}$$

$$\mathrm{cov}[G^{k/2}, G^{(k+2)/2}] = \mathbb{E}[G^{k/2}G^{(k+2)/2}] - \mathbb{E}[G^k]\mathbb{E}[G^{(k+2)/2}] = v_{k+2} - v_k v_{k+2}.$$

Therefore, the covariance matrix becomes

$$\Sigma_k = \begin{bmatrix} v_4 - v_2^2 & v_{k+2} - v_2 v_k & v_{k+4} - v_2 v_{k+2} \\ v_{k+2} - v_2 v_k & v_{2k} - v_k^2 & v_{2k+2} - v_k v_{k+2} \\ v_{k+4} - v_2 v_{k+2} & v_{2k+2} - v_k v_{k+2} & v_{2k+4} - v_{k+2}^2 \end{bmatrix}. \tag{5.104}$$

If we define

$$f_k(x, y, z) = \frac{k}{2\left(\frac{z}{xy}\right) - 1}, \tag{5.105}$$

the gradient of $f_k(x, y, z)$ can be found to be

$$\nabla f_k(x, y, z) = \frac{2f_k^2(x, y, z)}{kxy}\left[\frac{z}{x}, \frac{z}{y}, -1\right]^T. \tag{5.106}$$

131

Evaluate $\nabla f_k(x,y,z)$ at $[v_2, v_k, v_{k+2}]^T$ and use the fact that $f_k(v_2, v_k, v_{k+2}) = m$ and $v_2 = m$, we have

$$\nabla f_k(v_2, v_k, v_{k+2}) = \frac{m}{(k/2)v_k} \left[\frac{v_{k+2}}{v_2}, \frac{v_{k+2}}{v_k}, -1 \right]^T. \tag{5.107}$$

By the multivariate delta method stated in Section 5.2.1, we obtain the asymptotic variance σ_k^2 as

$$\sigma_k^2 = \left(\nabla f_k(v_2, v_k, v_{k+2}) \right)^T \Sigma_k \left(\nabla f_k(v_2, v_k, v_{k+2}) \right) \tag{5.108}$$

where the above expression can be evaluated using quadratic form expansion as

$$\sigma_k^2 \left[\frac{(k/2)^2 v_k^2}{m^2} \right]$$

$$= \left[\frac{v_{k+2}}{v_2}, \frac{v_{k+2}}{v_k}, -1 \right] \begin{bmatrix} v_4 - v_2^2 & v_{k+2} - v_2 v_k & v_{k+4} - v_2 v_{k+2} \\ v_{k+2} - v_2 v_k & v_{2k} - v_k^2 & v_{2k+2} - v_k v_{k+2} \\ v_{k+4} - v_2 v_{k+2} & v_{2k+2} - v_k v_{k+2} & v_{2k+4} - v_{k+2}^2 \end{bmatrix} \begin{bmatrix} \frac{v_{k+2}}{v_2} \\ \frac{v_{k+2}}{v_k} \\ -1 \end{bmatrix}$$

$$= \frac{v_{k+2}^2}{v_2^2} (v_4 - v_2^2) + \frac{v_{k+2}^2}{v_k^2} (v_{2k} - v_k^2) + v_{2k+4} - v_{k+2}^2 + 2(v_{k+2} - v_2 v_k)\frac{v_{k+2}^2}{v_2 v_k}$$

$$- 2(v_{k+4} - v_2 v_{k+2})\frac{v_{k+2}}{v_2} - 2(v_{2k+2} - v_k v_{k+2})\frac{v_{k+2}}{v_k}.$$

Now using the fact that

$$v_4 = v_2^2 + v_2$$

$$v_{k+2} = \left(m + \frac{k}{2} \right) v_k$$

$$v_{2k+4} = (m + k + 1) v_{2k+2}$$

$$v_{k+4} = \left(m + \frac{k}{2} + 1 \right) v_{k+2}$$

$$v_{2k+2} = (m + k) v_{2k},$$

we have

$$\sigma_k^2 \left[\frac{(k/2)^2 v_k^2}{m^2} \right]$$

$$= \frac{v_{k+2}^2}{v_2} + \left(m + \frac{k}{2} \right)^2 (v_{2k} - v_k^2) + (m + k + 1)v_{2k+2} - v_{k+2}^2 + 2 \left[\left(m + \frac{k}{2} \right) \frac{v_{k+2}^2}{v_2} - v_{k+2}^2 \right]$$

$$- 2 \left[v_{k+2}^2 - \left(m + \frac{k}{2} + 1 \right) \frac{v_{k+2}^2}{v_2} \right] - 2 \left[v_{k+2}^2 - \left(m - \frac{k}{2} \right) v_{2k+2} \right]$$

132

$$
= -\frac{v_{k+2}^2}{v_2} + \left(\frac{k}{2}\right)^2 v_{2k} + m(m+k)v_{2k} - v_{k+2}^2 + (1-m)v_{2k+2} + v_{k+2}^2
$$

$$
-\frac{v_{k+2}^2}{v_2} + \left(\frac{k}{2}\right)^2 v_{2k} + mv_{2k+2} + (1-m)v_{2k+2}
$$

$$
= -\frac{v_{k+2}^2}{v_2} + \left(\frac{k}{2}\right)^2 v_{2k} + v_{2k+2}. \tag{5.109}
$$

After rearrangement, we obtain (5.92) as desired.

For $\hat{m}_0$, we first note the following identity is true

$$
\mathbb{E}[G^i (\ln G)^j] = \frac{\frac{d^j}{dm^j}\Gamma(m+i)}{\Gamma(m)}, \; i > 0, \; j = 0,1,2,\ldots \quad . \tag{5.110}
$$

Let $\gamma_1 = \mathbb{E}[G \ln G]$, $\gamma_2 = \mathbb{E}[G]$, $\gamma_3 = \mathbb{E}[\ln G]$, and let $\hat{\gamma}_1$, $\hat{\gamma}_2$, $\hat{\gamma}_3$ be the sample means for $G \ln G$, G, and $\ln G$, respectively. By the Weak Law of Large Number, we have $\hat{\gamma}_k \xrightarrow{Pr} \gamma_k$. Since $\hat{m}_0$ is also a continuous function of $\hat{\gamma}_k$, we establish the consistency for $\hat{m}_0$ as

$$
\hat{m}_0 \xrightarrow{Pr} \left(\frac{\gamma_1}{\gamma_2} - \gamma_3\right)^{-1} = m. \tag{5.111}
$$

By the multivariate Central Limit Theorem, we have

$$
\sqrt{N} \begin{bmatrix} \hat{\gamma}_1 - \gamma_1 \\ \hat{\gamma}_2 - \gamma_2 \\ \hat{\gamma}_3 - \gamma_3 \end{bmatrix} \xrightarrow{L} \mathcal{N}(0, \Sigma_0) \tag{5.112}
$$

where $\mathcal{N}(0, \Sigma_0)$ is a trivariate normal distribution with mean vector $0 = [0,0,0]^T$ and covariance matrix Σ_0 given by

$$
\Sigma_0 = \begin{bmatrix} \mathrm{var}[G \ln G] & \mathrm{cov}[G, G \ln G] & \mathrm{cov}[G \ln G, \ln G] \\ \mathrm{cov}[G, G \ln G] & \mathrm{var}[G] & \mathrm{cov}[G, \ln G] \\ \mathrm{cov}[G \ln G, \ln G] & \mathrm{var}[G, \ln G] & \mathrm{var}[\ln G] \end{bmatrix}. \tag{5.113}
$$

Using (5.110), we obtain

$$
\Sigma_0 = \begin{bmatrix} \frac{\Gamma''(m+2)}{\Gamma(m)} - \left(\frac{\Gamma'(m+1)}{\Gamma(m)}\right)^2 & \frac{\Gamma'(m+2)}{\Gamma(m)} - \frac{m\Gamma'(m+1)}{\Gamma(m)} & \frac{\Gamma''(m+1)}{\Gamma(m)} - \frac{\Gamma'(m)\Gamma'(m+1)}{\Gamma^2(m)} \\ \frac{\Gamma'(m+2)}{\Gamma(m)} - \frac{m\Gamma'(m+1)}{\Gamma(m)} & m & \frac{\Gamma'(m+1)}{\Gamma(m)} - \frac{m\Gamma'(m)}{\Gamma(m)} \\ \frac{\Gamma''(m+1)}{\Gamma(m)} - \frac{\Gamma'(m)\Gamma'(m+1)}{\Gamma^2(m)} & \frac{\Gamma'(m+1)}{\Gamma(m)} - \frac{m\Gamma'(m)}{\Gamma(m)} & \frac{\Gamma''(m)}{\Gamma(m)} - \left(\frac{\Gamma'(m)}{\Gamma(m)}\right)^2 \end{bmatrix}. \tag{5.114}
$$

133

If we define

$$f_0(x,y,z) = \frac{1}{\frac{x}{y} - z},$$ (5.115)

the gradient of $f_0(x,y,z)$ can be found as

$$\nabla f_0 = \frac{f_0^2(x,y,z)}{y} \left[-1, \frac{x}{y}, y \right]^T.$$ (5.116)

Evaluate $\nabla f_0(x,y,z)$ at $[\gamma_1, \gamma_2, \gamma_3]^T$ and use the fact that

$$f_0(\gamma_1, \gamma_2, \gamma_3) = f_0(\mathbb{E}[G \ln G], \mathbb{E}[G], \mathbb{E}[\ln G]) = m,$$

we have

$$\nabla f_0(\gamma_1, \gamma_2, \gamma_3) = m \left[-1, \frac{\Gamma'(m+1)}{m\Gamma(m)}, m \right]^T.$$ (5.117)

Again, by the multivariate delta method, the asymptotic variance σ_0^2 can be found as

$$\sigma_0^2 = \left(\nabla f_0(\gamma_1, \gamma_2, \gamma_3) \right)^T \Sigma_0 \left(\nabla f_0(\gamma_1, \gamma_2, \gamma_3) \right)$$ (5.118)

Substituting (5.117) and (5.114) into (5.118), after some tedious algebra, we obtain (5.93) as required.

Alternatively, we can also obtain σ_0^2 in (5.93) by taking the limit k to 0 in (5.92) and using the l'Hôpital's rule multiple times. However, this approach requires us to justify the condition of interchanging the limit and the integration operators. ∎

A confidence interval on m, with asymptotic coverage $1 - \alpha$, is given by $\hat{m}_k \pm z_{\alpha/2} \frac{\hat{\sigma}_k}{\sqrt{N}}$ where the consistent estimate $\hat{\sigma}_k$ can be obtained by replacing m by $\hat{m}$ in (5.92). With the aid of Maple, it can be shown that the variance σ_k^2 is $2m^2(1 + O(m^{-1}))$. It suggests that the width of the confidence interval increases, approximately, linear with m. This undesirable point can be improved by using the delta method to obtain

$$\sqrt{N}(\ln \hat{m}_k - \ln m) \overset{L}{\longrightarrow} \mathcal{N}(0, V_k^2)$$ (5.119)

where $V_k^2 = \sigma_k^2/m^2$. The log transformation is chosen since $\left(\frac{d}{dm} \ln m \right)^2 = 1/m^2$, which is used to compensate the m^2 factor in σ_k^2. We comment that the delta method is used here to stabilize the variance, while the delta method is used to obtain the asymptotic variance in the proof of Theorem 4.5.1. After the log transformation on $\hat{m}_k$, the confidence interval on $\ln m$ becomes $\ln \hat{m}_k \pm z_{\alpha/2} \hat{V}_k / \sqrt{N}$.

134

The asymptotic variance V_k^2 of $\ln \hat{m}_k$ is plotted against m in Fig. 5.2 for $k = 2, k = 0$ and for the maximum likelihood estimator $\ln \hat{m}_{ML}$. Using the CRLB derived in (5.36), the asymptotic attainable variance for $\ln \hat{m}_{ML}$ is

$$V_{ML}^2 = \left[m^2 \left(\psi'(m) - \frac{1}{m} \right) \right]^{-1}. \tag{5.120}$$

Therefore the asymptotic relative efficiency (ARE) of $\ln \hat{m}_0$ with respect to $\ln \hat{m}_{ML}$ (or equivalently, ARE of $\hat{m}_0$ with respect to $\hat{m}_{ML}$) is

$$
\begin{aligned}
\text{ARE} &= \frac{V_{ML}^2}{V_0^2} \\
&= \frac{1}{m^2 (\psi'(m) - \frac{1}{m})(1 + m\psi'(m+1))} \\
&= 1 - \frac{1}{12m} + O(m^{-2}) \tag{5.121}
\end{aligned}
$$

where the last equality is obtained using Maple and the asymptotic expansion for the digamma function. Therefore, we conclude that $\hat{m}_0$ is almost fully efficient, in particular for large values of m, as it is shown in Fig. 5.2.

5.6 Numerical Results and Discussions

In this section, we use Monte Carlo simulation to assess the performances of those estimators proposed in Sections 5.4 and 5.5 when sample size is finite. For large and infinite sample size, we will draw several conclusions based on the asymptotic properties of those estimators. Our performance metrics are (sample) mean, (sample) variance (or standard deviation), and root mean square error. Unless otherwise specified, all simulated results are obtained by averaging over 30,000 experiments. The i.i.d. Nakagami random variates are generated for $\Omega = 1$ and for a useful range of m parameters $\{m = 0.5k, k = 1, 2, \dots 40\}$.

Fig. 5.3 compares the mean of four estimators, $\hat{m}_{ML(1)}$, $\hat{m}_{ML(2)}$, $\hat{m}_t$, $\hat{m}_s$, with the true m values. For $N = 100$, our close inspection of the numerical data indicates that $\hat{m}_{ML(2)}$, $\hat{m}_t$, and $\hat{m}_s$ are positively biased for all values of m, that $\hat{m}_t$ has smaller bias values than those of $\hat{m}_s$, and that $\hat{m}_{ML(1)}$ is negatively biased for small values of m (though these results are hard to discern from Fig.
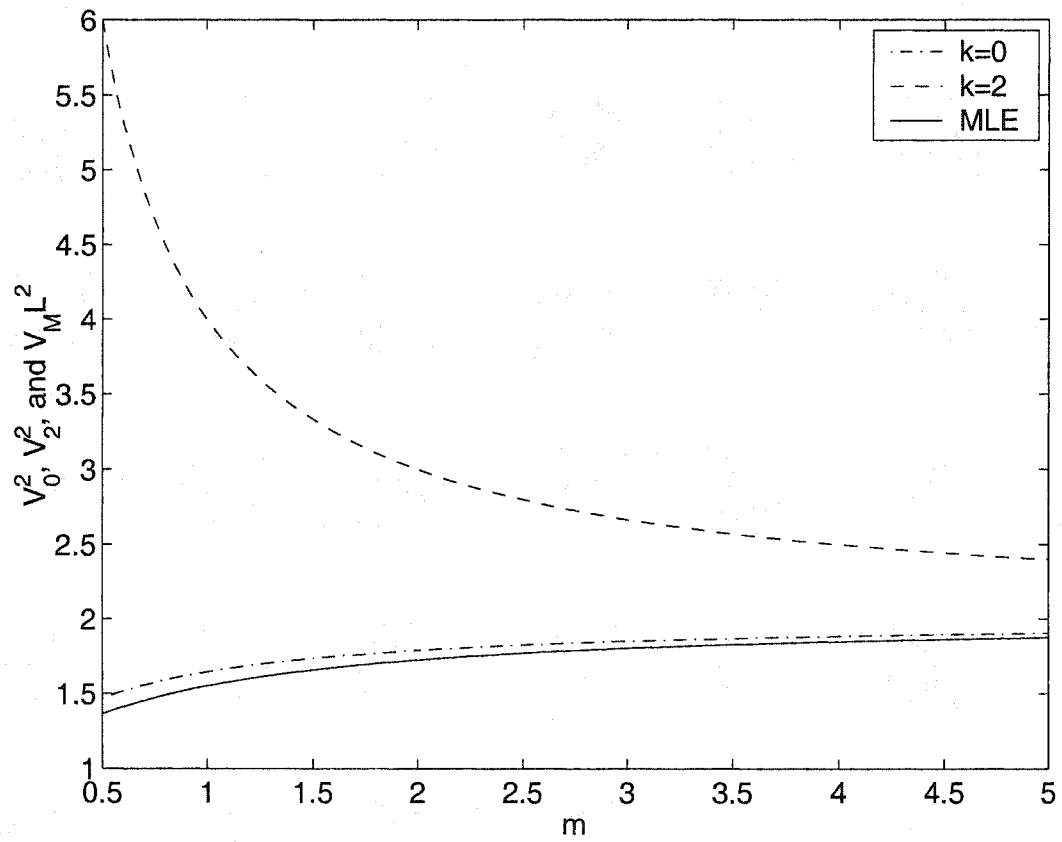
135

Figure 5.2. Asymptotic variances of $\ln \hat{m}_{k=2}$, $\ln \hat{m}_{k=0}$, and $\ln \hat{m}_{ML}$ vs. m.
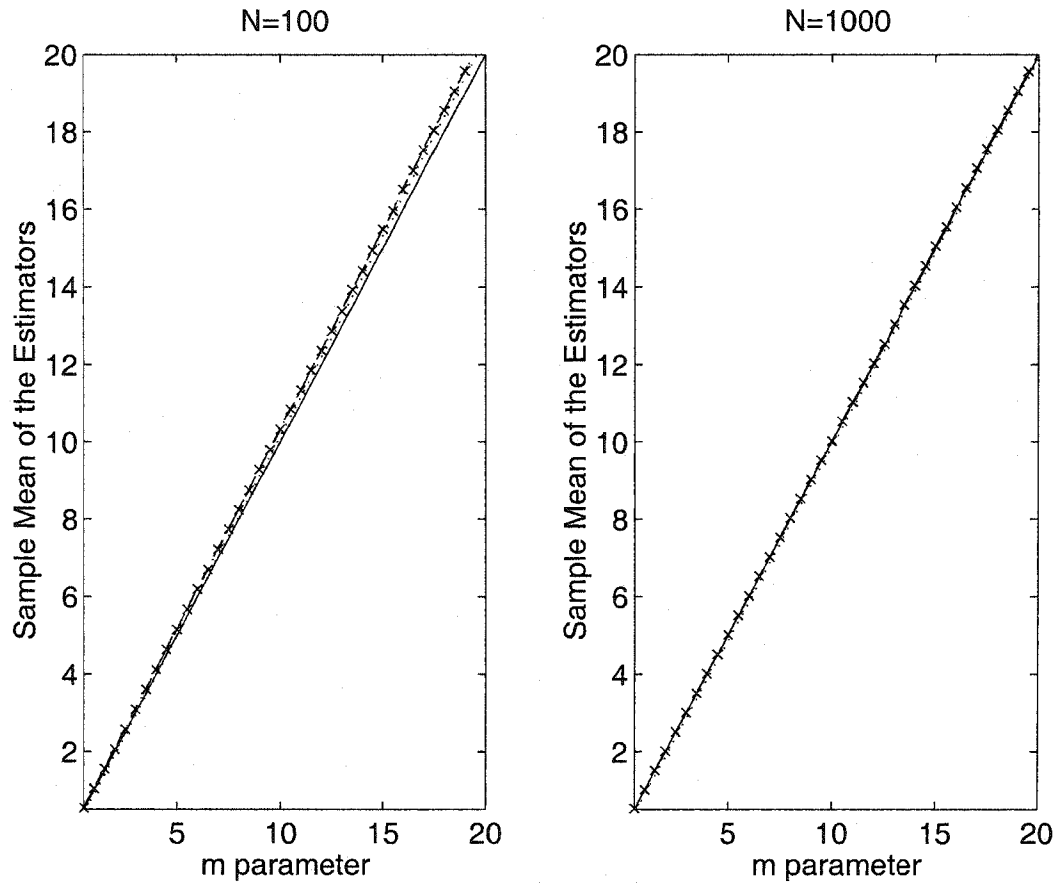
136

Figure 5.3. Comparisons of the sample means of the estimators for $\hat{m}_{ML(1)}$ (dotted line), $\hat{m}_{ML(2)}$ (crossed line), $\hat{m}_t$ (dashed and dotted line), $\hat{m}_s$ (dashed line) with the true m (solid line) parameter values for $N = 100$ and $N = 1,000$.

5.3) and positively biased for large value of m. However, the magnitude of the bias for $\hat{m}_{ML(1)}$ is typically smaller than the magnitude of the bias of the other estimators. For a larger sample size of $N = 1,000$, Fig. 5.3 indicates that, for practical applications, all four estimators are essentially unbiased.

Fig. 5.4 compares the variances of the same four estimators with the CRLB derived in (5.36). For $N = 100$, the variances of all four estimators are greater than the CRLB. However, the variances of $\hat{m}_{ML(1)}$ and $\hat{m}_{ML(2)}$ are smaller than that of $\hat{m}_t$, which is in turn smaller than that of $\hat{m}_s$. For $N = 1,000$, the variances of $\hat{m}_{ML(1)}$ and $\hat{m}_{ML(2)}$ graphically attain the CRLB whereas the variances
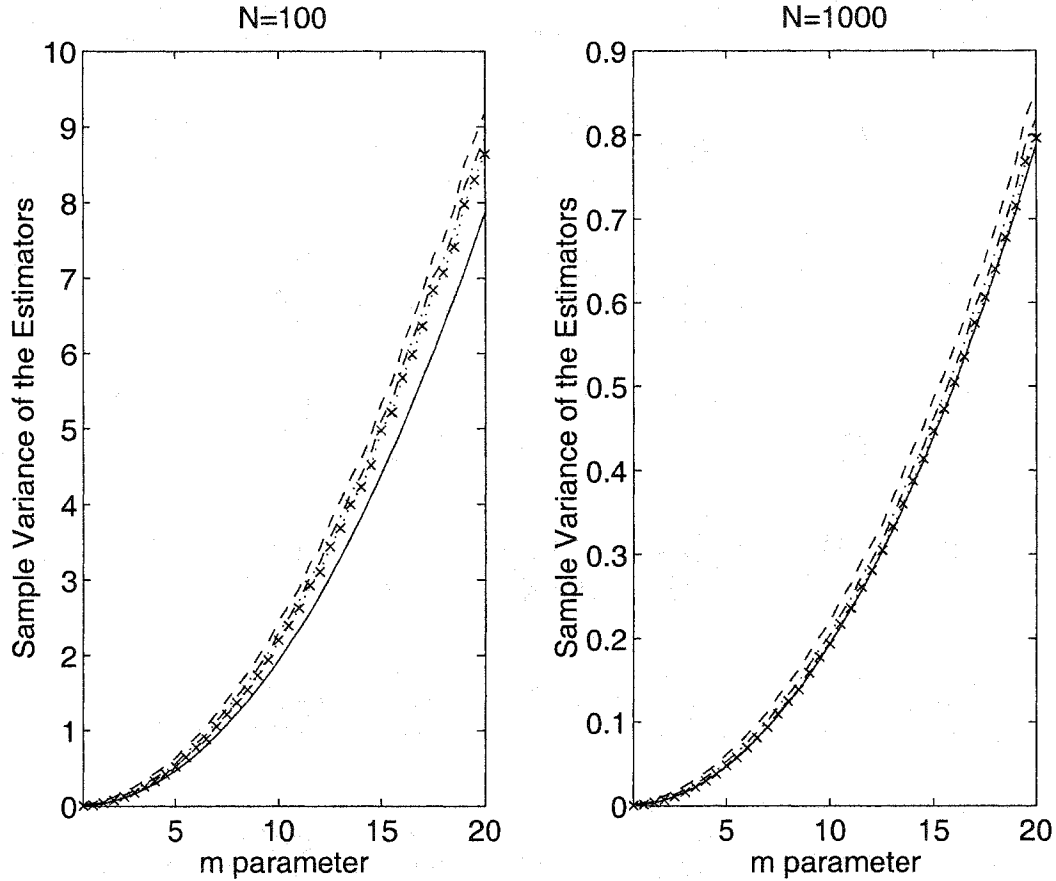
137

Figure 5.4. Comparisons of the sample variances of the estimators for $\hat{m}_{ML(1)}$ (dotted line), $\hat{m}_{ML(2)}$ (crossed line), $\hat{m}_t$ (dashed and dotted line), $\hat{m}_s$ (dashed line) with the CRLB (solid line) $N = 100$ and $N = 1,000$.

of $\hat{m}_t$ and $\hat{m}_s$ are clearly greater than the CRLB. This suggests that the two ML-based estimators, $\hat{m}_{ML(1)}$ and $\hat{m}_{ML(2)}$, are efficient for $N = 1,000$. This is expected since the asymptotic property of MLE predicts that ML estimators are asymptotically efficient.

We observe that the variances of the estimators increase with m. The same observation can be made from figures in [2], where, however, no explanation for this behavior was offered. Here, using the expressions for the ML estimators, we provide a simple explanation as follows. When m approaches infinity, the parameter Δ of (5.43), which appears in the *denominators* of (5.45) and (5.46), approaches zero. Therefore, the estimator becomes more sensitive to small changes in Δ. In

the sequel, using large sample analysis, we will show rigorously that the asymptotic variances of our proposed estimators as well as the CRLB are proportional, approximately, to m^2.

Fig. 5.5 compares the normalized variances of the four estimators against the normalized CRLB, where the normalizations are performed by dividing the variances and the CRLB by m^2. As discussed in Section 5.5, this normalization is equivalent to taking the log transformation of the estimator, i.e., $\ln \hat{m}_k$. It is seen that, for large m values, the normalized CRLB are essentially flat, or *stabilized*. This suggests that the variances are proportional, approximately, to m^2 for large m values. For small values of m, it is interesting to observe that the behaviors of the normalized variances for $\hat{m}_t$ and $\hat{m}_s$ are contrary to the behaviors of $\hat{m}_{ML(1)}$ and $\hat{m}_{ML(2)}$ and the normalized CRLB. In particular, Fig. 5.5 suggests that the performances of $\hat{m}_s$ is relatively poor for small m values. This behavior is explained as follows. It is well-known that moment-based estimators are inefficient because large outlying samples corrupt the estimate disproportionally (due to the power operations). In the case of small m values, the mode of the Nakagami distribution is near zero (it is zero for $m = 0.5$). Thus, for small m values, there is small likelihood of samples having values less than the mode occurring. Therefore, the large positive distortion caused by samples much larger than the mode is not offset by samples much smaller than the mode, as is the case for large m values.

Fig. 5.6 compares the normalized variances of $\hat{m}_k$ indexed by $k = 2.0, 1.0, 0.5$, and 0.01. The behaviors of these normalized variance curves are shown for varying index k values. It is seen that when k value decreases, the performance of $\hat{m}_k$, in particular for small values of m, approaches that of ML-based estimator. This confirms our early expectation since when k value decreases, the highest order sample moment that $\hat{m}_k$ uses also decreases. Therefore, the performance of the moment-based estimator $\hat{m}_k$ is less sensitive to the corruption of outlying samples.

What interests us the most is the limiting case of $\hat{m}_k$ when k goes to zero. Figs. 5.7-5.9 compares the performances of $\hat{m}_0$ and the Greenwood-Durand estimator, denoted by $\hat{m}_{GDE}$, a popular ML estimator. In these figures, we have plotted the bias, (sample) standard deviation, and root mean square error versus sample size for $m = 3.5$ (Similar observations can be made for other values of m). The simulation results for these figures are obtained by averaging over $3,000$ experiments. As shown,

139
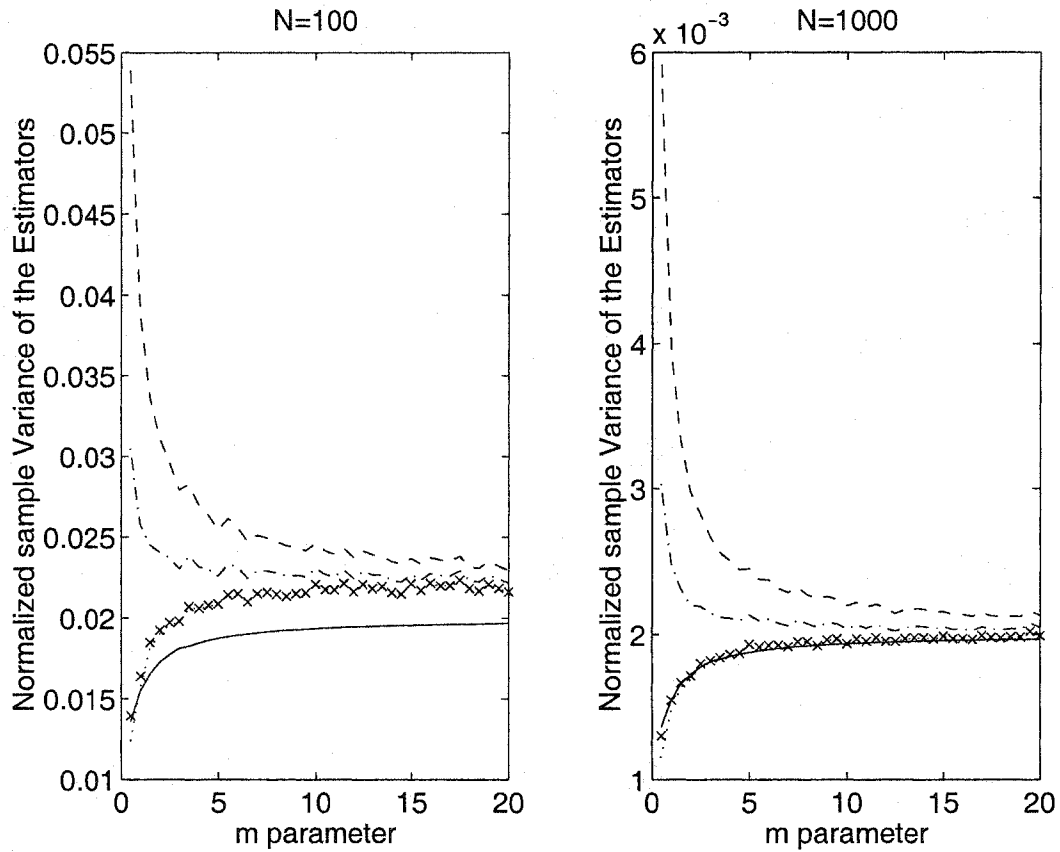
Figure 5.5. Comparisons of the normalized sample variances of the estimators for $\hat{m}_{ML(1)}$ (dotted line), $\hat{m}_{ML(2)}$ (crossed line), $\hat{m}_t$ (dashed and dotted line), $\hat{m}_s$ (dashed line) with the normalized CRLB (solid line) $N = 100$ and $N = 1,000$.
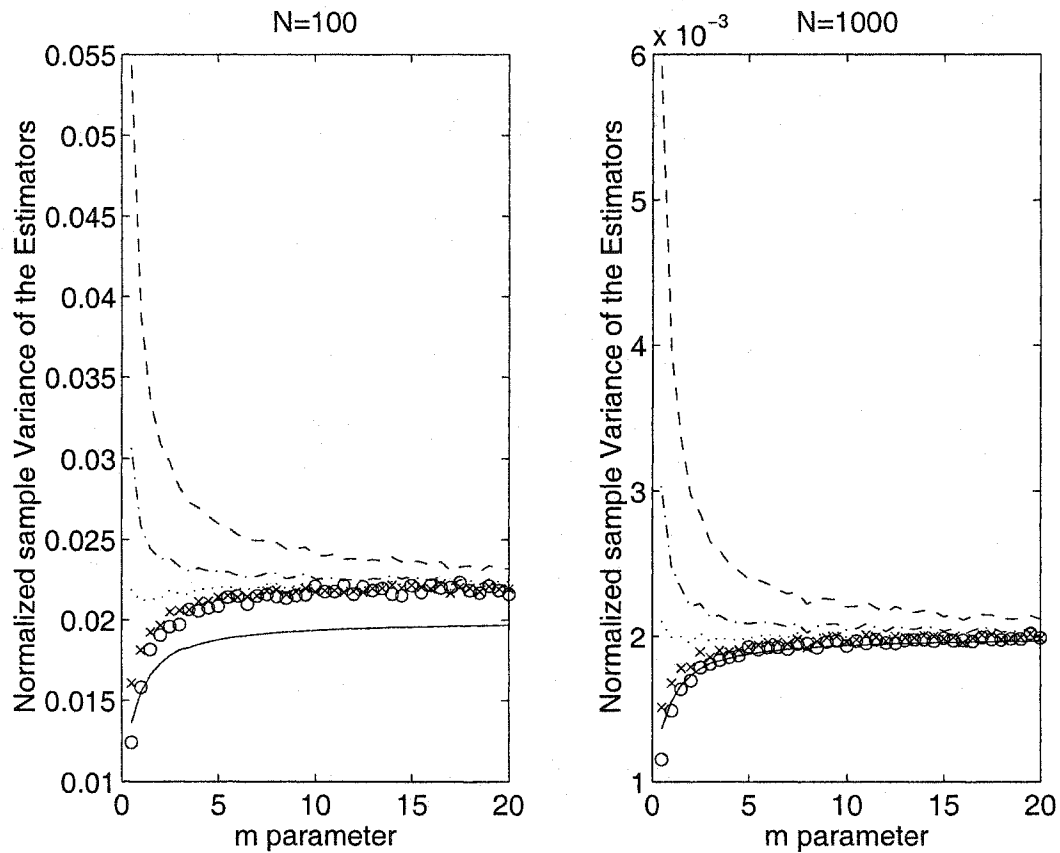
140

Figure 5.6. Comparisons of the normalized variances of the estimators for $\hat{m}_{k=2}$ (dashed line), $\hat{m}_{k=1}$ (dashed and dotted line), $\hat{m}_{k=0.5}$ (dotted line), $\hat{m}_{k=0.01}$ (crossed line), $\hat{m}_{ML(1)}$ (circled line) with the normalized CRLB (solid line) for $N = 100$ and $N = 1,000$.
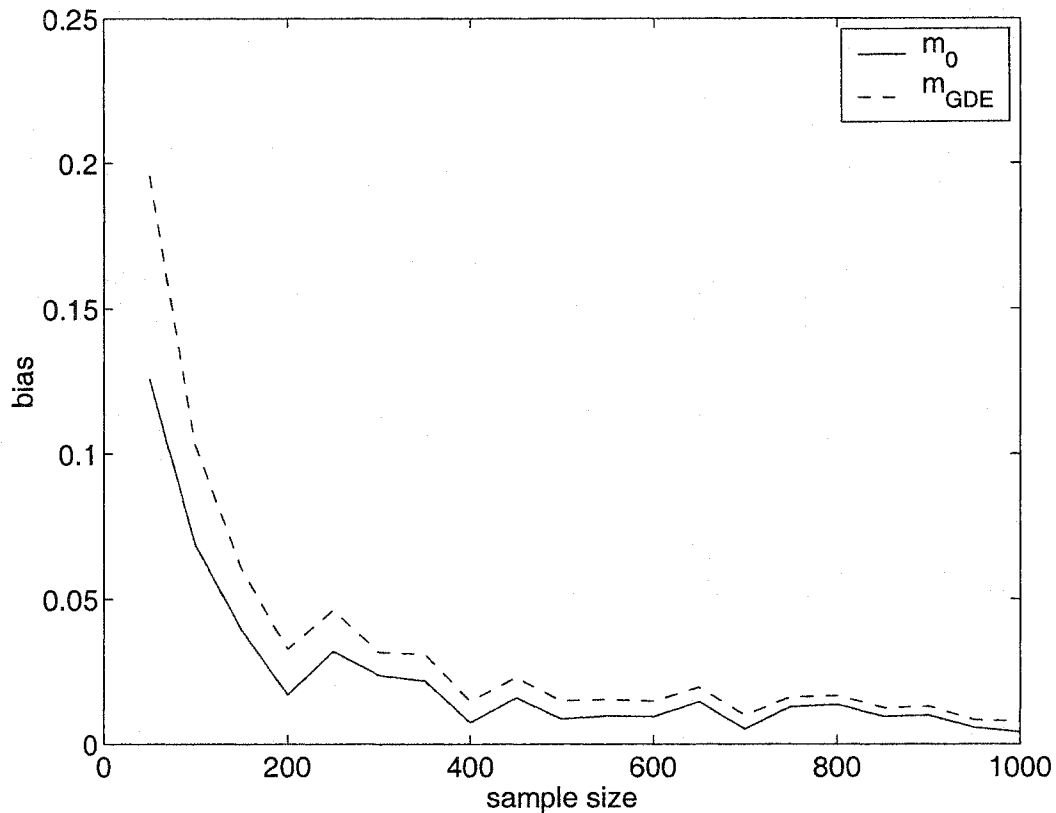
141

Figure 5.7. Comparisons of the bias of the estimator $\hat{m}_0$ (solid line) and $\hat{m}_{GDE}$ (dashed line) for

$m = 3.5$ with different sample sizes.

for $m = 3.5$, in terms of (sample) standard deviation and root mean square error, the performances

for $\hat{m}_0$ and $\hat{m}_{GDE}$ are almost indistinguishable. However, Fig. 5.7 indicates that $\hat{m}_{GDE}$ has larger

bias over $\hat{m}_0$ for a wide range of sample sizes. This suggests that $\hat{m}_0$ is slightly in favor over $\hat{m}_{GDE}$

if smaller bias is required. Recall that GDE is based on rational approximation and requires the

knowledge (or storage) of coefficients with accuracy in the sixth significant digits. The analytical

expression for $\hat{m}_0$ is, however, more elegant, thus, more suitable for on-line implementation.

Numerical results in Fig. 5.6 lead us to believe initially that when the index k goes to zero, the

variance of $\hat{m}_k$ is minimized at $\hat{m}_0$. This believe is, strictly speaking, incorrect. Figs. 5.10 and 5.11

plot the asymptotic variance versus index k values for $m = 1$. In these two figures, the horizontal

line denotes V_0^2, the normalized asymptotic variance for $\hat{m}_0$. When $m = 1$, it can be shown using
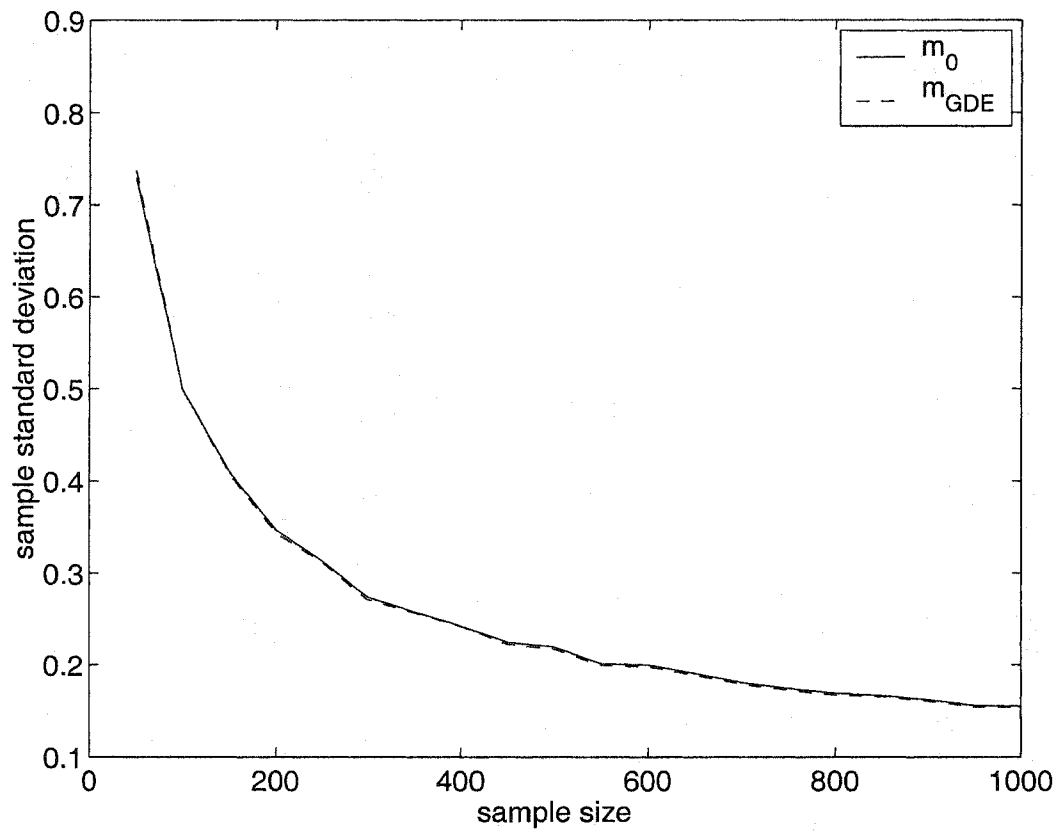
142

Figure 5.8. Comparisons of the sample standard deviation of the estimator $\hat{m}_0$ (solid line) and $\hat{m}_{GDE}$ (dashed line) for $m = 3.5$ with different sample sizes.

143
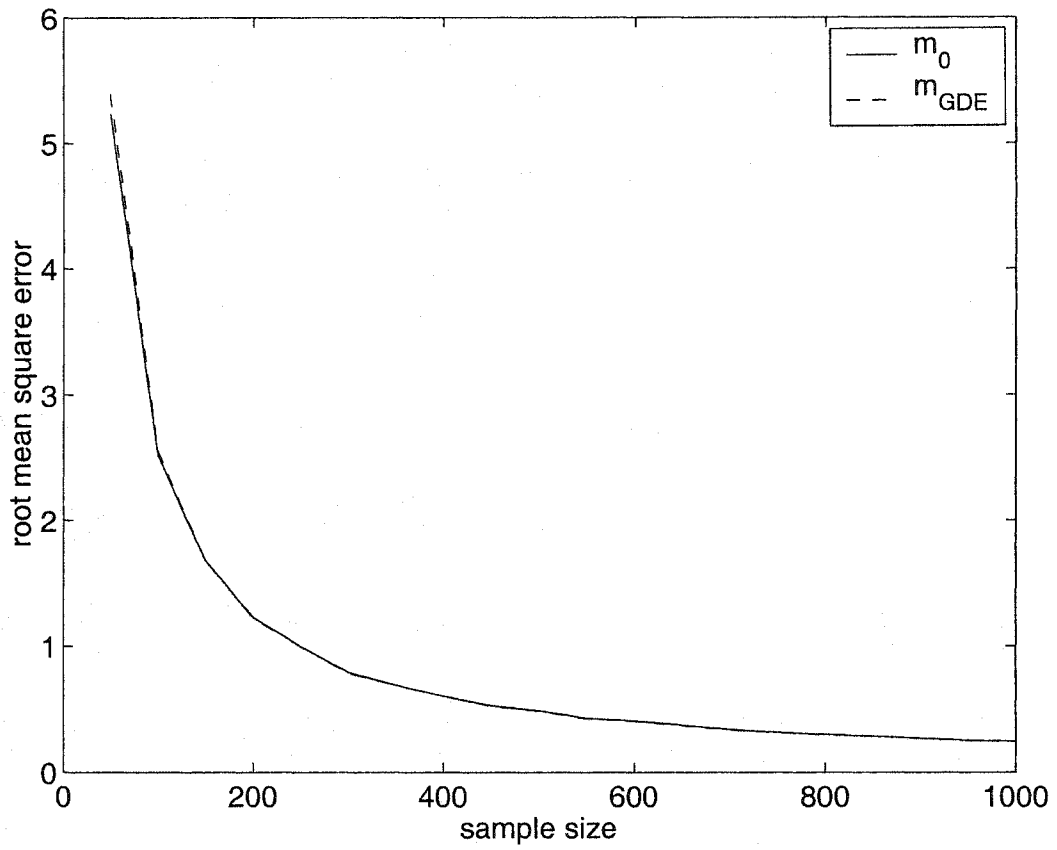
Figure 5.9. Comparisons of the root mean square error of the estimator $\hat{m}_0$ (solid line) and $\hat{m}_{GDE}$ (dashed line) for $m = 3.5$ with different sample sizes.

144
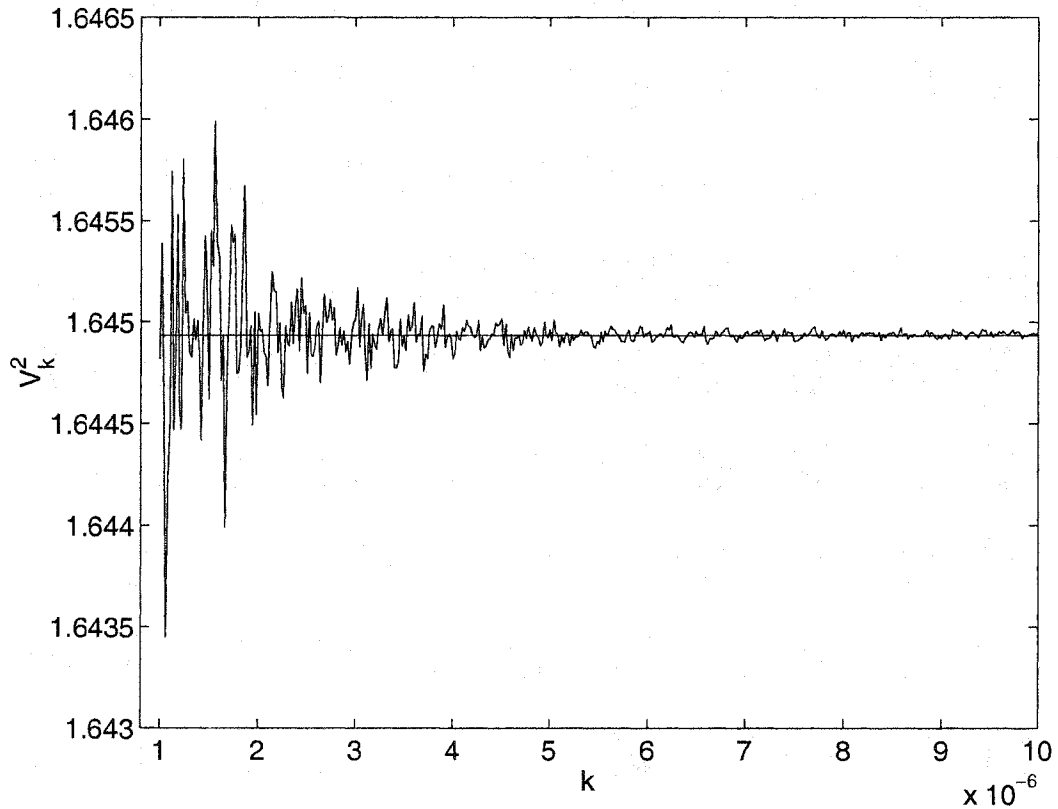
Figure 5.10. Asymptotic variances V_k^2 of $\ln \hat{m}_k$ vs. k for $10^{-6} \leq k \leq 10^{-5}$ with $m = 1$. The horizontal line is at $V_0^2 = \pi^2/6$.

(5.93) that $V_0^2 = 1 + \psi'(2) = \pi^2/6$. As shown in Fig. 5.10, for very small k values (less then 10^{-5}), V_k^2 is oscillatory and can drop below V_0^2, albeit a practically insignificant amount. For larger index k values, Fig. 5.11 shows V_k^2 is always above V_0^2. Figs. 5.12 and 5.13 also show the same V_k^2 and V_0^2 comparison for a different values of m (horizontal line V_0^2 for $m = 3.5$ is approximately $V_0^2 \approx 1.8705$), and similar observations can be made. Therefore, we conclude that, for practical engineering applications, we can consider the variance of $\hat{m}_0$ is smaller than that of $\hat{m}_k$, for $k > 0$.

145
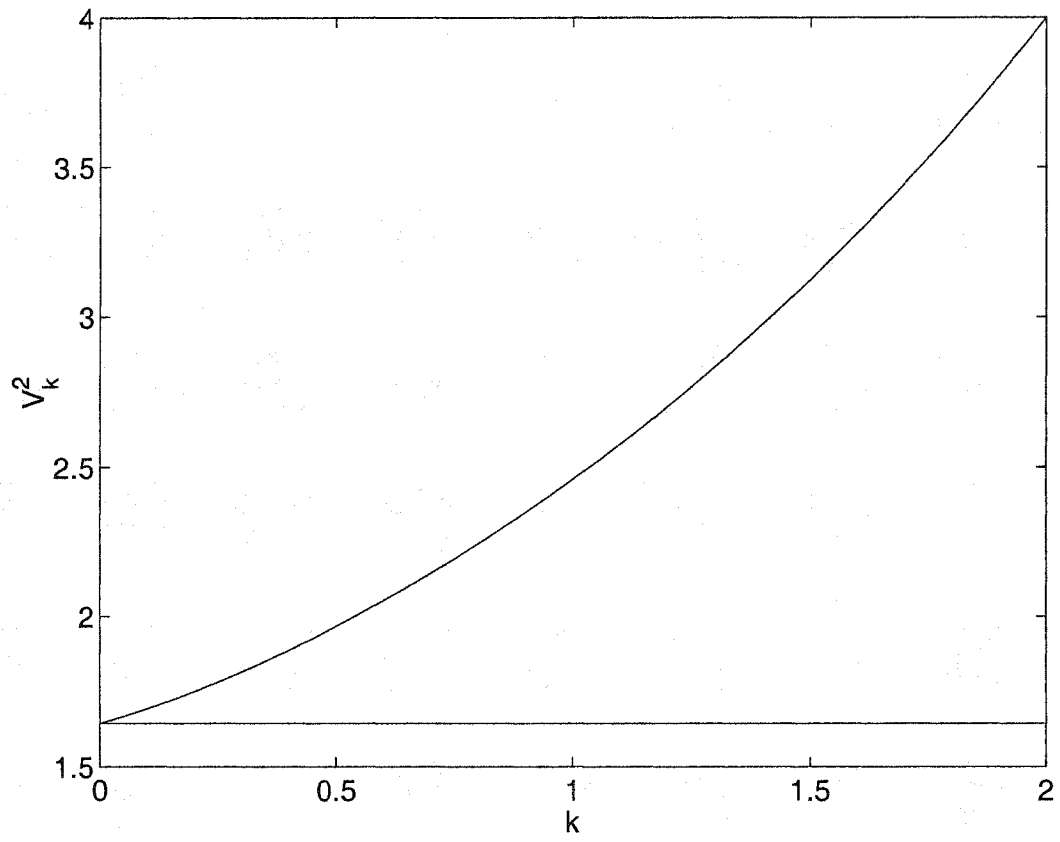
Figure 5.11. Asymptotic variances V_k^2 of $\ln \hat{m}_k$ vs. k for $0 \le k \le 2$ with $m = 1$. The horizontal line is at $V_0^2 = \pi^2/6$.
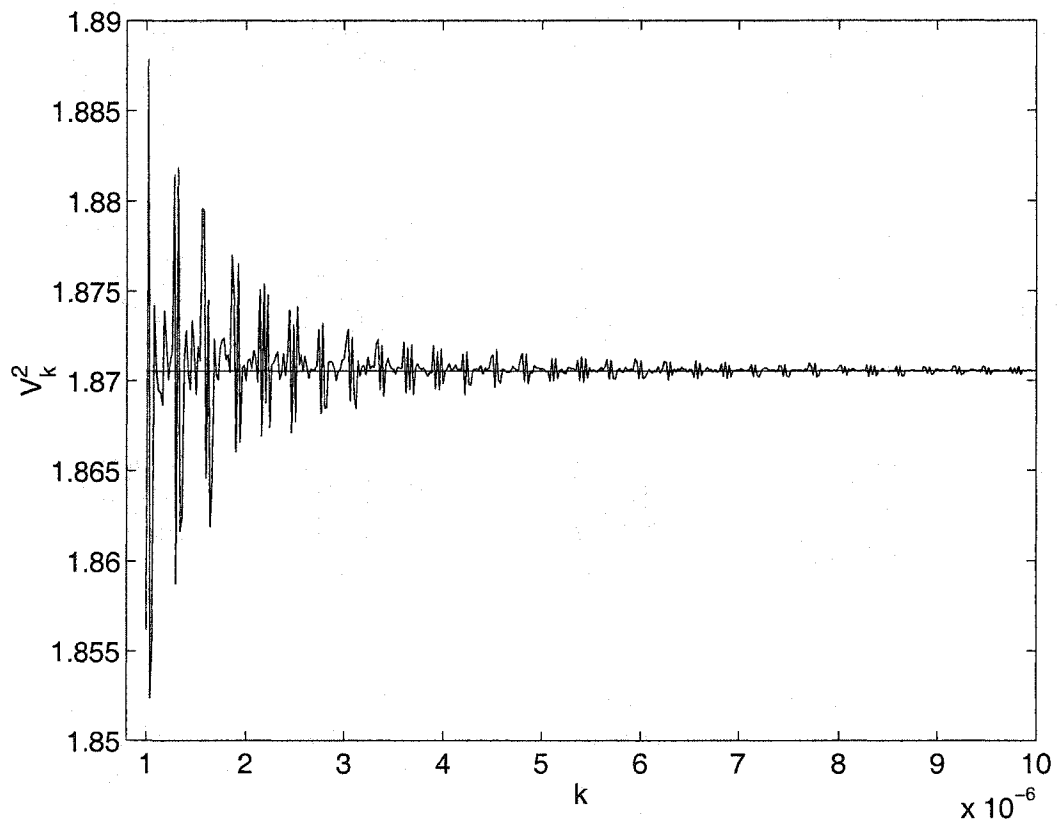
Figure 5.12. Asymptotic variances V_k^2 of $\ln \hat{m}_k$ vs. k for $10^{-6} \leq k \leq 10^{-5}$ with $m = 3.5$. The horizontal line is at $V_0^2 = 1.8705$.

147
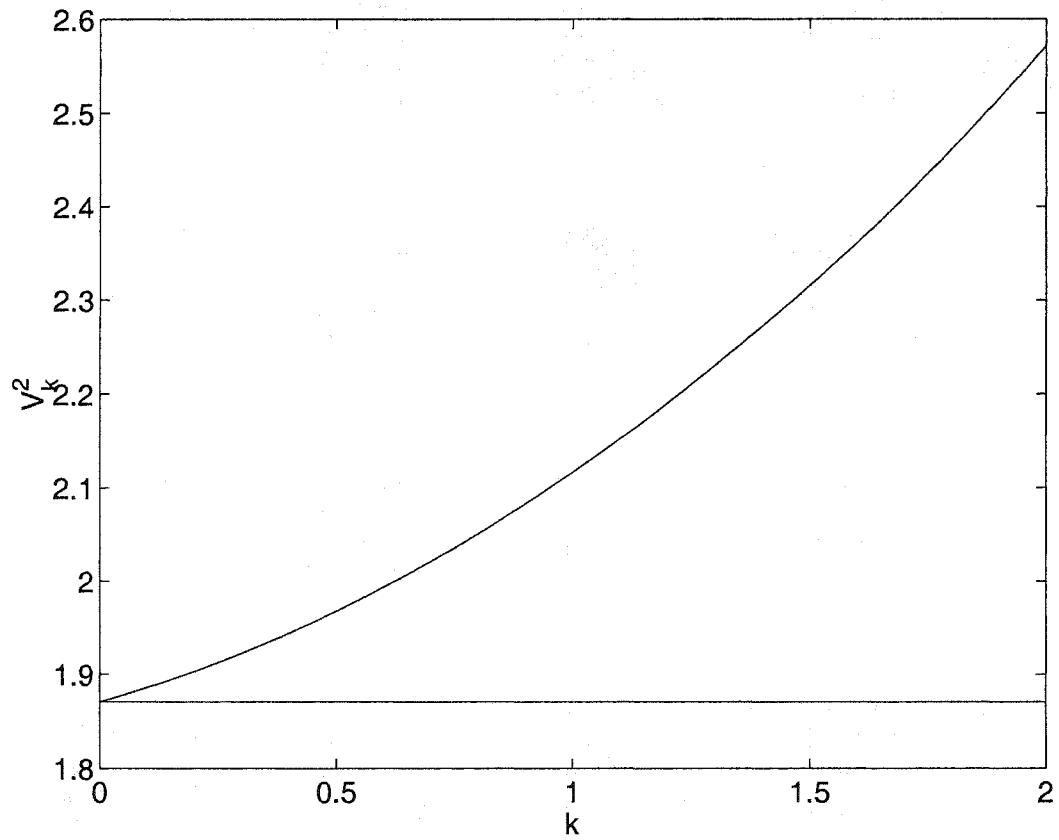
Figure 5.13. Asymptotic variances V_k^2 of $\ln \hat{m}_k$ vs. k for $0 \leq k \leq 2$ with $m = 3.5$. The horizontal line is at $V_0^2 = 1.8705$.

148

5.7 Summary

In this chapter, we considered estimation of the Nakagami fading parameters. In doing so, we showed that the Nakagami-m distribution is a member of the two-parameter exponential family, from which we obtained the complete sufficient statistic for the fading parameters. The CRLB's for the fading parameters were derived. Two approximate ML estimators were proposed. Numerical study indicates that these ML estimators can attain the CRLB with a moderate sample size. A family of new moment-based estimators, which use both integer and non-integer sample moments, were derived and their asymptotic variances were found analytically. The limiting case of this family is, in particular, of interest. This estimator, which uses only integer sample moments and sample covariance, has small variance and is almost fully efficient. The performance of this estimator is comparable to the popular Greenwood-Durand estimator. In addition, our new estimator is more suitable for on-line implementation.

Chapter 6

Conclusions and Suggestions for Future Work

In this conclusion chapter, we first highlight important findings of this thesis, and then suggest several topics for future research

6.1 Conclusions

1. It is possible to further simplify a well-known decision statistic at the output of a correlator receiver for a BPSK DS-CDMA signal using random spreading sequences. This simplification can significantly reduce the computational complexity of exact BER calculation.

2. A new closed-form expression has been obtained for the characteristic function of the multiple access interference.

3. The exact average BER of a coherent BPSK DS-CDMA system with Rayleigh-faded asynchronous users can be expressed in terms of a single integral. The integrand is positive and well behaved. With modest computational complexity, it is possible to calculate the exact BER for a system with large processing gains.

4. The accuracies of the standard Gaussian approximation and the simplified improved Gaussian approximation have been assessed. It has been found that both approximations can give accurate BER estimates in Rayleigh fading. These approximations are valid even for a system with a processing gain of 255 and for a system with a small number of users.

150

5. The exact average BER of coherent BPSK DS-CDMA system with Nakagami-m faded asynchronous users can also be expressed in terms of a single integral. The integrand can take both positive and negative values. A new closed-form expression for the CF of the MAI has been found for this fading and interference environment. It is shown that the BER obtained using the standard Gaussian approximation can be poor for a system with a small number of users in a lightly faded environment.

6. Closed-form expressions have been derived for the first-order PDF and the CF of the quadrature components of the Nakagami fading process (assuming uniform phase distribution). In the special case when m takes integer values, the PDF (CF) takes the form of a product of a Gaussian PDF (CF) with a polynomial function of even powers. These closed-form results can be useful in error analysis for other digital modulation schemes with Nakagami-faded cochannel interference.

7. A tractable analytical BER expression has been developed for the performance of bandwidth efficient BPSK in Nakagami fading and cochannel interference. It has been verified that the cochannel interference is exactly Gaussian distributed in the special case when all the interfering signals are Rayleigh and symbol synchronous with desired user signal.

8. The performance of a new novel pulse shape in fading and cochannel interference has been investigated. It has been shown both analytically and numerically that this novel pulse outperforms the widely used raised-cosine pulse shape. When the BER is at 10^{-6}, it has been demonstrated that approximately 0.86 dB savings in SNR can be achieved at no additional cost.

9. It has been shown numerically as well as argued using the convexity property of the Q-function that fading of an interfering signal worsens (increases) the BER of the desired signal rather than improving (decreasing) it, a result perhaps contrary to conventional thinking.

10. It has been shown that the Nakagami-m distribution is a member of two-parameter exponential

151

family. The complete sufficient statistics for the fading parameters have been derived.

11. A CRLB for estimation of the Nakagami-m fading parameters has been derived. We have shown that there exists no unbiased estimator for m that attains the CRLB with finite sample size.

12. Two approximate ML estimators have been proposed. Numerical results suggest that $\hat{m}_{ML(1)}$ slightly outperforms $\hat{m}_{ML(2)}$. When the sample size is $N = 1,000$, both estimators are practically unbiased and attain the CRLB.

13. A new compact definition of the Nakagami m parameter is derived. Based on this definition, the Nakagami fading figure can be interpreted alternatively as the covariance of the instantaneous fading power and its value in dB normalized by its average fading power.

14. A family of new moment-based estimators using both integer and non-integer moments have been proposed for estimation of the Nakagami m parameter. As a limiting case of this family, a new moment estimator using only integer moments is suitable for on-line implementation and its performance approaches that of ML estimators.

15. The family of new moment-based estimators have been shown to be consistent. Closed-form expressions for the asymptotic variances of these estimators have been found.

16. It has been proved that the new estimator $\hat{m}_0$ is almost fully efficient asymptotically. Numerical studies have indicated that this estimator and the classical Greenwood-Durand estimator perform equally well when the sample size is finite. In addition, $\hat{m}_0$ can possibly provide smaller bias.

6.2   Suggestions for Future Work

1. A DS-CDMA signal is inherently wideband; therefore, a frequency-selective fading channel followed by a RAKE receiver is a more appropriate system model. In [24], Eng and Milstein

152

carried out a performance analysis for coherent DS-CDMA in frequency-selective Nakagami fading using a Gaussian approximation. It is therefore of interest to extend our accurate analysis technique to this practical system model. However, challenges remain in doing such exact performance analysis since it can be shown that the self-interference terms on different RAKE fingers are highly correlated.

2. It has been demonstrated that Holtzman's approximation can be used to improve the accuracy of error estimation using the standard Gaussian approximation for a DS-CDMA system. It is of interest to apply this technique to improve the standard Gaussian approximation for bandwidth efficient BPSK in our generalized fading and interference environment. To our best knowledge, Holtzman's technique has not been applied to any bandwidth-limited system.

3. It is of interest to consider the exact BER analysis for a bandlimited BPSK or MPSK system in fading and CCI with some popular diversity combining schemes.

4. Finding the phase distribution of the Nakagami-m fading process remains an open problem. Often, for convenience, the phase of the Nakagami fading process is assumed to be uniformly distributed. This assumption is questionable since the quadrature components of the Nakagami fading process, $X = R\cos\Theta$ and $Y = R\sin\Theta$, are only statistically independent when $m = 1$ (Rayleigh) if uniform distribution is assumed for Θ. We speculate that the phase distribution of the Nakagami fading process is dependent on the m parameter. Therefore, one plausible way to formulate the problem is to search for a family of distributions indexed by m, $f_\Theta(\theta; m)$, such that two quadrature components are statistically independent. One evidence to support this thinking is that the phase distributions of two special values of m parameter, namely $m = 1$ and $m = +\infty$, indeed satisfy this criterion. We are currently investigating this topic.

5. The complete sufficient statistic for the Nakagami m parameter has been determined in this thesis. However, the MVUE for m is yet to be found, provided it exists. If any unbiased

estimator for m is known, we can use this complete sufficient statistic to determine the MVUE by the Rao-Blackwell-Lehmann-Scheffé theorem.

6. It is of interest to study the problem of Nakagami m parameter estimation in a noisy environment (finite SNR). Cheng and Beaulieu [14] first investigated this problem for an AWGN environment using the method of moments. This work has recently been extended by Tepedelenlioglu [74]. It has been shown that a large performance gap remains between the CRLB and the variance of the best known estimator.

154

References

[1] V. A. Aalo and J. Zhang. On the effect of cochannel interference on average error rates in Nakagami-fading channels. *IEEE Communications Letters*, 3:136–138, May 1999.

[2] A. Abdi and M. Kaveh. Performance comparison of three different estimators for the Nakagami m parameter using Monte Carlo simulation. *IEEE Communications Letters*, 4:119–121, April 2000.

[3] M. Abramowitz and I. Stegun. *Handbook of Mathematical Functions*. Dover, New York, 1971.

[4] A. A. Abu-Dayya and N. C. Beaulieu. Diversity MPSK receivers in cochannel interference. *IEEE Transactions on Vehicular Technology*, 48:1959–1965, November 1999.

[5] N. C. Beaulieu and A. A. Abu-Dayya. Bandwidth efficient QPSK in cochannel interference and fading. *IEEE Transactions on Communications*, 43:2464–2474, September 1995.

[6] N. C. Beaulieu, C. C. Tan, and M. O. Damen. A "Better Than" Nyquist pulse. *IEEE Communications Letters*, 5:367–368, September 2001.

[7] D. E. Borth and M. B. Pursley. Analysis of direct-sequence spread spectrum multiple-access communication over Rician fading channels. *IEEE Transactions on Communications*, 25:795–799, August 1979.

[8] K. O. Bowman and L. R. Shenton. *Properties of Estimators for the Gamma Distribution*. Marcel Dekker, New York, 1988.

[9] G. Casella and R. L. Berger. *Statistical Inference*. Duxbury, 2nd edition, Pacific Grove, CA, 2002.

[10] U. Charash. Reception through Nakagmai fading multipath channels with random delays. *IEEE Transactions on Communications*, 27:657–670, April 1979.

[11] K. L. Cheah, S. W. Oh, and K. H. Li. Efficient performance analysis of asynchronous cellular CDMA over Rayleigh-fading channels. *IEEE Communications Letters*, 1:71–73, May 1997.

[12] J. Cheng and N. C. Beaulieu. Estimation of the Nakagami-m Parameter. In *Wireless Calgary*, pages 84–88, Calgary, A.B., July 9-11 2001.

[13] J. Cheng and N. C. Beaulieu. Maximum-likelihood based estimation of the Nakagami m parameter. *IEEE Communications Letters*, 5:101–103, March 2001.

[14] J. Cheng and N. C. Beaulieu. Moment-based estimation of the Nakagami-m fading parameter. In *PACRIM*, pages 361–364, Victoria, B.C., August 26-28 2001.

[15] J. Cheng and N. C. Beaulieu. Generalized moment estimators for the Nakagami fading parameter. *IEEE Communications Letters*, 6:144–146, April 2002.

[16] M. Chiani. Analytical distribution of linearly modulated cochannel interferers. *IEEE Transactions on Communications*, 45:73–79, January 1997.

[17] P. H. J. Chong and C. Leung. NCFSK bit-error rate with unsynchronized slowly fading interferers. *IEEE Transactions on Communications*, 49:272–281, February 2001.

[18] R. H. Clarke. A statistical theory of mobile radio reception. *Bell System Technical Journal*, 47:957–1000, July 1968.

[19] T. M. Cover and J. A. Thomas. *Elements of Information Theory*. John Wiley & Sons, New York, 1991.

[20] D. Cox. A radio system proposal for widespread low-power tetherless communications. *IEEE Transactions on Communications*, 39:324–335, February 1991.

[21] H. Cramér. *Mathematical Methods of Statistics*. Princeton University Press, NJ, 1946.

[22] P. J. Crepeau. Uncoded and coded performance of MFSK and DPSK in Nakagami fading channels. *IEEE Transactions on Communications*, 40:487–493, March 1992.

[23] R. R. Davidson and D. L. Solomon. Moment-type estimation in the exponential family. *Communications in Statistics*, 3:1101–1108, 1974.

[24] T. Eng and L. B. Milstein. Coherent DS-CDMA performance in Nakagami mutipath fading. *IEEE Transactions on Communications*, 43:1134–1143, February/March/April 1995.

[25] P. G. Flikkema. Spread-spectrum techniques for wireless communication. *IEEE Signal Processing Magazine*, pages 26–36, May 1997.

[26] C. S. Gardner and J. A. Orr. Fading effects on the performance of a spread spectrum multiple-access communication system. *IEEE Transactions on Communications*, 27:143–149, January 1979.

[27] E. A. Geraniotis. Performance of coherent direct-sequence spread-spectrum communications over specular multipath fading channels. *IEEE Transactions on Communications*, 33:502–508, June 1985.

[28] E. A. Geraniotis. Direct-sequence spread-spectrum multiple-access communications over nonselective and frequency-selective Rician fading channels. *IEEE Transactions on Communications*, 34:756–764, August 1986.

[29] E. A. Geraniotis and B. G. Ghaffari. Performance of binary and quaternary direct sequence spread-spectrum multiple-access systems with random signature sequences. *IEEE Transactions on Communications*, 39:713–724, May 1991.

[30] E. A. Geraniotis and M. B. Pursley. Error probability for direct-sequence spread-spectrum multiple-access communication– Part 2: Approximations. *IEEE Transactions on Communications*, 30:985–995, May 1982.

[31] G. A. Gibson. *Advanced Calculus*. Macmillan, London, 1931.

[32] K. S. Gilhousen, I. M. Jacob, R. Padovani, A. J. Viterbi, L. A. Weaver, and C. E. Weatley. On the capacity of a cellular CDMA system. *IEEE Transactions on Vehicular Technology*, 40:309–312, May 1991.

[33] I. S. Gradshteyn and I. M. Ryzhik. *Table of Integrals, Series and Products*. Wiley, San Diego: Academic Press, 1995.

[34] J. A. Greenwood and D. Durand. Aids for fitting the Gamma distribution by maximum likelihood. *Technometrics*, 2:55–65, February 1960.

[35] C. Hastings. *Approximation for Digital Computers*. Princeton University Press, NJ, 1955.

[36] S. Haykin. *Digital Communications*. Wiley, New York, 1988.

[37] R. V. Hogg and A. T. Craig. *Introduction to Mathematical Statistics*. Prentice Hall, 5th ed., Upper Saddle River, NJ, 1995.

[38] J. M. Holtzman. A simple, accurate method to calculate spread-spectrum multiple-access error probabilities. *IEEE Transactions on Communications*, 40:461–464, March 1992.

[39] Y.-C. Jenq. Does a larger intersymbol interference result in higher probability of error? *IEEE Communications on Communications*, 28:1771–1773, September 1980.

[40] M. Kavehrad. Performance of nondiversity receivers for spread spectrum in indoor wireless communication. *AT& T Technical Journal*, 64:1181–1210, July-August 1985.

[41] S. M. Kay. *Fundamentals of Statistical Signal Processing: Estimation Theory*. Prentice-Hall, Englewood, NJ, 1993.

[42] Y.-C. Ko and M.-S. Alouini. Estimation of Nakagami-m fading channel parameter with application to optimized transmitter diversity systems. *In submission to IEEE Transactions on Wireless Communications.*

[43] R. Krishnamurthi and S. C. Gupta. The error performance of Gray encoded QPSK and 8-PSK schemes in a fading channel with cochannel interference. *IEEE Transactions on Communications*, 41:1773–1776, December 1993.

[44] W. C. Lee. Overview of cellular CDMA. *IEEE Transactions on Vehicular Technology*, 40:291–302, May 1991.

[45] E. L. Lehmann. *Elements of Large-Sample Theory.* Springer-Verlag, New York, 1999.

[46] E. L. Lehmann and G. Casella. *Theory of Point Estimation.* Springer-Verlag, New York, 1998.

[47] J. S. Lehnert and M. B. Pursley. Error probabilities for binary direct sequence spread spectrum communications with random signature sequences. *IEEE Transactions on Communications*, 35:87–98, November 1987.

[48] D. Liu, C. L. Despins, and W. A. Krzymien. Low-complexity performance evaluation of binary and quaternary DS-SSMA over Rician fading channels via the characteristic function method. *Wireless Personal Communications*, 7:257–273, August 1998.

[49] B. Q. Long, J. D. Hu, and P. Zhang. Method to improve Gaussian approximation accuracy for calculation of spread-spectrum multiple-access error probabilities. *IEE Electronics Letters*, 31:529–531, 1995.

[50] Y. Ma, T. J. Lim, and S. Pasupathy. Error probability for coherent and differential PSK over arbitrary Rician fading channels with multiple cochannel interferers. *IEEE Transactions on Communications*, 50:429–441, March 2002.

[51] H. V. MacDonald. The cellular concept. *Bell System Technical Journal*, 58:15–41, January 1979.

159

[52] R. Maciejko. Digital modulation in Rayleigh fading in the presence of cochannel interference. *IEEE Transactions on Communications*, 29:1379–1386, September 1981.

[53] L. B. Milstein, T. S. Rappaport, and R. Barghouti. Performance evaluation for cellular CDMA. *IEEE Journal on Selected Areas in Communications*, 10:680–689, May 1992.

[54] A. M. Monk, M. Davis, L. B. Milstein, and C. W. Helstrom. A noise-whitening approach to multiple-access noise rejection– Part 1: Theory and background. *IEEE Journal on Selected Areas in Communications*, 12:817–827, 1994.

[55] R. K. Morrow. Accurate CDMA BER calculations with low computational complexity. *IEEE Transactions on Communications*, 46:1413–1417, November 1998.

[56] R. K. Morrow and J. S. Lehnert. Bit-to-bit error dependence in slotted DS/SSMA packet systems with random signature sequences. *IEEE Transactions on Communications*, 37:1052–1061, October 1989.

[57] M. Nakagami. The m-distribution, a general formula of intensity distribution of rapid fading. In *Statistical Methods in Radio Wave Propagation*, W. G. Hoffman, Ed. Oxford, England: Pergamon, 1960.

[58] H. H. Nguyen and E. Shwedyk. On error probability of DS-CDMA systems with arbitrary chip waveforms. *IEEE Communications Letters*, 5:78–80, March 2001.

[59] A. Papoulis. *The Fourier Integral and its Applications*. McGraw-Hill, New York, 3rd edition, 1962.

[60] A. Papoulis. *Probability, Random Variables, and Stochastic Processes*. McGraw-Hill, New York, 3rd edition, 1991.

[61] R. L. Pickholtz, L. B. Milstein, and D. L. Schilling. Spread spectrum for mobile communications. *IEEE Transactions on Vehicular Technology*, 40:313–322, May 1991.

160

[62] H. V. Poor. *An Introduction to Signal Detection and Estimation*. Springer, New York, 3rd edition, 1994.

[63] J. G. Proakis. *Digital Communications*. McGraw-Hill, New York, 4th edition, 2001.

[64] M. B. Pursley. Performance evaluation for phase-coded spread-spectrum multiple-access communication– Part I: System analysis. *IEEE Transactions on Communications*, 25:795–799, August 1977.

[65] T. S. Rappaport. *Wireless Communications Principles and Practice*. Prentice Hall PTR, New Jersey, 2nd edition, 2002.

[66] T. S. Rappaport, A. Annamalai, R. M. Buehrer, and W. H. Tranter. Wireless communications: past events and a future perspective. *IEEE Communications Magazine*, pages 148–161, 50th Anniversary Commemorative Issue, May 2002.

[67] K. V. Sairam, N. Gunasekaran, and S. R. Reddy. Bluetooth in wireless communication. *IEEE Communications Magazine*, pages 90–96, June 2002.

[68] M. K. Simon and M.-S. Alouini. *Digital Communication over Fading Channels: A Unified Approach to Performance Analysis*. Wiley, New York, 2000.

[69] S. Stein. Unified analysis of certain coherent and noncoherent binary communication systems. *IEEE Transactions on Information Theory*, 10:43–51, January 1964.

[70] G. L. Stüber. *Principles of Mobile Communication*. Kluwer Academic Publishers, Norwell, MA, 2nd edition, 2001.

[71] M. O. Sunay and P. J. McLane. Calculating error probability for DS CDMA systems: When not to use the Gaussian approximation. In *Proc. IEEE GLOBECOM*, pages 1744–1749, London, UK, November 1996.

[72] M. O. Sunay and P. J. McLane. Probability of error for diversity combining in DS-CDMA systems with synchronization errors. *European Transactions on Telecommunications*, 9:449–463, September-October 1998.

[73] H. Suzuki. A statistical model for urban radio channel model. *IEEE Transactions on Communications*, 25:673–680, February 1977.

[74] C. Tepedelenlioglu. Analytical performance analysis of moment-based estimators of the Nakagami parameter. In *IEEE VTC-2002 Fall*, Vancouver, B.C., Sept. 24-28 2002.

[75] H. C. Thom. A note on the Gamma distribution. *Monthly Weather Review*, 86:117–122, April 1958.

[76] O. K. Tonguz and M. M. Wang. Cellular CDMA networks impaired by Rayleigh fading: System performance with power control. *IEEE Transactions on Vehicular Technology*, 43:515–527, August 1994.

[77] D. J. Torrieri. Performance of direct-sequence systems with long pseudonoise sequences. *IEEE Journal on Selected Areas in Communications*, 10:770–781, May 1992.

[78] S. Verdú. Minimum probability of error for asynchronous Gaussian multiple-access channels. *IEEE Transactions on Information Theory*, 32:85–96, January 1986.

[79] S. Verdú. *Multiuser Detection*. Academic University Press, Cambridge: UK, 1998.

[80] G. N. Watson. *A treatise on the theory of Bessel functions*. Cambridge University Press, 2nd ed., Cambridge: UK, 1958.

[81] J. M. Wozencraft and I. M. Jacobs. *Principles of Communication Engineering*. John Wiley and Sons, New York, 1965.

[82] K.-T. Wu and S.-A. Tsaur. Error performance for diversity DS-SSMA communication in fading channels. *Proc. Inst. Elect. Eng. Commun.*, 64:357–363, October 1994.

[83] K. Yao. Error probability of asynchronous spread spectrum multiple access communications systems.

[84] Y. Yao and A. U. H. Sheikh. Investigation into cochannel interference in microcellular mobile radio systems. *IEEE Transactions on Vehicular Technology*, 41:114–123, May 1992.

[85] Y. C. Yoon. A simple and accurate method of probability of bit error analysis for asynchronous band-limited DS-CDMA systems. *IEEE Transactions on Communications*, 50:656–663, April 2002.

[86] Q. T. Zhang. A note on the estimation of Nakagami-m fading parameter. *IEEE Communications Letters*, 6:237–238, June 2002.

[87] R. E. Ziemer and W. H. Tranter. *Principles of Communication*. John Wiley & Sons, New York, 5th edition, 2002.

Appendix A

In this appendix, we simplify the decision statistic at the output of the correlator receiver for an asynchronous BPSK DS-CDMA system using random spreading sequences. In the first half of the appendix we review a well-known random sequence decision statistic simplified by Lehnert and Pursley [47]. In the second half of the appendix, we propose a simplified random sequence decision statistic and study its statistical properties in detail. The study of these decision statistics is crucial in the exact average BER performance analysis for our system model.

Following the system model and the notations described in Chapter 2, we have the unfaded amplitude of the kth interference term, W_k, as

$$W_k = \int_0^T b_k(t - \tau_k) a_k(t - \tau_k) a_1(t)\, dt \tag{A.1}$$

where T is the duration of one data symbol, τ_k is the kth user's random time delay assumed to be uniform over $[0, T)$. The kth user's data signal is $b_k(t) = \sum_{j=-\infty}^{+\infty} b_j^{(k)} P_T(t - jT)$ where $P_T(t)$ is a unity height rectangular pulse limited to $[0, T)$. The spreading signal of the kth user is $a_k(t) = \sum_{l=-\infty}^{+\infty} a_l^{(k)} \psi(t - lT_c)$ where T_c is the chip duration and $\psi(t)$ is a chip waveform time-limited to T_c. In our system model, the data symbol duration is assumed to be an integer multiple of the chip duration, i.e., $T = GT_c$, where G is the processing gain. Fig. A.1 shows the timing diagram (modified from [65]) of the PN sequences for User 1 (the desired user) and User k. In this figure, the delay τ_k is expressed as

$$\tau_k = \gamma_k T_c + S_k \tag{A.2}$$

where γ_k is an integer and S_k, which accounts for the fractional chip displacement of the kth interferer's chip relative to User 1, is uniform over $[0, T_c)$.

164
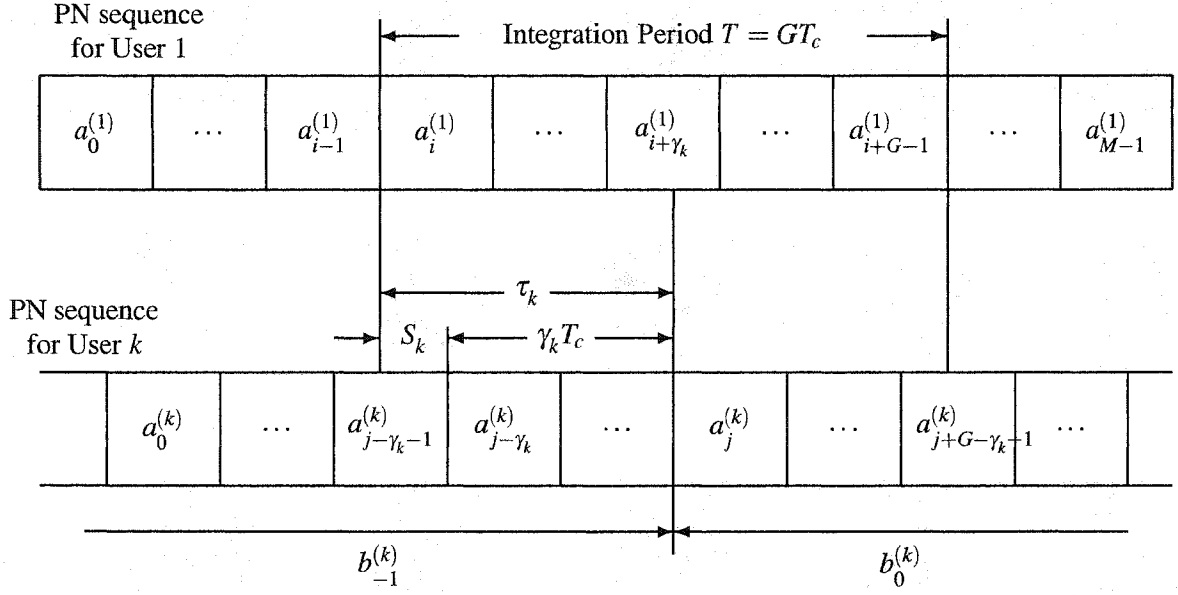
Figure A.1. Timing diagram of the PN sequences for User 1 and User k.

In Chapter 2 we have shown that

$$W_k = b_{-1}^{(k)} R_{k,1}(\tau_k) + b_0^{(k)} \hat{R}_{k,1}(\tau_k) \tag{A.3}$$

where $R_{k,1}(\tau)$ and $\hat{R}_{k,1}(\tau)$ are the partial cross-correlation functions defined in (2.14) and (2.15), respectively. With the pictorial aid from Fig. A.1, we can write the partial cross-correlation function $R_{k,1}(\tau_k)$ as

$$
\begin{aligned}
R_{k,1}(\tau_k) &= \int_0^{\tau_k} a_k(t - \tau_k) a_1(t) \, dt \\
&= \sum_{l=j-\gamma_k-1}^{j-1} a_l^{(k)} a_{l+i-j+\gamma_k+1}^{(1)} \int_0^{S_k} \psi(t)\psi(t + T_c - S_k) \, dt \\
&\quad + \sum_{l=j-\gamma_k}^{j-1} a_l^{(k)} a_{l+i-j+\gamma_k}^{(1)} \int_{S_k}^{T_c} \psi(t)\psi(t - S_k) \, dt
\end{aligned}
\tag{A.4}
$$

and write the other partial cross-correlation function $\hat{R}_{k,1}(\tau_k)$ as

$$\hat{R}_{k,1}(\tau_k) = \int_{\tau_k}^{T} a_k(t - \tau_k) a_1(t) \, dt$$

165

$$= \sum_{l=j}^{j+G-\gamma_k-2} a_l^{(k)} a_{l-j+i+\gamma_k+1}^{(1)} \int_0^{S_k} \psi(t)\psi(t + T_c - S_k)\, dt$$

$$+ \sum_{l=j}^{j+G-\gamma_k-1} a_l^{(k)} a_{l-j+i+\gamma_k}^{(1)} \int_{S_k}^{T_c} \psi(t)\psi(t - S_k)\, dt. \tag{A.5}$$

If we define the partial autocorrelation functions of the chip waveform as

$$R_\psi(s) = \int_0^s \psi(t)\psi(t + T_c - s)\, dt, \quad 0 \le s \le T_c \tag{A.6}$$

and

$$\hat{R}_\psi(s) = \int_s^{T_c} \psi(t)\psi(t - s)\, dt, \quad 0 \le s \le T_c, \tag{A.7}$$

applying (A.4), (A.5), (A.6) and (A.7) in (A.3), we can express W_k as

$$W_k = \left(b_{-1}^{(k)} \sum_{l=0}^{\gamma_k-1} a_{l+j-\gamma_k}^{(k)} a_{l+i}^{(1)} + b_0^{(k)} \sum_{l=\gamma_k}^{G-1} a_{l+j-\gamma_k}^{(k)} a_{l+i}^{(1)} \right) \hat{R}_\psi(S_k)$$

$$+ \left(b_{-1}^{(k)} \sum_{l=-1}^{\gamma_k-1} a_{l+j-\gamma_k}^{(k)} a_{l+i+1}^{(1)} + b_0^{(k)} \sum_{l=\gamma_k}^{G-2} a_{l+j-\gamma_k}^{(k)} a_{l+i+1}^{(1)} \right) R_\psi(S_k) \tag{A.8}$$

$$= \left(\sum_{l=0}^{\gamma_k-1} b_{-1}^{(k)} a_{l+j-\gamma_k}^{(k)} a_{l+i}^{(1)} + \sum_{l=\gamma_k}^{G-2} b_0^{(k)} a_{l+j-\gamma_k}^{(k)} a_{l+i}^{(1)} + b_0^{(k)} a_{G-1+j-\gamma_k}^{(k)} a_{N-1+i}^{(1)} \right) \hat{R}_\psi(S_k)$$

$$+ \left(\sum_{l=0}^{\gamma_k-1} b_{-1}^{(k)} a_{l+j-\gamma_k}^{(k)} a_{l+i+1}^{(1)} + \sum_{l=\gamma_k}^{G-2} b_0^{(k)} a_{l+j-\gamma_k}^{(k)} a_{l+i+1}^{(1)} + b_{-1}^{(k)} a_{j-\gamma_k-1}^{(k)} a_i^{(1)} \right) R_\psi(S_k). \tag{A.9}$$

The rest of this appendix addresses further simplification of W_k to a form which is suitable for accurate BER performance analysis of our DS-CDMA system. To simplify W_k further, Lehnert and Pursley introduced auxiliary RV's $Z_l^{(k)}$, $l = 0, \ldots, G$, defined as [47]

$$Z_l^{(k)} = \begin{cases} b_{-1}^{(k)} a_{l+j-\gamma_k}^{(k)} a_{l+i}^{(1)} & l = 0, \ldots, \gamma_k - 1 \\[2mm] b_0^{(k)} a_{l+j-\gamma_k}^{(k)} a_{l+i}^{(1)} & l = \gamma_k, \ldots, G-2 \\[2mm] b_0^{(k)} a_{G-1+j-\gamma_k}^{(k)} a_{G-1+i}^{(1)} & l = G-1 \\[2mm] b_{-1}^{(k)} a_{j-\gamma_k-1}^{(k)} a_i^{(1)} & l = G; \end{cases} \tag{A.10}$$

and stated that given User 1's spreading sequence $\{a_l^{(1)}\}$, RV's $Z_l^{(k)}$, $l = 0, 1, \ldots G$, are mutually independent. To show this statement is true, for convenience, we introduce a useful lemma.

166

Lemma A.1: *Suppose that α and $\{\beta_1, \beta_2, \cdots, \beta_M\}$ are mutually independent symmetric Bernoulli random variables taking values from $\{+1, -1\}$ with equal probabilities. Then $\{\alpha\beta_1, \alpha\beta_2, \cdots, \alpha\beta_M\}$ are also mutually independent.*

Proof: Let $\Pr(\alpha\beta_1 = a_1, \alpha\beta_2 = a_2, \cdots, \alpha\beta_M = a_M)$ denote the joint probability where a_i takes value of -1 or $+1$. In order to show that $\alpha\beta_1, \alpha\beta_2, \cdots, \alpha\beta_M$ are independent, we need to show that the joint probability equals product of the marginals, i.e.,

$$\Pr(\alpha\beta_1 = a_1, \alpha\beta_2 = a_2, \cdots, \alpha\beta_M = a_M) = \Pr(\alpha\beta_1 = a_1)\Pr(\alpha\beta_2 = a_2)\cdots\Pr(\alpha\beta_M = a_M).$$

$$\text{(A.11)}$$

To establish the equality in (A.11), we invoke the theorem of total probability and write

$$\begin{aligned}
&\Pr(\alpha\beta_1 = a_1, \alpha\beta_2 = a_2, \cdots, \alpha\beta_M = a_M)\\
=\ & \Pr(\alpha\beta_1 = a_1, \alpha\beta_2 = a_2, \cdots, \alpha\beta_M = a_M, \alpha = 1)\\
& + \Pr(\alpha\beta_1 = a_1, \alpha\beta_2 = a_2, \cdots, \alpha\beta_M = a_M, \alpha = -1)\\
=\ & \Pr(\beta_1 = a_1, \beta_2 = a_2, \cdots, \beta_M = a_M, \alpha = 1)\\
& + \Pr(\beta_1 = -a_1, \beta_2 = -a_2, \cdots, \beta_M = -a_M, \alpha = -1)\\
=\ & \Pr(\beta_1 = a_1)\Pr(\beta_2 = a_2)\cdots\Pr(\beta_M = a_M)\Pr(\alpha = 1)\\
& + \Pr(\beta_1 = -a_1)\Pr(\beta_2 = -a_2)\cdots\Pr(\beta_M = -a_M)\Pr(\alpha = -1)
\end{aligned}$$

where in obtaining the above result we have used the condition that α and $\{\beta_1, \beta_2, \cdots, \beta_M\}$ are mutually independent. Since $\Pr(\alpha = 1) = \Pr(\alpha = -1) = 1/2$ and $\Pr\left(\beta_j = a_j\right) = \Pr\left(\beta_j = -a_j\right)$, we have

$$\Pr(\alpha\beta_1 = a_1, \alpha\beta_2 = a_2, \cdots, \alpha\beta_M = a_M) = \Pr(\beta_1 = a_1)\Pr(\beta_2 = a_2)\cdots\Pr(\beta_M = a_M). \quad \text{(A.12)}$$

On the other hand,

$$\begin{aligned}
\Pr\left(\alpha\beta_j = a_j\right) &= \Pr\left(\alpha\beta_j = a_j, \alpha = 1\right) + \Pr\left(\alpha\beta_j = a_j, \alpha = -1\right)\\
&= \Pr\left(\beta_j = a_j, \alpha = 1\right) + \Pr\left(\beta_j = -a_j, \alpha = -1\right)\\
&= \Pr\left(\beta_j = a_j\right)\Pr(\alpha = 1) + \Pr\left(\beta_j = -a\right)\Pr(\alpha = -1)
\end{aligned}$$

167

$$= \Pr\left(\beta_j = a_j\right). \tag{A.13}$$

Combining (A.11), (A.12), and (A.13), we complete the proof of Lemma A.1. ∎

Lemma A.1 can also be argued using a coin tossing experiment. One might toss a first fair coin to determine α. A second toss determines β_1 and therefore $\alpha\beta_1$. A third toss determines β_2 and therefore $\alpha\beta_2$. Continuing this process, the $(M+1)$th toss will determine β_M and hence $\alpha\beta_M$. Clearly, the M outcomes are mutually independent.

Since the joint independence implies pairwise independence, Lemma A.1 can be specialized to that $\alpha\beta_i$ and $\alpha\beta_j$ for $i \neq j$, a result due to Torrieri [77]:

We now show that RV's $Z_l^{(k)}, l = 0,\dots,G$, are jointly independent given User 1's spreading sequence. To show this, we write the joint probabilities of $Z_l^{(k)}$, $l = 0,\dots,G$, as

$$\Pr\left(Z_0^{(k)} = z_0, \cdots Z_{\gamma_k-1}^{(k)} = z_{\gamma_k-1}; Z_{\gamma_k}^{(k)} = z_{\gamma_k}, \cdots, Z_{G-1}^{(k)} = z_{G-1}; Z_G^{(k)} = z_G \,\Big|\, a_l^{(1)}\right)$$

$$= \Pr\left(b_{-1}^{(k)}a_{l+j-\gamma_k}^{(k)} = z_l/a_{l+i}^{(1)}, l = 0,1,\dots\gamma_k - 1; b_{-1}^{(k)}a_{j-\gamma_k-1}^{(k)} = z_G/a_i^{(1)} \,\Big|\, a_l^{(1)}\right)$$

$$\times \Pr\left(b_0^{(k)}a_{l+j-\gamma_k}^{(k)} = z_l/a_{l+j}^{(1)}, l = \gamma_k,\dots,G-1 \,\Big|\, a_l^{(1)}\right) \tag{A.14}$$

$$= \Pr\left(b_{-1}^{(k)}a_{j-\gamma_k-1}^{(k)} = z_G/a_i^{(1)} \,\Big|\, a_l^{(1)}\right) \prod_{l=0}^{\gamma_k-1} \Pr\left(b_{-1}^{(k)}a_{l+j-\gamma_k}^{(k)} = z_l/a_{l+i}^{(1)} \,\Big|\, a_l^{(1)}\right)$$

$$\times \prod_{l=\gamma_k}^{G-1} \Pr\left(b_0^{(k)}a_{l+j-\gamma_k}^{(k)} = z_l/a_{l+j}^{(1)} \,\Big|\, a_l^{(1)}\right) \tag{A.15}$$

where in obtaining (A.14) we have used the independence condition between the data symbols as well as the independence condition between the random chip sequences, and (A.15) follows immediately from Lemma A.1. Since each RV $Z_l^{(k)}$ is also a symmetric Bernoulli, according to (A.15), we conclude that RV's $Z_l^{(k)}, l = 0,1,\dots,G$, are mutually independent given User 1's spreading sequence.

Using the definition of $Z_l^{(k)}$ in (A.10) and the fact that $a_l^{(1)}a_l^{(1)} = 1$, we can express (A.9) as

$$W_k = \sum_{l=0}^{G-2} Z_l^{(k)}\hat{R}_\psi(S_k) + Z_{G-1}^{(k)}\hat{R}_\psi(S_k) + \sum_{l=0}^{G-2} Z_l^{(k)}a_{l+i}^{(1)}a_{l+i+1}^{(1)}R_\psi(S_k) + Z_G^{(k)}R_\psi(S_k)$$

$$= \sum_{l=0}^{G-2} Z_l^{(k)}\left(\hat{R}_\psi(S_k) + a_{l+i}^{(1)}a_{l+i+1}^{(1)}R_\psi(S_k)\right) + Z_{G-1}^{(k)}\hat{R}_\psi(S_k) + Z_G^{(k)}R_\psi(S_k). \tag{A.16}$$

168

Let us denote $\mathcal{A}$ as the set of all integers in $[0, G-2]$ such that $a^{(1)}_{l+i} a^{(1)}_{l+i+1} = 1$, and denote $\mathcal{B}$ as the set of all integers in $[0, G-2]$ such that $a^{(1)}_{l+i} a^{(1)}_{l+i+1} = -1$. Then (A.16) becomes

$$W_k = \sum_{l \in \mathcal{A}} Z^{(k)}_l \left(\hat{R}_\psi(S_k) + R_\psi(S_k) \right) + \sum_{l \in \mathcal{B}} Z^{(k)}_l \left(\hat{R}_\psi(S_k) - R_\psi(S_k) \right)$$
$$+ Z^{(k)}_{G-1} \hat{R}_\psi(S_k) + Z^{(k)}_G R_\psi(S_k). \tag{A.17}$$

Now define

$$X_k = \sum_{l \in \mathcal{A}} Z^{(k)}_l \tag{A.18}$$

$$Y_k = \sum_{l \in \mathcal{B}} Z^{(k)}_l \tag{A.19}$$

$$P_k = Z^{(k)}_G \tag{A.20}$$

$$Q_k = Z^{(k)}_{G-1} \tag{A.21}$$

and equation (A.17) becomes

$$W_k = P_k R_\psi(S_k) + Q_k \hat{R}_\psi(S_k) + X_k \left(\hat{R}_\psi(S_k) + R_\psi(S_k) \right) + Y_k \left(\hat{R}_\psi(S_k) - R_\psi(S_k) \right). \tag{A.22}$$

Recall that given User 1's spreading sequence, $\{Z^{(k)}_l\}$ is a set of i.i.d. Bernoulli RV's. From (A.18)-(A.21), it follows immediately that P_k, Q_k, X_k, and Y_k are independent RV's conditioned on User 1's sequence. Since mean of the Bernoulli RV is zero, RV's P_k, Q_k, X_k, and Y_k also have zero mean. From (A.22), it is seen that W_k is a function of P_k, Q_k, X_k, Y_k, and S_k. It is obvious that, conditioned on User 1's sequence, $\{P_k, Q_k, X_k, Y_k, S_k\}$ and $\{P_{k+1}, Q_{k+1}, X_{k+1}, Y_{k+1}, S_{k+1}\}$ are mutually independent since the kth interferer's data bits and chip sequences are independent of the $(k+1)$th interferer's data bits and chip sequences. Therefore, W_k and W_{k+1} are also independent given User 1's sequence. If we denote the cardinality of the set $\mathcal{A}$ by A and denote the cardinality of the set $\mathcal{B}$ by B, the respective probability mass functions for X_k and Y_k are

$$p_{X_k}(i) = \binom{A}{\frac{i+A}{2}} 2^{-A}, \quad i = -A, -A+2, \ldots, A-2, A \tag{A.23}$$

and

$$p_{Y_k}(j) = \binom{B}{\frac{j+B}{2}} 2^{-B}, \quad j = -B, -B+2, \ldots, B-2, B. \tag{A.24}$$

169

For a sequence with length G, there are $G-1$ chip boundaries. With the definition of the sets $\mathscr{A}$ and $\mathscr{B}$, these two sets form the partition of the index set denoting the chip boundaries, thus, $A + B = G - 1$. It is important to note that, with (A.22), given G, the conditioning on User 1's sequence has been reduced to the conditioning on the value of B, the number of transitions at the chip boundaries. The value of B can be thought as a measure of the amount of spreading in User 1's spreading sequence. When $B = G - 1$, it corresponds the maximum spreading where there is a transition at every chip boundary. On the other hand, when $B = 0$, it corresponds the minimum spreading where there is no transition at any chip boundaries.

The decision statistic presented in (A.22) was originally derived by Lehnert and Pursley [47]. This work has been widely cited and has appeared, for example, in two popular wireless textbooks [65], [70]. This form of decision statistic, as shown in Chapter 1, allows us to examine the BER dependence on the amount of spreading in User 1's sequence. However it can be very cumbersome to use and even prohibitive to compute the exact average BER for a system with large processing gain (G). Therefore, it is our motivation to search for another simpler form of W_k, which is statistically equivalent to (A.22). To do so, we re-examine the unsimplified expression for W_k in (A.8) and write W_k as

$$W_k = \Gamma_k \hat{R}_\psi(S_k) + \Delta_k R_\psi(S_k) \tag{A.25}$$

where

$$\Gamma_k = b_{-1}^{(k)} \sum_{l=0}^{\gamma_k - 1} a_{l+j-\gamma_k}^{(k)} a_{l+i}^{(1)} + b_0^{(k)} \sum_{l=\gamma_k}^{G-1} a_{l+j-\gamma_k}^{(k)} a_{l+i}^{(1)} \tag{A.26}$$

and

$$\Delta_k = b_{-1}^{(k)} \sum_{l=-1}^{\gamma_k - 1} a_{l+j-\gamma_k}^{(k)} a_{l+i+1}^{(1)} + b_0^{(k)} \sum_{l=\gamma_k}^{G-2} a_{l+j-\gamma_k}^{(k)} a_{l+i+1}^{(1)}. \tag{A.27}$$

We now make following important claims:

Claim 1: RV Γ_k is a sum of G i.i.d. symmetric Bernoulli RV's.

Claim 2: RV Δ_k is a sum of G i.i.d. symmetric Bernoulli RV's.

Claim 3: RV's Γ_k and Δ_k are statistically independent.

170

These claims are useful in the accurate BER estimation for the problem discussed in Chapter 2, in particular for a system with large processing gain. In the remainder of this appendix, we will show that all four claims are indeed true.

We first show that the auxiliary RV's $\{Z_l^{(k)}\}$ are mutually independent unconditionally. We state this result as a lemma and provide a detailed proof.

Lemma A.2: *The random variables $Z_l^{(k)}$, $l = 0, 1, \ldots, G$, defined in (A.10) are mutually independent symmetric Bernoulli random variables, regardless of User 1's spreading sequence.*

Proof: Clearly the discrete random variables $Z_l^{(k)}$, $l = 0, 1, \ldots, G$, are Bernoulli. To show they are mutually independent, we need to show that

$$\Pr\left(Z_0^{(k)} = z_0, Z_1^{(k)} = z_1, \cdots, Z_G^{(k)} = z_G\right) = \Pr\left(Z_0^{(k)} = z_0\right)\Pr\left(Z_1^{(k)} = z_1\right)\cdots\Pr\left(Z_G^{(k)} = z_G\right)$$

(A.28)

where z_i takes value of -1 or $+1$. From the definition of $Z_l^{(k)}$ in (A.10), we have

$$\begin{aligned}
&\Pr\left(Z_0^{(k)} = z_0, Z_1^{(k)} = z_1, \cdots, Z_G^{(k)} = z_G\right)\\
&= \Pr\left(b_{-1}^{(k)}a_{l+j-\gamma_k}^{(k)}a_{l+i}^{(1)} = z_l,\ l = 0, 1, \ldots, \gamma_k - 1;\ b_{-1}^{(k)}a_{j-\gamma_k-1}^{(k)}a_i^{(1)} = z_G;\right.\\
&\qquad\qquad \left. b_0^{(k)}a_{l+j-\gamma_k}^{(k)}a_{l+i}^{(1)} = z_l,\ l = \gamma_k, \ldots, G - 1\right)\\
&= \Pr\left(b_{-1}^{(k)}a_{l+j-\gamma_k}^{(k)}a_{l+i}^{(1)} = z_l,\ l = 0, 1, \ldots, \gamma_k - 1;\ b_{-1}^{(k)}a_{j-\gamma_k-1}^{(k)}a_i^{(1)} = z_G\right)\\
&\qquad\qquad \times\Pr\left(b_0^{(k)}a_{l+j-\gamma_k}^{(k)}a_{l+i}^{(1)} = z_l,\ l = \gamma_k, \ldots, G - 1\right)
\end{aligned}$$

(A.29)

where the last equality results from the independence assumption among the data bits, as well as the independence assumption among the chip sequence (with distinct chip index). To show that the first joint probability in (A.29) can be factored into products of the marginal probabilities, we observe that (assuming α_i or β_j takes value of -1 or $+1$)

$$\begin{aligned}
&\Pr\left(a_{j-\gamma_k-1}^{(k)}a_i^{(1)} = \alpha_1,\ a_{j-\gamma_k}^{(k)}a_i^{(1)} = \alpha_2,\ a_{1+j-\gamma_k}^{(k)}a_{i+1}^{(1)} = \beta_1, \cdots, a_{j-1}^{(k)}a_{\gamma_k-1+i}^{(1)} = \beta_{\gamma_k-1}\right)\\
&= \Pr\left(a_{j-\gamma_k-1}^{(k)}a_i^{(1)} = \alpha_1,\ a_{j-\gamma_k}^{(k)}a_i^{(1)} = \alpha_2\right)\prod_{l=1}^{\gamma_k-1}\Pr\left(a_{l+j-\gamma_k}^{(k)}a_{l+i}^{(1)} = \beta_l\right)\\
&= \Pr\left(a_{j-\gamma_k-1}^{(k)}a_i^{(1)} = \alpha_1\right)\Pr\left(a_{j-\gamma_k}^{(k)}a_i^{(1)} = \alpha_2\right)\prod_{l=1}^{\gamma_k-1}\Pr\left(a_{l+j-\gamma_k}^{(k)}a_{l+i}^{(1)} = \beta_l\right)
\end{aligned}$$

(A.30)

171

where the last equality follows from Lemma A.1 since $a^{(k)}_{j-\gamma_k-1}$ and $a^{(k)}_{j-\gamma_k}$ are independent Bernoulli

RV's. Therefore, the $\gamma_k + 1$ composite random variables

$$\left\{ a^{(k)}_{l+j-\gamma_k} a^{(1)}_{l+i}, \; l = 0, 1, \ldots, \gamma_k - 1; \; a^{(k)}_{j-\gamma_k-1} a^{(1)}_i \right\}$$

are mutually independent and Bernoulli. They are also independent of the Bernoulli RV $b^{(k)}_{-1}$. Applying Lemma A.1 to the first joint probability in (A.29), we obtain

$$\Pr\left(b^{(k)}_{-1} a^{(k)}_{l+j-\gamma_k} a^{(1)}_{l+i} = z_l, \; l = 0, 1, \ldots, \gamma_k - 1; \; b^{(k)}_{-1} a^{(k)}_{j-\gamma_k-1} a^{(1)}_i = z_G \right)$$

$$= \Pr\left(b^{(k)}_{-1} a^{(k)}_{j-\gamma_k-1} a^{(1)}_i = z_G \right) \prod_{l=0}^{\gamma_k-1} \Pr\left(b^{(k)}_{-1} a^{(k)}_{l+j-\gamma_k} a^{(1)}_{l+i} = z_l \right). \tag{A.31}$$

Similarly, since the $G - \gamma_k$ composite random variables

$$\left\{ a^{(k)}_{l+j-\gamma_k} a^{(1)}_{l+i} = z_l, l = \gamma_k, \ldots, G - 1 \right\} \tag{A.32}$$

are also mutually independent and Bernoulli; and they are independent of the Bernoulli RV $b^{(k)}_0$. Applying Lemma A.1 to the second joint probability in (A.29), we obtain

$$\Pr\left(b^{(k)}_0 a^{(k)}_{l+j-\gamma_k} a^{(1)}_{l+i} = z_l, l = \gamma_k, \ldots, G - 1 \right) = \prod_{l=\gamma_k}^{G-1} \Pr\left(b^{(k)}_0 a^{(k)}_{l+j-\gamma_k} a^{(1)}_{l+i} = z_l \right). \tag{A.33}$$

Collecting results from (A.29), (A.31), and (A.33), we complete our proof for Lemma A.2. ∎

Claim 1 is a direct consequence of Lemma A.2 because we have, from (A.26),

$$\begin{aligned}
\Gamma_k &= \sum_{l=0}^{\gamma_k-1} b^{(k)}_{-1} a^{(k)}_{l+j-\gamma_k} a^{(1)}_{l+i} + \sum_{l=\gamma_k}^{G-1} b^{(k)}_0 a^{(k)}_{l+j-\gamma_k} a^{(1)}_{l+i} \\
&= \sum_{l=0}^{\gamma_k-1} Z^{(k)}_l + \sum_{l=\gamma_k}^{G-1} Z^{(k)}_l \\
&= \sum_{l=0}^{G-1} Z^{(k)}_l.
\end{aligned} \tag{A.34}$$

By Lemma A. 2, Claim 1 immediately becomes true, that is, RV Γ_k is a sum of G i.i.d. symmetric Bernoulli random variables.

Clearly, from (A.27), Δ_k is a sum of Bernoulli RV's. To show that Claim 2 is true, we are left to show that these Bernoulli RV's are mutually independent. To show this, assuming α_l or β_l takes

172

value of -1 or $+1$, we have from (A.27)

$$
\begin{aligned}
&\Pr\left(b^{(k)}_{-1}a^{(k)}_{l+j-\gamma_k}a^{(1)}_{l+i+1} = \alpha_l, \, l=-1,\ldots,\gamma_k-1; \right.\\
&\qquad\qquad \left. b^{(k)}_0 a^{(k)}_{l+j-\gamma_k}a^{(1)}_{l+i+1} = \beta_l, \, l=\gamma_k,\ldots,G-2\right)\\
&= \Pr\left(b^{(k)}_{-1}a^{(k)}_{l+j-\gamma_k}a^{(1)}_{l+i+1} = \alpha_l, \, l=-1,\ldots,\gamma_k-1\right)\\
&\qquad \times \Pr\left(b^{(k)}_0 a^{(k)}_{l+j-\gamma_k}a^{(1)}_{l+i+1} = \beta_l, \, l=\gamma_k,\ldots,G-2\right)\\
&= \left[\prod_{l=-1}^{\gamma_k-1}\Pr\left(b^{(k)}_{-1}a^{(k)}_{l+j-\gamma_k}a^{(1)}_{l+i+1} = \alpha_l\right)\right]\cdot\left[\prod_{l=\gamma_k}^{G-2}\Pr\left(b^{(k)}_0 a^{(k)}_{l+j-\gamma_k}a^{(1)}_{l+i+1} = \beta_l\right)\right]
\end{aligned}
$$

$$(A.35)$$

where the first product term is a result of the direct application of Lemma A.1 since the composite random variables

$$
\left\{a^{(k)}_{l+j-\gamma_k}a^{(1)}_{l+i+1}, \, l=-1,\ldots,\gamma_k-1\right\}
$$

are i.i.d. symmetric Bernoulli and they are independent of the symmetric Bernoulli RV $b^{(k)}_{-1}$. Similarly, the second product term is a result of the direct application of Lemma A.1 since the composite random variables

$$
\left\{a^{(k)}_{l+j-\gamma_k}a^{(1)}_{l+i+1}, \, l=\gamma_k,\ldots,G-2\right\}
$$

are i.i.d. symmetric Bernoulli and they are independent of the symmetric Bernoulli RV $b^{(k)}_0$. Therefore, according to (A.35), we conclude that Claim 2 is also true, that is, RV Δ_k is a sum of G i.i.d. symmetric Bernoulli random variables.

The proof for Claim 3 is slightly more involved. It is convenient for us to label the G summands of Γ_k given in (A.26) as $U_1, U_2, \cdots, U_G$ and enumerate them as

$$
\mathcal{U} = \left\{ U_1 = b^{(k)}_{-1}\underbrace{a^{(k)}_{j-\gamma_k}}_{g_3}\underbrace{a^{(1)}_i}_{g_2}, \, U_2 = b^{(k)}_{-1}\underbrace{a^{(k)}_{1+j-\gamma_k}}_{g_5}\underbrace{a^{(1)}_{1+i}}_{g_4}, \, \cdots, \, U_{\gamma_k} = b^{(k)}_{-1}\underbrace{a^{(k)}_{-1+j}}_{g_{2\gamma_k+1}}\underbrace{a^{(1)}_{\gamma_k-1+i}}_{g_{2\gamma_k}}, \right.
$$

$$
U_{\gamma_k+1} =
$$

$$
\left. \underbrace{b^{(k)}_0 a^{(k)}_j}_{g_{2\gamma_k+3}}\underbrace{a^{(1)}_{\gamma_k+i}}_{g_{2\gamma_k+2}}, \, \cdots, \, U_{G-1} = b^{(k)}_0 \underbrace{a^{(k)}_{G-2+j-\gamma_k}}_{g_{2G-1}}\underbrace{a^{(1)}_{G-2+i}}_{g_{2G-2}}, \, U_G = b^{(k)}_0 \underbrace{a^{(k)}_{G-1+j-\gamma_k}}_{g_{2G+1}}\underbrace{a^{(1)}_{G-1+i}}_{g_{2G}} \right\},
$$

173

and similarly we label the G summands of Δ_k given in (A.27) as $V_1, V_2, \cdots, V_G$ and enumerate them as

$$\mathscr{V} = \left\{ V_1 = \underbrace{b_{-1}^{(k)} a_{-1+j-\gamma_k}^{(k)}}_{g_1} \underbrace{a_i^{(1)}}_{g_2}, \; V_2 = \underbrace{b_{-1}^{(k)} a_{j-\gamma_k}^{(k)}}_{g_3} \underbrace{a_{1+i}^{(1)}}_{g_4}, \; \cdots, \; V_{\gamma_k} = \underbrace{b_{-1}^{(k)} a_{-2+j}^{(k)}}_{g_{2\gamma_k-1}} \underbrace{a_{\gamma_k+i-1}^{(1)}}_{g_{2\gamma_k}}, \right.$$

$$\left. V_{\gamma_k+1} = \underbrace{b_{-1}^{(k)} a_{-1+j}^{(k)}}_{g_{2\gamma_k+1}} \underbrace{a_{\gamma_k+i}^{(1)}}_{g_{2\gamma_k+2}}, \; V_{\gamma_k+2} = \underbrace{b_0^{(k)} a_j^{(k)}}_{g_{2\gamma_k+3}} \underbrace{a_{\gamma_k+i+1}^{(1)}}_{g_{2\gamma_k+4}}, \; \cdots, \; V_G = \underbrace{b_0^{(k)} a_{G-2+j-\gamma_k}^{(k)}}_{g_{2G-1}} \underbrace{a_{G-1+i}^{(1)}}_{g_{2G}} \right\}$$

where, after a careful examination of the sequence pattern in $\mathscr{U}$ and $\mathscr{V}$, we have denoted the chip sequences of the desired user by $g_2, g_4, \ldots g_{2G}$, and denote the composite RV's, which consist of the kth interferer's data bits and chip sequences, by $g_1, g_3, \ldots, g_{2G+1}$. These latter random terms are defined as

$$
\begin{bmatrix}
g_1 \triangleq b_{-1}^{(k)} a_{-1+j-\gamma_k}^{(k)} \\[2mm]
g_3 \triangleq b_{-1}^{(k)} a_{j-\gamma_k}^{(k)} \\[2mm]
\vdots \\[2mm]
g_{2\gamma_k-1} \triangleq b_{-1}^{(k)} a_{-2+j}^{(k)} \\[2mm]
g_{2\gamma_k+1} \triangleq b_{-1}^{(k)} a_{-1+j}^{(k)} \\[2mm]
g_{2\gamma_k+3} \triangleq b_0^{(k)} a_j^{(k)} \\[2mm]
\vdots \\[2mm]
g_{2G-1} \triangleq b_0^{(k)} a_{G-2+j-\gamma_k}^{(k)} \\[2mm]
g_{2G+1} \triangleq b_0^{(k)} a_{G-1+j-\gamma_k}^{(k)}
\end{bmatrix}
\begin{bmatrix}
g_2 \triangleq a_i^{(1)} \\[2mm]
g_4 \triangleq a_{1+i}^{(1)} \\[2mm]
\vdots \\[2mm]
g_{2\gamma_k} \triangleq a_{\gamma_k-1+i}^{(1)} \\[2mm]
g_{2\gamma_k+2} \triangleq a_{\gamma_k+i}^{(1)} \\[2mm]
g_{2\gamma_k+4} \triangleq a_{\gamma_k+1+i}^{(1)} \\[2mm]
\vdots \\[2mm]
g_{2G-2} \triangleq a_{G-2+i}^{(1)} \\[2mm]
g_{2G} \triangleq a_{G-1+i}^{(1)}
\end{bmatrix}
. \qquad \text{(A.36)}
$$

Therefore, for simplicity, we can rewrite the set $\mathscr{U} = \{U_1, U_2, \cdots, U_G\}$ as

$$\mathscr{U} = \left\{ U_1 = g_2 g_3, U_2 = g_4 g_5, \cdots, U_{\gamma_k} = g_{2\gamma_k} g_{2\gamma_k+1}, U_{\gamma_k+1} = g_{2\gamma_k+2} g_{2\gamma_k+3}, \right.$$

$$\left. \cdots, U_{G-1} = g_{2G-2} g_{2G-1}, U_G = g_{2G} g_{2G+1} \right\}, \qquad \text{(A.37)}$$

and rewrite the set $\mathscr{V} = \{V_1, V_2, \cdots, V_G\}$ as

$$\mathscr{V} = \left\{ V_1 = g_1 g_2, V_2 = g_3 g_4, \cdots, V_{\gamma_k} = g_{2\gamma_k-1} g_{2\gamma_k}, V_{\gamma_k+1} = g_{2\gamma_k+1} g_{2\gamma_k+2}, \right.$$

$$\ldots, V_{G-1} = g_{2G-3}g_{2G-2}, V_G = g_{2G-1}g_{2G} \Bigg\}. \qquad (A.38)$$

A close study of g_k defined in (A.36) reveals that the $2G+1$ RV's $\{g_1, g_2, g_3, \ldots, g_{2G-1}, g_{2G}, g_{2G+1}\}$ are i.i.d. Bernoulli, where in making this observation Lemma A.1 has been invoked wherever required. This key observation leads us to conclude that the $2G$ RV's $\{U_1, U_2, \ldots, U_G\}$ and $\{V_1, V_2, \cdots, V_G\}$ are mutually independent. This result can be seen from a fair coin tossing experiment. According to (A.37) and (A.38), one may toss a first fair coin to determine the value of g_1. A second toss determines g_2, therefore the value of $g_1 g_2$ or V_1. A third toss determines g_3 therefore the value of $g_2 g_3$ or U_1. A forth toss determines g_4 hence the value of $g_3 g_4$ or V_2. We continue this process until the last toss which determines g_{2G+1} hence the value of $g_{2G}g_{2G+1}$ or U_G. Clearly $\{U_1, U_2, \ldots, U_G\}$ and $\{V_1, V_2, \ldots, V_G\}$ are mutually independent. Since functions of statistically independent random vectors are also statistically independent, we conclude, as a result, that $\sum_{i=1}^{G} U_i$ and $\sum_{i=1}^{G} V_i$ are statistically independent. In other words, Γ_k and Δ_k are statistically independent and this completes the proof of Claim 3.

In general, the MAI terms at the output of the correlator receiver are dependent. This is true for both deterministic and random spreading sequences. However, as shown in Chapter 2, the loss in accuracies for BER's is negligible if we make the independence assumption for these MAI terms. Finally, we comment that the simplification of the decision statistic does not rely on the periodicity assumption in random sequences (see Fig. A.1).

175

Vita

Julian Zhishen Cheng

EDUCATION

University of Alberta	Ph.D. Candidate	Electrical and Computer Engineering January 2000 – Present
Queen's University	Ph.D. Candidate (Transferred)	Electrical and Computer Engineering September 1997 – December 2000
Queen's University	M.Sc. (Eng.)	Mathematics and Engineering January 1996 – August 1997
University of Victoria	B.Eng. (First Class)	Electrical and Computer Engineering September 1990 – April 1995

WORK EXPERIENCE

University of Alberta (iCORE Wireless Communications Laboratory)	Research Assistant	Jan. 2000 - Present
Queen's University (Electrical and Computer Engineering)	Research Assistant Teaching Assistant	Sept. 1997 - Dec. 2000
Nortel Networks (Advanced Wireless Technology)	Summer Intern	May 1997 - Sept. 1997
University of Victoria (Electrical and Computer Engineering)	Research Assistant	1993, 1994, 1995
Northern Telecom Ltd. (Semiconductor Group)	Co-op Student	Sept. 1994 - December 1994

AWARDS

NSERC (the Natural Sciences and Engineering Research Council of Canada) Postdoctoral Fellowship, 2002.

Ontario Graduate Scholarships in Science and Technology (OGSST), Queen's University, Kingston, Ontario, 2000 (Declined).

NSERC (the Natural Sciences and Engineering Research Council of Canada) Postgraduate Scholarship, 1997-1999.

Queen's Graduate Fellowship, Queen's University, Kingston, Ontario, 1999-2000.

R. S. McLaughlin Fellowship, Queen's University, Kingston, Ontario, 1996-1997.

President's Scholarship, University of Victoria, Victoria, British Columbia, 1994, 1995.

J. Bullick Memorial Scholarship, University of Victoria, Victoria, British Columbia, 1993, 1994, 1995.

NSERC (the Natural Sciences and Engineering Research Council of Canada) Undergraduate Scholarship, 1993, 1994, 1995.

PUBLICATIONS

Julian Cheng and Norman C. Beaulieu, "Generalized Moment Estimators for the Nakagami Fading Parameter," *IEEE Communications Letters*, vol. 6, pp. 144-146, April 2002.

Julian Cheng and Norman C. Beaulieu, "Accurate DS-CDMA Bit Error Probability Calculation in Rayleigh Fading," *IEEE Transactions on Wireless Communications*, vol. 1, pp. 3-15, January 2002.

Julian Cheng and Norman C. Beaulieu, "Maximum-Likelihood Based Estimation of the Nakagami m Parameter," *IEEE Communications Letters*, vol. 5, pp. 101-103, March 2001.

Yi Song, Steven D. Blostein and Julian Cheng, "Exact Outage Probability for Equal Gain Combining with Cochannel Interference in Rayleigh Fading," To appear in *IEEE Transactions on Wireless Communications*.

Douglas P. Wiens, Julian Cheng and Norman C. Beaulieu, "A Class of Method of Moments Estimators for the Two-Parameter Gamma Family," To appear in *Pakistan Journal of Statistics*.

N. C. Beaulieu and J. Cheng, "Precise Error Rate Analysis of Bandwidth Efficient BPSK in Nakagami Fading and Cochannel Interference," Submitted to *IEEE Transactions on Communications*.

177

Julian Cheng, Maria A. Stuchly, C. DeWagter and L. Martens, "Magnetic Field Induced Currents in a Human Head from Use of Portable Appliances", *Physics in Medicine and Biology,* vol. 40, pp. 495-510, April 1995.

Julian Cheng and Norman C. Beaulieu, "Error Rate of BPSK in Generalized Fading Channels with Co-Channel Interference," *VTC Spring,* Birmingham, Alabama, pp. 1786-1790, May 6-10 2002.

Julian Cheng and Norman C. Beaulieu, "Moment-Based Estimation of the Nakagami-m Fading Parameter," *PACRIM 2001,* Victoria, British Columbia, Canada, pp. 361-364, August 26-10 2002.

Julian Cheng and Norman C. Beaulieu, "Estimation of the Nakagami-m Parameter," *Wireless 2001,* Calgary, Alberta, Canada, pp. 84-88, July 9-11, 2001.

Julian Cheng and Norman C. Beaulieu, "Precise Bit Error Rate Calculation for Asynchronous DS-CDMA in Nakagami Fading," *GLOBECOM 2000,* San Francisco, CA, pp. 980-984, November 27- December 1 2000.

Julian Cheng and Norman C. Beaulieu, "Exact Bit Error Probability of DS-CDMA in Rayleigh Fading," *International Conference on Telecommunications ICT 2000,* Acapulco, Mexico, pp. 587-591, May 22-25 2000.

Julian Cheng and Fady Alajaji, "Channel Optimized Quantization of Images Over Bursty Channels," *1997 Canadian Workshop on Information Theory,* Toronto, Ontario, June 1997.

Maria. A. Stuchly, Julian Cheng, L. Martens and C. DeWagter, "Magnetic Field Induced Currents in a Human Head from Use of Portable Appliances," *BEMS Annual Conference,* Boston, MA, June 1995.